Norsk Geologisk Tidsskrift

Volume 72

Proceedings of the 7th TSGS Conference held in Stavanger,
3–5 October 1990

POST-CRETACEOUS UPLIFT AND SEDIMENTATION ALONG THE WESTERN FENNOSCANDIAN SHIELD

Edited by

LARS N. JENSEN, FRIDTJOF RIIS & ROGNVALD BOYD

SCANDINAVIAN UNIVERSITY PRESS · OSLO – STOCKHOLM

ISSN 0029-196X

July 1992

Norsk Geologisk Tidsskrift
Vol. 72, No. 3, pp. 221–338

POST-CRETACEOUS UPLIFT AND SEDIMENTATION ALONG THE WESTERN FENNOSCANDIAN SHIELD

Contents

Acknowledgments

All the papers in this volume of Norsk Geologisk Tidsskrift have been revised by experts from the various research fields represented. The editors express their thanks to: B. G. Andersen, A. Andresen, K. Anundsen, K. Bjørlykke, P. Blystad, H. Brekke, T. Eidvin, J. I. Faleide, R. Feyling-Hansen, W. Fjeldskaar, R. B. Færseth, R. H. Gabrielsen, S. Gudlaugsson, E. Jansen, A. Koestler, A. G. Krill, B. T. Larsen, S. Lippard, H. Løseth, A. G. Milnes, A. Solheim, A. M. Spencer, O. Stephanson, E. Swensson, J. Sættem, K. Sørensen, E. Thomsen, A. Thon, B. Tørudbakken, S. Vassmyr.

Financial support for the conference was given by: Amerada Hess, Conoco Norway, Institutt for Kontinentalsokkelundersøkelser og Petroleumsteknologi, Mobil, Norsk Hydro and Statoil.

Printing of this expanded proceedings volume has been made possible through financial support from Statoil.

Preface

The 7th annual meeting of the Tectonics and Structural Geology Studies Group (TSGS) of the Geological Society of Norway (NGF) was held in Stavanger from October 3rd to 5th, 1990. The topic of the conference was: Post-Cretaceous uplift and sedimentation along the western Fennoscandian Shield. A one-day field trip focusing on neotectonism in the vicinity of Stavanger was held in connection with the meeting.

The aim of the TSGS is to organize annual meetings on different topics in the fields of tectonics and structural geology and to bring together people from academia and industry for information exchange and discussion. Approximately 150 participants from six countries attended this meeting, at which 28 oral and 5 poster contributions were presented.

The present volume of *Norsk Geologisk Tidsskrift* contains 20 of the contributions presented at the meeting, covering all the main topics discussed at the conference. This volume is therefore the first collected attempt to cover the various aspects of Tertiary erosion and sedimentation in Scandinavia. We hope that it will be used as a reference book during further research in academia and industry.

Four speakers were specially invited by the TSGS organizing committee: Sierd Cloetingh (Vrije Universitet, Amsterdam), Anthony G. Doré (Conoco Norway), Hans Christian Larsen (GGU, Copenhagen) and Jan I. Skagen (Statoil).

The organizing committee consisted of: Karl Anundsen, Roy H. Gabrielsen, Lars N. Jensen, Andreas Koestler, Fridtjof Riis and Eivind Swensson.

LARS N. JENSEN, Statoil
FRIDTJOF RIIS, Oljedirektoratet
ROGNVALD BOYD, Norges geologiske undersøkelse

Introduction: Measuring uplift and erosion – proposal for a terminology

FRIDTJOF RIIS & LARS N. JENSEN

Riis, F. & Jensen, L. N.: Introduction: Measuring uplift and erosion – proposal for a terminology. *Norsk Geologisk Tidsskrift*, Vol. 72, pp. 223–228. Oslo 1992. ISSN 0029-196X.

To avoid confusion in further discussions concerning uplift and erosion a number of terms are defined, e.g. uplift of rocks, tectonic and isostatic uplift, surface uplift, net uplift and erosion. A proposal for a Norwegian terminology is also presented. The terminology is discussed with reference to a hypothetical subsidence/uplift history relevant to the Norwegian shelf. Further aspects of Late Tertiary uplift and sedimentation in Norway are discussed in relation to two regional profiles: one from northern Norway and the Barents Sea and one from Telemark to the Central Graben.

Fridtjof Riis, Oljedirektoratet, PO Box 600, N-4001 Stavanger, Norway; Lars N. Jensen, Statoil a.s, PO Box 300, N-4001 Stavanger, Norway.

This volume of *Norsk Geologisk Tidsskrift* comprises presentations from the 7th TSGS conference in Stavanger (1990), where post-Cretaceous uplift and subsidence, erosion and sedimentation were discussed. A considerable amount of research has been focused on this topic in the last few years, but in spite of that many aspects of the Tertiary and Quaternary vertical movements of Scandinavia are not yet understood. As an introduction to this volume we discuss the methodology used for measuring, and propose a terminology for the basic concepts of uplift and erosion. Hopefully this will facilitate further discussion.

Terminology of uplift and erosion

This proposal for a terminology of uplift and erosion is based on the definitions and discussions of Brown (1991), Molnar & England (1990) and England & Molnar (1990). The confusion in the literature arises from the fact that 'uplift' is used in different senses (England & Molnar 1990). Two types of uplift have to be clearly distinguished. These are:

1. *Uplift of rocks* (U), which refers to the vertical movement of a rock body or marker horizon with respect to a given datum. U is the difference in elevation with respect to the chosen datum at a given point at two different instants in time. Upward movement is positive (i.e. uplift, *Norwegian: heving*), downward movement is negative (i.e. subsidence, *Norwegian: innsynkning*). Uplift (subsidence) of rocks can be due to different causes and the parameter U can be subdivided into components according to the different effects. For instance, *tectonic uplift* (Ut) is the component of uplift in response to tectonic forces or temperature changes, whereas *isostatic uplift* (Ui) is the component of uplift in response to loading (or unloading) of the Earth's crust. In the following we use mean sea level (approximately the geoid, see England & Molnar 1990) as our reference datum. This means that the complicating factor of eustatic sea level change does not enter into the discussion. Also, we have not taken compaction of sediments into account. A hypothetical uplift/subsidence curve of this type is shown in Fig. 1.

2. *Surface uplift* or surface rise (R), which refers to the vertical movement of the Earth's surface (sea bottom or land surface) with respect to a given datum. R is the difference in elevation with respect to the chosen datum at a given point at two different instants in time. Using mean sea level as datum, a hypothetical variation of surface height/depth with time is shown in Fig. 1.

As shown by England & Molnar (1990), the difference between the uplift parameter U and the uplift parameter R is a measure of the *erosion/deposition* (what they call 'exhumation') according to the equation:

$$U = Ut + Ui = R + E \quad \text{and} \quad R = Ho - Hi \tag{1}$$

where E is the change in the thickness of overburden above the marker horizon at a given point at two different instants of time. Decreasing thickness of overburden (i.e. erosion, *Norwegian: erosjon*), which can be submarine or subaerial, is positive here, whereas increasing thickness of overburden (i.e. deposition, *Norwegian: avsetning*) is negative. In the hypothetical example of Fig. 1, E can be obtained by plotting the difference between the two uplift/subsidence curves. Ho is the present elevation and Hi is the initial paleo-elevation.

Unfortunately, rocks contain no precise paleo-altimeters, and for practical measurements of uplift we are often confined to a thermal or sediment compaction frame of reference. To relate these frames of reference to the sea level, we often need additional independent information

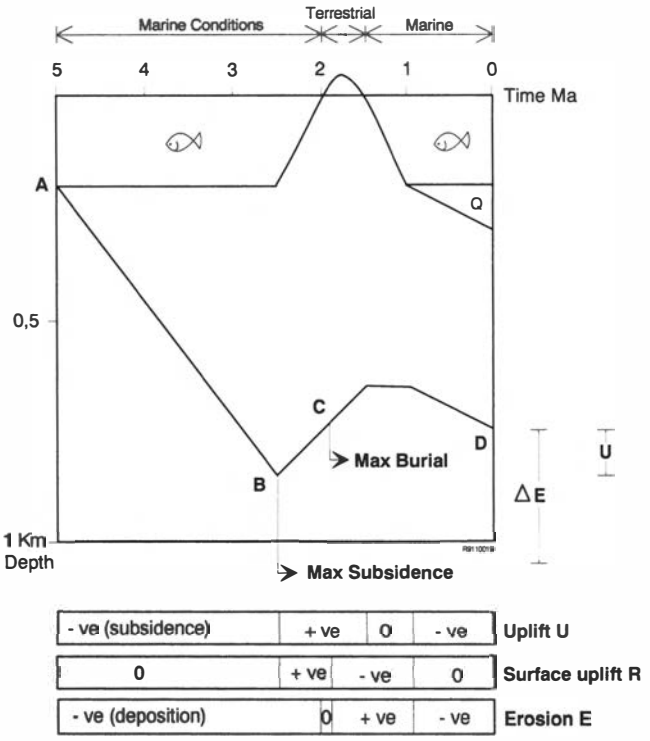

Fig. 1. A hypothetical subsidence/uplift curve (ABCD) for a marker horizon deposited 5 m.y. ago, together with a surface subsidence/uplift curve. Points B and C show maximum subsidence and maximum burial respectively. Q is Quaternary sediments. Indicated at the base of the figure are the times uplift, surface uplift and erosion were positive, negative or zero. The erosion before 1 Ma is indicated with a vertical bar ΔE and the uplift between points B and D is labeled U.

about paleo-elevation. In a thermal frame of reference, erosion is called *denudation* (Brown 1991), and methods such as apatite fission-track analysis (AFTA, Green 1989, Brown 1991), vitrinite reflectance trends (Jensen & Schmidt, this volume) and fluid inclusion studies (Walderhaug, this volume) are used to quantify the erosion. In a sediment compaction frame of reference we measure erosion (i.e. missing overburden) relative to a set of standard compaction curves (Magara 1976; Sclater & Christie 1980).

In addition to the above terminology and definitions, some useful terms are described below.

Denudation and exhumation (*Norwegian: blottlegging*): The process of erosion seen in a thermal (denudation) and general overburden (exhumation) frame of reference.

Maximum burial and maximum subsidence (*Norwegian: maksimal begravning og maksimal innsynkning*): Maximum burial refers to the maximum overburden of a marker horizon, whereas the maximum subsidence refers to the minimum altitude of this horizon. The time of maximum burial (i.e. overburden) is not necessarily equal to the time of maximum subsidence measured from sea level (Fig. 1).

Net uplift (*Norwegian: netto heving*): A quantity introduced by Nyland et al. (in press) and Jensen & Schmidt (in press), who define net uplift as the difference between maximum burial and the present elevation of a marker bed. This parameter is easier to calculate and to contour than erosion. Net uplift may be a useful parameter, in particular in basin modelling studies where the main concern is maturation of source rocks, so that absolute elevations and water depths are not of primary importance. In a marine setting (like offshore Norway) the maximum difference between net uplift and true uplift (U, eq. 1) is the water depth at onset of uplift of the marker horizon (point B, Fig. 1).

Some of the complications inherent in Eq. 1 are illustrated in Fig. 1, which shows the uplift/subsidence history of a hypothetical marker horizon deposited five million years ago, together with a possible surface uplift/subsidence curve (change in depth below, or height above mean sea level). The following points should be noted: (1) Under marine conditions, deposition may continue after the time of maximum subsidence. This means that the time of maximum burial is not necessarily the time of maximum subsidence. (2) Similarly, erosion may take place during periods of subsidence or static conditions as well as in periods of uplift. In our hypothetical case, the period of static conditions is accompanied by considerable submarine erosion by shelf ice. At 1 m.y. deposition resumes due to the retreat of the ice (Quaternary sediments, Q on Fig. 1). (3) Net uplift may differ from both eroded thickness (E) and from the uplift (U). In Fig. 1, net uplift is zero. This illustrates that the net uplift should not be confused with the eroded thickness (e.g. the reduction in thickness of the overburden) or with the uplift (e.g. the decrease in depth of the marker bed).

Methods

Table 1 shows the methods used to quantify uplift and erosion. The regional methods are used on uplift and erosion in a given drainage area, while the local methods are used to calculate uplift and erosion in single wells.

Table 1. Methods used to quantify uplift and erosion.

REGIONAL METHODS (analysis of map, profile and velocity data)
Subcrop maps
Extrapolation from seismic profiles
Geomorphology and paleogeographical reconstructions
Seismic velocity analysis
LOCAL METHODS (analysis of rock parameters and well data)
Shale compaction (sonic velocity, density, porosity)
Sandstone porosity and diagenesis
Clay mineral diagenesis
Vitrinite reflectance trends
Colour of microfossils (TAI)
Organic geochemistry (pyrolysis data, geochemical markers)
Fluid inclusion analysis
Fission track studies
Opal A – Opal CT – quartz transformations
PVT modelling of hydrocarbon accumulations
Drilling parameters (Dx component)
Kinetic modelling

Local methods

Calculations of uplift and erosion by the local methods are based on the physical and chemical changes caused by burial. In general, temperature and lithostatic pressure (sediment compaction) are the most important factors causing these changes. Therefore, the local methods give an estimate of the maximum paleo-temperature and/or overburden. The maximum overburden may be calculated using well/reference well methods (e.g. Magara 1976) or kinetic modelling (e.g. Forbes et al. 1991). Since we are concerned with overburden, the zero level used for the calculations is the ground surface or the sea floor.

To obtain reliable results using local methods one must establish a reference well which is lithologically similar to the studied well and which has a similar geological history. Also, one must be confident that the temperature gradient of the reference well at present is similar to the temperature gradient of the studied well at its maximum burial, and that the compaction trends were similar (e.g. no overpressure).

Kinetic modelling is a method commonly applied to geochemical reactions in sedimentary basins (e.g. Forbes et al. 1991). In such modelling paleo-temperatures are a major factor of uncertainty. In addition, the present temperatures may not be in equilibrium with the heat flow at depth. In eroded areas temperatures should be slightly higher than expected from the heat flow through the crust, and in areas with rapid deposition temperatures should be lower.

Regional methods

The mass balance method was important in establishing the large amount of glacial erosion in the Barents Sea (Nøttvedt et al. 1988; Eidvin & Riis 1989; Vorren et al. 1990). In this method, the volume of the clastic sediments of a given age in a depocenter is compared with the size of the eroded drainage area. The method gives a qualitative idea of the average amount of erosion in the drainage area. The major uncertainties of this method are discussed by Vorren et al. (1990).

The paleogeographic reconstruction method is used by Riis & Fjeldskaar (in press) and Doré (this volume). This method can be used regionally or on profiles to estimate the eroded section. The simplest way of applying the method is to extrapolate the dipping and eroded Mesozoic and Cenozoic strata to the onshore and measure directly how much has been eroded along the depth-converted profile.

The regional methods (except for seismic velocity analysis) differ from the local methods in that the eroded section is measured directly (in m or m^3), while in the local methods erosion is inferred from rock parameters. Regional methods should therefore always be used together with local methods to ensure geological control on the interpretation.

Post-Cretaceous vertical movements of the Norwegian shelf

Many of the papers presented in this volume give examples of Tertiary and Quaternary vertical movements, and these observations fit into a regional picture. The western parts of Fennoscandia and the Barents Sea were uplifted 1000–2000 m in the Tertiary and Quaternary to form structural domes and platforms which were strongly eroded. Deposition of the erosional products took place on the subsiding parts of the shelf and at the shelf margin. The Paleozoic to Cenozoic sedimentary cover shows a gentle dip away from this basement-cored dome in Scandinavia. This is illustrated in two key profiles (Figs. 2 and 3).

Figure 2a, b shows the relationship between basement and the sedimentary cover in a profile across the southwestern Barents Sea. The profile is based on Gabrielsen et al. (1990) and Sigmond (in press). The Pliocene–Pleistocene Bjørnøya wedge covers the western part of the profile, and the eroded Tertiary and pre-Tertiary strata is seen to the east. The dotted line (Mo) shows the amount of erosion based on vitrinite and pyrolysis data from wells, as well as on seismic interpretation of the opal A to CT transition (Riis & Fjeldskaar, in press). There are no data from the Finnmark Platform and the onshore area. It is interesting, however, that the surface defined by the missing overburden line fits so well with the base of the Pliocene to the west and with the highest mountains to the east. The profile also shows that the Permian and Triassic strata on the Finnmark Platform have such a dip that they can be extrapolated onshore to reach a level slightly higher than the highest mountains.

These observations suggest that much of the dip in the Tertiary section is related to an isostatic response to the Plio-Pleistocene erosion, and that the coastal parts of Finnmark were covered by Paleozoic and Mesozoic sediments before the Neogene and Quaternary uplift. There also seems to be a relationship between the amount of erosion offshore and the summit level of the mountains onshore. The subsidence curves (Fig. 2b) illustrate the importance of the major Late Cretaceous and Eocene tectonic phases as well as the Plio-Pleistocene erosion and deposition.

Figure 3a, b shows the relationship between basement and sedimentary cover in a profile from the Central Graben, across the Farsund Basin to the central part of southern Norway. The profile is modified from Jensen & Schmidt (in press). The Neogene depocentre in the central North Sea covers the western part of the profile, and from location 2 (Fig. 3b) the Neogene uplift and erosion increases towards the Norwegian coast. The dotted line (Mo) shows a reconstruction of the eroded strata. The magnitude of uplift and erosion is based on vitrinite reflectance data and shale compaction from wells along the profile. From reconstruction of the eroded strata it is evident that Mesozoic sediments must have covered the coastal parts of southern Norway. The Late Cretaceous

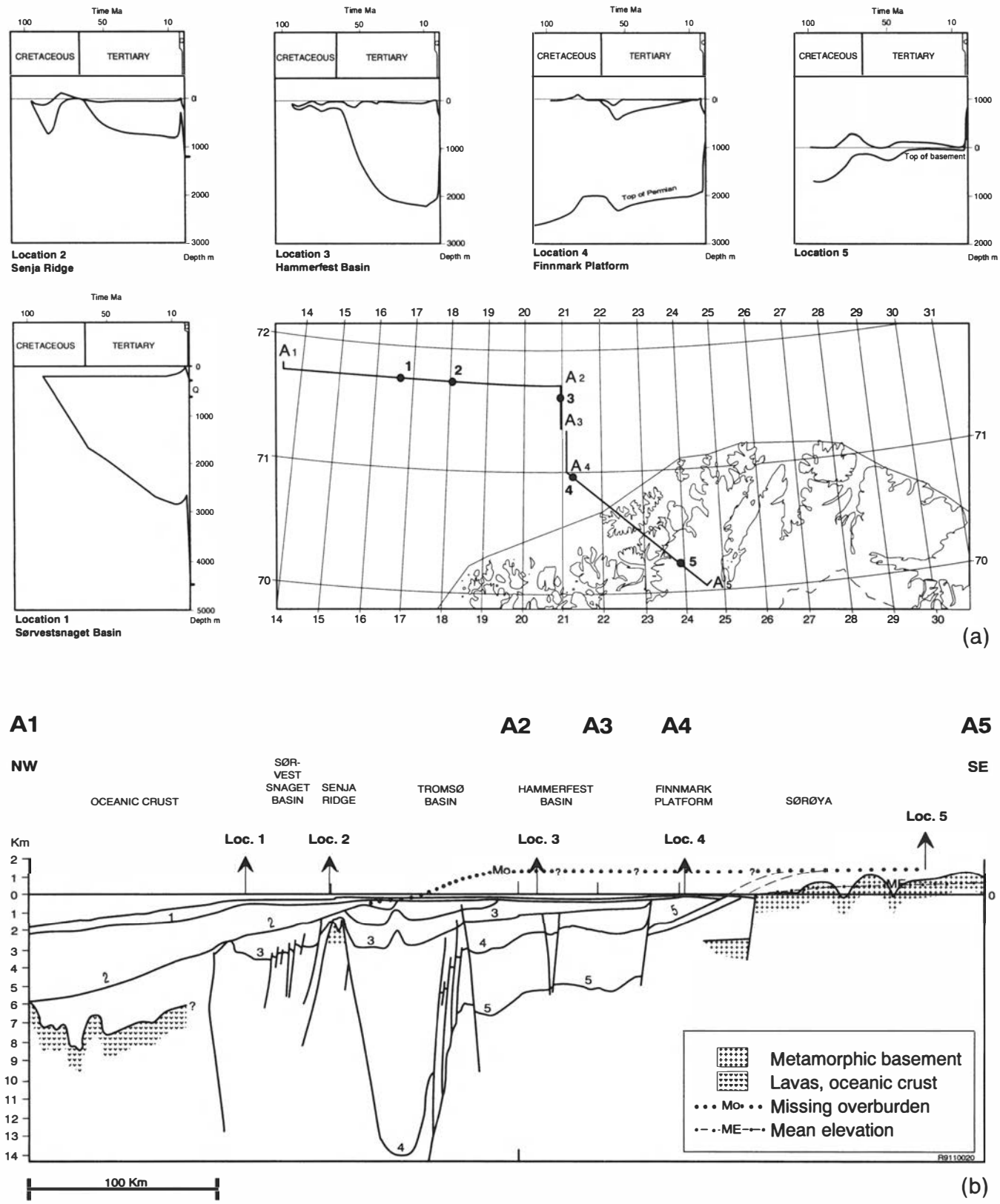

Fig. 2. (a) The location of the regional profile across the Barents Shelf and the subsidence history at five locations along this profile. (b) A regional profile across the Barents Shelf to Sørøya, Finnmark. The five locations shown as subsidence diagrams (Fig. 2a) are indicated. Reflectors: 1 – Base Quaternary, 2 – Base of Upper Pliocene, 3 – Base Tertiary, 4 – Base Cretaceous, 5 – Base Triassic. Depth in km.

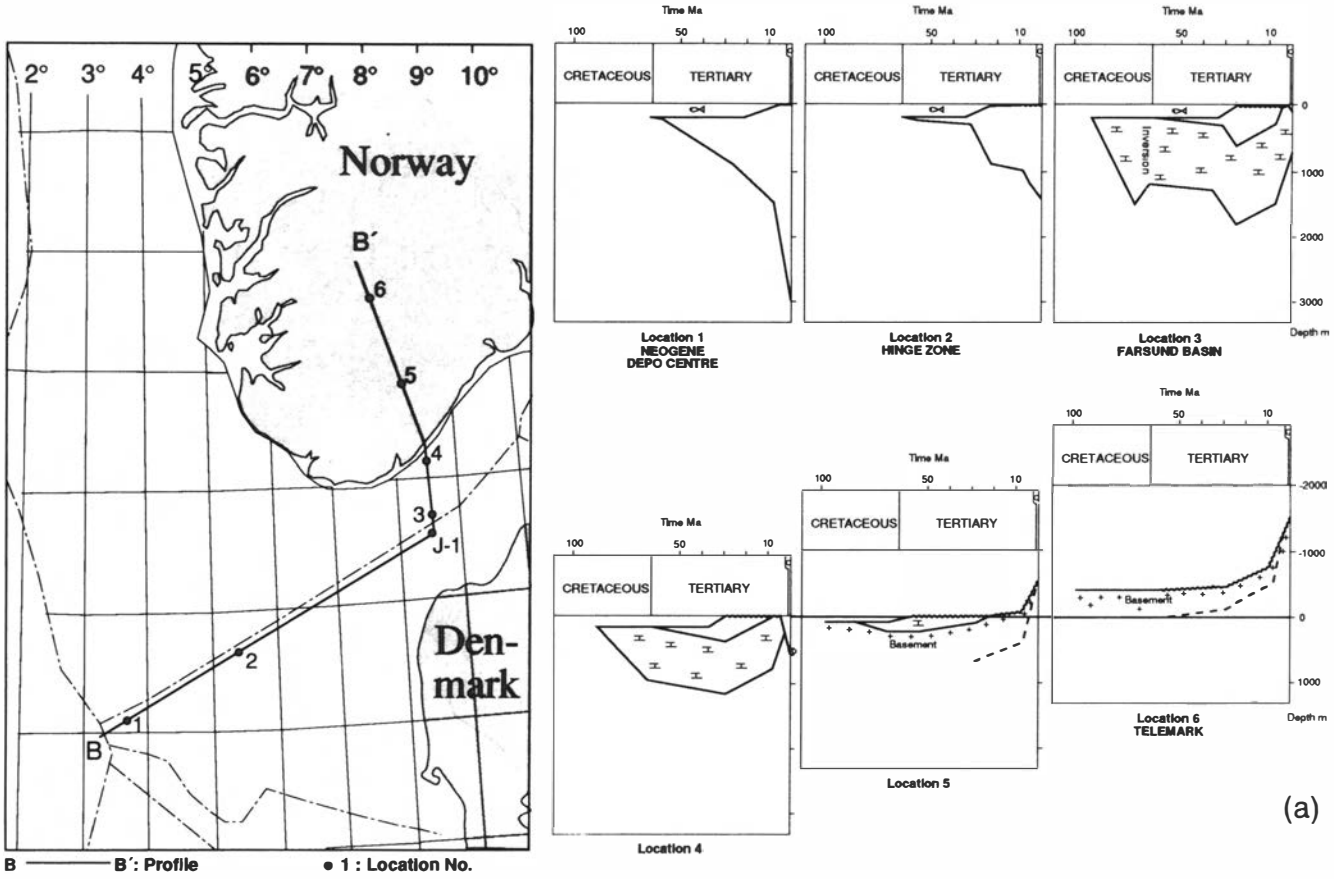

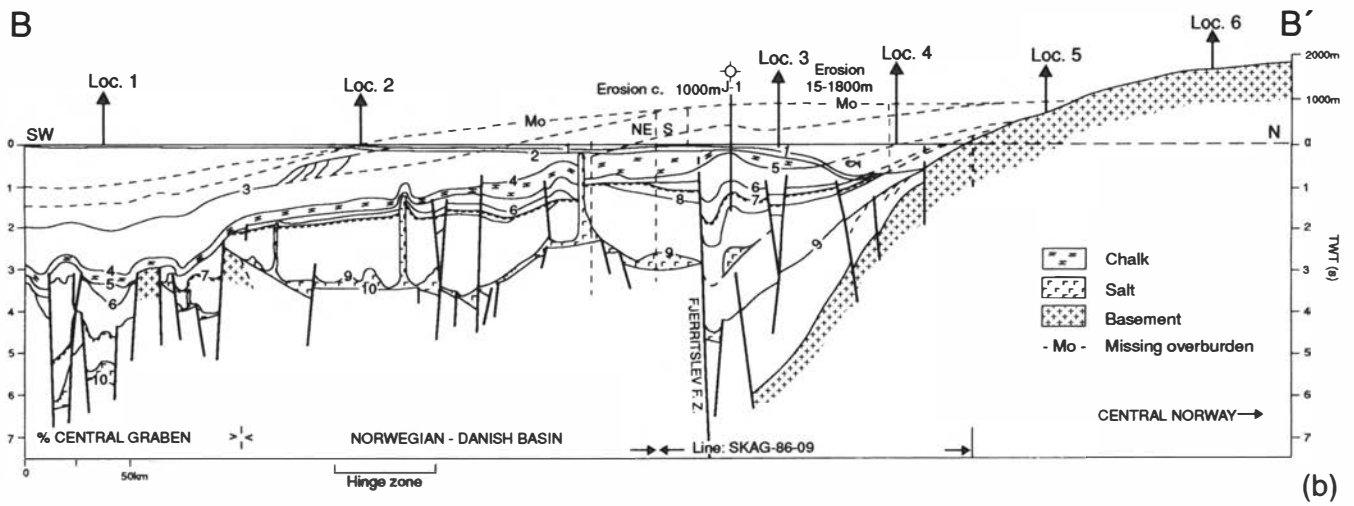

Fig. 3. (a) The location of the regional profile across the central North Sea and southern Norway. The subsidence history at six locations along this profile is also shown. (b) A regional profile across the central North Sea and southern Norway. The six locations shown as subsidence diagrams (Fig. 3a) are indicated. Reflectors: 1 – Sea bed, 2 – Base Quaternary, 3 – Base Neogene, 4 – Base Tertiary, 5 – Base Chalk, 6 – Base Cretaceous, 7 – Middle Jurassic unconformity, 8 – Base Jurassic, 9 – Base Triassic, 10 – Top Pre-Zechstein, Depth in two-way travel time, height in meters.

and Tertiary subsidence/uplift history of six locations along the profile are shown in Fig. 3a.

Manuscript received February 1992

References

Brown, R. W. 1991: Backstacking apatite fission-track 'stratigraphy': a method for resolving the erosional and isostatic rebound components of tectonic uplift histories. *Geology 19*, 74–77.

Doré, A. G. 1992: The Base Tertiary Surface of southern Norway and the northern North Sea. *Norsk Geologisk Tidsskrift 72.* This volume, pp. 259–265.

Eidvin, T. & Riis, F. 1989: Nye dateringer av de tre vestligste borehullene i Barentshavet. Resultater og konsekvenser for den tertiære hevingen. *Norwegian Petroleum Directorate Contribution No. 27*, 43 pp.

England, P. & Molnar, P. 1990: Surface uplift, uplift of rocks, and exhumation of rocks. *Geology 18*, 1173–1177.

Fjeldskaar, W. 1989: Rapid eustatic changes – never globally uniform. *In* Collison, J. D. (ed.): *Correlation in Hydrocarbon Exploration*, 13–19. Norwegian Petroleum Society. Graham & Trotman.

Forbes, P. L., Ungerer, P. M., Kuhfuss, A. B., Riis, F. & Eggen, S. 1991: Compositional modelling of petroleum generation and expulsion: trial application to a local mass balance in the Smørbukk Sør Field, Haltenbanken area, Norway. *American Association of Petroleum Geologists Bulletin*, 873–893.

Gabrielsen, R. H., Færseth, R. B., Jensen, L. N., Kalheim, J. E. & Riis, F. 1990: Structural elements of the Norwegian continental shelf. Part I: The Barents Sea Region. *Norwegian Petroleum Directorate Bulletin 6*, 33 pp.

Jensen, L. N. & Schmidt, B. J. 1992: Late Tertiary uplift and erosion in the Skagerrak area: magnitude and consequences. *Norsk Geologisk Tidsskrift 72.* This volume, pp. 275–279.

Jensen, L. N. & Schmidt, B. J.: Neogene uplift and erosion in the northeastern North Sea; magnitude and consequences for hydrocarbon exploration in the Farsund Basin. *In* Spencer, A. M. (ed.): *Generation, Accumulation and Production of Europe's Hydrocarbons III. Special Publication E.A.P.G. No. 3.* Springer Verlag (in press).

Magara, K. 1976: Thickness of removed sedimentary rocks, paleopore pressure and paleotemperature, southwestern part of Western Canada Basin. *American Association of Petroleum Geologists Bulletin 60*, 554–565.

Molnar, P. & England, P. 1990: Late Cenozoic uplift of mountain ranges and global climate change: chicken or egg? *Nature 346*, 29–34.

Nyland, B., Jensen, L. N., Skagen, J., Skarpnes, O. & Vorren, T. 1992: Tertiary uplift and erosion in the Barents Sea; magnitude, timing and consequences. *In* Larsen R. M. et al. (eds.): *Structural and Tectonic Modelling and Its Application to Petroleum Geology*. Norwegian Petroleum Society. Elsevier (in press).

Nøttvedt, A., Berglund, T., Rasmussen, E. & Steel, R. 1988: Some aspects of Tertiary tectonics and sediments along the western Barents Shelf. *In* Morton, A. C. & Parson, L. M. (eds.): Early Tertiary volcanism and the opening of the NE Atlantic. *Geol. Soc. Spec. Publ. 39*, 421–425.

Riis, F. & Fjeldskaar, W. 1992: On the magnitude of the Late Tertiary and Quaternary erosion and its significance for the uplift of Scandinavia and the Barents Sea. *In* Larsen, R. M. et al. (eds.): *Structural and Tectonic Modelling and Its Application to Petroleum Geology*. Norwegian Petroleum Society, Elsevier (in press).

Sclater, J. G. & Christie, P. A. F. 1980: Continental stretching: an explanation of the Post-Mid-Cretaceous subsidence of the central North Sea Basin. *J. Geophys Res 85, No. B7*, 3711–3739.

Sigmond, E. M. 1992: Berggrunnskart over Norge og kontinentalsokkelen. 1:3 000 000. Norges geologiske undersøkelse.

Vorren, T. O., Richardsen, G., Knutsen, S. M. & Henriksen, E. 1990: The western Barents Sea during the Cenozoic. *In* Bleil, U. & Thiede, J. (eds.): *Geologic History of the Polar Oceans: Arctic versus Antarctic*, 95–118. NATO ASI Series, Kluwer.

Intraplate stresses and the post-Cretaceous uplift and subsidence in northern Atlantic basins

SIERD CLOETINGH, PAUL REEMST, HENK KOOI & STEIN FANAVOLL

Cloetingh, S., Reemst, P., Kooi, H. & Fanavoll, S.: Intraplate stresses and the post-Cretaceous uplift and subsidence in northern Atlantic basins. *Norsk Geologisk Tidsskrift*, Vol. 72, pp. 229–235. Oslo 1992. ISSN 0029-196X.

Subsidence curves of basins around the northern Atlantic show an acceleration of subsidence during the late Neogene deviating from predictions of stretching models of basin formation. Results from quantitative stratigraphic modelling of the Barents Sea demonstrate that an increase in compressive intraplate stress can explain the observed subsidence pattern. At the same time, uplift of rift flanks adjacent to the basins occurs. Stress-induced tectonic uplift of rift flanks could be an important factor in the initiation of glaciations during the late Neogene, augmenting the post-glacial rebound of Scandinavia. Contributions by intraplate stresses to the post-Cretaceous uplift and subsidence history of the Norwegian margin are important in view of implications for the reservoir properties and the depth of hydrocarbon windows.

S. Cloetingh, P. Reemst & H. Kooi, Institute of Earth Sciences, Vrije Universiteit, De Boelelaan 1085, 1081 HV Amsterdam, The Netherlands; S. Fanavoll, IKU – Continental Shelf and Petroleum Technology Research Institute, N-7034, Trondheim, Norway.

The post-Cretaceous uplift of onshore regions around the northern Atlantic is accompanied by phases of subsidence in adjacent rifted basins, as documented by quantitative subsidence analysis (Cloetingh et al. 1990; Kooi et al. 1991). The observed acceleration in tectonic subsidence comes after a phase of general quiescence in subsidence and deviates from predictions of stretching models (McKenzie 1978) characterized by a decay of subsidence with time after Mesozoic–Tertiary basin formation. Temporal fluctuations in stress caused by changes in plate tectonic regime (Philip 1987) have a strong effect on the record of vertical motions in sedimentary basins (Cloetingh et al. 1985, 1989; Cloetingh 1988), yielding displacement rates well in excess of values associated with thermal subsidence.

The observed patterns of anomalous subsidence can, therefore, be explained by an increase in the level of intraplate compression in the Atlantic region associated with the dynamics of African/Eurasian collision processes and a reorganization of spreading directions in the Atlantic, possibly reflecting a plate reorganization of global nature (Cloetingh et al. 1990). Stress-induced topography in the onshore parts of the Norwegian continental margin, coupled with the stress-induced subsidence in the offshore, deeper parts of the margin basins, has probably also contributed to recent phases of uplift in Scandinavia, augmenting the uplift induced by glacial unloading (Fig. 1). This can affect estimates of ice thicknesses which are directly inferred from the observed uplift ignoring other driving mechanisms. Topography plays a crucial role in the dynamics of (de)glaciation (Van der Veen 1987) and it is also for this reason important to quantify the interplay of rapid tectonic phases of uplift and subsidence with external agents in Plio-Quaternary times.

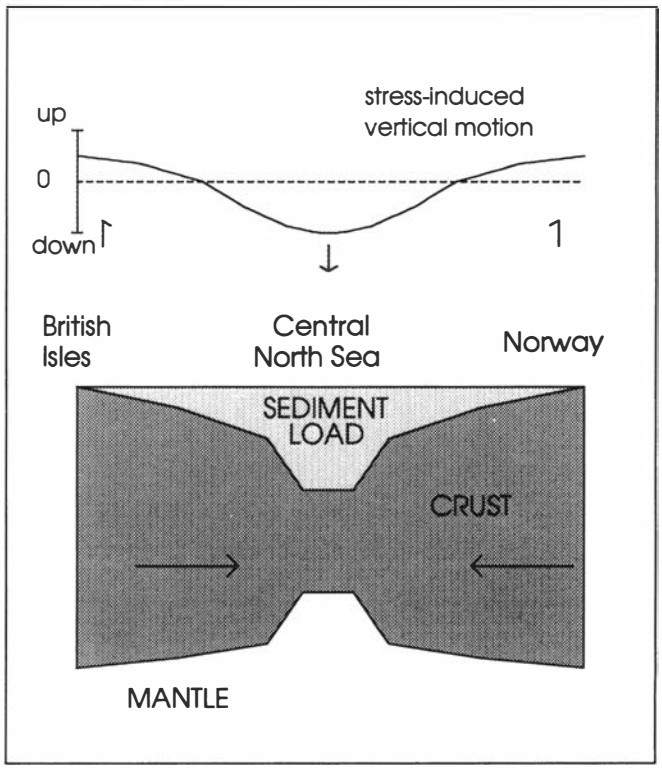

Fig. 1. Cartoon illustrating the spatial relationship between stress-induced downbending resulting in an acceleration in late Neogene subsidence in the Central North Sea and stress-induced uplift of the British Isles and onshore Norway.

In this paper, we discuss the post-Cretaceous uplift of the Norwegian continental margin in the context of the observed record of vertical motions in a number of rifted basins in the Atlantic region. This is followed by a discussion of results of stratigraphic modelling along a cross section in the Barents Sea. Subsequently, we discuss

the interplay of stress-induced changes in uplift and subsidence patterns with the dynamics of Plio-Quaternary (de)glaciation.

Plio-Quaternary subsidence in the northern Atlantic

Evidence is accumulating for particularly strong deviations from the subsidence patterns predicted by thermal models for rifted basins in the northern Atlantic region (locations given in Fig. 2) in late Neogene times (Tørudbakken & Gabrielsen 1987; Ziegler 1988, 1990; Cloetingh et. 1990; Kooi et al. 1991). Figure 3 shows a panel with curves of tectonic subsidence of these basins obtained from quantitative subsidence analysis. Previous modelling studies (Cloetingh et al. 1990; Kooi et al. 1991) of the North Sea Basin have shown that maximum estimates of paleobathymetry inferred from study of faunal assemblages cannot account for the basin subsidence, demonstrating the tectonic nature of the observed acceleration, with rates up to 0.1 cm/year. An explanation for the rapid late Neogene accelerations in basin subsidence in terms of an increased level of intraplate compression is more likely than a phase of renewed stretching, as the present-day stress field in NW Europe and the northern Atlantic is compressional in character (Zoback 1992; Spann et al. 1991). The acceleration in subsidence in the North Sea is expressed in up to 1 km thick sedimentary Plio-Quaternary wedges documented by Cameron et al. (1987). As pointed out by these authors, some of the major faults in the southern North Sea basin have been active during Pleistocene times, leading locally to displacements of the base Quaternary by more than 100 m.

A reorganization of spreading directions and rates occurred at 2.5 Ma along the entire Atlantic spreading center (Klitgord & Schouten 1986). Important tectonic phases during late Neogene times also occurred on the western side of the Atlantic Ocean. A climax in compressional tectonics in the Artic of northern Alaska and northern Canada occurred at about 6 Ma, possibly connected with the formation of an incipient convergent plate boundary (Hubbard et al. 1987). Episodicity in plate motions and associated coupled changes in the Pacific and Atlantic plates in the Upper Miocene (9 Ma) and Pliocene (4 Ma) have been documented in great detail by Pollitz (1988).

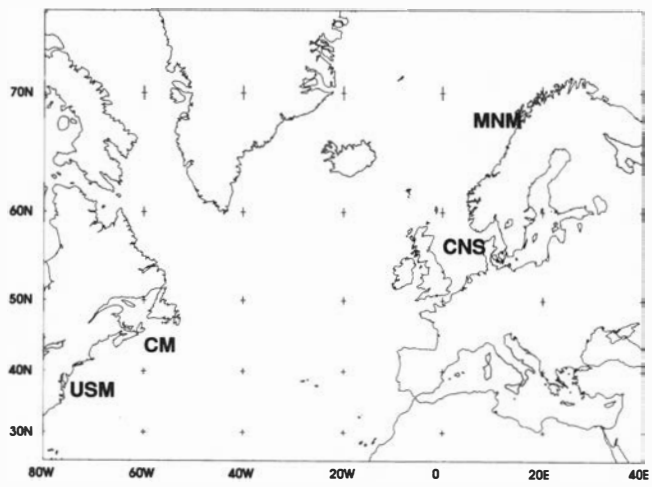

Fig. 2. Location map showing areas in the northern Atlantic with distinct phases of rapid acceleration in tectonic subsidence during late Neogene times. CNS, MNM, CM, USM indicate the Central North Sea, Mid-Norway margin, Eastern Canadian margin, Eastern US margin, respectively.

Stratigraphic modelling of the Barents Sea

We have carried out stratigraphic modelling along three deep seismic lines (Gudlaugsson et al. 1987) in a NW–SE direction across the Barents Sea (see Fig. 4 for the location) to test the predictions of the subsidence analysis of rifted basins discussed above. In this paper we limit ourselves to a discussion of the results of the stratigraphic modelling of one of these lines (IKU-84-C). Constraints on the timing of tectonic phases of the area are provided by a large number of studies on the geologic evolution of the Barents Sea (e.g. Rønnevik & Jacobsen 1984; Faleide et al. 1984; Riis et al. 1986; Eldholm et al. 1987). Based on these investigations, we have incorporated the following four periods of rifting in our forward modelling using the Harland (1990) time scale: Devonian–Carboniferous (375–325) Ma), Triassic (245–241 Ma), Jurassic–Cretaceous (157–97 Ma), and Paleocene–Eocene (60–50 Ma). Following earlier work (Wood 1989; Roufosse 1987), we have incorporated the stretching formulation (McKenzie 1978) in the subsidence modelling. Our work differs from the previous modelling studies by incorporating multiple stretching phases of finite duration (Jarvis & McKenzie 1980) as well as changing intraplate stress fields and necking of the lithosphere. The model parameters used are shown in Table 1. A paleo-waterdepth profile based on faunal assemblages is incorporated for each stratigraphic horizon. Compaction of sediments is incorporated in the forward model using a standard porosity-depth relation

Table 1. Parameters used in the forward modelling of basin stratigraphy.

Parameter	Symbol	Value
Initial lithospheric thickness	L	120 km
Initial crustal thickness	C	32.1 km
Coefficient of thermal expansion	α	3.4×10^{-5}°C^{-1}
Asthenospheric temperature	T_m	1333°C
Thermal diffusivity	κ	0.008 cm^{2}s^{-1}
Mantle density	ρ_m	3.33 gcm^{-3}
Crustal density	ρ_c	2.8 gcm^{-3}
Isotherm describing EET	T_e	300°C
Water density	ρ_w	1.03 gcm^{-3}
Surface porosity of sediment infill	$\phi(0)$	0.55
Characteristic depth constant	c	0.55 km^{-1}

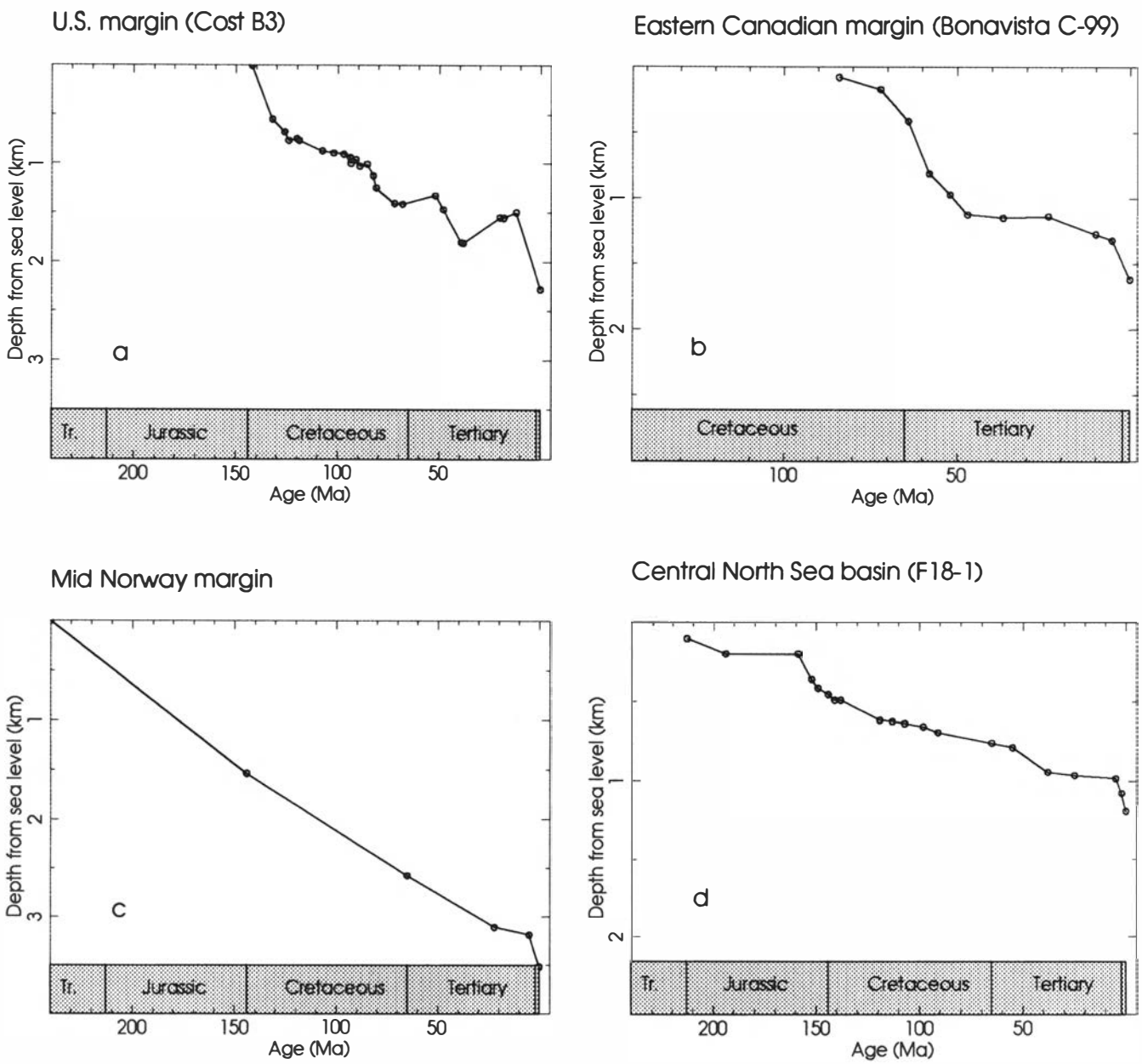

Fig. 3. Deviations from thermal patterns of subsidence observed for a number of rifted basins in the northern Atlantic region. (a) Eastern US continental margin (after Heller et al. 1982), (b) Eastern margin of Canada (after Cloetingh et al. 1990), (c) Mid-Norway margin (after Pedersen & Skogseid 1989), (d) Central North Sea basin (after Kooi et al. 1992).

$\phi(z) = 0.55e^{-0.55z}$ for all sediments at the margin. Depth-dependent stretching (Royden & Keen 1980) and lithospheric necking using regional isostasy (Kooi et al. 1992) is required to produce the characteristic block basin shape of the Barents Sea margin during rifting. Lithospheric flexure is taken into account in the analysis adopting a 300°C isotherm describing the equivalent elastic thickness (EET). The locus of maximum stretching, during subsequent periods of rifting, migrates from the southeast to the northwest. The maximum stretching factors are 1.20 in the Hammerfest Basin (Devonian–Carboniferous extension), 1.15 in the Hammerfest Basin (Triassic extension), 2.30 in the Tromsø Basin (Jurassic–Cretaceous extension), and 2.30 in the Sørvestsnaget Basin (Paleocene–Eocene extension). The distribution of the cumulative stretching factors is shown in Fig. 5.

The Tertiary and Quaternary development of the Barents Sea has been extensively studied by Spencer et al. (1984), Eidvin & Riis (1989) and Vorren et al. (1990). As elsewhere around the northern Atlantic, a rapid phase of uplift occurs in the Barents Sea simultaneously with the development of thick Plio-Quaternary sediment wedges more oceanward. Different estimates for the magnitude of the uplift inferred from a wide range of techniques, including vitrinite reflectance, fission tracks, shale compaction and diagenesis of clay minerals, extrapolation of seismic sequence geometries and volumetric mass balance between eroded and deposited sediments (Nyland et al.

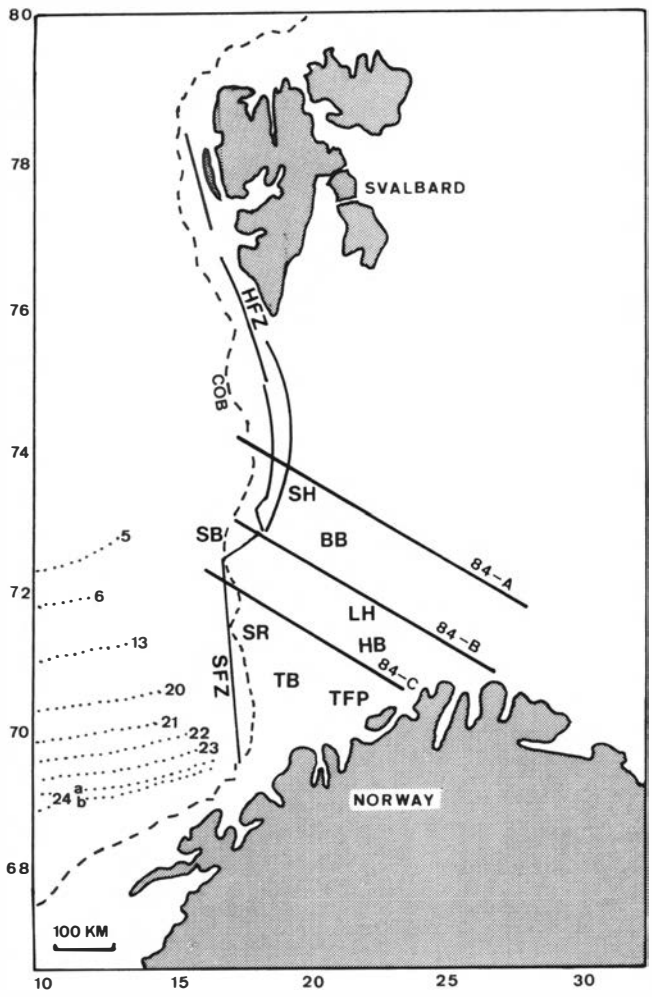

1992; Riis & Fjeldskaar 1992), range from the order of 500 to 2000 m (Lippard et al. 1990). Maximum estimates of 500 to 1000 m of this amount can be contributed to glacial processes (Cogan & Lerche 1990; Sættem et al. in press), suggesting a dominantly tectonic control.

For the Tertiary part of the subsidence record on the platform three major phases of uplift and/or erosion can be identified. The first period of uplift corresponds to the timing of break-up during the earliest Eocene of the Norwegian–Greenland Sea resulting in flank uplift, probably in response to necking of the lithosphere (Kooi et al. 1992), and coincides with the timing of the Eurekan orogeny on Svalbard (Steel et al. 1985). The second period of uplift and erosion coincides with a major plate reorganization in the Oligocene and a widely recognized major fall in sea level (Haq et al. 1987). As shown by Fig. 5, the most recent phase of uplift can be explained by an increase in the level of intraplate compression, which is also consistent with the rapid phase of subsidence and associated thickening of the Pliocene–Quaternary wedge more oceanward in the Sørvestsnaget Basin. A late Neogene increase in compressive intraplate forces perpendicular to the margin which starts at 15 Ma and

Fig. 4. Location map showning position of three seismic lines used for our stratigraphic modelling project of the Barents Sea margin. SH = Stappen High, SB = Sørvestsnaget Basin, BB = Bjørnøya Basin, SR = Senja Ridge, TB = Tromsø Basin, LH = Loppa High, HB = Hammerfest Basin, TFP = Tromsø Finnmark Platform, HFZ = Hornsund Fault Zone, SFZ = Senja Fracture Zone, COB = Continent-ocean boundary, dotted lines are magnetic lineations.

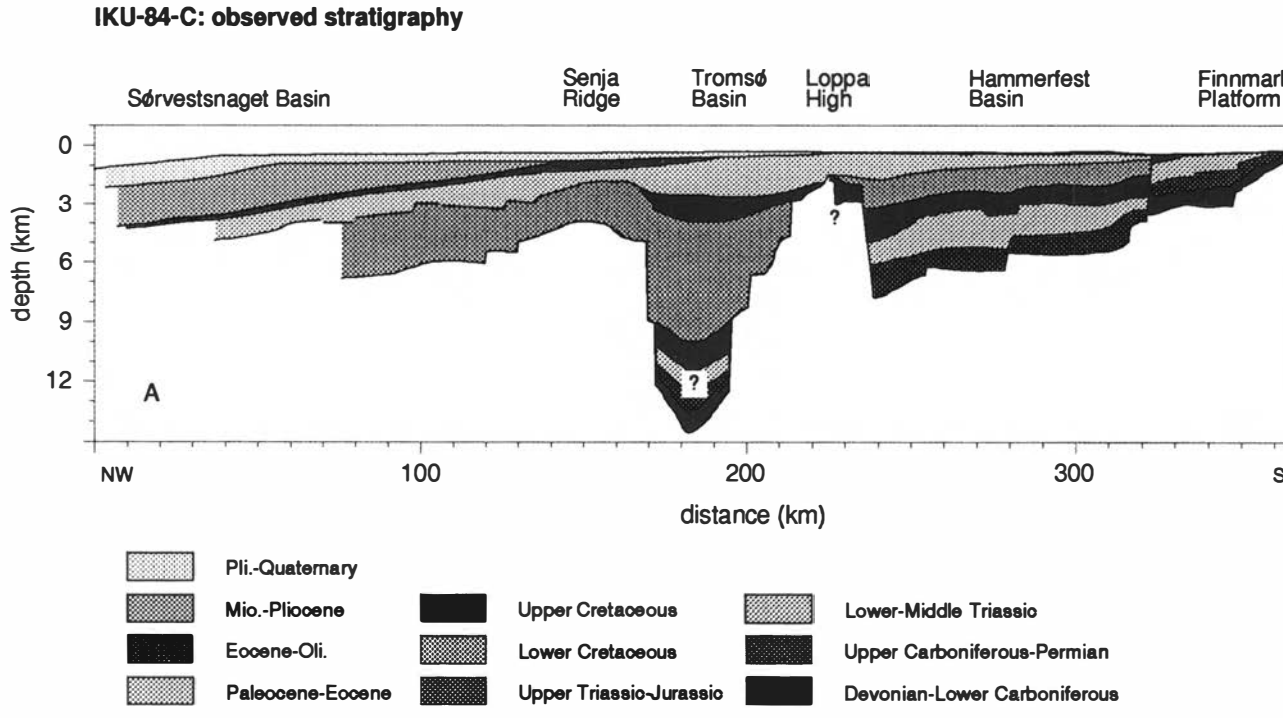

Fig. 5. (a) Observed Barents Sea margin stratigraphy along line IKU-84-C (location given in Fig. 4) and ages of stratigraphic units. (b) Modelled Barents Sea stratigraphy for fluctuating stress regime incorporating a Plio-Quaternary increase in compression. (c) Stratigraphy modelled in the absence of a fluctuating stress field. (d) Distribution of cumulative crustal and subcrustal extension factors α and β during each period of rifting.

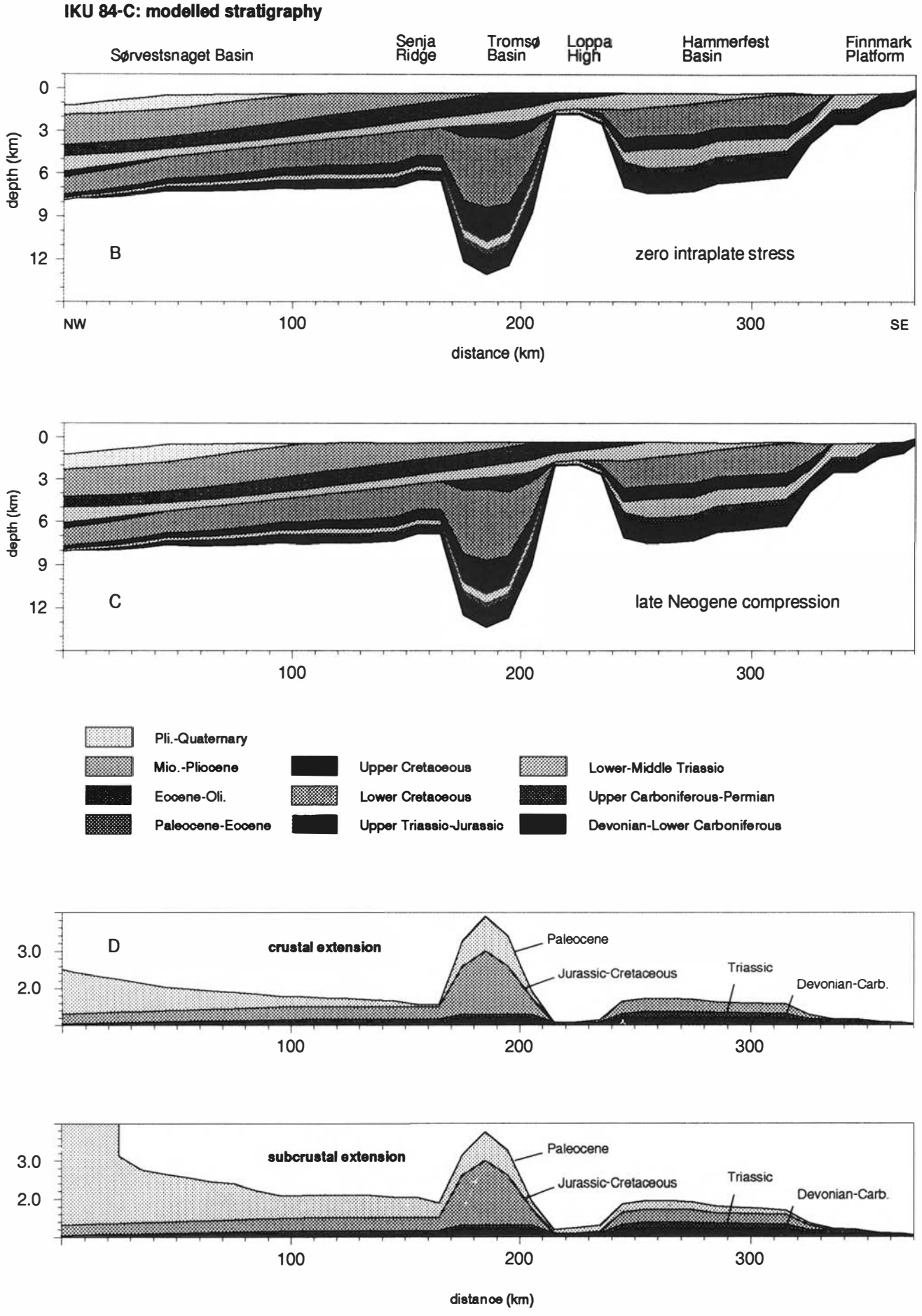
IKU 84-C: modelled stratigraphy
Sørvestsnaget Basin
Senja Ridge
Tromsø Basin
Loppa High
Hammerfest Basin
Finnmark Platform
depth (km)
0
3
6
9
12
B
zero intraplate stress
NW
100
200
300
SE
distance (km)
C
late Neogene compression
Pli.-Quaternary
Mio.-Pliocene
Eocene-Oli.
Paleocene-Eocene
Upper Cretaceous
Lower Cretaceous
Upper Triassic-Jurassic
Lower-Middle Triassic
Upper Carboniferous-Permian
Devonian-Lower Carboniferous
D
crustal extension
Paleocene
Jurassic-Cretaceous
Triassic
Devonian-Carb.
3.0
2.0
subcrustal extension
distance (km)

reaches a level of $15 \times 10^{12}\ Nm^{-1}$ (equivalent to a stress of 5 kbar in a 30 km thick elastic plate) at 5 Ma continuing to the present is required to induce the observed acceleration in tectonic subsidence. This value should be considered as an overestimate, as the incorporation of depth-dependent rheological properties significantly reduces the stress levels inferred from models adopting an elastic plate (Cloetingh et al. 1989). Previous stratigraphic modelling (Cloetingh et al. 1990) has shown that the presence of thick Plio-Quaternary sedimentary wedges along the eastern Canadian continental margin is also consistent with a similar increase in the level of compression.

Interplay of tectonics and (de)glaciation

The onset of the rapid vertical motions along the northern Atlantic continental margins is well before the first occurrence of glaciation at 5.1–5.0 Ma (Jansen et al. 1990). While the differential character of the uplift and subsidence at different positions within the rifted basins around the northern Atlantic rules out glaciation as the main cause of the late Neogene subsidence phases, it is also known that periods of increased elevation promote the development of glaciation (e.g. Raymo 1991; Stuevold 1989). Mapping of the Base Tertiary horizons for profiles perpendicular to the Norwegian continental margin has demonstrated a flexural shape of the lithospheric deflection, with a coupling of offshore subsidence and onshore uplift (Doré 1992). The wavelength of the observed deflection is consistent with flexure induced by sediment loading (Cloetingh et al. 1982), while the observed amplitude of the vertical deflection points to an amplification by intraplate compression. The present-day stress field off the Norwegian margin has been investigated using borehole break-out techniques (Spann et al. 1991) and is characterized by the existence of a significant component of compression perpendicular to the margin.

The northern Atlantic and the Arctic have been the site of a relatively high level of tectonic activity in Late Cenozoic times, while recent studies of neotectonics and seismicity (Karpuz et al. 1991; Stein et al. 1989) also demonstrates a high level of intraplate deformation for the Norwegian 'passive' continental margin. Although, unloading of Scandinavia and associated glacial erosion provide an important contribution to the vertical motions in the Barents Sea and Norwegian margin, another mechanism is required to generate the observed thickness of offshore Plio-Quaternary sedimentary wedges and to explain the magnitude of the inferred inner margin erosion. As stated by Ruddiman (1991), tectonic induced uplift of the Rocky Mountains and Himalayan plateaus affects the climate, resulting in global cooling and glaciations. This far field, uplift induced cooling could be reinforced by local uplift along the northern Atlantic itself.

In addition to the stress-induced topography created during the late-stage phase of rift basin evolution, flank uplift due to necking of the lithosphere during the early stages of basin formation has played an important role in some Antarctic and Arctic basins. This process has, for example, controlled the formation of the Transantarctic Mountains (Fitzgerald et al. 1987) in Tertiary times, while seismic profiling of sedimentary sequences in the Ross Sea embayment (Bartek et al. 1991) demonstrates phases of tilting and associated truncation of Paleogene and Neogene strata at the inner parts of the continental margin during late Neogene times. Similarly, necking of the lithosphere in association with Tertiary rifting of the Norwegian Greenland Sea has probably contributed to the formation of steep rift flanks in the Svalbard area.

Tectonically induced post-Cretaceous vertical motions along northern Atlantic margins have a number of obvious consequences for hydrocarbon exploration. For example, stress-induced flank uplift of basins has an important effect on the dynamics of fluid flow, salt diapirism, faulting and fracturation affecting reservoir properties (Cloetingh & Kooi 1992), while the associated accelerations in subsidence in deeper parts of rifted basins are relevant for estimates of the depths of hydrocarbon windows (Kooi & Cloetingh 1989).

Acknowledgements. – Statoil and Saga Petroleum generously provided support and data for the modelling of the Barents Sea margin. Valuable discussions with Dr B. T. Larsen, Dr D. Worsley, Dr A. Mørk, Professor O. Eldholm and Professor R. Gabrielsen are acknowledged.

Manuscript received October 1991

References

Bartek, L. R., Vail, P. R., Anderson, J. B., Emmet, P. A. & Wu, S. 1991: Effect of Cenozoic ice sheet fluctuations in Antarctica on the stratigraphic signature of the Neogene. *Journal of Geophysical Research 96*, 6753–6778.

Cameron, T. D. J., Stoker, M. S. & Long, D. 1987: The history of Quaternary sedimentation in the UK sector of the North Sea basin. *Journal of the Geological Society of London 144*, 43–58.

Cloetingh, S. 1986: Intraplate stresses: a new tectonic mechanism for the fluctuations of relative sea level. *Geology 14*, 617–620.

Cloetingh, S. 1988: Intraplate stresses: A new element in basin analysis. *In* Kleinspehn, K. L. & Paola, C. (eds.): *New Perspectives in Basin Analysis*, 205–230. Springer-Verlag, New York.

Cloetingh, S., Kooi, H. & Groenewoud, W. 1989: Intraplate stresses and sedimentary basin evolution. *American Geophysical Union, Geophysical Monograph 48*, 1–16.

Cloetingh, S., Gradstein, F., Kooi, H., Grant, A. C. & Kaminski, M. 1990: Did plate reorganisation cause rapid late Neogene subsidence around the Atlantic? *Journal of the Geological Society of London 147*, 495–506.

Cloetingh, S. & Kooi, H. 1992: Intraplate stresses and dynamical aspects of rift basins. *Tectonophysics*, in press.

Cloetingh, S., McQueen, H. & Lambeck, K. 1985: On a tectonic mechanism for regional sea level variations. *Earth and Planetary Science Letters 75*, 157–166.

Cloetingh, S., Wortel, M. J. R. & Vlaar, N. J. 1982: Evolution of passive continental margins and initiation of subduction zones. *Nature 297*, 139–132.

Cogan, J. & Lerche, I. 1990: Flexural plate dynamics of Barents Sea, northern Norway and impact of Quaternary ice loading. *In* Arctic Geology and Petroleum Potential, Tromsø, Norway, 15–17 August, abstracts.

Doré, A. G. 1992: The Base Tertiary surface of Southern Norway and the northern North Sea. *In* Jensen, L. N. & Riis, F. (eds.): Post-Cretaceous uplift and sedimentation along the western Fennoscandian Shield. *Norsk Geologisk Tidsskrift*. This volume, pp. 259–265.

Eidvin, T. & Riis, F. 1989: Nye dateringer av de tre vestligste borehullene i Barentshavet. Resultater og konsekvenser for den Tertiære hevning. *NPD contribution 27*, Norwegian Petroleum Directorate, Harstad, 44 pp.

Eldholm, O., Faleide, J. L. & Myhre, A. M. 1987: Continent-ocean transition at the western Barents Sea/Svalbard continental margin. *Geology 15*, 1118–1122.

Faleide, J. I., Gudlaugsson, S. T. & Jacquart, G. 1984: Evolution of the western Barents Sea. *Marine and Petroleum Geology 1*, 123–150.

Fitzgerald, P. G., Sandiford, M., Barrett, P. J. & Gleadow, A. J. W. 1987: Asymmetric extension associated with uplift and subsidene in the Transantarctic Mountains and Ross Sea Embayment. *Earth and Planetary Science Letters 81*, 67–78.

Gudlaugsson, S. T., Faleide, J. I., Fanavoll, S. & Johansen, B. 1987: Deep seismic reflection profiles across the western Barents Sea. *Geophysical Journal of the Royal Astronomical Society 89*, 273–278.

Haq, B., Hardenbol, J. & Vail, P. R. 1987: Chronology of fluctuating sea level since the Triassic (250 million years to present). *Science 235*, 1156–1167.

Harland, W. B. 1990: *A Geologic Time Scale* 1989. Cambridge University Press, Cambridge.

Heller, P. L., Wentworth, C. M. & Poag, C. W. 1982: Episodic post-rift subsidence of the United States Atlantic continental margin. *Geological Society of America Bulletin 93*, 379–390.

Hubbard, R. J., Edrich, S. P. & Rattey, R. P. 1987: The geological evolution and hydrocarbon habitat of the Arctic Alaska microplate. *Marine and Petroleum Geology 4*, 2–32.

Jansen, E., Sjøholm, J., Bleil, U. & Erichsen, J. A. 1990: Neogene and Pleistocene glaciations in the Northern Hemisphere and Late Miocene–Pliocene global ice volume fluctuations: evidence from the Norwegian Sea. *In* Bleil, U. & Thiede, J. (eds.): *Geological History of the Polar Oceans: Arctic versus Antarctic*, 677–705. Kluwer, Dordrecht.

Jarvis, G. T. & McKenzie, D. P. 1980: Sedimentary basin formation with finite extension rates. *Earth and Planetary Science Letters 48*, 42–52.

Karpuz, M. R., Gabrielsen, R. H., Engell-Sorensen, L. & Anundsen, K. 1991: Seismotectonic significance of the January 29, 1989 Etne Earthquake, southwest Norway. *Terra Nova 3(5)*, 540–549.

Klitgord, K. D. & Schouten, H. 1986: Plate kinematics and the Central Atlantic. *In* Vogt, P. R. & Tucholke, B. E. (eds.): *The Geology of North America, vol. M., The Western North Atlantic Region*, 351–378. Geological Society of America.

Kooi, H. & Cloetingh, S. 1989: Some consequences of late-stage compression for extensional models of basin evolution. *Geologische Rundschau 78*, 183–195.

Kooi, H., Hettema, M. & Cloetingh, S. 1991: Lithospheric dynamics and the rapid Pliocene/Quaternary subsidence phase in the southern North Sea basin. *Tectonophysics 192*, 245–259.

Kooi, H. Burrus, J. & Cloetingh, S. 1992: Lithospheric necking and regional isostasy at extensional basins: part 1, subsidence and gravity modeling with an application to the Gulf of Lions margin (SE France). *Journal of Geophysical Research*, submitted.

Lippard, S. J., Liu Guojiang, Fanavoll, S., Doré, A. G., Skjervoy, S. & Vassmyr, S. 1990: Quantitative geodynamic modelling of Tertiary uplift in the Barents Sea and its significance for Fennoscandian/North Atlantic marginal uplift. *In* Arctic Geology and Petroleum Potential, Tromsø Norway, 15–17 August, abstracts.

McKenzie, D. P. 1978: Some remarks on the development of sedimentary basins. *Earth and Planetary Science Letters 40*, 25–32.

Nyland, B., Jensen, L. N., Skagen, J. I., Skarpnes, O, & Vorren, T. 1992: Tertiary uplift and erosion in the Barents Sea; magnitude, timing and consequences. *In* Larsen, R. M. & Parson, L. M. (eds.): *Structural and Tectonic Modelling and its Application to Petroleum Geology*. Norwegian Petroleum Society, Elsevier, Amsterdam, in press.

Pedersen, T. & Skogseid, J. 1989: Vøring Plateau volcanic margin: extension, melting and uplift, *In* Eldholm, O., Thiede, J., Taylor, et al. *Proceedings ODP, Scientific Results, 104: College Station, TX (Ocean Drilling Program)*, 985–991.

Philip, H. 1987: Plio-Quaternary evolution of the stress field in Mediterranean zones of subduction and collision. *Annales Geophysicae 5B*, 301–320.

Pollitz, F. F. 1988: Episodic North America and Pacific plate motions. *Tectonics 7*, 711–726.

Raymo, M. E. 1991: Geochemical evidence supporting T. C. Chamberlin's theory of glaciation. *Geology 19*, 344–347.

Riis, F. & Fjeldskaar, W. 1992: The importance of erosion and mantle phase changes for the Late Tertiary uplift of Scandinavia and the Barents Sea. *In* Larsen, R. M. & Parson L. M. (eds.): *Structural and Tectonic Modelling and its Application to Petroleum Geology*. Norwegian Petroleum Society, Elsevier, Amsterdam, in press.

Riis, F., Vollset, J. & Sand, M. 1986: Tectonic development of the western margin of the Barents Sea and adjacent areas. *American Association of Petroleum Geologists Memoir, 40*, 661–676.

Rønnevik, H. & Jacobsen, H. P. 1984: Structural highs and basins in the western Barents Sea. *In* Spencer, A. M. et al. (eds.): *Petroleum Geology of the North European Margin*, 19–32. Norwegian Petroleum Society, Graham & Trotman, London.

Roufosse, M. C. 1987: The formation and evolution of sedimentary basins in the Western Barents Sea. *In* Brooks, J. & Glennie, K. (eds.): *Petroleum Geology of North West Europe*, 1149–1161. Graham & Trotman, London.

Royden, L. & Keen, C. E. 1980: Rifting processes and thermal evolution of the continental margin of eastern Canada determined from subsidence curves. *Earth and Planetary Science Letters 51*, 343–361.

Ruddiman, W. F. 1991: Notes on long-term forcing of Arctic climate. *Norsk Geologisk Tidsskrift 71*, 167–168.

Spann, H., Brudey, A. & Fuchs, K. 1991: Stress evaluation in offshore regions of Norway. *Terra Nova 3*, 148–152.

Spencer, A. M., Home, P. C. & Berglund, L. T. 1984: Tertiary structural development of the western Barents Shelf: Troms to Svalbard. *In* Spencer, A. M. et al. (eds.): *Petroleum Geology of the North European Margin*, 199–209. Graham & Trotman, London.

Steel, R., Gjelberg, J., Nøtvedt, A., Helland-Hansen, W., Kleinspehn, K. & Rye-Larsen, M. 1985: The Tertiary strike-slip basins and orogenic belt of Spitsbergen. *Society of Economic Paleontologists and Mineralogists Special Publication 37*, 339–360.

Stein, S., Cloetingh, S., Sleep, N. H. & Wortel, R. 1989: Passive margin earthquakes, stresses and rheology. *In* Gregersen, S. & Basham, P. (eds.): *Earthquakes at North-Atlantic Passive Margins: Neotectonics and Postglacial Rebound*, 231–259. Kluwer, Deventer.

Stuevold, L. M. 1989: Den tertiære fennoskandiske landheving i lys av vertikalbevegelser pa midtnorsk kontinentalmargin. Unpublished thesis, University of Oslo, 160 pp.

Tørudbakken, B. O. & Gabrielsen, R. 1987: Subsidence-rates versus tectonic position in grabens: an example from the Norwegian Continental Shelf. *Norsk Geologisk Tidsskrift 67*, 438 (abstract).

Van der Veen, C. J. 1987: Longitudinal stresses and basal sliding: a comparative study. *In* Van der Veen, C. J. & Oerlemans, J. (eds.): *Dynamics of the West Antarctic Ice Sheet*, 223–248, Reidel, Dordrecht.

Vorren, T. O., Richardson, G., Knutsen, S.-M. & Hendriksen, E. 1990: The western Barents Sea during the Cenozoic. *In* Bleil, U. & Thiede, J. (eds.): *Geological History of the Polar Oceans: Arctic versus Antarctic*, 95–118. Kluwer, Dordrecht.

Wood, R. J., Edrich, S. P. & Hutchison, I. 1989: Influence of North Atlantic tectonics on the large-scale uplift of Strappen High and Loppa High, Western Barents Shelf. *In* Tankard, A. J. & Balkwill, H. R. (eds.): Extensional tectonics and stratigraphy of the North Atlantic Margins. *American Association of Petroleum Geologists Memoir 46*, 559–566.

Ziegler, P. A. 1988: Evolution of the Arctic-North Atlantic and the western Tethys. *American Association of Petroleum Geologists Memoir 43*, 198 pp.

Ziegler, P. A. 1990: *Geological Atlas of Western and Central Europe*, 2nd ed., 239 pp. Shell International and Geological Society of London Publishers, London.

Zoback, M. L. 1992: First and second order patterns of stress in the lithosphere: the World Stress Map Project. *Journal of Geophysical Research*, in press.

The state of stress in the North Sea and in the offshore regions of Norway (abstract)

HOLGER SPANN

Spann, H.: The state of stress in the North Sea and in the offshore regions of Norway (abstract). *Norsk Geologisk Tidsskrift*, Vol. 72, pp. 237–238. Oslo 1992. ISSN 0029-196X.

Knowledge of the orientation and magnitude of the state of stress in offshore regions of Norway and in the North Sea has immediate implications for hydrocarbon production. Knowledge of the in situ stress field is also of importance for understanding the sources of the lithospheric stress field and the nature of intraplate processes, such as the formation of sedimentary basins or mountain ranges. To improve this knowledge on the stress field, a joint German–Norwegian project 'Determination of stress trajectories in northern Europe and the significance of stress field orientation for hydrocarbon production and local and regional tectonics' was established. The information on the stress field is derived from borehole breakout analysis, but fault plane solutions are also used in our project. The resulting stress orientations are presented on a regional map of the stress trajectories (Fig. 1). For use in the oil industry more detailed maps of local stress patterns will be compiled.

Stress directions (SH_{max}, Fig. 1) derived from borehole breakout analysis along the Norwegian coast demonstrate the influence of the plate boundaries on the global stress field. In the Central Graben a bimodal stress distribution is seen. One direction lies parallel to the strike of the graben, the other perpendicular to it (Fig. 1). To obtain a comparison with the analysed stress data, various finite element models of Europe are developed. A simple model of a local linear inclusion can probably explain the rapid changes in stress orientation. Modelling of the Central Graben indicates that the stress field is also affected locally by the structural environment. A more detailed description of the project is published by Spann et al. (1991).

Holger Spann, Geophysical Institute, University of Karlsruhe, Hertzstrasse 16, D-7500 Karlsruhe 21, Germany.

Manuscript received October 1991

Reference

Spann, H., Brudi, M. & Fuchs, K. 1990. Stress evaluation in offshore regions of Norway. *Terra Nova 3*, 148–152.

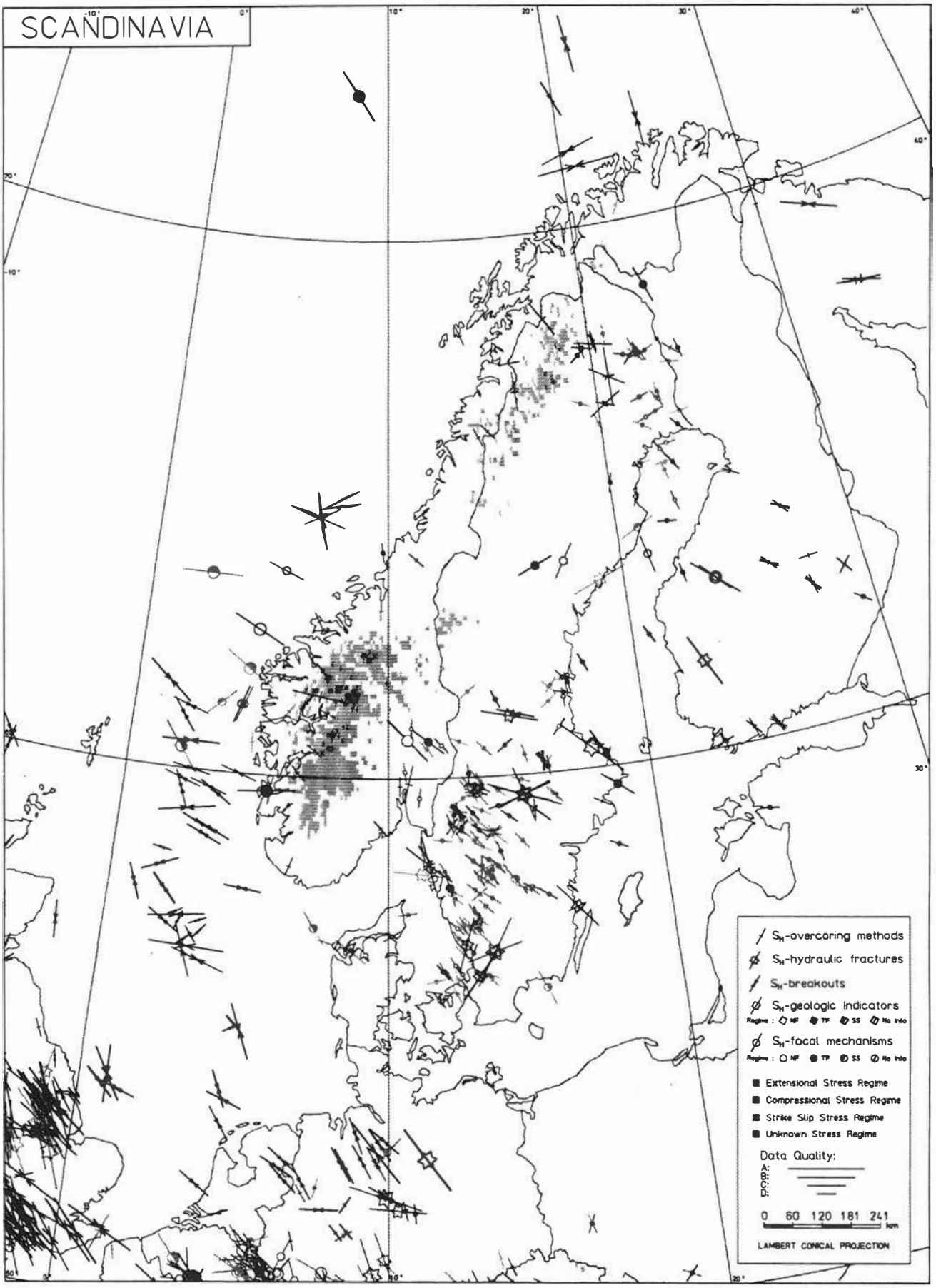

Fig. 1. SH_{max} directions from different stress measurements in northern Europe. The quality factors (A, B and C) determine the size of the stress symbol.

Mapping the rate of crustal uplift in Norway: parameters, methods and results

SIVERT BAKKELID

Bakkelid, S. Mapping the rate of crustal uplift in Norway: parameters, methods and results. *Norsk Geologisk Tidsskrift*. Vol. 72, pp. 239–246. Oslo 1992. ISSN 0029-196X.

The paper intends to show the status of our present knowledge about crustal uplift in Norway. It presents relevant data together with data acquisition methods and observed crustal uplift values, their accuracy and geographical coverage. The paper also draws attention to the present and future possibilities of increasing and improving existing data sets, and outlines future problems.

S. Bakkelid, Statens kartverk, Geodesidivisjonen, Kartverksveien, N-3500 Hønefoss, Norway.

In this paper the term 'crustal uplift' is used to refer to the rate of apparent crustal uplift or the vertical velocity of the land relative to the mean sea surface. We denote this parameter by U.

The data that can be used to determine U are of five different types: (1) Remeasurements of the height of man-made sea level indicators, (2) continuous tide-gauge records, (3) shore-level displacement curves, (4) shore-level diagrams, (5) relevelling.

Remeasurements of man-made sea level indicators

U can be and is at present determined by observation of the vertical movement of a bench mark preferably in rock, relative to the mean sea surface (Figs. 1 and 2)

$$U = V_c - V_s = \frac{d}{dt}(H_c - H_s) = \frac{d}{dt}(\Delta H)$$

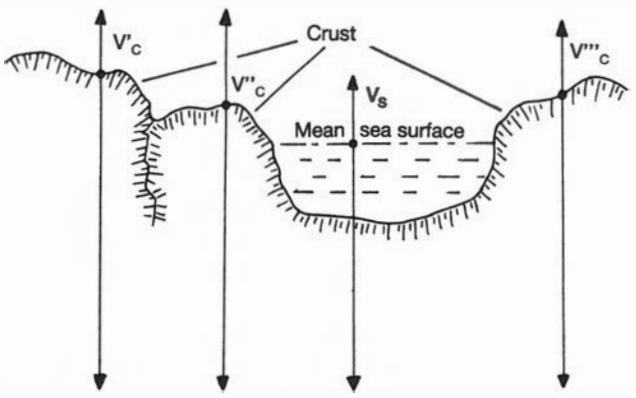

Fig. 1. Uplift parameters. H_c – Height/distance from the mass centre of the Earth (M) to crustal surface points. H_s – Height/distance from M to the surface of the sea. V_c – Vertical velocity of crustal points relative to M. V_s – Vertical velocity of sea surface relative to M.

Fig. 2. The 1839 mean sea-level mark at Kragerø.

U is defined as the change over time of the height of a mark in rock relative to mean sea level. What is measured directly, however, is the height of the mark over the instantaneous sea level. This parameter can differ significantly (several metres) in height from mean sea level and has strong, irregular, height variations over time.

This problem is overcome in different ways in the different methods used. As there is always an error (ε) left in the determination of ΔH, and because U has a very small value, we have to make the observation period long and determine U as

$$U = \frac{\Delta H_2 - \Delta H_1 + \sqrt{2}\varepsilon}{T_2 - T_1}$$

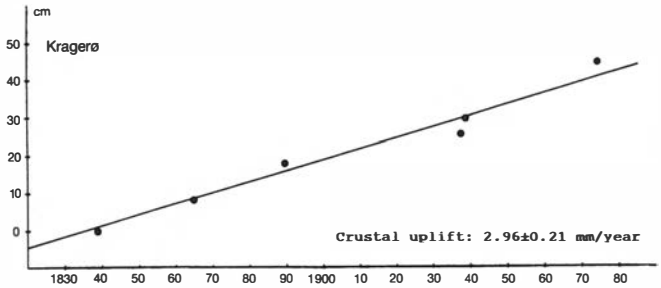

Fig. 3. U at Kragerø determined from the slope of the regression line to the observed variation over time in the height of the mean sea-level mark (Norges geografiske oppmåling).

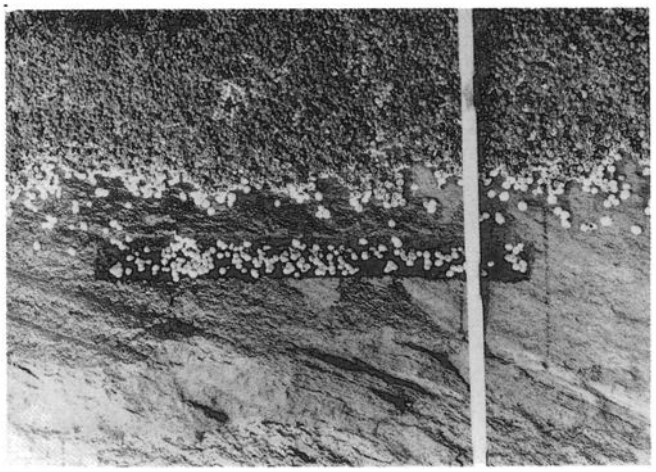

Fig. 4. Rim of acorn barnacle colonies and bladder-wrack attachments, and mark placed in 1897 at Gurihola, Havøysund photographed in August 1990.

where the indices 1 and 2 denote two observation epochs several decades apart. In doing this, however, we assume that U is constant over the observation period. This means that the present methods for determination of U only give consistent values if both V_c and V_s are constant over time.

The old sea-level marks along the coast of Norway are of two different types: (1) Mean sea-level marks, placed in 1839, in the 1840s and in the 1860s. (2) Acorn barnacle (*Balanus balanoides*) or bladder wrack (*Fucus vesiculosus*) marks placed during the period 1889–1897.

The mean sea-level marks are grooves cut into faces of steep rock at the height of mean sea level at that time, as determined from sea-level observations over a few weeks (Fig. 2). The height of the marks originally placed in 1839 relative to mean sea level have been remeasured a number of times (Fig. 3). (Tolpinrud 1989).

Considering the strong and rapid variation in the height of sea level, an unacceptable error in the value of U determined from remeasurement of the height of the old sea-level marks could be expected. Firstly because the height of the mark relative to the sea level is determined from a single or a limited number of observations of the instanteneous sea level, and secondly, because U is computed from observations of ΔH at only two epochs – when the mark was placed and when it was remeasured.

Acceptable accuracy in U can be obtained in the following ways: When U is determined from remeasurements of a mean sea-level mark, ΔH is observed at the times of highest and lowest water level when the tidal variation is at a minimum. The average of the two water levels is taken to be the sea level measured in the middle of this time period. We assume the short-periodic and small-amplitude sea-level variations at the site of the mark and at the nearest tide-gauge to be about the same. This allows us to assume that the 'anomalies' in sea level at the two sites (as defined below) are about the same. They can be determined at the site of the gauge and applied as corrections to the sea-level observations at the site of the mark.

The acorn barnacle/bladder wrack marks mostly comprise a groove cut into rock at or immediately above the upper rim of acorn barnacle colonies, or bladder wrack attachment zones. U is determined from remeasurement of the height of the groove relative to these rims.

A large number of these marks have been found and remeasured (Fig. 4).

When U is determined from remeasurement of an old acorn barnacle or bladder-wrack mark the accuracy is dependent on the time scale for the reaction in the growth of acorn barnacles and bladder wracks to variations in the height of mean sea level.

The map in Fig. 5 shows the location of sites of old sea-level marks of the two categories.

U determined from tide-gauge records

Tide-gauges record ΔH. Figure 6 shows a plot of the annual means of hourly readings. It should be remembered that the values of ΔH recorded by a gauge represent the tidal components with the high-frequency variations caused by wind and current filtered out. Nevertheless, the plot shows variations between consecutive annual means of several centimetres.

U at a tide-gauge site is determined as the slope of the straight line determined by least squares regression of the observed annual means. Continuous recordings over 50–100 years are required to determine U, giving an accuracy of 0.2–0.3 mm/year.

If we correct the observed ΔH for the influence of variations in atmospheric pressure the annual means will give a smoother graph and we will obtain the same accuracy in U with a shorter observation period. This pressure reduction is, however, a very time-consuming process, and as such has not been carried out in all cases by the Norwegian Mapping Authority.

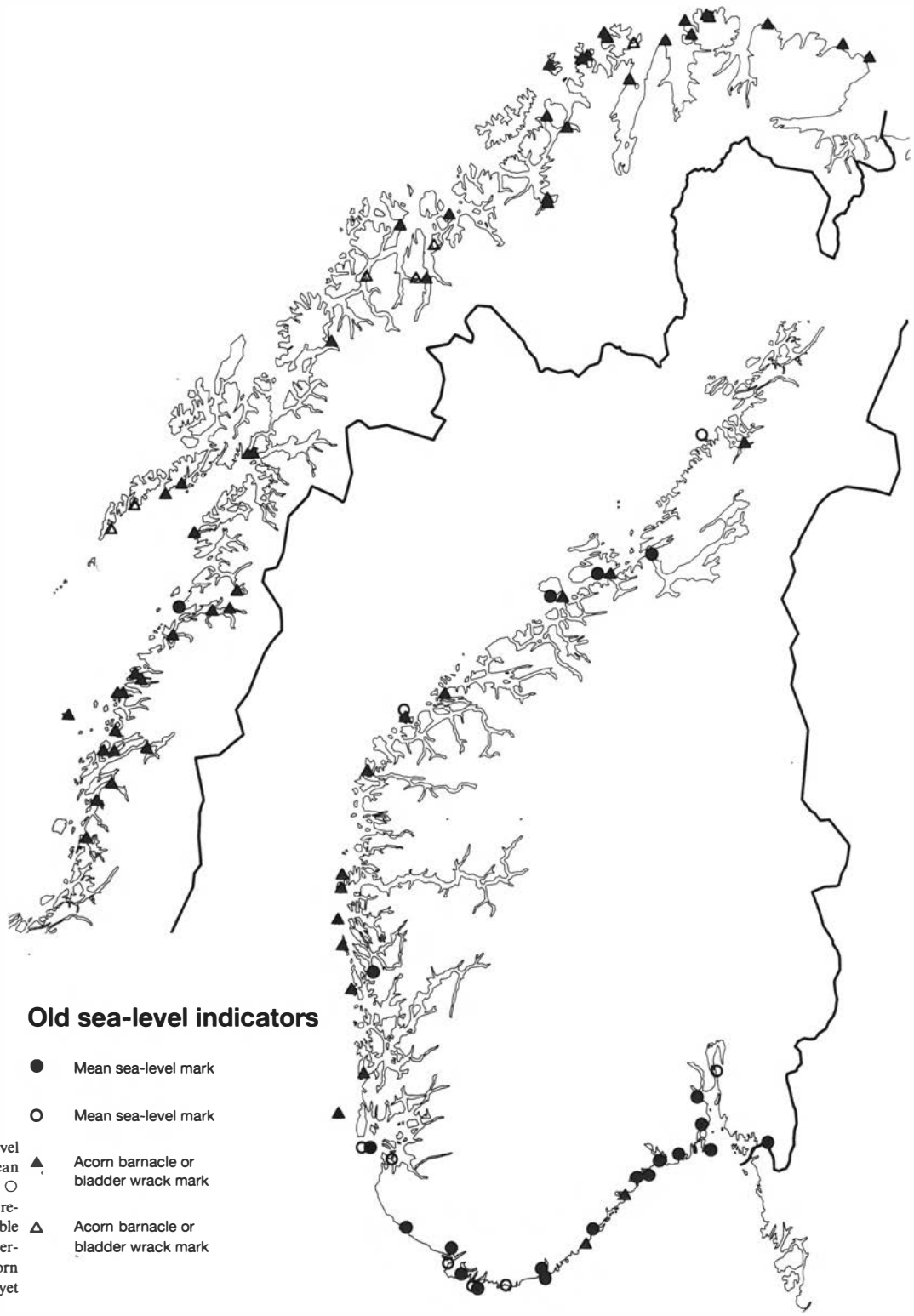

Fig. 5. Location of sites of old sea-level marks of the two categories. ● Mean sea-level marks – Remeasured. ○ Mean sea-level marks which require re-measurement to give U with acceptable accuracy. ▲ Acorn barnacle/bladder-wrack marks. Remeasured. △ Acorn barnacle/bladder-wrack marks. Not yet remeasured.

The straight line represents what may be termed 'long-term mean sea level' and the height difference between the observed and the long-term mean sea level for a particular year represents the 'anomaly of the observed annual mean'.

The map in Fig. 7 shows the location of sites where a tide-gauge has been in operation.

Determination of U from shore-level displacement curves

Up to the present, 15 to 20 shore-level displacement curves have been determined in Norway using modern stratigraphic and dating techniques (Fig. 8).

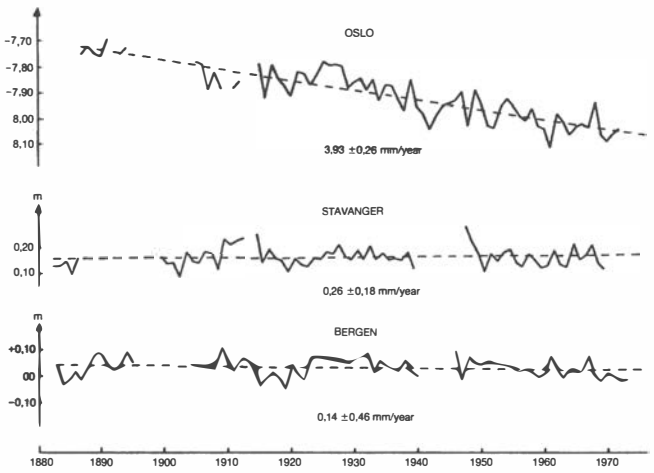

Fig. 6. Variations in annual mean sea level at the site of the gauges in Oslo, Stavanger and Bergen. Rates of crustal uplift are indicated (Norges geografiske oppmåling).

The rate of crustal uplift for any epoch covered by a shore-level displacement curve is given by the tangent to the curve at that epoch. As it is difficult to estimate accurately the zero level of the curve there will be an uncertainty in the rate of uplift determined by the tangent to the point corresponding to the present. In practise we can assume a constant rate over the last 3000–4000 years BP, and determine this rate to an accuracy of about 0.5 mm/year.

The Norwegian Mapping Authority has so far made little use of shore-level diagrams and shore-level displacement curves for determination of the apparent crustal uplift rate. These diagrams and curves would become more useful for this purpose if a reliable value for the rate of crustal uplift had been established at some of the localities for which a displacement curve has been determined.

Determination of U for inland crustal sites

U can be directly observed only at the coast. To determine U for inland crustal points we have to make use of the relative crustal uplift differences determined by precise levelling and by shoreline diagrams constructed from radiometrically dated shorelines whose altitudes are precisely measured. Starting at a datum point with an arbitrary vertical velocity we can compute consistent relative uplift values over a continuous area network. Choosing a datum point for which U has been determined we find consistent U values also for the inland points.

Figure 9 shows the precise levelling network in Norway and the lines that have been relevelled. Out of 14,500 km that have been levelled only 2500 km have been relevelled.

The present map of the rate of crustal uplift in Norway

Bakkelid (1979) constructed a model for the rate of crustal uplift in Norway (Fig. 10) based on a smooth standard curve for the uplift along a profile from the coast to the centre of maximum uplift in the Gulf of Bothnia (Fig. 11). The profile for Norway was determined from observed rates of uplift along profiles in Finland and Sweden, adjusted to a best fit with the few uplift values available in Norway at that time. The model represents a coarse first approximation to the real situation and has been proved correct in its main features where new data are available in the coastal area, with the exception of outer Oslofjord, where adjustments are required.

Remeasurements of old bladder-wrack marks on the coast of Nordland and Lofoten in 1990 indicate that the isobases there should be moved 0.5 mm/year closer to the coast (Fig. 12). Remeasurements of such marks on the coast of Finnmark in 1989 indicate that the isobases of the model in outer Varangerfjord should be moved seawards a distance corresponding to 1.0 mm/year.

For the inland areas we find greater deviations from the 1979 model (Fig. 12). The author remains sceptical of some of these features and of some of the published uplift values (Sørensen et al. 1987).

Future problems, possibilities and methods

If global warming by greenhouse gases is established as a real factor influencing the melting of polar ice, there will be changes in V_s not accounted for in this study. As a consequence, the values determined for U will be arbitrary and consequently invalid. It may be argued, however, that the relevant geological information lies mainly in the spatial variation in V_c and less in its absolute magnitude.

It may therefore be anticipated that consistent V_c differences from repeated precise levelling will be used to determine U_r values on an arbitrary datum.

$$U_r = V_c + C_1 = U + C_2$$

where C_1 and C_2 are constants.

Two new methods to determine the spatial variation in V_c will probably also be available in the future: (1) Using satellite methods, H_c can now be measured directly, but only to an accuracy of approximately ± 0.5 m. (2) Using LLR (Lunar Laser Ranging) techniques the station's distance from the Earth's centre of mass can be determined with a precision of a few centimetres.

With present techniques, height differences of crustal points can be measured to an accuracy of about 10 mm over distances of up to about 100 km. Relative vertical velocities (ΔV_c) of crustal points within an area of this size can therefore be determined to an accuracy of about 0.3 mm/year, using an observation period (ΔT) of about 50 years, which is about what can be achieved by repeated precise levelling.

The state of the art in absolute gravity meters allows V_c to be determined as $\Delta H_c/\Delta T$ where ΔH_c is determined

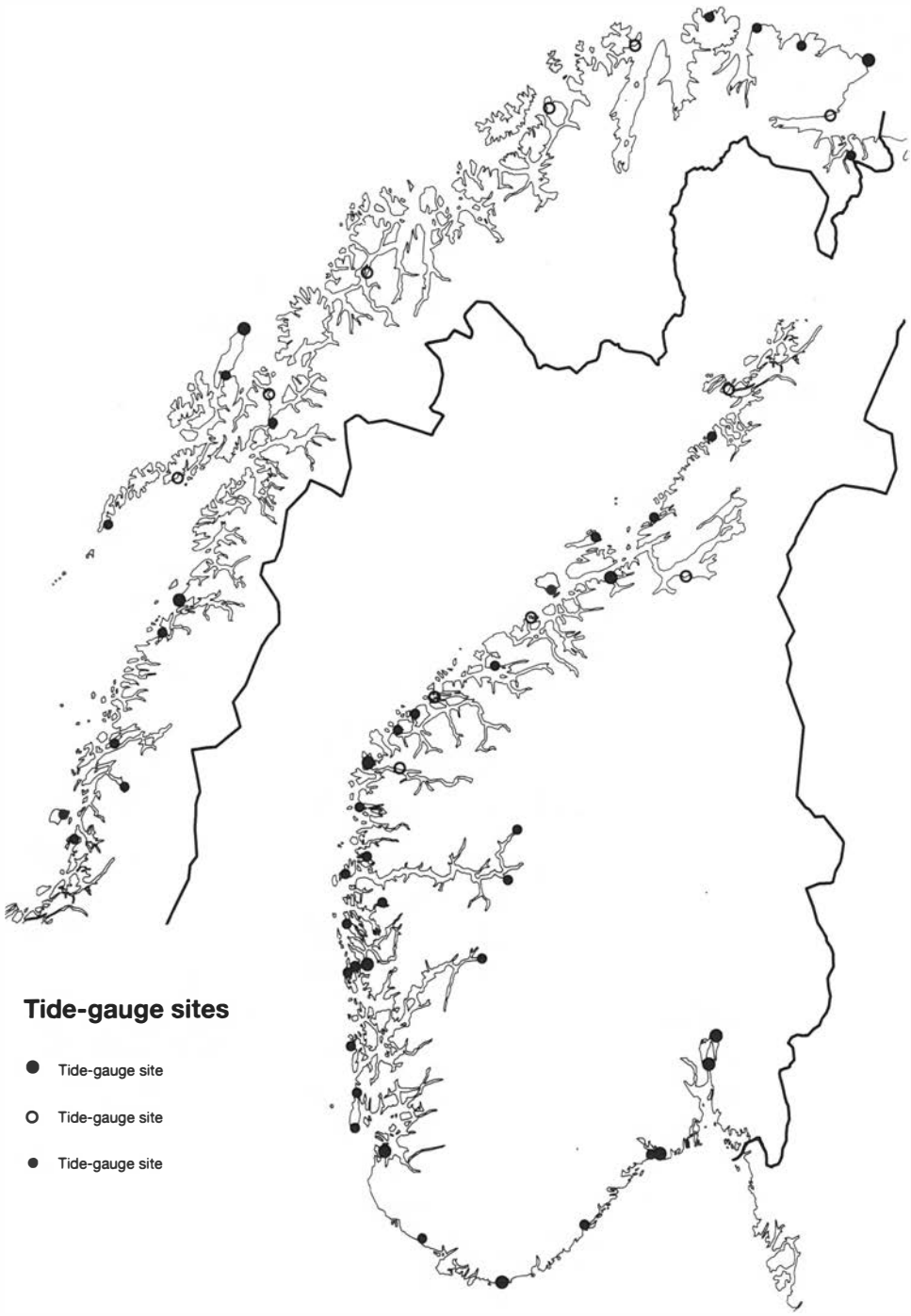

Fig. 7. Location of sites of tide gauges of different categories. ● Gauge sites where the available recordings have given a U with an accuracy better than 0.5 mm/year. Most of the sites have gauges still in operation, making the updating of U possible. ○ Gauge sites where the available recordings so far have failed to give a U with an accuracy better than 0.5 mm/year but where the gauges are still in operation. ● Sites where a gauge has been in operation for a period of a few weeks up to a few years. The greater number of these gauges were in operation between 1945 and 1967. For these sites a crustal uplift rate could be determined if a gauge is remounted at the site for a period of time in the future, provided the gauge benchmark can be found.

by repeated absolute gravity observations. It is assumed that using this method we will at present require a repeat period of 70 years to obtain an accuracy of 0.5 mm/year in V_c. Direct determination of ΔH_c by these methods, however, would have to be corrected for the tidal deformations of the Earth.

It can be concluded that it will probably be necessary in the future to shift from a consideration of apparent crustal uplift to the new parameters of relative crustal uplift (U_r) or absolute crustal uplift (V_c). We have noticed that variations in V_s may make determinations of U invalid. A significant rise in sea level will also invalidate the precise levelling method for determination of differential vertical crustal velocities in the coastal region due to the changes in the potential surfaces of the gravity field.

Conclusion

Much work remains to be carried out before we can construct a complete, detailed and correct map of the rate of crustal uplift in Norway. To achieve this, a great number of improved data points are required. If we are

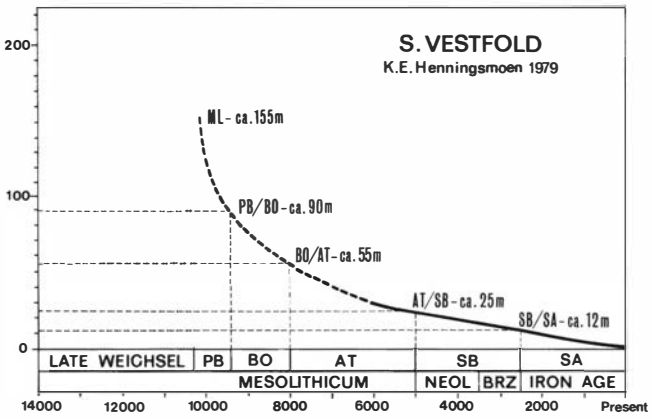

Fig. 8. Shore-level displacement curve for southern Vestfold (from Henningsmoen 1979).

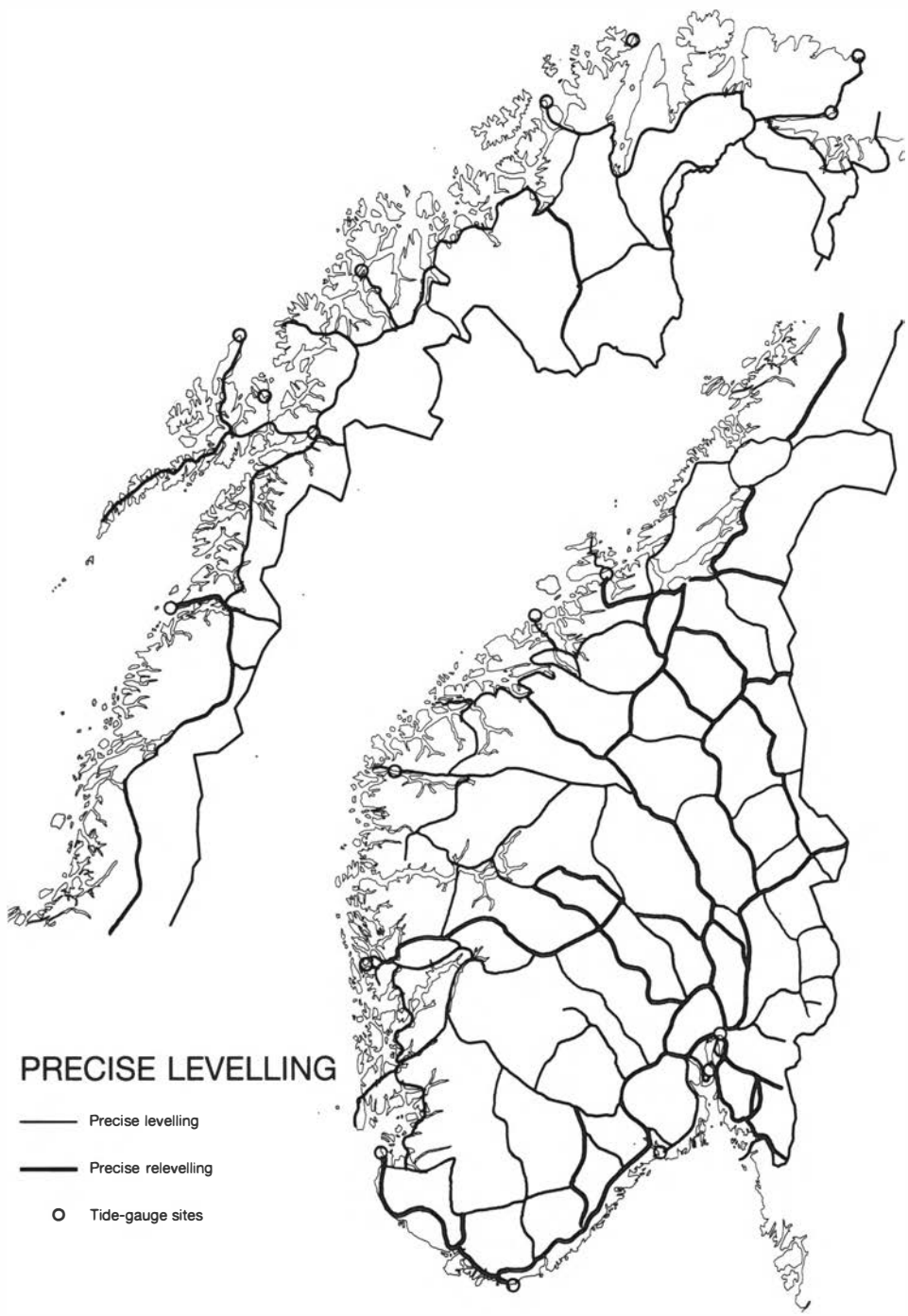

Fig. 9. Precise levelling and precise relevelling network in Norway.

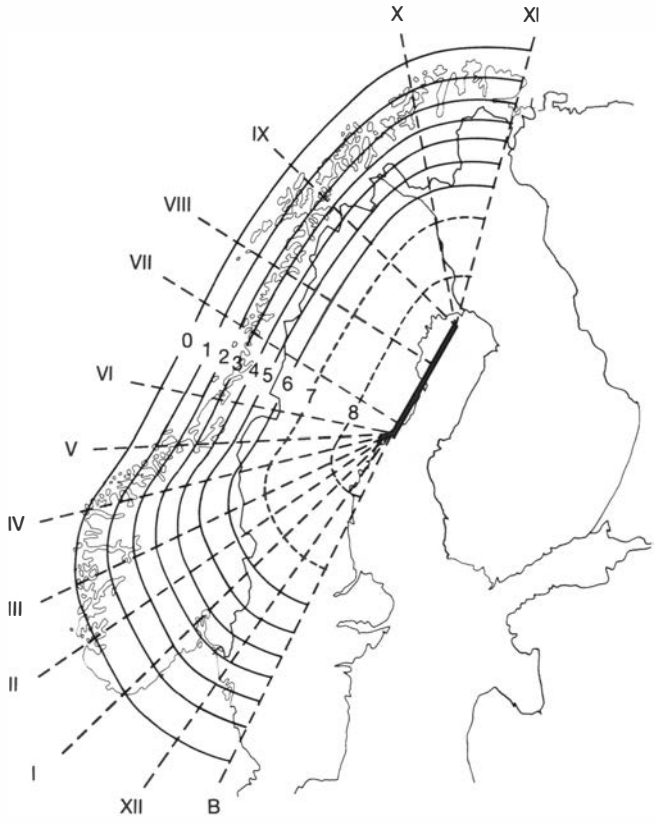

Fig. 10. Isobases for the rate of crustal uplift (U) in Norway (Bakkelid 1979).

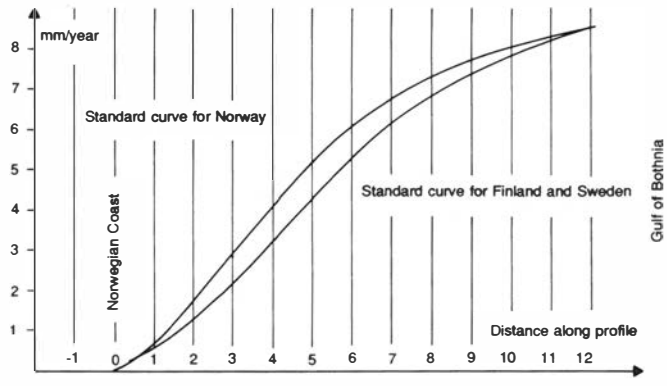

Fig. 11. Rate of crustal uplift profile. Standard curve for Norway (Bakkelid 1979).

to prepare such a map within three to five decades from now, it should be realized that we must depend on the established methods and the data points at which such observations have already been recorded. It will take some time for the new methods to reveal values of crustal uplift rates of guaranteed quality and reliability.

Internationally, it has long been realized that recent crustal movements, and in particular the present rate of crustal uplift, are one of the most important indicators of processes going on in the Earth's interior.

Very little coordinated effort has been made until now in Norway to establish a strategy for the mapping of the crustal uplift rate.

Recently, a working group has been established by the International Association of Geodesy (IAG) and the International Earth Rotation Service (IERS) to discuss, design and implement the establishment of a 'Common, global, integrated and fundamental Network' to satisfy the overall goals of a 'Global GPS International Service' which, apart from geodetic objectives, should provide effective and economical means for acquiring, analysing and archiving the data sets required to solve global problems such as the monitoring of: (1) Global sea-level change, (2) Post-glacial rebound, (3) Tectonic motion and deformation.

A multidisciplinary cooperation of geoscientists is required to achieve these goals (International GPS Service, 1991).

Manuscript received October 1991

References

Bakkelid, S. 1979: Et foreløpig totalbilde av landhevningen i Norge. Norges geografiske oppmåling, 22 pp.

Henningsmoen, K. E. 1979: En karbon-datert strandforskyvningskurve fra Søndre Vestfold. *In* Nydal, R., Westin, S., Hafsten, U. & Gulliksen, S. (eds.): *Fortiden i søkelyset. ^{14}C datering gjennom 25 år.* Laboratoriet for radiologisk datering, Trondheim.

International GPS Service, 1991: Report prepared by the Network Design Panel, 21 pp.

Sørensen, R., Bakkelid, S. & Torp, B. 1987: Landhevning. *In*: *Nasjonalatlas for Norge. Hovedtema 2: Landformer, berggrunn og løsmasser.* Kartblad 2.3.3. Statens kartverk.

Tolpinrud, H. 1989: *Landheving utrekna etter den seinaste ommålinga av middelvassmerka frå 1839.* Statens kartverk.

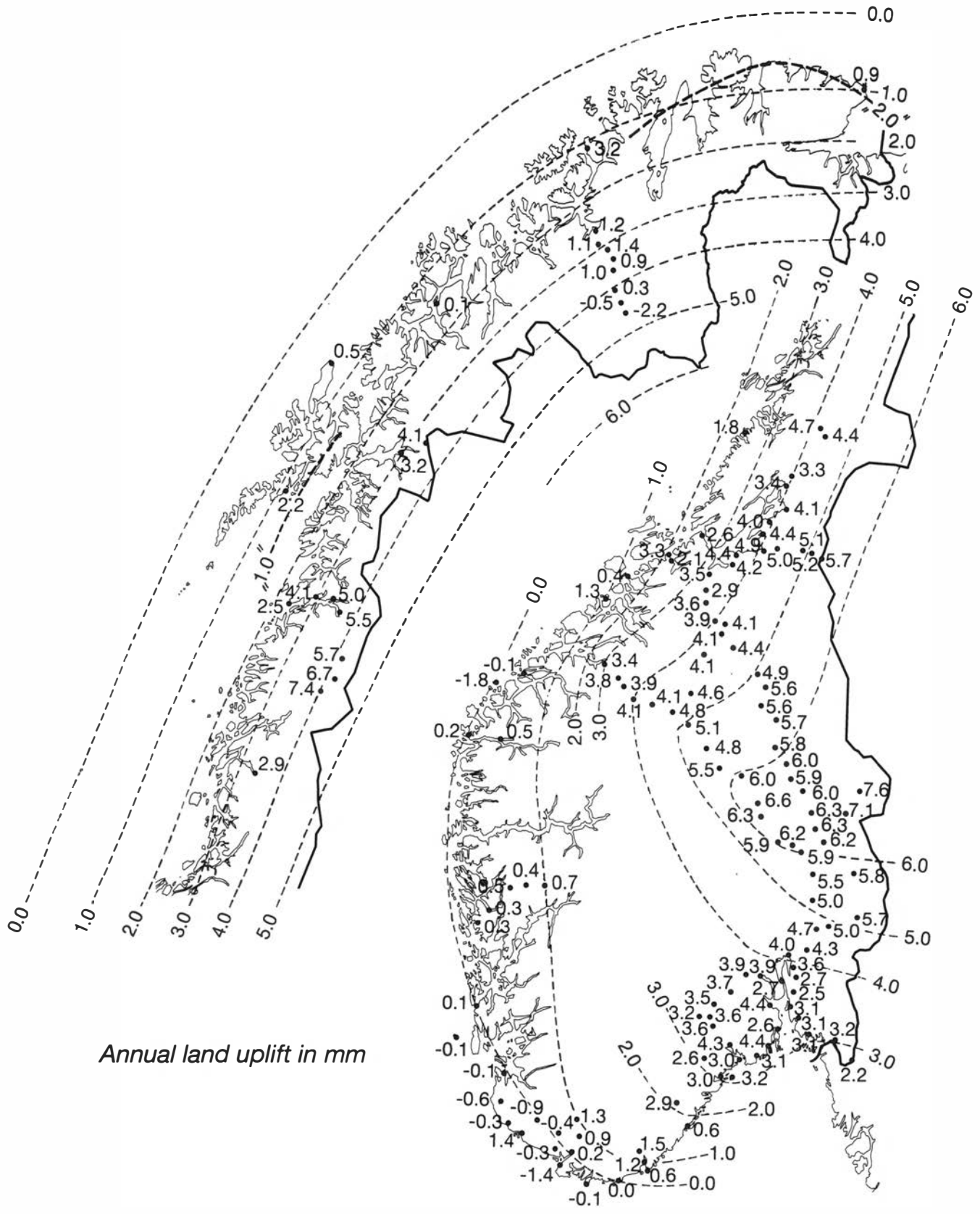

Fig. 12. Isobases for the rate of crustal uplift (Fig. 10) adjusted by some recently observed rate values (Sørensen et al. 1987).

Modelling the effect of glaciation, ice flow and deglaciation on the Lansjärv region in north Sweden

PANAYIOTIS CHRYSSANTHAKIS & NICK BARTON

Chryssanthakis, P. & Barton, N.: Modelling the effect of glaciation, ice flow and deglaciation on the Lansjärv region in north Sweden. *Norsk Geologisk Tidsskrift*, Vol. 72, pp. 247–251. Oslo 1992. ISSN 0029-196X.

The Universal Distinct Element Code UDEC-BB was used for modelling a rock mass of 4 × 4 km. In UDEC-BB the rock mass is modelled by describing the response of every discontinuity and deformable block separately with non-linear stiffness according to the Barton–Bandis model for the discontinuities. The modelled rock mass contained two sets of intersecting joints/faults of 30° and 110° dip, to represent elements of the Lansjärv region in north Sweden. An initial ice body of 3 km in height and 4 km in length simulated the glacier, first as a static load, then in motion. This ice load was then reduced in steps to simulate the deglaciation. On the final unloading stages, i.e. today's situation where all the ice was removed, glacial rebounds of the ground surface of 0.8 to 3.8 m were indicated. The simulated faults of Model 2 exhibited greater rebound than Model 1 joints, the overshoot effect probably caused by the reduced shear resistance predicted during reversed shear.

P. Chryssanthakis & N. Barton, Norwegian Geotechnical Institute, PO Box 40 Tåsen, 0801 Oslo 8, Norway.

The effect of glaciation and deglaciation has been studied in two-dimensional generic models of faulted rock masses. Six loading cases were modelled for the 4 × 4 km rock mass (Fig. 1). After consolidation and application of boundary stresses, where the models were loaded by horizontal stresses from both sides (case 1), an ice sheet, 3 km thick, was applied at the surface of the model (case 2). An interface was introduced at the ice-rock boundary. Ice flow was then simulated by velocity applied at the left vertical boundary (case 3). For simulation of deglaciation, the ice thickness was reduced in two steps. First, two-thirds of the ice sheet was removed and the response in stress and displacement was studied (case 4). Later, all ice was removed from one-half of the model and a triangular ice load was left (case 5). Finally, all ice was removed to represent today's situation (case 6). In modelling the effect of glaciation and deglaciation the vertical displacements at the bottom of the model were restricted to zero. In nature, the ice load will cause deeper subsidence and rebound due to the viscoelastic behaviour of the earth's mantle (Bakkelid 1986; Stephansson et al. 1986). These effects are not considered in this study.

The rock mass contained two sets of intersecting joints/faults of 30° and 110° dip, to broadly represent the Lansjärv region in north Sweden. Two different models were studied with variations mainly in the normal and shear stiffness of the joints/faults in the rock mass. Model 1 simulated the stiffer joints and Model 2 the faults. See Table 1 for stiffness values. The term 'rock joint' is used to describe the mechanical discontinuities of geological origin that intersect almost all near-surface rock masses. The term 'fault' is used in this paper to describe the discontinuities with substantially lower normal and shear stiffness values. These numerical 'faults' still have wall-to-wall contact. The reduction in stiffness values simulated the presence of filling material in the faults. In the cases of both joints and faults, roughness coefficient and stiffness values are of primary importance (see Singh et al. 1988; Barton et al. 1985). The two numerical models showed substantial differences in behaviour under the different load sequences.

Details on the application of this code can be found in Barton & Chryssanthakis (1988) and Chryssanthakis (1989). Modelling with the UDEC-BB model (Cundall 1980) permits determination of mechanical and conductive (hydraulic) fault or joint apertures. These two joint properties are very important parameters in deciding the final location of a repository for radioactive waste (Stephansson 1987).

Modelling with the UDEC non-linear Barton–Bandis joint model

The geometry of the joint/fault sets that were modelled with the UDEC-BB model is shown in Fig. 2. Results from the two applications of the generic models – called Model 1 and Model 2 – are presented. In Model 1 effective tectonic stresses were applied. By the term 'effective tectonic stresses' we mean absolute stresses minus pore water pressure. Model 1 has joint stiffnesses that are two to four orders of magnitude stiffer than the faults for Model 2.

Model 2 is subjected to an initial horizontal stress (total $\sigma_H = 5 + 32 \cdot Z$) acting at both the vertical

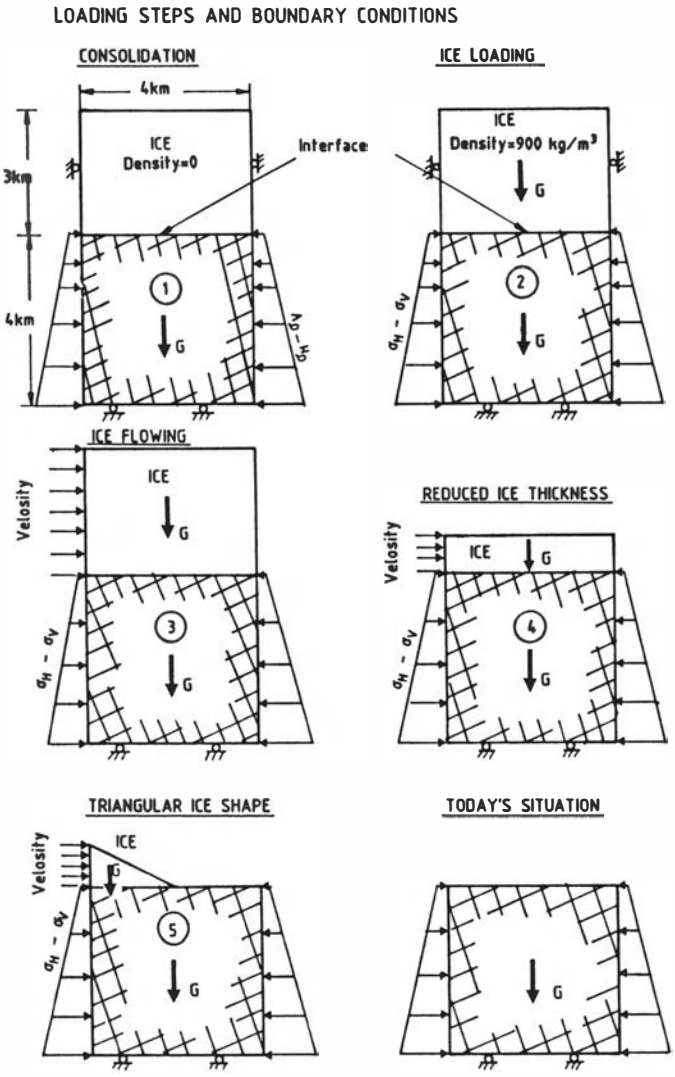

Fig. 1. Generic models for glaciation, glacial flow and deglaciation. Roller boundaries are placed at the bottom and sides of the model. Loading cases, boundary conditions and geometry. Two different boundary conditions were used. During consolidation, loading case 1, no ice load was applied.

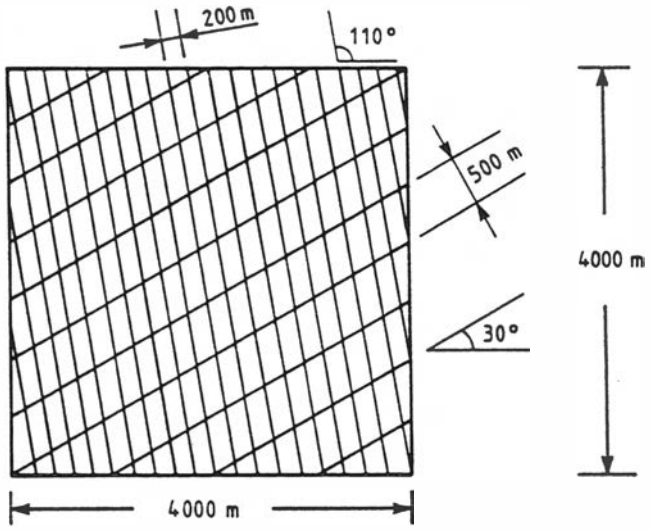

Fig. 2. Joint fault set geometries in generic modelling.

boundaries and a vertical stress of $\sigma_v = 27 \cdot Z$) where Z is the depth in kilometres and stresses are in MPa).

The large problem size and the differences between the joint stiffnesses and the surrounding rock mass in Model 2 resulted in a very long consolidation procedure (loading case 1) which proceeded slowly during successive loading and unloading stages. The downward displacements of the ground surface after ice loading were found to be 3.8 m and 3.9 m for Models 1 and 2, respectively. The application of effective tectonic stresses to the model made no major changes in magnitudes of stresses and displacements.

An important difference in the behaviour of Models 1 and 2 can be seen in the last stage (case 6), which is today's situation, where all ice has been removed from the rock mass. Model 1 exhibits an upwards movement of 0.8 m, indicating a moderate hysteresis effect with no overshooting. On the contrary, Model 2 (soft faults) shows no hysteresis and as much as 3.8 m of overshooting. The overshooting effect of Model 2 can be understood more easily by considering the forward shear and reversal shear behaviour of a rock joint. In general, when shearing a joint in the reverse direction it exhibits lower dilation and shear strength values, due to damage in joint roughness coefficient (JRC reduction). The Barton–Bandis joint model integrated in UDEC-BB contains a shear reversal 'loop' similar in principle to the one reported by Celestino & Goodman (1979) for a plaster replica of a joint in sandstone. Greater shear and JRC damage occurred in Model 2.

The principle stress plots for Models 1 and 2 indicate no dramatic changes in terms of stress rotation under the various loading and unloading cases. Changes in horizontal and vertical stresses at 500 m below ground surface are in close agreement with other modelling results except for the case of reduced stresses caused by deglaciation in Model 2 (cf. Fig. 3).

The computation mesh used in the central and uppermost 1000 m of Model 2 was made finer in order to study the change in displacements and stresses in the vicinity of a repository in detail. Figure 4 shows a slight re-orientation of the principal stresses due to ice loading and ice flow from left to right for Model 2.

The shear displacements obtained vary between 1.2 mm and 80 mm for Model 1 down to a depth of 1000 m. A maximum shear displacement of 0.89 m was obtained for the 'soft faults' in Model 2. For more details about the specific value of mechanical and hydraulic apertures used in this study the reader is referred to the work by Chryssanthakis (1989).

Modelling with the UDEC-BB code (Cundall 1980) permits determination of hydraulic joint/fault apertures. The hydraulic or conductive aperture shows direct similarities with the mechanical aperture since it is derived from the empirical formula $e = E^2/\mathrm{JRC}^{2.5}$ where e = conducting aperture, E = mechanical aperture, JRC = joint roughness coefficient.

The mechanical apertures during the different loading cases are relatively stable for Model 1, which exhibits a

Table 1. Rock material and joint properties used for Models 1 and 2. After Chryssanthakis (1989).

Properties	Intact rock	Model 1†		Model 2	
		Subvertical	Subhorizontal	Subvertical fault set	Subhorizontal fault set
Young's Mod. (GPa)	39.9*				
Poisson's ratio	0.19*				
Density (kg/m^3)	2700				
Bulk Mod. (MPa)	2.1E3*				
Shear Mod. (MPa)	8.2E3*				
JRC (Joint roughness coefficient)		5	10	5	10
JKN (MPa/m) Joint normal stiffness limit		2.4E8	1E9	2.4E4	1E5
JKS (MPa/m) Joint shear stiffness limit		2.9E4	7.8E4	2.0E2	6.0E2
KN (MPa/m) Point contact normal stiffness		2.4E7	1E8	2.4E3	1E4
KS (MPa/m) Point contact shear stiffness		2.9E3	7.8E3	2.0E1	6.0E2
APER (mm) Zero load aperture		0.150	0.200	0.150	0.200

* Equivalent properties.
† Effective tectonic stresses applied.
JCS (Joint wall compressive strength) is 150 MPa for all joint sets.
ϕ (Residual friction angle) is 30 for all joint sets.
L_o (Laboratory scale joint length) is 0.1 m for all joint sets.
σ_c (Uniaxial compressive strength of intact rock) is 220 MPa for all joint sets.
L_n Assumed block size is 0.5 m and 3.0 m for the subhorizontal and subvertical joint sets respectively.

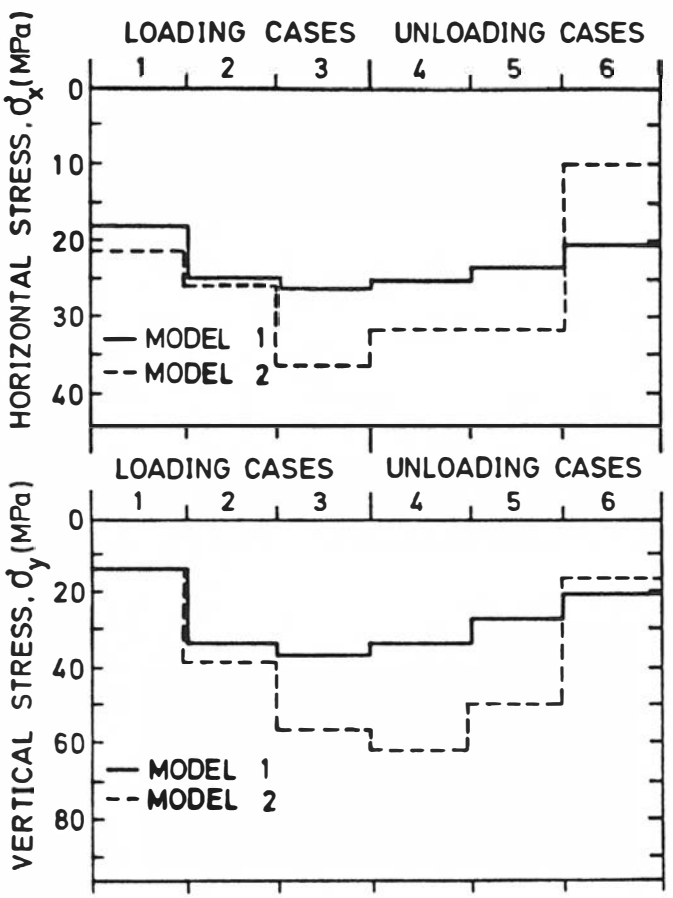

Fig. 3. Horizontal and vertical stresses at 500 m depth versus loading and unloading cases for Models 1 and 2, UDEC with the Barton–Bandis joint model. Based on data taken from Chryssanthakis (1989).

small variation in apertures and closures down to a depth of about 200–300 m. Below this depth the joints of Model 1 (properties from Table 1) cannot close any further, they have reached maximum closure (100 μm for the subhorizontal and 40 μm for the subvertical joint set). In the last loading case Model 1 exhibits a slight opening of 40 μm of the subvertical joint set down to a depth of 800 m. The behaviour of the 'soft' faults of Model 2 differs significantly. The fault apertures change with depth during the loading cases. The apertures at the top and bottom of Model 2 vary betwen 90 μm and 40 μm for the subvertical fault set. The corresponding values for the subhorizontal fault set are 160 μm and 110 μm respectively. During the last unloading case, Model 2 exhibited an opening for both fault sets down to a depth of about 1500 m. The maximum variations for the subhorizontal and subvertical faults set at the top and bottom of the model were 90 μm and 100 μm respectively. A typical mechanical aperture plot is shown in Fig. 4B.

Conclusions

For UDEC-modelling with the Barton–Bandis joint model, the vertical displacement of the ground surface after glaciation was found to be 3.8 and 3.9 m for Models 1 (stiff joints) and 2 (soft faults), respectively. Modelling with stiff joints was satisfactory while modelling two sets of intersecting fault sets and soft fault

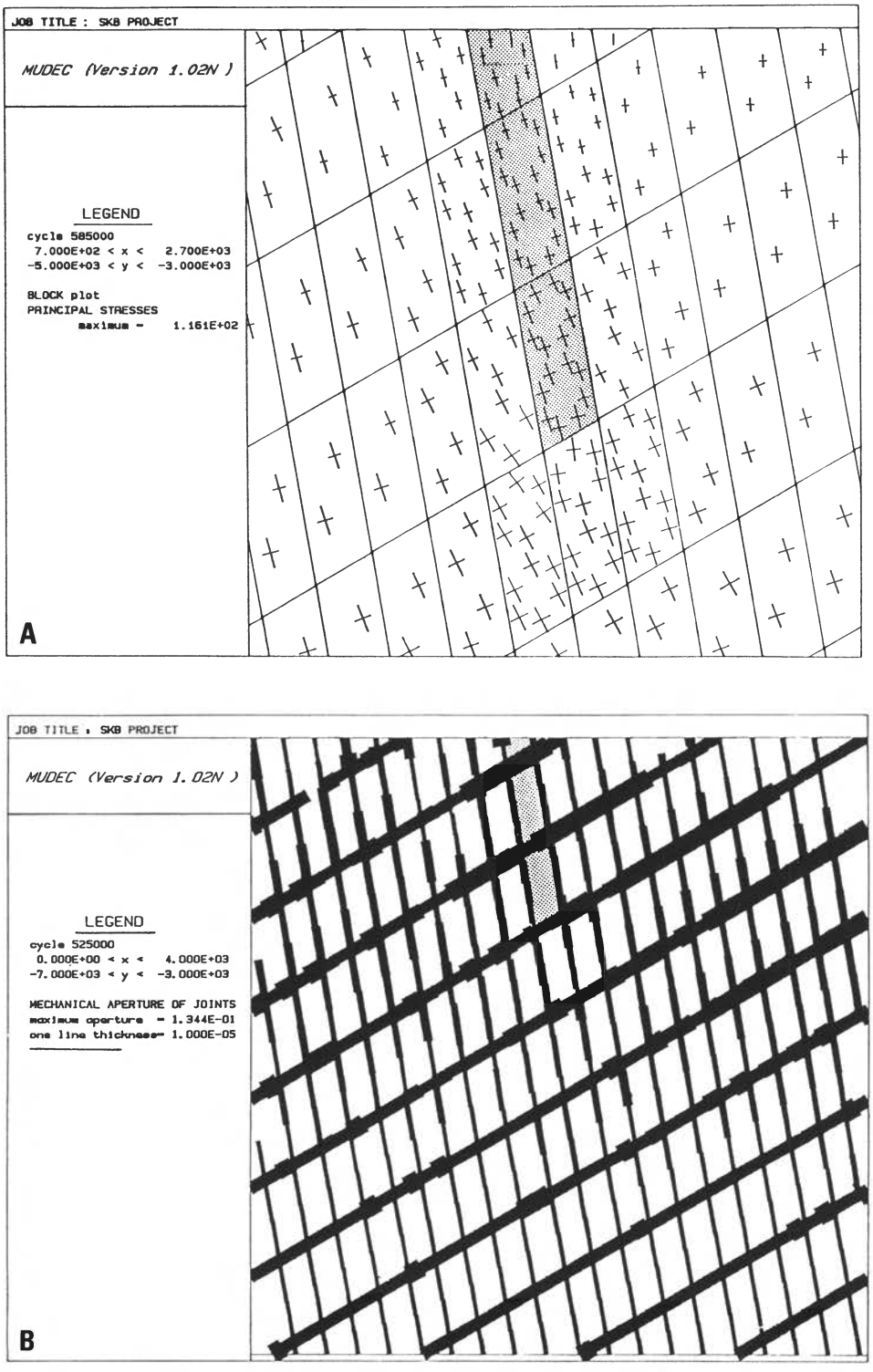

Fig. 4. Loading case 3 with 3 km of ice and ice flow analysed with the UDEC non-linear Barton–Bandis joint model. (A) Principal stress vector in the central portion of Model 2. There is no significant stress rotation observed. (B) Mechanical aperture plot of the whole of Model 2. On the subvertical fault set the variation of apertures on the top and bottom of the model ranges between 90 μm and 40 μm (after Chryssanthakis 1989).

stiffnesses gave very high vertical stresses when ice flow was introduced. Application of effective tectonic stresses, i.e. total stress minus pore pressure, made no major change in the magnitude of stresses and displacements.

On the final unloading case (today's situation) where all ice was removed, the joints simulated in Model 1 (stiff joints) showed a hysteresis effect, while the simulated 'soft' faults of Model 2 exhibited a major rebound (above original ground level) of 3.8 m. The greater release of strain energy in this case can cause changes in the mechanical and conducting aperture of the faults and consequently change the groundwater flow during deglaciation.

Modelling with the UDEC Barton–Bandis joint model permitted determination of mechanical and hydraulic fault apertures. Aperture varied from 40 to 100 μm for the subvertical and subhorizontal joints sets respectively for

Model 1 down to a depth of 200–300 m. In contrast to Model 1, Model 2 exhibited apertures changing with depth. The change of apertures at the top and bottom of the model ranged between 90 μm and 40 μm for the subhorizontal and between 160 μm and 110 μm for the subvertical fault sets respectively.

The load of a 3 km thick ice sheet superimposed on the virgin vertical rock stress gave an additional vertical stress of 30 MPa. This stress was superimposed on the virgin state of rock stress. Construction of a repository, thermal loadings and loading from swelling bentonite will further influence the stress around the repository. The results of the modelling demonstrate the change in stresses (magnitudes and directions) due to glaciation and deglaciation and favour a location of a repository around 500 m depth.

Acknowledgements. – The work of this paper was supported by the Swedish Nuclear Fuel and Waste Management Co. (SKB). Special thanks are due to G. Bäckblom for his interest and support during this work.

Manuscript received October 1991

References

Bakkelid, S. 1986: The determination of rates of land uplift in Norway. *Tectonophysics 130*, 307–326.

Barton, N., Bandis, S. & Bakhtar, K. 1985: Strength, deformation and conductivity coupling of rock joints. *International Journal of Rock Mechanics, Mining Sciences & Geomechanical Abstracts 22*, 121–140.

Barton, N. & Chryssanthakis, P. 1988: *Validation of MUDEC against Colorado School of Mines Block Test Data.* SKB Technical Report 88-14, Swedish Nuclear Fuel and Waste Management Co., Stockholm, 94 pp.

Celestino & Goodman 1979: Path dependency of rough joints in bi-directional shearing. *Proceedings of the Fourth International Congress on Rock Mechanics*, 91–98. Montreaux, Vol. 1

Chryssanthakis, P. 1989: *Distinct Element Modelling of the Influence of Glaciation and Deglaciation on the Behaviour of a Faulted Rock Mass.* SKB Working Report 89, Swedish Nuclear Fuel and Waste Management Co., Stockholm, 41 pp. and 84 App.

Cundall, P. A. 1980: *UDEC – A Generalized Distinct Element Program for Modelling Jointed Rock.* Report PCAR-1-80, Peter Cundall Associate, Contract DAJA 37-79-C-0548, European Research Office, US Army.

Singh, U., Savilahti, T. & Stephansson, O. 1988: *Generic Model Analysis of Large Faulted Rock Masses with Hard Fault Stiffness.* SKB Working Report 88–22, Swedish Nuclear Fuel and Waste Management Co., Stockholm, 13 pp. and 15 App.

Stephansson, O. 1987: *Modelling of Crustal Rock Mechanics for Radioactive Waste Storage in Fennoscandia.* SKB Technical Report 87-11, Swedish Nuclear Fuel and Waste Management Co., Stockholm, 79 pp.

Stephansson, O., Särkkä, P. & Myrvang, A. 1986: State of stress of Fennoscandia. *Proceedings of the International Symposium on Rock Stress and Rock Stress Measurements*, 21–32. Centek Publishers, Luleå.

Uplift and subsidence of northwestern Europe: possible causes and influence on hydrocarbon productivity

JOHN K. SALES

Sales, J. K.: Uplift and subsidence of northwestern Europe: possible causes and influence on hydrocarbon productivity. *Norsk Geologisk Tidsskrift*, Vol. 72, pp. 253–258. Oslo 1992. ISSN 0029-196X.

Northwestern Europe has experienced several uplift and subsidence events that influenced hydrocarbon prospectivity. Several tectonic mechanisms, related to the opening history of the Atlantic, might explain the distribution of these events. Except for Paleogene transpression between Greenland and Svalbard, these are extensional and associated with (1) early rifting, (2) later pre-subduction instability. Possible mechanisms and controls on sedimentation are summarized first, followed by their affect on uplift and subsidence history of northwestern Europe. Glaciation is included to separate its contribution to uplift from the tectonic component of uplift. This is followed by consideration of the influence that these events have had on hydrocarbon accumulation.

J. K. Sales, Mobil Exploration Norway Inc., PO Box 510, N-4001 Stavanger, Norway.

Early-stage rift mechanisms

Although rifts may show asymmetry (Wernicke 1986), the stretching model (Beaumont 1978; McKenzie 1978) applies and explains co-axial distribution of syn- and post-rift sediments (White 1990). Initial stretching plus hangingwall weighting cause early subsidence, concentrated along the rift axis. Plaster models sometimes show over 20% stretching before visible faulting. Similar amounts may precede seismically visible faulting (minimum of approximately 50 m throw) in nature. Models also show low-angle detachments evolving from domino-style tilt blocks (Fig. 1), though they are also initiated at low angles.

The asthenosphere swell (McKenzie 1978) and footwall buoyancy (Jackson & McKenzie 1983) cause broad regional uplift, rift shoulders, and high blocks. The swell causes a taller isostatic column than adjacent colder mantle. This supports regionally high topography and produces broad wavelength gravity minima under active rifts like East Africa (Girdler 1975). Individual blocks are elevated by footwall uplift (Jackson & McKenzie, 1983) or depressed in proportion to relative amount of footwall or hangingwall. The Ruwenzori Uplift (5120 m) in Africa is an extreme case where a pyramid-shaped block, surrounded by footwalls, may have been driven abnormally high (Fig. 2).

Early-stage interplay with sedimentation

Sediment accommodation (Jarvey 1988) results from stretching and hangingwall weighting overcoming the positive effect of the thermal swell. Regional uplift due to the asthenosphere swell and more local highs driven by footwall buoyancy combine to control provenance areas for syn-rift sediments. Zones of asymmetry-change provide entry points for major drainages. Wide variations in accommodation space relative to sediment supply occur, with one of the largest variables being the distribution of drainage, specifically the presence or absence of a trunk river system in the rift. Thus, Lakes Baikal and Tanganyika, with no trunk drainage flowing into them, have accommodation space so dominant over sediment input that they are about 2 km and 1 km deep respectively. Conversely, the Reelfoot Rift in the USA, through which the Mississippi River flows, is so overwhelmed by that great river that a tenfold increase in accommodation space might have little effect. As another example, the Gulf of Suez would contain a much greater proportion of shallow-marine and continental clastics if the Nile River had been channeled through it, instead of beind deflected out of it by the elevated rift shoulder.

Rift blocks evolve in variable vertical positions relative to base level, depending on rate of stretching, degree of asymmetry, time in the cycle of opening in which they form, and their position in the rift. Northwestern Wyoming, USA is in such an elevated setting that even the hangingwall of the famous Teton–Jackson Hole half-graben is being elevated and incised, while the Precambrian metamorphics on the footwall stand at over 4000 m in the Tetons. Other blocks that form late, especially in a slow spreading rift, may never raise their crests above sea level. Some of the blocks in the northern Viking Graben, such as Gullfaks, are relatively weakly eroded and in some cases low-angle detachment surfaces high on the block (Fig. 1) may be misinterpreted as erosion and thus erosion may be overestimated.

Stretching and thermal decay finally dominate over the active asthenosphere swell and footwall buoyancy. Thus,

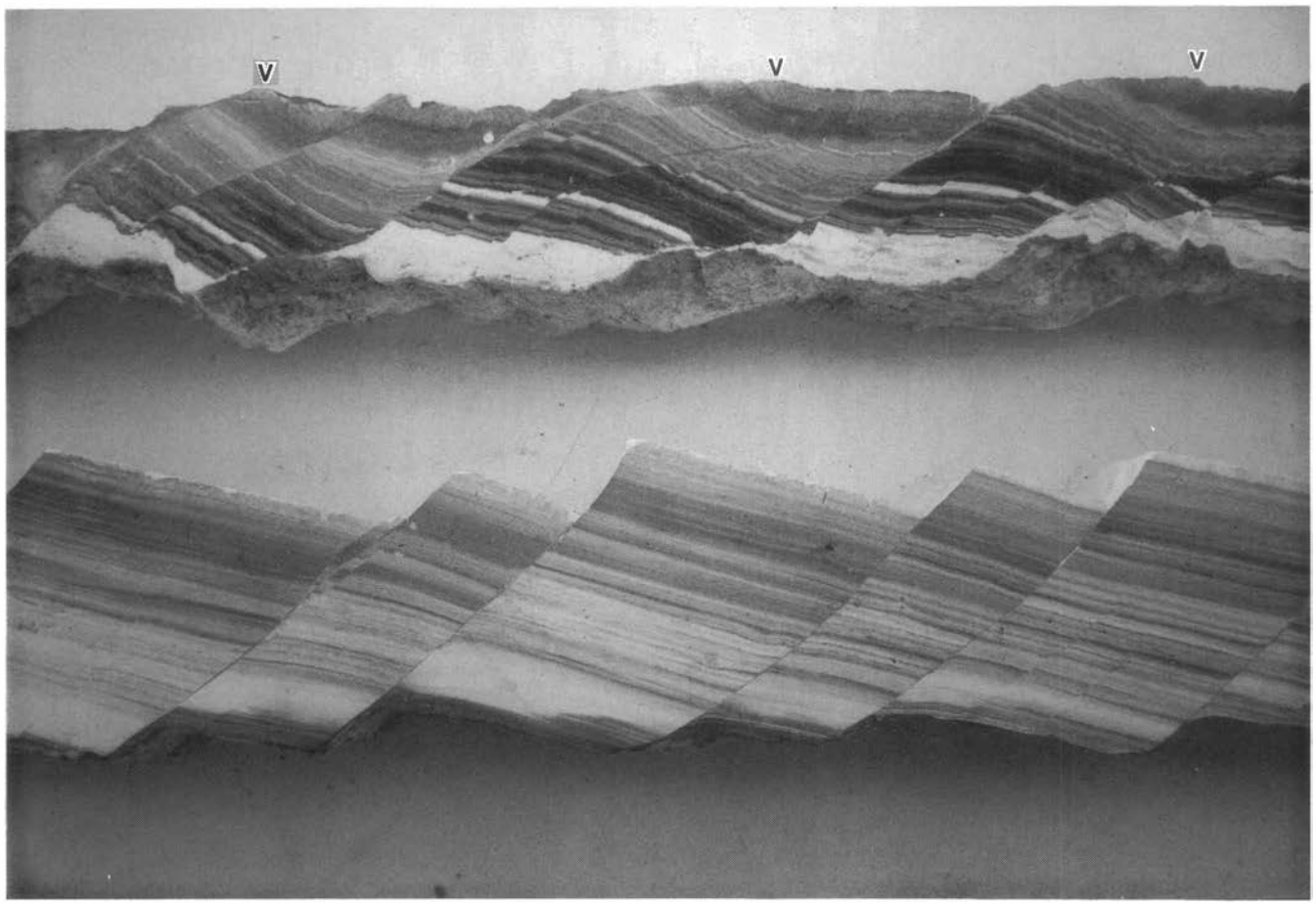

Fig. 1. Otherwise nearly identical domino tilt block plaster models with roughly 15% and 100% extension. In the lower model only about 6% extension shows as measurable fault heave, the rest being pervasive stretching and microscopic faulting roughly similar to sub-seismically visible (approx. 50 m offset) faulting in nature. Upper model with 100% extension shows scarps flattened into nearly horizontal low-angle detachment surfaces, easily mistaken for post-rift (breakup) unconformity surfaces. Small arrow points are placed at the tops of the 'scarps' to emphasize their flatness. Fluid barite sub-crust removed prior to photographing, original thickness of faulted plaster crust is 10–15 cm. See Sales (1987) for additional detail on the technique.

all rifts finally subside and are erosionally transgressed to form the 'post-rift' or 'breakup' unconformity, separating syn- and post-rift sections. Interplay between rate of transgression, competence of the erosional processes, and rock resistance can cause great variations in the degree of bevelling. At one extreme the entire syn-rift section might be removed, at the other there may be continuous though condensed sedimentation, even over the highest blocks.

Transgression, initiated by stretching and block weighting and finalized by thermal subsidence is economically important. Using classic northern North Sea terminology, high-energy nearshore deposits generate Brent-type reservoirs. They may prograde even though the overall long-term setting is transgressive. These are transgressed by nearshore Heather-type 'cold' shales that form seals. These are in turn transgressed by deeper water 'hot' shales that often become prolific source rocks. Highest blocks may not be brought below base level until later and are sealed by Cretaceous marls, with Kimmeridge and Heather shales wedging out on their flanks (Spencer & Larsen 1990).

Thus, as a rift goes into thermal subsidence, shorelines retreat and local high blocks drop below base level, causing a sharp transition from high-energy to pelagic sedimentation. Optimum conditions apparently develop when a rift 'shales out' before open marine circulation is established. This configures rifts to take advantage of any organic productivity bloom induced by plate distribution and/or climate. The Late Jurassic (Kimmeridge-type) source rocks result from this setting in such diverse areas as the North Sea, Hammerfest Basin, and West Siberian Basin.

Late-stage pre-subduction mechanisms

As pointed out by Cloetingh et al. (1992), as Atlantic margins mature, subsidence and decompacted sedimentation rates finally exceed what is predicted by oceanic cooling curves (Sclater & Celerier 1988) and stretching models (Beaumont 1978; McKenzie 1978). The accelerated sedimentation is not merely due to glacial erosion, because it is seen in more equatorial areas also (for example

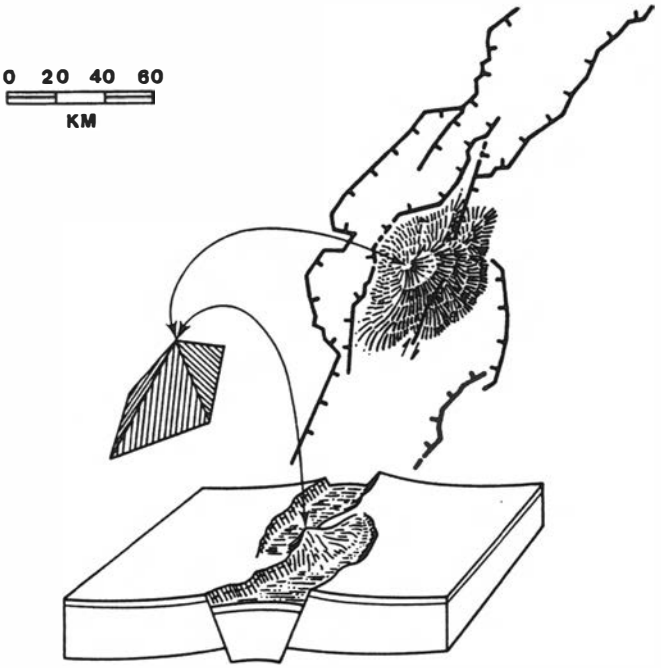

Fig. 2. Block diagram interpreting the Ruwenzori Uplift in East Africa's western rift as an extreme example of footwall uplift. Because it is located in a kink in the rift, boundary faults from the north and south having opposite throw wrap around the massif, forming a pyramid-shaped block, giving it abnormal positive buoyancy and raising basement rocks to 6000 m. Fault pattern from Holmes & Holmes (1978).

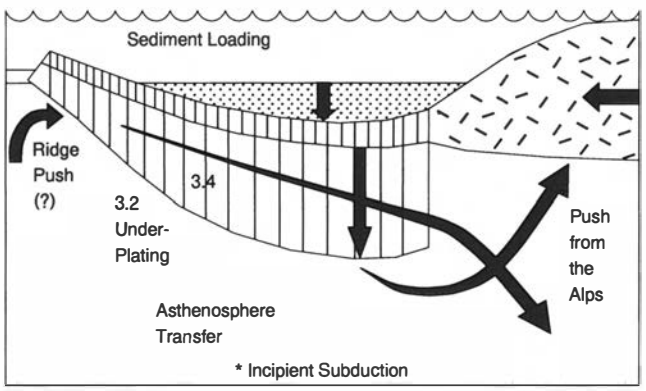

Fig. 3. Cross-section suggesting the factors that might contribute to formation of a peripheral bulge, under the assumption that it is a result of pre-subduction instability.

Mohriak et al. 1989). This does not mean that the models are wrong, only that there is a terminal stage in the evolution of Atlantic-type oceans, after the stability predicted by the flat part of the oceanic cooling curve, when instability sets in prior to subduction. That the end product of Atlantic evolution is subduction and not stability is suggested by the fact that there is no ocean crust older than about 200 m.y.

At approximately the same time that subsidence and sedimentation accelerate, a landward 'Peripheral bulge' develops. 'Peripheral bulge', 'bulge' for short, is used for high topography around the Atlantic, e.g. in Scandinavia; 'asthenosphere swell' is used for the upwelling of asthenosphere into basal lithosphere under a rift. They are at opposite ends of the rifting cycle and top and bottom of the lithosphere. This bulge may be a response to weighting caused by a combination of ocean underplating, sediment loading (Magara 1989), end-load compression (Cloetingh et al. 1992) as the slab begins to be deflected margin-ward prior to subduction, and flexural rigidity of the slab (Beaumont 1978). An attempt to illustrate this is shown in Fig. 3.

Since peripheral bulges exist in areas not glaciated (eastern South America, southern Appalachians), the mechanism is tectonic and not caused by glacial rebound. Also, glaciation shortens and densifies the isostatic column, and must result in a lowered, not raised topographic or bathymetric surface. Bulges cannot result from the simple shear mechanism (Wernicke & Tilke, 1989) because: (1) they are several tens to a few hundred m.y. later than associated rift-stage extension, (2) a period of stability intervenes between rifting and rise of the bulge, (3) there are symmetrical bulges across some oceans, i.e. Scandinavia (Riis 1992) and East Greenland (Christiansen et al. 1992), not predicted by the simple shear model, and (4) The Oldenberg & Brune (1972) wax experiment suggests that the simple shear mechanism could not operate across oceanic crust, even though it is viable during the rifting stage. Briefly, the spreading center stays centered because it is continually the weakest part of the system and has symmetrical accretion to both sides of the 'crack'. For this to happen the asthenosphere swell must stay centered under that ridge. Thus, that swell cannot remain available under the margin of that ocean to cause uplift as Wernicke & Tilke suggest. Christiansen et al. (1992) pointed out this time-space discrepancy in relation to E. Greenland uplift.

Bulges cannot be delayed rebound from a compressive mountain root because some exist where no root exists, and some that are located over previous mountain roots show a long period of stability between root-rebound and bulge-formation.

Peripheral bulges can be seen in the older rock record (Bally et al. 1966) as the unconformity separating the passive and active margin mega-suites. The unconformity that results from the bulge is overtopped by orogenic strata with an outboard source in the rising contraction belt caused by subduction. The duration of the peripheral bulge and of pre-subduction instability is poorly known and constrained. At one extreme, probably because of the dynamic setting, ocean crust subducts and reorganizes at a young age in very small ocean basins in the back-arc setting (Hamilton 1979). At the other extreme, when Pangea came together on one side of the globe, and Atlantic-type ocean must have encompassed nearly three-fourths of the globe. Since the oldest sea floor is Jurassic, an age limit of 200 m.y. may be appropriate for the spreading stage. As Ziegler (1989) points out, however, the duration of the rifting stage may be extremely variable. In summary, peripheral bulges are the upwarp, still coupled to the downwarp that will become the subducting slab when the margin breaks.

Application to evolution of northwestern Europe

Figure 4 summarizes the following discussion. Extension ceased in the North Sea after the Jurassic and caused a distinct Base-Cretaceous post-rift uncomformity separating syn- and post-rift sediments. By contrast, the Atlantic continued opening, first through an extended rifting phase (Ziegler 1989), and then with its spreading center moving continuously farther offshore. In contrast, the Viking Graben went dormant and extension jumped to the west of the UK to produce the final Atlantic, thus leaving the Viking Graben as a failed arm. Rifting propagated northeast into the basins of the western Barents Shelf over a more protracted time (Faleide et al. 1984; Ziegler 1989), with strata at least as young as Aptian being bevelled by the equivalent post-rift unconformity. The Arctic (Eurasian) Basin opened en echelon to the Atlantic and the two had early-stage rift shoulders (West Halten High, Northern Svalbard) and high blocks such as the Loppa High (Wood et al. 1989). Especially in the north, ideas are converging on the model continuing to be refined by many workers, but most notably by the University of Oslo group (Talwani & Eldholm 1977; Faleide et al. 1984; Myhre & Eldholm 1988, Vågnes et al. 1988; Vågnes et al. 1992; to cite a few salient papers).

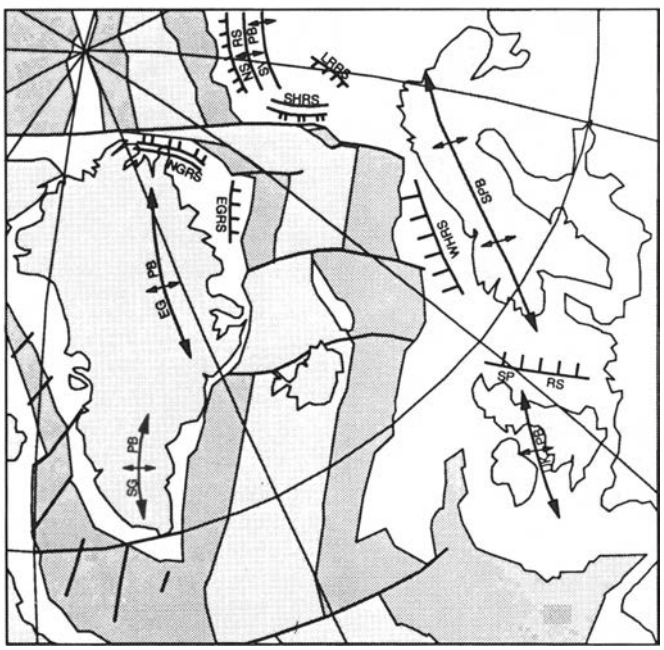

Fig. 4. Sketch map of the North Atlantic Region showing a simplified representation of features discussed in the text. Land stippled, shelves clear, pre-anomaly 13 seafloor dark gray, post-anomaly 13 seafloor light gray. Single fault symbols are Cretaceous rift shoulders, double fault symbols early Neogene rift shoulders, plunging anticline symbols are late Neogene peripheral bulges. SPRS = Shetland Platform Rift Shoulder, WHRS = West Halten Rift Shoulder, LRRS = Loppa Ridge Rift Shoulder, NSRS = North Svalbard Rift Shoulder, EGRS = East Greenland Rift Shoulder; SHRS = Stappen High Rift Shoulder, NGRS = North Greenland Rift Shoulder; UKPB = United Kingdom Peripheral Bulge, SPB = Scandinavian Peripheral Bulge, SVPB = Svalbard Peripheral Bulge, EGPB = East Greenland Peripheral Bulge, SGPB = South Greenland Peripheral Bulge. Basic map modified from Ziegler (1988).

Initiation of shearing along the then in-line Senja–Greenland–Troll land Fjord strand of the Transform in Late Cretaceous–Paleocene: (1) caused the Eureka Orogeny as a restraining bend related to that shear and, (2) shielded the southwest Barents Basins from further extension (Vågnes et al. 1988). As extension halted, thermal subsidence began in these basins, as evidenced by the more blanket-like sedimentation of the Paleogene (Spencer et al. 1984; Ziegler 1988). Breakthrough of spreading to the Hornsund Strand of the transform zone in Eocene: (1) caused structuring of the Sørvestsnaget Basin (Gabrielsen & Færseth 1988) and, (2) initiated Spitsbergen's Western Uplift and Central Basin as a restraining bend related to that shear (Vågnes et al. 1988). Vergence of the two belts was dictated by the rift–rift transform configuration, the N. Spitsbergen rift shoulder thrusting over Greenland and the NE Greenland rift shoulder thrusting over Spitsbergen.

A Mid-Tertiary westward shift in Greenland's trajectory: (1) slowed or halted extension in the Labrador Trough (Ziegler 1988), (2) arrested transpression on Spitsbergen, (3) probably initiated Forelandsundet and related basins (Vågnes et al. 1988) and, (4) created the Stappen High Rift Shoulder along the NW Barents Shelf (Wood et al. 1989) and in NE Greenland. When thrusting ceased, crust over-thickened by compression rebounded. The Askeladden Delta Sequence (Nøttvedt 1985) and Battfjellet Formation (Helland-Hansen 1990) appear to predate the lockup of the thrusts and grade into the foredeep, probably because accommadation-space was being provided by thrust loading. The overlying continental clastics of the Aspelintoppen Formation appear to be graded to base levels exterior of the foredeep, probably because accomodation space was no longer being created in the local basin when thrusting stopped – both basin and uplift should rebound. If the amount of eroded section is accounted for (Manum & Throndsen 1978), the transition was probably initiated at approximately the same anomaly 13 (Early Oligocene) which seems to indicate the time of change of motion of Greenland, based on the seafloor record (Myhre & Eldholm 1988; Vågnes et al. 1988).

The change in plate motion turned the Hornsund transpressional transform into the Hornsund obliquely opening rift. Since the Atlantic and Eurasian basins had opened previously, the only area of the newly defined plate boundary in which the early-stage asthenosphere swell was available under continental crust to create a rift shoulder was along the west rim of the Barents shelf form the Stappen High north, and the conjugate margin of NE Greenland. This accounts for the presence of a Neogene rift shoulder, giving greater amounts of uplift centered on the Stappen High (Wood et al. 1989).

Neogene peripheral bulges formed adjacent to the Arctic's Eurasian Basin (Svalbard) and Atlantic Basin (Scandinavia, Great Britain, and east Greenland). Onshore relations on N. Spitsbergen suggest that peripheral bulge has risen 1.5 km or more within the last 11 m.y.

Offshore relations off Mid-Norway suggest that Scandinavia rose as a peripheral bulge starting in the Miocene. A master maximum flooding surface at T20 (near top Miocene) appears to underlie the westward prograding and downlapping Sula Group, constraining initiation of the uplift. Riis (1992) suggests that much of this uplift has taken place within the last 2–3 m.y. The North Sea's denser rifted crust repressed fromation of a peripheral bulge, thereby isolating the British and Scandinavian segments of the bulge. The situation is similar in eastern South America, where the Amazon failed rift separates the Brazilian and Guayana segments of that peripheral bulge.

Glacial erosion removes the youngest and least-dense sediments. It has to leave the isostatic column shorter and with a greater average density after glaciation than before. To accommodate this, the surface must be lowered, even though strata under the surface are raised (Vågnes et al. 1992). These authors suggest: 'Assuming that the eroded areas in the Barents Sea were at sea level prior to the onset of glaciations, a simple relation should exist between present water depth and the amount of erosion. For example, a water depth of 100 m implies that 200–300 m of overburden have been removed, depending on the density of the eroded material.' Greater amounts were removed where tectonic causes had elevated the crust so that it was more vulnerable to glaciation. This mechanism explains much of the Barents Shelf's bathymetry, but it cannot account for Scandinavia's uplift, which is almost surely tectonic, i.e. a peripheral bulge.

Influence on petroleum accumulations

Rapid late subsidence and sedimentation, due to both pre-subduction instability and accelerated glacial erosion, maximize recent hydrocarbon expulsion and seal integrity. This is important to hydrocarbon accumulation, reducing the need for long-term retention at the same time inhibiting fracturing of the seal rocks. The biggest single indicator of a productive Mesozoic rift is the presence of a thick overlying Tertiary subsidence basin.

Uplift generally degrades productivity, though variably. Geochemical burnout levels are raised and reservoir diagenesis and seal brittleness are enhanced. Expanding gas may flush oil from some traps, though other traps may actually have more room for oil after uplift than before. Sealed pressure compartments are apt to be damaged by uplift, whereas those areas of reservoir open to the sea floor are less vulnerable. Shallow traps may be most at risk because they are uplifted proportionally more than deeper ones, and because there is less pressure difference between the hydrostatic and the fracture (80% of lithostatic) gradient at shallow depths. Yet deeper traps are often not viable because of elevated burnout or advanced diagenesis. Thus the prospecting depth window is narrowed by uplift.

Glacial erosion further increases sedimentation rates already accelerated by pre-subduction instability. This improved productivity in the Viking Graben and Mid-Norway, but hindered it in the Barents Shelf, since the latter was a source area for clastics, rather than a depocentre. Rapid glacial onset, erosion and melting may stress traps more than slower tectonic mechanisms, because pressure regimes have more difficulty equilibrating.

A logical master picture seems to be emerging in which a few basic tectonic mechanisms, active at appropriate times and places in the cycle of the opening Atlantic, produced the observed uplift and subsidence history. These in turn influenced hydrocarbon accumulation in a predictable fashion.

Manuscript received October 1991

References

Bally, A. W., Gordy, P. L. & Stewart, G. A. 1966: Structure, seismic data and orogenic evolution of southern Canadian Rocky Mountains. *Canadian Petroleum Geology Bulletin 14*, 337–381.

Beaumont, C. 1978: The evolution of sedimentary basins on a visco-elastic lithosphere: theory and examples. *Geophysical Journal of the Royal Astronomical Society 55*, 471–498.

Christiansen, F. G., Larsen, H. C., Marcussen, C., Hansen, K., Krabbe, H., Larsen, L. M., Piasecki, S., Stemmerik, L. & Watt, W. S. 1992: Uplift study of the Jameson Land basin, East Greenland, *Norsk Geologisk Tidsskrift 72*. This volume, pp. 291–294.

Cloetingh, S., Reemst, P., Kooi, H. & Fanavoll, S. 1992: Intraplate stresses and the post-Cretaceous uplift and subsidence in northern Atlantic basins. *Norsk Geologisk Tidsskrift 72*. This volume, pp. 229–235.

Faleide, J. I., Gudlaugsson, S. T. & Jacquart, G. 1984: Evolution of the Western Barents Sea. *Marine and Petroleum Geology 1*, 123–150.

Gabrielsen, R. H. & Færseth, R. R. 1988: Cretaceous and Tertiary reactivation of master fault zones of the Barents Sea. *In* Dallmann, Ohta & Andresen (eds.): *Tertiary Tectonics of Svalbard. Norsk Polarinstitutt Report 46*, 93–97.

Girdler, R. W. 1975: The great negative Bouguer gravity anomaly over Africa. EOS Transactions. *American Geophysical Union 56*, 516–519.

Hamilton, W. 1979: Tectonics of the Indonesian Region. *United States Geological Survey Professional Paper 1078*, 345 pp.

Helland-Hansen, W. 1990: Paleogene foreland basin, Spitsbergen. *American Association of Petroleum Geologists Bulletin 74*, 260–272.

Heller, P. L., Wentworth, C. M. & Poag, C. W. 1982: Episodic post-rift subsidence of the United States Atlantic continental margin. *Geological Society of America Bulletin 93*, 379–390.

Holmes, A. & Holmes, D. L. 1978: *Holmes Principles of Physical Geology*. 3rd ed., 738 pp. Nelson & Sons Ltd., Middlesex, UK.

Jackson, J. A. & McKenzie, D. P. 1983: The geometric evolution of normal fault systems. *Journal of Structural Geology 5*, 471–482.

Jarvey, M. T. 1988: Quantitative geological modeling of siliciclastic rock sequences and their seismic expression. *Society of Exploration Paleontologists and Minerologists Special Publication 42*, 47–69.

Magara, K. 1989: Isostatic balance during sediment loading and unloading in continental margins. *Journal of Petroleum Geology 12*, 437–452.

Manum, S. & Throndsen, T. 1978: Rank of coal and dispersed organic matter and its geological bearing on Spitsbergen Tertiary. *Norsk Polarinstitutt Årbok, 1977*, 159–177.

McKenzie, D. P. 1978: Some remarks on the development of sedimentary basins. *Earth and Planetary Science Letters 40*, 25–32.

Mohriak, V. U., Mello, M. R., Kerner, G. D., Dewey, J. F. & Maxwell, J. R. 1989: Structural and Stratigraphic evolution of the Campos Basin, Offshore Brazil. *In* Tankard, A. J. & Balkwill, H. R.: Extensional tectonics and stratigraphy of the North Atlantic margins. *American Association of Petroleum Geologists Memoir 46*, 557–598.

Myhre, A. M. & Eldholm, O. 1988: The west Svalbard margin. Marine and Petroleum Geology *5*, 134–156.

Nøttvedt, A. 1985: Askeladden delta sequence (Paleocene) on Spitsbergen – sedimentation and controls on delta formation. *Polar Research 3*, 21–48.

Oldenburg, D. W. & Brune, J. N. 1972: Ridge-transform fault spreading pattern in freezing wax. *Science (AAAS) 178*, 301–304.

Riis, F. 1992: Dating and measuring of erosion, uplift and subsidence in Norway and the Norwegian shelf in glacial periods. *Norsk Geologisk Tidsskrift 72.* This volume, pp. 325–331.

Sales, J. K. 1987: Tectonic models. *In* Seyfert, C. K. (ed.): *Encyclopedia of Structural Geology and Plate Tectonics*, 785–794. Van Nostrand Reinhold, New York.

Sclater, J. G. & Celerier, B. 1988: Extensional models for the formation of sedimentary basins and continental margins. *Norsk Geologisk Tidsskrift 67*, 253–268.

Spencer, A. M., Home, P. C. & Berglund, L. T. 1984: *Tertiary Structural Development of the West Barents Shelf. Petroleum Geology of North European Margin*, 199–210. Norwegian Petroleum Society. Graham & Trotman, London.

Spencer, A. M. & Larsen, V. B. 1990: Fault traps in the northern North Sea. *In* Hardman, R. F. P. & Brooks, J. (eds.): Tectonic events responsible for Britain's oil and gas reserves. *Geological Society of London Special Publication 55*, 281–298.

Talwani, M. & Eldholm, O. 1977: Evolution of the Norwegian–Greenland Sea. *Geological Society of America Bulletin 88*, 969–999.

Vågnes, E. Reksnes, P. A., Faleide, J. I. & Gudlaugsson, S. T. 1988: Plate tectonic constraints on the formation of the Spitsbergen fold and thrust belt. *In* Dallmann, W. K., Ohta, Y. and Andresen, A. (eds.): *Tertiary Tectonics of Svalbard. Norsk Polarinstitutt Report Series 46*, 105–108.

Vågnes, E., Faleide, J. I. & Gudlaugsson, S. T. 1992: Glacial erosion and tectonic uplift in the Barents Sea. *Norsk Geologisk Tidsskrift 72.* This volume, pp. 333–338.

Wernicke, B. 1986: Whole-lithosphere normal simple shear: an interpretation of deep reflection profiles in Great Britain. *American Geophysical Union Geodynamic Series 14*, 331–339.

Wernicke, B. & Tilke, P. G. 1989: Extensional tectonic framework of the U.S. Central Atlantic passive margin. *In* Tankard, A. J. & Balkwill, H. R. (eds.): Extensional tectonics and stratigraphy of the North Atlantic Margins. *American Association of Petroleum Geologists Memoir 46*, 7–22.

White, N. 1990: Nature of lithospheric extension in the North Sea. *Geology 17*, 111–114.

Wood, R. J., Edrich, S. P. & Hutghinson, I. 1989: Influence of North Atlantic tectonics on the large-scale uplift of the Stappen High and Loppa High, western Barents Shelf. *In* Tankard, A. J. & Balkwill, H. R. (eds.) Extensional tectonics and stratigraphy of north Atlantic margins. *American Association of Petroleum Geologists Memoir 46*, 559–575.

Ziegler, P. A. 1988: Evolution of the Arctic–North Atlantic and the Western Tethys. *American Association of Petroleum Geologists Memoir 43*, 198 pp., plus 30 plates under separate cover.

Ziegler, P. A. 1989: Evolution of the North Atlantic – an overview. *American Association of Petroleum Geologists Memoir 46*, 111–129.

The Base Tertiary Surface of southern Norway and the northern North Sea

ANTHONY GEORGE DORÉ

Doré, A. G. The Base Tertiary Surface of southern Norway and the northern North Sea. *Norsk Geologisk Tidsskrift*, Vol. 72, pp. 259–265. Oslo 1992. ISSN 0029-196X.

Sketch maps and sections across the high-level planation surface of southern Norway (roughly represented by the summit-height envelope) and the Base Tertiary offshore suggest that these two surfaces can be regarded as a single coherent feature. Arguments are presented that the surface resulted from late Mesozoic base levelling and major Late Cretaceous transgression. Subsequent gentle warping of the surface is ascribed to variations in the regional stress field during the Cenozoic. This process was accentuated by erosion of the upwarped landmass, isostatic rebound and flexural response to sediment loading in the adjacent basin. Such effects were particularly prominent during the late Cenozoic glaciations.

A. G. Doré, Conoco Norway Inc., PO Box 488, N-4001 Stavanger, Norway.

Introduction and historical review

The simple exercise of hill-walking in western Norway, or flying over the region, cannot fail to impress upon the observer the remarkable summit height concordance of the highlands. This is a local illustration of a regional phenomenon. The 'summit height envelope', merging into flat-topped 'vidde' terrain, defines a gently graded surface that cuts across a wide variety of bedrock structures. It has been recognized for more than a century as one of the most distinctive aspects of Norway's geomorphology. There is general agreement that the feature must represent the remains of a planation surface, formed prior to, or during the Tertiary, and subsequently uplifted and gently deformed. In southern Norway, elements of a much older planation surface – the 'sub-Cambrian peneplain' formed by the contact between transgressive Cambrian shales and eroded Archean/Proterozoic basement – may be incorporated into the overall envelope (Strøm 1948). The surface shows evidence of weathering, probably under much warmer climatic conditions than those of the present, giving rise to a distinctive suite of geomorphological features recognized throughout Norway and sometimes referred to as the 'paleic surface' (Gjessing 1967). High-level autochthonous block fields described in parts of southern Norway have also been interpreted as representing a preglacial weathering surface (Nesje et al. 1988). These features are distinct from the more extreme, younger forms, dominated by incised fluvial systems and glacial erosion, which deeply dissect the old planation surface.

From the aforegoing discussion, it can readily be appreciated that the literature defines a wide variety of 'surfaces' in southern Norway (summit height, sub-Cambrian, block-field) and that these are often implied to be distinct from one another. It is significant, however, that the surfaces often occupy approximately the same level and frequently merge into each other. This observation leads to the central hypothesis of this paper – that a single, first-order surface can be defined which incorporates pre-existing unconformities and which has been extensively modified since its formation. This feature, together with its postulated extension into the subsurface offshore, is herein termed the 'Base Tertiary Surface'.

The present elevation and attitude of the surface is a topic that has generated much speculation. A link with the Tertiary mountain-building episodes in the Alpine domain has been postulated by Gjessing (1967) and others. Holtedahl (1953) drew attention to the concentration of highlands along the western margin of Fennoscandia and suggested that the Tertiary uplift was oblique in nature, facilitated by movements on faults bordering the present coastline. It is now recognized that such faults do exist, although they are essentially Mesozoic features and the degree to which they were active during the Tertiary is still a matter for debate. Widespread acceptance of plate tectonic theory in the late 1960s led to speculation that elevation of the Fennoscandian surface may relate to the early Eocene opening of the North Atlantic (Torske 1972). Torske documented the Tertiary surface of Southern and Mid-Norway (Fig. 1) and described it in terms of Red Sea-style rift-shoulder uplift occurring prior to, and during, continental separation.

The importance of these ideas was probably not realized until the 1980s, when drilling results in the Barents Sea provided unequivocal evidence that this area also, was subjected to major uplift and erosion in Cenozoic times. A reasonable conclusion from the available evi-

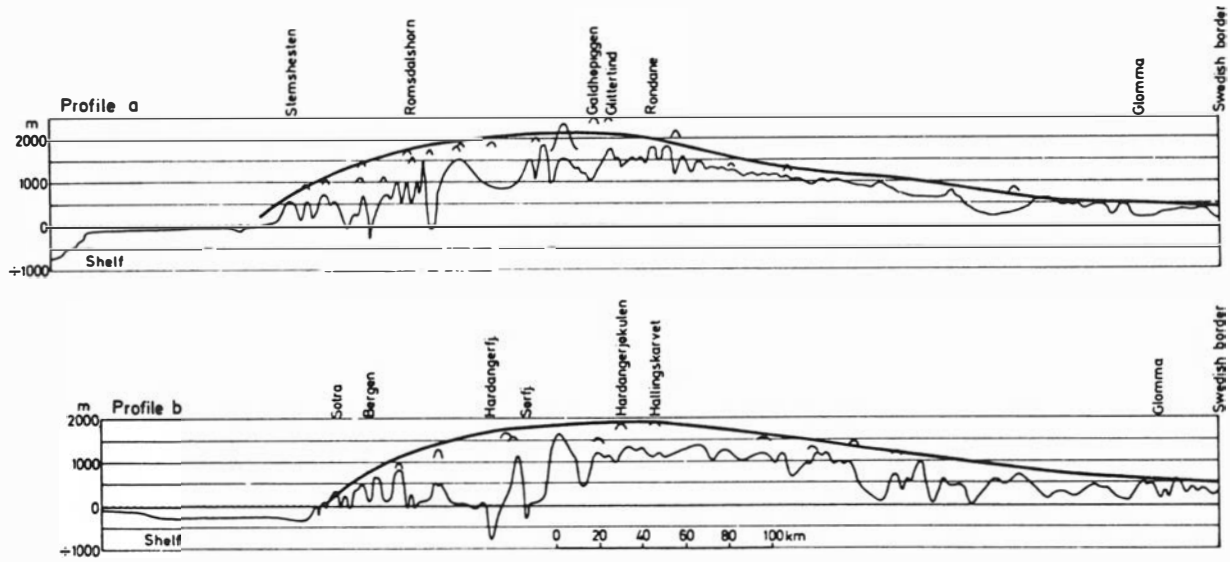

Fig. 1. Schematic profiles of the Norwegian landmass from Torske (1972), indicating the summit height envelope. Location of profiles is shown in Fig. 2. Vertical exaggeration 20×.

dence was that the Barents Sea and Fennoscandian uplift were related phenomena of similar magnitude, despite the obvious differences between these two areas in terms of erosion and present relief. This concept is shown in Fig. 2. Cenozoic uplift is now known to have extended from Spitsbergen, through the Barents Sea and western Norway, to the Farsund Basin off the southern Norwegian coast. A large number of hypotheses is now available to explain this phenomenon, and multiple causes seem likely. However, there is some consensus that a link must exist between the uplift and its position immediately adjacent to the North Atlantic passive margin. This direct causality cannot, however, exist for southern Norway and the Skagerrak, which border the intracratonic basin system of the northern North Sea.

Origin and definition of the Base Tertiary Surface

Formation of the high-level planation surface of southern Norway must represent a prolonged period of base-levelling. Although some authors have implied an intra-Tertiary origin, the evidence for repeated landmass rejuvenation in the Tertiary (see other papers in this volume) suggests little scope for the extended period of stability required to form such a widespread surface. It is proposed here that the surface more probably developed during the great rifting events of the Mesozoic, when vast quantities of coarse clastic material were eroded from the rift margins and transported into the adjacent, rapidly subsiding basins. The rifting reached its acme in the Late Jurassic, after which there was a long period during which relief was progressively reduced. These events were followed by the major transgression of the Late Cretaceous, an episode of global scale that produced one of the greatest inundations of continental margins in geological history (Hancock & Kauffman 1979). Lithostratigraphic correlation in the Norwegian North Sea (Isaksen & Tonstad, 1989, Figs. 7–11) shows that, by the end of this period, virtually all of the remaining paleohighs had been transgressed. This situation probably also prevailed off parts of Mid-Norway, where bevelling and transgression of intra-basinal highs during the Late Cretaceous is spectacularly demonstrated on seismic lines (e.g. Brekke & Riis 1987). Deposition during the latest Cretaceous was almost universally fine grained – pelagic carbonates and mudstones – indicating that any remaining areas of relief must have been subdued.

The extent to which the Late Cretaceous transgression eroded and flooded the main Fennoscandian Shield is unknown. However, it is largely immaterial whether the 'summit height envelope' represents a marine planation surface (i.e. an exhumed unconformity originally produced by gradual rise in sea level during the Late Cretaceous) or a peneplain (i.e. a surface formed by a prolonged period of continental erosion). What is important here is that, by the end of the Cretaceous, a very gently graded surface probably existed between the deeply-eroded landmass and the adjacent seabed. This postulate can be summarized as follows: *SUMMIT HEIGHT ENVELOPE ONSHORE is equivalent to BASE TERTIARY HORIZON OFFSHORE equals 'BASE TERTIARY SURFACE'*.

From this hypothesis, it follows that the present attitude of the surface (the depth of the Base Tertiary horizon and the height of the 'envelope') can be taken to represent the net deformation, on a first-order scale, that has occurred since the beginning of the Tertiary. The credibility of this idea can, therefore, be tested by combining the two surfaces to determine whether they form a coherent feature. Such an exercise is shown in Fig. 3, produced by juxtaposing a regional Base Tertiary map of the North Sea and a smoothed summit height elevation map of southern Norway.

This map, its isometric projection (Fig. 4) and the E–W cross-sections of Fig. 5, can all be seen to define a gentle,

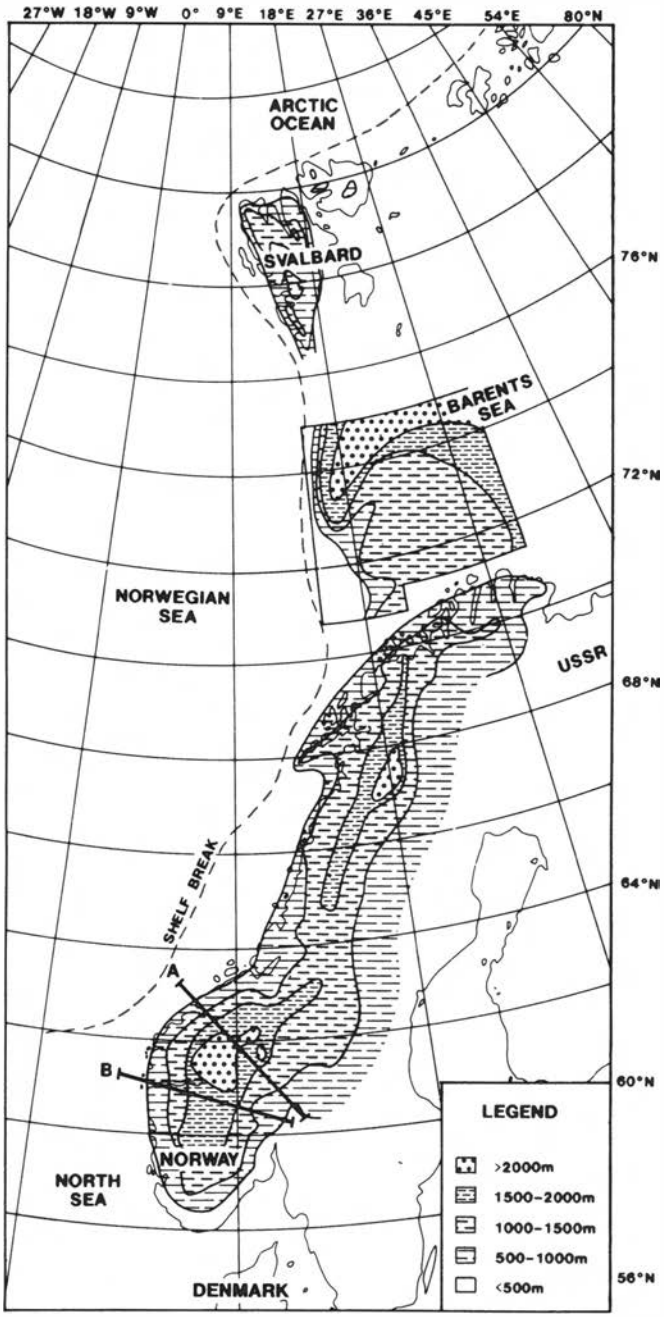

Fig. 2. Combined Cenozoic uplift (Barents Shelf) and smoothed relief map of western Scandinavia.

rather symmetrical flexure. The amplitude of the feature varies surprisingly little; from 4.65 km in the north to 4.15 km in the south, and the half-wavelength is remarkably constant at about 300 km measured in an E–W direction. Elevation of the surface with respect to present sea level varies significantly, however. The highlands of the north, including the Jotunheimen peaks rising to ca. 2450 m, lie adjacent to a Tertiary basin about 2200 m deep. In the south, the entire surface is depressed with lower peaks on the mainland and a correspondingly deeper adjacent basin. Further south still, the entire surface lies below present sea level.

Deformation of the Base Tertiary Surface

The map of Fig. 3 and cross-sections of Fig. 5 all suggest that gentle warping can for the most part account for the deformation of the surface, without necessity for significant displacement on Mesozoic marginal fractures such as the Horda–Øygarden Fault Zone. This conclusion has also been reached by Ghazi (this volume) and Jensen & Schmidt (this volume) from detailed observation of the Tertiary sequences flanking the present landmass. It contrasts strongly with the interpretation of the Northern North Sea by Rundberg (1989), who invokes substantial Tertiary reactivation along the Øygarden Fault Zone and cites as evidence the wedge-shaped nature of several of the offshore sequences. It is significant, however, that due to subsequent truncation these wedges were nowhere observed to intersect the Mesozoic fault system. Without additional evidence, therefore, this geometry can equally well be described as a series of truncated progradational units, derived from a flexurally uplifted landmass. Such an interpretation does not preclude more limited Cenozoic activity on the fault zone, resulting from thermal subsidence and/or sediment loading in the adjacent basin, and from post-glacial isostatic readjustment (e.g. Gabrielsen 1989).

It is tempting to envisage a purely passive origin for the deformation of the Base Tertiary Surface. Flexural bulge associated with sediment loading in the adjacent basin, coupled with an Early Tertiary drop in sea level, could have resulted in erosion and unloading of the exposed landmass, which will then have been isostatically uplifted. Rapid deposition of erosion products in the basin will have produced more load-induced subsidence, more flexural bulge, and so on until an equilibrium is reached. Accelerated erosion and deposition during the glacial episodes should logically have been a major contributor to this effect (Fig. 6). In such a scenario, the increasing height of the surface towards the north could be a function of proximity to the Atlantic margin, where the cumulative deformation may include thermal uplift of the rift margins during Early Tertiary plate separation. There are, however, two major difficulties with this 'self-perpetuating' passive model:

1. The strongly episodic nature of Tertiary sedimentation adjacent to the landmass, indicating periods of accelerated rejuvenation. In the Northern North Sea, Rundberg (1989) identifies such important phases as occurring in Paleocene, Late Eocene–Early Oligocene and Pliocene times. In the Stord Basin, Ghazi (this volume) describes a broadly similar picture with the exception of the mid-Tertiary episode, which he dates as Late Oligocene–Miocene. Both are agreed on the particular significance of the Pliocene rejuvenation. Unless such episodes are purely a result of eustatic sea level fall, they must surely indicate a more active and temporally variable tectonic drive for the deformation.

2. Mechanical simulation of passive margin deformation for a wide range of lithospheric models (Stein et al.

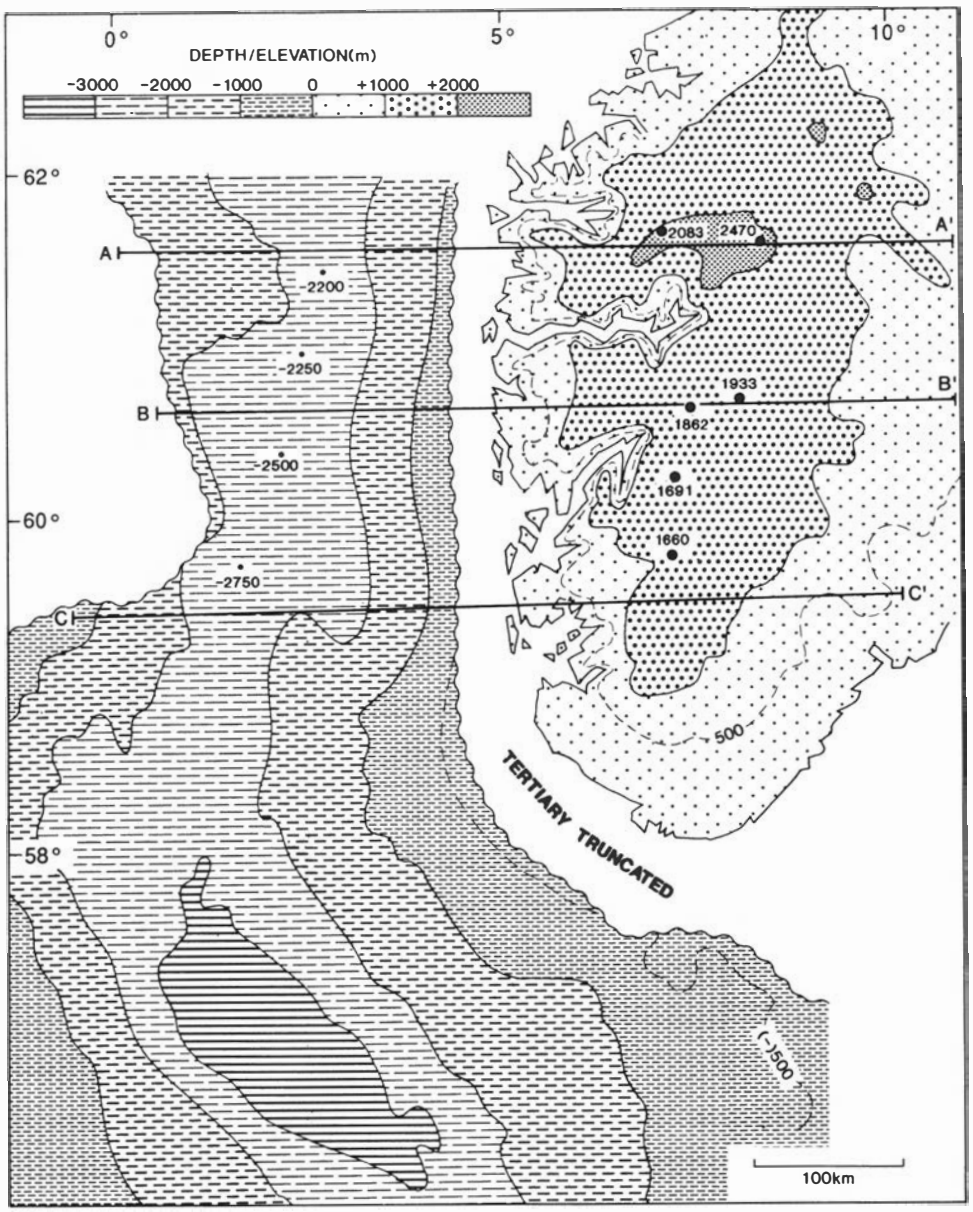

Fig. 3. Southern Norway: map of depth subsea to Base Tertiary (offshore) and smoothed summit height envelope (onshore) defining the 'Base Tertiary Surface'.

1989) consistently fails to predict the amount of peripheral bulge, resulting from sediment downloading alone, necessary to explain the current elevation of southern Norway. This seems to suggest the necessity for an additional tectonic mechanism for the uplift. Note, however, that passive mechanisms (flexural bulge and isostasy) can produce a significant elevation of the *summit height surface* while producing only a minor effect on the *mean elevation* if deeply incised valleys are the geomorphological norm (Molnar & England 1990).

If an additional tectonic mechanism is required, it should probably be sought in the varying stress field that must have existed within the NW European plate during the Cenozoic, resulting from the combined effect of spreading reorganizations in the North Atlantic and closure events in the Tethyan domain to the southeast. It seems inconceivable that these well-documented events, taking place at the plate margin, would have had no effect whatsoever on the deformation of the Base Tertiary Surface.

A final note is desirable here on the association between glaciation and Neogene uplift. The broad contemporaneity of the glacial epoch and the latest (and most important) uplift phase of Fennoscandia has led Riis & Fjeldskaar (in press) to propose that glacial erosion and isostatic re-equilibration is the primary mechanism for uplift of the 'summit height envelope'. Riis & Fjeldskaar admit that the present elevation of western Fennoscandia (particularly southern Norway) cannot be fully explained by this mechanism, and postulate that phase changes in the lower lithosphere may contribute to the uplift effect. It is possible, however, to reverse the argument and propose that tectonically-driven uplift in the Neogene, in combination with the known global climatic cooling trend of the Cenozoic, may have itself triggered the glaciations (Fig. 6). The onset of glaciation due to the

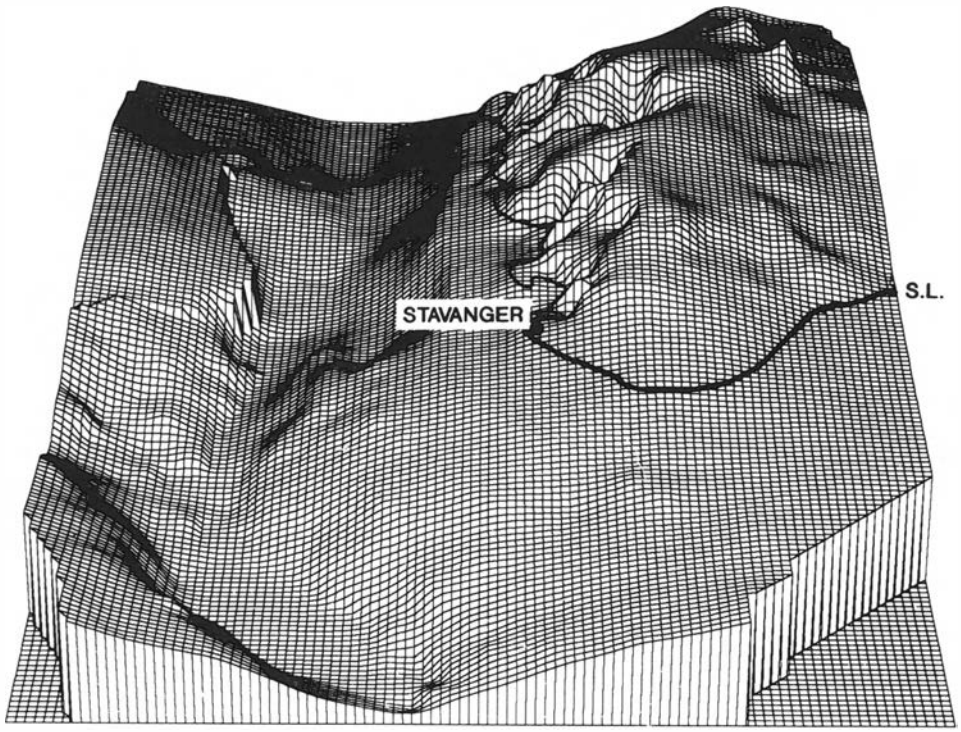

Fig. 4. Isometric projection of the 'Base Tertiary Surface' shown in Fig. 3. Viewed from the south with 30 × vertical exaggeration.

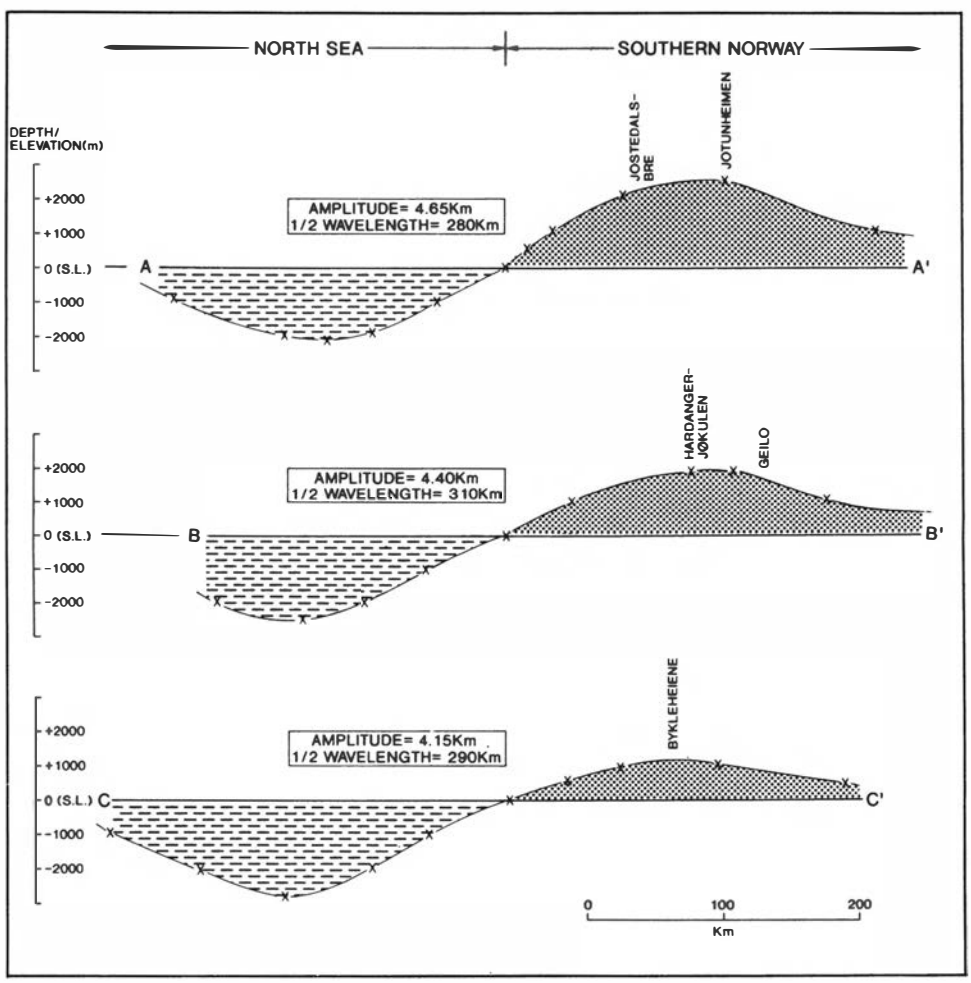

Fig. 5. Smoothed E–W cross-sections of the 'Base Tertiary Surface' produced from Fig. 3. The Quaternary strandflat and the offshore Tertiary truncation zone are eliminated by the smoothing. Locations shown in Fig. 3. Vertical exaggeration 25 ×.

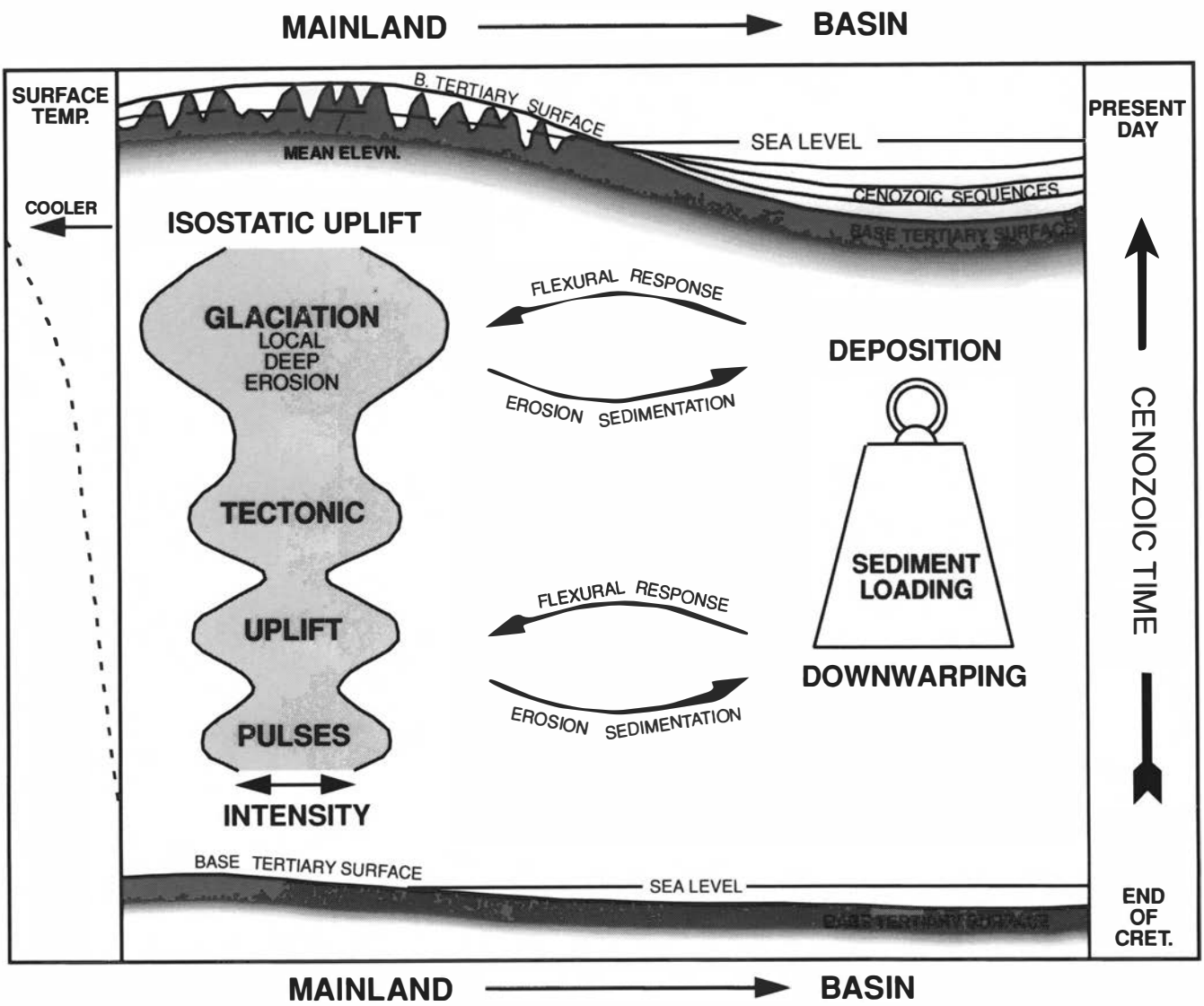

Fig. 6. Cartoon showing an integrated concept for deformation of the 'Base Tertiary Surface'. The initial low-relief surface produced by Mesozoic base-levelling and Late Cretaceous transgression undergoes gentle tectonic warping, further emphasized by erosion, isostasy and flexural response to sediment loading. The topography thereby produced provides the focus for glaciation, intense differential erosion and consequent isostatic elevation of the surface.

creation of extensive highlands is an old idea that is gaining new support (e.g. Cloetingh et al. 1990). It is an attractive hypothesis, since it specifies a single causal mechanism (Neogene change in the regional stress field) with the potential to explain the inception of the Neogene uplift/subsidence phenomenon, its magnitude, and the commencement of glacial activity.

Conclusions

1. It is postulated that the Base Tertiary horizon offshore and summit height envelope of southern Norway represent a coherent and roughly time-equivalent surface, produced by prolonged late Mesozoic base-levelling and major Late Cretaceous transgression.

2. Cenozoic deformation of the surface in southern Norway and the Northern North Sea occurred primarily by gentle warping without significant reactivation of offshore Mesozoic faults.

3. Elevation of southern Norway, adjacent to a subsiding intracratonic basin, cannot be explained by 'Red Sea', rift-shoulder uplift associated with North Atlantic opening. This effect may, however, contribute to the increased elevation of the surface in the north.

4. A passive model involving erosion and sediment loading may explain part of the net deformation of the Base Tertiary Surface. However, it seems likely that the main episodes of differential movement represent accentuation by other means. A varying stress regime, associated with North Atlantic plate reorganization and Tethyan closure events, is considered the most likely mechanism. These effects probably created the initial topography that allowed the continental ice sheets to nucleate, with consequent deep erosion and further isostatic elevation of the remnant Base Tertiary Surface.

Acknowledgements. – My thanks to Samir Ghazi and Ian Walker for critical reading the manuscript, and to Donald Dorn-Lopez for creating the perspective plot shown in Fig. 4.

Manuscript received October 1991

References

Brekke, H. & Riis, F. 1987: Tectonics and basin evolution of the Norwegian shelf between 62° and 72° *Norsk Geologisk Tidsskrift 67*, 295–321.

Cloetingh, S., Goradstein, F. M., Kooi, H., Grant, A. C. & Kaminski, M. 1990: Plate reorganization: a cause of rapid late Neogene subsidence and sedimentation around the North Atlantic. *Journal of the Geological Society 147*, 495–506.

Gabrielsen, R. H. 1989: Reactivation of faults on the Norwegian Continental Shelf and its implication for earthquake occurrence. *In* Gregersen, S. & Basham, P. W. (eds): *Earthquakes at North-Atlantic Passive Margins: Neotectonics and Postglacial Rebound*, 67–90. Kluwer, Dordrecht.

Ghazi, S. A. 1992: Cenozoic uplift in the Stord Basin area and its consequences for exploration. *Norsk Geologisk Tidsskrift 72.* This volume, pp. 285–290.

Gjessing, J. 1967: Norway's Paleic Surface. *Norsk Geographisk Tidsskrift 21*, 69–132.

Hancock, J. M. & Kauffman, E. G. 1979: The great transgressions of the Late Cretaceous. *Journal of the Geological Society 136*, 175–186.

Holtedahl, O. 1953: On the oblique uplift of some Northern lands. *Norsk Geographisk Tidsskrift 21*, 69–132.

Jensen, L. N. & Schmidt, B. J. 1992: Late Tertiary uplift and erosion in the Skagerrak area; magnitude and consequences. *Norsk Geologisk Tidsskrift 72.* This volume, pp. 275–279.

Molnar, P. & England P. 1990: Late Cenozoic uplift of mountain ranges and global climate changes: chicken or egg? *Nature 346*, 29–34.

Nesje, A., Dahl, S. O., Anda, E. & Rye, N. 1988: Block fields in southern Norway: significance for the Late Weichselian ice sheet. *Norsk Geologisk Tidsskrift 68*, 149–169.

Riis, F. & Fjeldskaar, W.: On the magnitude of the Late Tertiary and Quaternary erosion and its significance for the uplift of Scandinavia and the Barents Sea. *In* Larsen, R. M. et al. (eds). *Structural and Tectonic Modelling and its Application to Petroleum Geology*. Norwegian Petroleum Society (NPF). Elsevier, Amsterdam (in press).

Rundberg, Y. 1989: Tertiary sedimentary history and basin evolution of the Norwegian North Sea between 60°N and 62°N. An integrated approach. Dr. ing. thesis, University of Trondheim, Norway.

Stein, S., Cloetingh, S., Sleep, N. H. & Wortel, R. 1989: Passive margin earthquakes, stresses and rheology. *In* Gregersen, S. & Basham, P. W. (eds): *Earthquakes at North-Atlantic Passive Margins: Neotectonics and Postglacial Rebound*, 231–259. Kluwer, Dordrecht.

Strøm, K. M. 1948: The geomorphology of Norway. *Geographical Journal 112*, 19–27.

Torske, T. 1972: Tertiary oblique uplift of Western Fennoscandia; crustal warping in connection with rifting and break-up of the Laurasian continent. *Norges Geologisk undersøkelse 273*, 43–48.

Neotectonism in the Jæren area, southwest Norway

EDITH M. G. FUGELLI & FRIDTJOF RIIS

Fugelli, E. M. G. & Riis, F.: Neotectonism in the Jæren area, southwest Norway. *Norsk Geologisk Tidsskrift*, Vol. 72, pp. 267–270. Oslo 1992. ISSN 0029-196X.

Glaciomarine clays of Weichselian age lie at about 200 m above sea level in the Jæren area. The high-lying sediments are located east of the Gannsfjord lineament, which seems to be developed as a fault in the area. The clays appear to be uplifted by recent tectonic movements caused by reactivation of this fault.

E. M. G. Fugelli, Statoil, Forushagen, PO Box 300, N-4001 Stavanger, Norway; F. Riis, Norwegian Petroleum Directorate, Prof. Olav Hanssensvei 10, PO Box 600, N-4001 Stavanger, Norway.

The Jæren area (Fig. 1) has been an area of interest for generations of geologists. Many of the geologic localities were well known as early as at the beginning of this century. Bio- and lithostratigraphic investigations show glaciomarine sediments and tills mainly of Weichselian age, 130,000–13,000 years BP (Fig. 2). The glaciomarine sediments, mainly clays, lie at about 200 m above sea level at Opstad and Høgemork (Milthers 1911, 1913; Feyling-Hanssen 1964, 1971; Andersen et al. 1987). Similar sediments have been described from Gjesdal (approximately 160 m a.s.l.) (Østmo 1971). The high-lying location of the sediments is difficult to explain by glacial isostasy, and our presentation is a contribution to this discussion.

The Gannsfjord lineament, described by several authors as the 'Gannsfjord-fault', follows a north–south trend (Fig. 1). The lineament extends southwards as an approximate boundary between the Caledonian gneiss/phyllite to the west and Precambrian gneiss to the east. The lineament represents a morphological boundary. Along the coast we observe flat-lying areas (Låg–Jæren). The mountains and higher areas rise to the east and are called Høg–Jæren. Both Opstad and Høgemork lie in the Høg–Jæren area. The trend of the Gannsfjord lineament seems to be parallel to the trend of the Paleozoic basins (Carboniferous–Permian) in the North Sea which were probably reactivated in Jurassic time (Fig. 1).

How can the high-lying sediments east of the lineament be explained? If the lineament is a fault, it could have been reactivated during periods with ice-melting because of pressure-release when the ice-cap disappeared. This fault has if not its continuation at least its analogy in the Vindafjord–Yrkjefjord fault system (Fig. 1). In this area Karl Anundsen has measured recent movements (Anundsen pers. comm.).

Using field observations and topographic maps, we have tried to map a pre- to Early Weichselian surface in Høg–Jæren. This surface is defined by the break in slope at the foot of several high areas (hills, etc.). The altitude of the surface rises from 60 m in the west to 300 m in the east. In Fig. 3, the shaded areas indicate ground above the mapped surface, and the approximate altitude of the break in slope is contoured. Further to the north of Jæren we observe the same phenomena, but for the time being we concentrate on south Rogaland. Here, the contour lines lie very close together at the fault line. This most likely reflects a young faulting. A rather steep rise to the east of the southern section of the surface possibly indicates a monoclinical structure. Off the coast a similar monoclinical structure is indicated by seismic reflection profiles where Quaternary layers dip from the coast in an offshore direction (Fig. 4b).

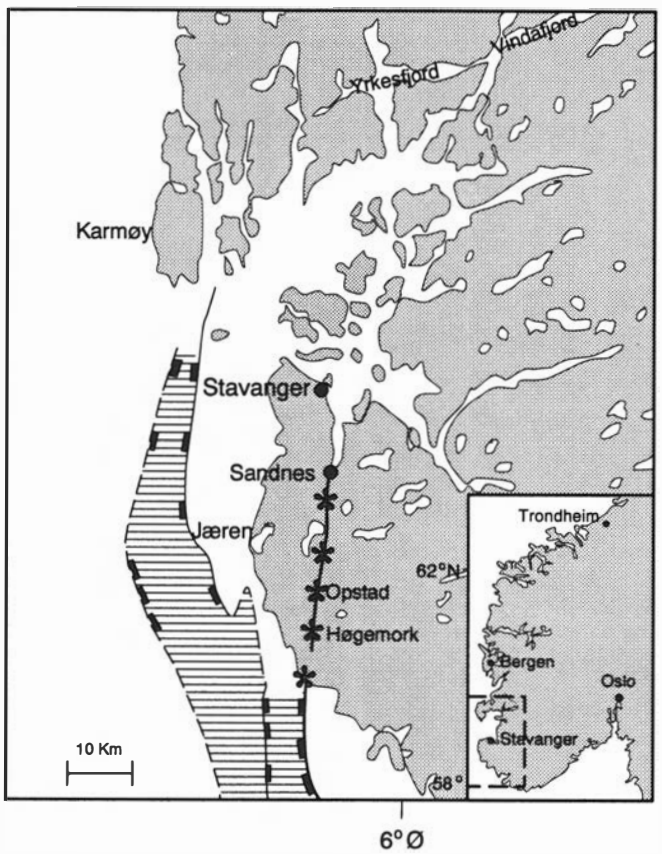

Fig. 1. Jæren with the investigated localities. The Paleozoic basin is marked with horizontal lines. The Gannsfjord lineament is marked with stars.

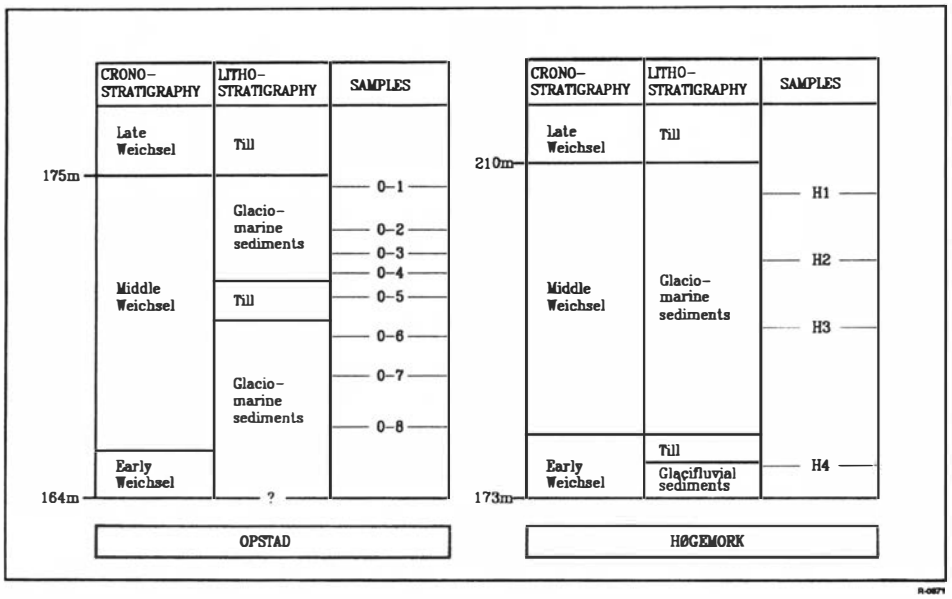

Fig. 2. Litho- and chronostratigraphic columns of the two described sections on Jæren.

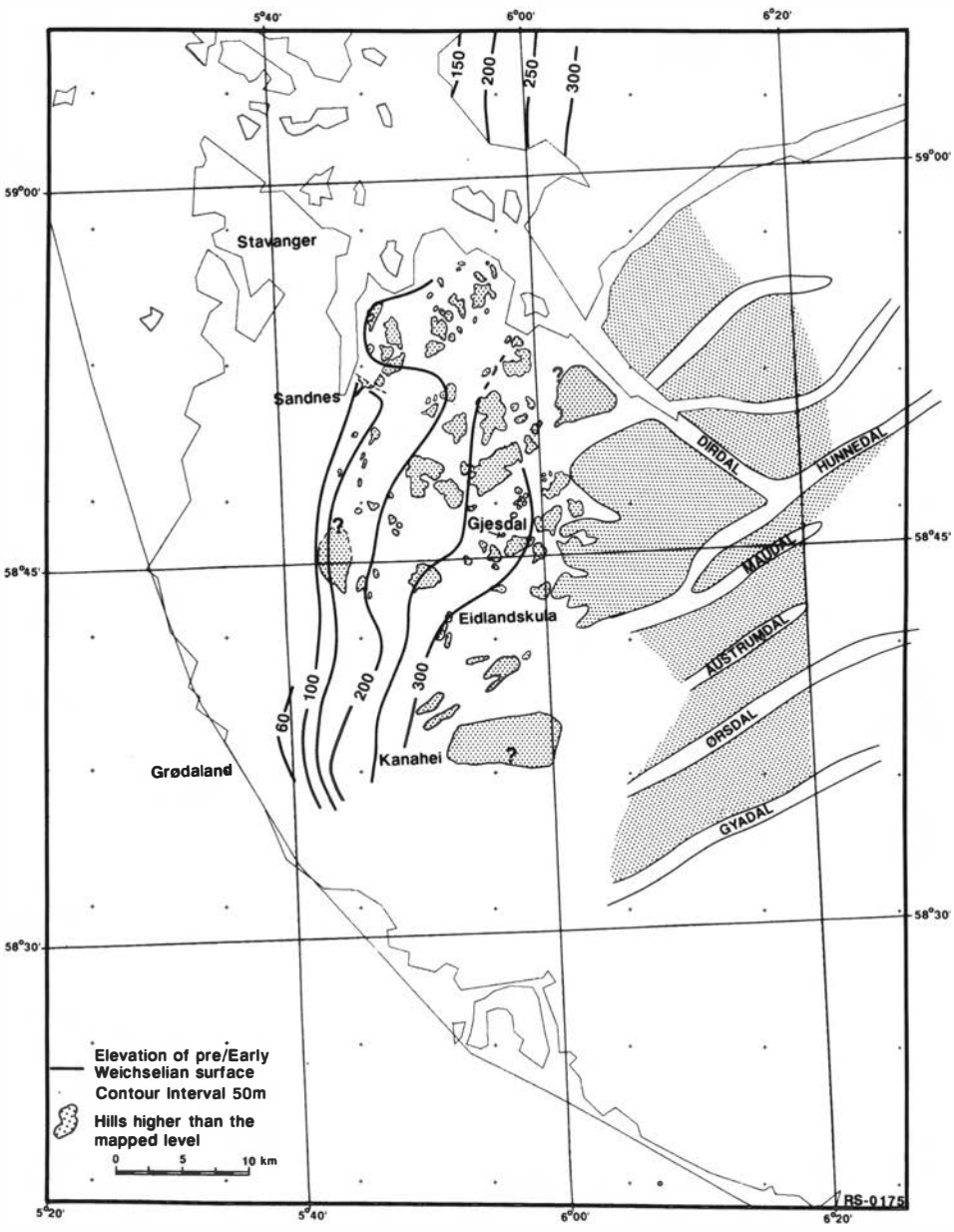

Fig. 3. Contour map of pre/early Weichselian surface, southern Rogaland.

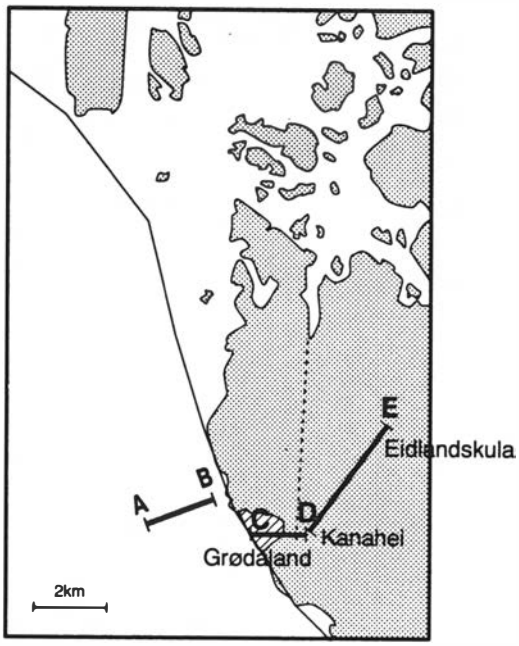

(a)

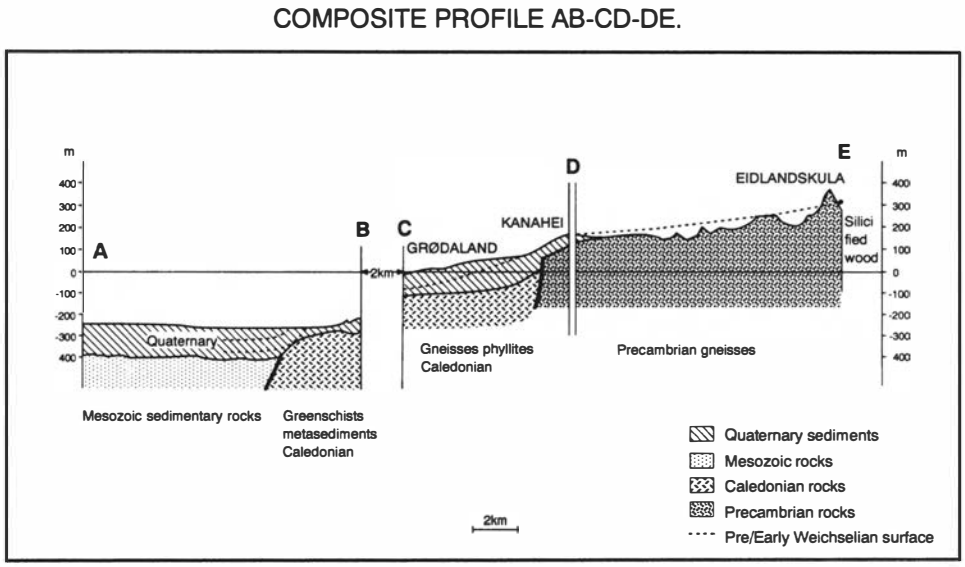

(b)

Fig. 4. (a) The three profiles mentioned in the text. The Gannsfjord lineament is marked with stippled lines. The area of coal findings (Jørstad 1964) is marked with diagonal lines. (b) Combination of the three profiles shown in Fig. 4a.

In Fig. 4, section AB represents a marine seismic line, section CD and DE was constructed using information from Grødaland (Bjørlykke 1908), Kanahei (Opstad) (Fugelli 1987), Eidlandskula (Låg & Skadsheim 1955) and the map presented in Fig. 3 (cf. Grimes 1909, 1910). We have also used a seismic refraction line shot by NGU (Norwegian Geological Survey) in the early 1960s (Andersen et al. 1987).

A borehole at Grødaland, which was drilled in the 1870s, reached basement at 93 m (Fig. 4a). Pre-Weichselian sediments occurred at approximately 45 m (Andersen et al. 1987). In the deeper parts, pieces of brown coal similar to Lias coals in England and Bornholm, Denmark, commonly occurred (Horn & Isachsen 1944).

A large piece of well-preserved, silicified wood, assumed to be of *Fraxinus*, was found near Eidlandskula at 300 m a.s.l. in 1920 (Låg & Skadsheim 1955). The nearest occurrence of fossil wood is in Denmark in layers of Miocene age. We suggest that this fragment of wood was transported into a pre-Weichselian coast by icebergs (cf. Feyling-Hanssen 1964). The dashed line on Fig. 4b illustrates a possible pre-Weichselian surface, perhaps a coastal plain.

The profile A–E suggests that the pre- to Early Weichselian surface has been disturbed by flexuring and/or faulting. In the seismic profile AB, the resolution is not good enough to determine whether the basement fault penetrates the Quaternary layers. The steep rise in topography from B to C could indicate another basement fault. In profile CD, the interpretation of the NGU seismic profile suggests that the Gannsfjord lineament is developed as a fault in this area. Observations of coal in

the Quaternary sediments of Jæren seem to be restricted to areas of the west side of the 'Gannsfjord fault' (Jørstad 1964, Fig. 4a). The high-lying sediments at Høg–Jæren thus appear to be uplifted by recent tectonic movements, resulting in monoclinal structures associated with basement faults (cf. Feyling-Hanssen 1966).

Manuscript received October 1991

References

Andersen, B. G., Wangen, O. P. & Østmo, S. R. 1987: Quaternary geology and adjacent areas, southwestern Norway. *Norges geologiske undersøkelse 411*, 1–55.

Bjørlykke, K. O. 1908: Jæderens Geologi. *Norges geologiske undersøkelse 48*, 160.

Feyling-Hanssen, R. W. 1964: Skagerakmorenen på Jæren. *Norsk Geografisk Tidsskrift 19*, 301–317.

Feyling-Hanssen, R. W. 1966: Geologiske observasjoner i Sandnes-området. *Norges geologiske undersøkelse 242*, 26–43.

Feyling-Hanssen, R. W. 1971: Weichselian Interstadial Foraminifera from the Sandnes–Jæren area. *Geological Society of Denmark Bulletin 21*, 72–116.

Fugelli, E. M. F. 1987: Bio- ag litostratigrafiske undersøkelser av sedimenter på Opstad og Høgemork, Syd-Jæren. *Cand. scient thesis Univ. i Oslo.*

Grimnes, A. 1909: Kart over Jæderen med Angivelse av Høideforholdene og Jordbundens Art. *Norges geologiske undersøkelse 52*a.

Grimnes, A. 1910: Jæderens Jordbund. *Norges geologiske undersøkelse 52*, 1–104.

Horn, G. & Isachsen, F. 1944: Et kullfund i Skagerakmorenen på Jæren. *Norsk Geologisk Tidsskrift 22*, 15–46.

Jørstad, F. 1964: Utgliding i Gannsområdet, Sandnes, august 1963. Kvartærgeologiske forhold på Jæren, spesielt i Sandnes området. Norges Geotekniske Institutt, Oslo. Unpubl. report F-256-6. s. 26.

Låg, J. & Skadsheim, M. 1955: Funn av forsteinet trestykke i Gjesdal, Rogaland. *Norsk Geologisk Tidsskrift 35*, 153–158.

Milthers, V. 1911: Preliminery report on boulders of Swedish and Baltic rocks in the southwest of Norway. *Meddelelser fra Dansk Geologisk Forening 3.*

Milthers, V. 1913: Ledeblokke i de skandinaviske Nedisningers sydvestlige Grænseegne og deres Bidrag til Kundskaben om Isströmretningenernes Skiften og Aldersfølge. *Meddelelser fra Dansk Geologisk Forening 4*, 1–114.

Østmo, S. R. 1971: En kvartærgeologisk undersøkelse på midtre Jæren og fjellområdene østenfor. *Hovedoppg. i geologi. Univ. i Oslo.*

Geometry, thickness and isostatic loading of the Late Weichselian Scandinavian ice sheet

ATLE NESJE & SVEIN OLAF DAHL

Nesje, A. & Dahl, S. O.: Geometry, thickness and isostatic loading of the Late Weichselian Scandinavian ice sheet. *Norsk Geologisk Tidsskrift*, Vol. 72, pp. 271–273. Oslo 1992. ISSN 0029-196X.

A consistent geographical and altitudinal distribution of autochthonous blockfields (mantle of bedrock weathered *in situ*) and trimlines in southern Norway suggests a multi-domed and asymmetric Late Weichselian ice sheet. The ice-thickness distribution of the Late Weichselian Scandinavian ice sheet is not in correspondence with the modern uplift pattern of Fennoscandia. Early Holocene crustal rebound was apparently determined by an exponential, glacio-isostatic rise. Later, however, crustal movements appear to have been dominated by a large-scale tectonic uplift of the Fennoscandian Shield, centred on the Gulf of Bothnia, the region of maximum lithosphere thickness.

Atle Nesje, Department of Geography, University of Bergen, Breiviken 2, N-5035 Bergen-Sandviken, Norway; Svein Olaf Dahl, Department of Geology, Sec. B, University of Bergen, Allégt. 41, N-5007 Bergen, Norway.

Records of glacio-isostatic recovery, together with glacial geological investigations and glacier profiles deduced from glaciological theory and modelling, have been the most common approaches in reconstructing Pleistocene ice sheets (Andrews 1982). In addition, weathering zonation and trimlines have been used in Scandinavia (Sollid & Sørbel 1979; Nesje et al. 1987, 1988), Iceland (Hjort et al. 1985), Scotland (Ballantyne 1990) and North America (Brookes 1985) to indicate former ice-sheet surfaces.

Reconstruction of Pleistocene ice sheets based on glaciological theory tend to assume a nearly symmetrical ice cover with a central dome (Denton & Hughes 1981). Models based on glacial geological observations (e.g. Nesje et al. 1988; Ehlers 1990), erratic dispersal trains (e.g. Prest 1984) and on uplift data (e.g. Peltier & Andrews 1983), however, indicate a complex of ice masses with several ice domes interconnected by saddles (Andrews 1987).

Previously published models of the thickness of the Late Weichselian Scandinavian ice sheet suggest an entirely covered land mass (Vorren 1977; Grosswald 1980; Andersen 1981; Boulton et al. 1985).

The main geological argument for ice-free areas during the Late Weichselian glacial maximum has been the consistent geographical and altitudinal distribution of trimlines marking the lower boundary of frost-weathered bedrock and continuous mantles of autochthonous blockfields with sharp lower weathering limits.

This extended abstract challenges the notion that the pattern of postglacial and present-day uplift in Scandinavia is a direct reflection of the pattern of former ice-sheet loading.

Ice-sheet loading

Isostatic adjustments depend primarily on the history of glaciation, crustal rigidity and the length scale of elastic flexure (Peltier 1987).

The model presented here for the Late Weichelselian Scandinavian ice sheet (Fig. 1a) indicates that ice thickness varied considerably, especially in western Scandinavia. According to the model, the regions of maximum ice thickness were located in the northern Baltic region, in the central lowland area of eastern Norway, and in the Trøndelag region (Fig. 1b).

If the present pattern of uplift across Scandinavia is exclusively a response to Weichselian ice-sheet loading, there should have been *several* centres of isostatic uplift supposing that the distances between centres of maximum ice thickness lie within Peltier's (1987) length scale of elastic flexure. In addition, low flexural rigidity to ice loading is demonstrated by a significant transgression that accompanied the Younger Dryas (10,000–11,000 years BP) glacier readvance in southwestern Norway (Anundsen & Fjeldskaar 1983; Anundsen 1985).

Recently published data on the present rate of isostatic uplift on a regional scale in Scandinavia, however, shows only *one* major centre of uplift located in the Gulf of Bothnia, with a mean rate of uplift of 9 mm/year (Ekman 1987).

Closer inspection of modern isostatic movements in southern Norway (Sørensen et al. 1987) and southern Sweden (Svensson 1989) on a more local scale, however, shows significant deviations from the regional pattern. In addition, the 6500 year BP isobases and the modern land uplift pattern in southern Norway (Sørensen et al. 1987)

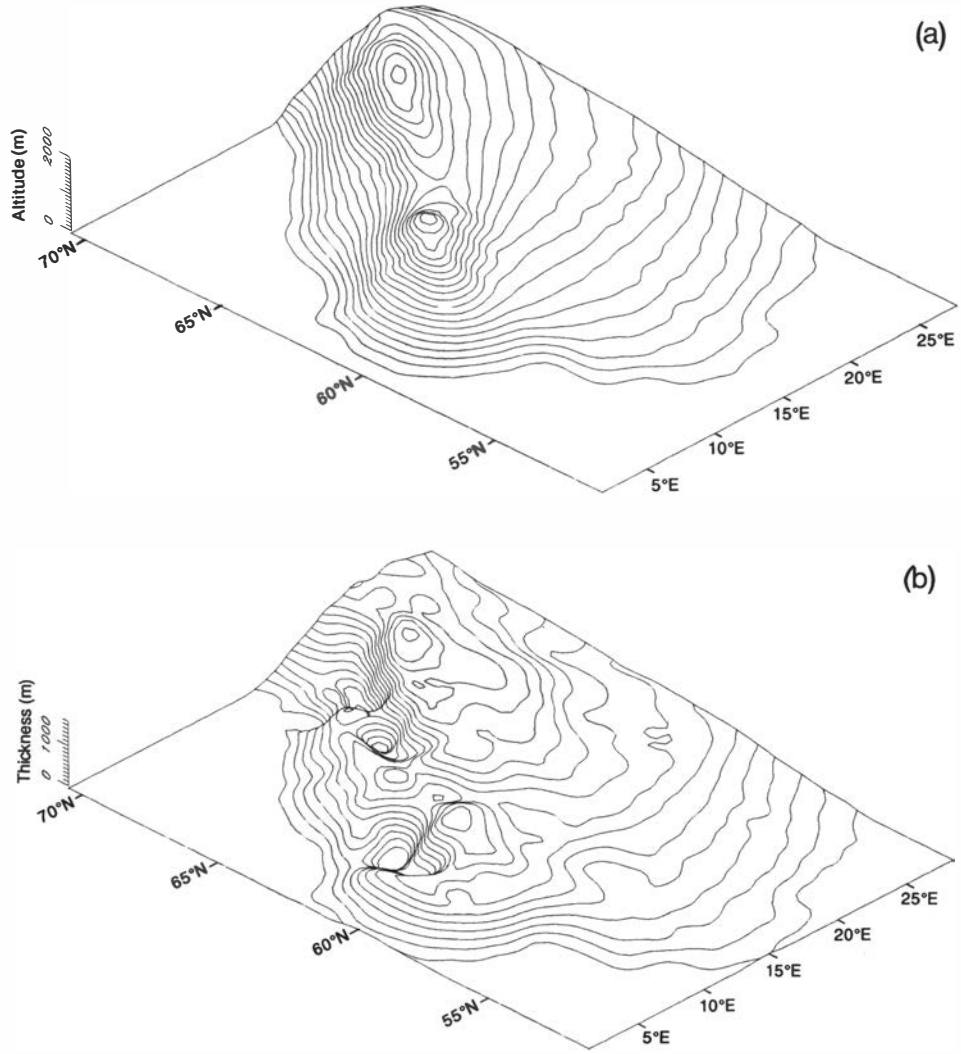

Fig. 1. (a) Oblique 3D reconstruction of the Late Weichselian Scandinavian ice sheet during its maximum. Contour interval 100 m. View from southwest toward northeast. (b) Ice-thickness distribution in Fennoscandia during the Late Weichselian glacial maximum. Contour interval 100 m. View from southwest toward northeast.

show significant discrepancies, strongly suggesting that modern isostatic movements are affected by a significant tectonic component.

Postglacial movements along old fracture- and fault-lines in Scandinavia (Kujansuu 1964; Lundquist & Lagerbäck 1976; Lagerlund 1977; Lagerbäck 1979, 1990; Olesen 1988; Anundsen 1989; Bäckblom & Stanfors 1989; Olesen et al. 1989; Roberts 1991) illustrate that the Fennoscandian Shield exhibits minor tectonic irregularities, and by no means consists of a rigid and stable crust.

Recently, redistribution of continental material due to glacier erosion and resulting large-scale accumulation of glacigenic deposits on the continental shelf off Norway have been introduced to explain parts of the isostatic and thermal imbalance in the Fennoscandian Shield during the Plio-Pleistocene (Riis et al. 1990).

Mörner (1980) suggested that the Fennoscandian uplift consists of two main components; one exponential, due to glacio-isostasy, and one linear and related to the lithosphere. The postglacial uplift pattern may, therefore, have been determined by two factors; The effect of deglaciation may have been dominated by an exponential, glacio-isostatic rise which died out a few thousand years ago, while an approximately linear uplift centred in the middle of the Fennoscandian Shield may still be active. This opinion is supported by the seismologically determined lithosphere thickness in Fennoscandia (Babuska et al. 1988) showing the thickest regions (160–180 km) corresponding to the area of maximum uplift in the Gulf of Bothnia (Fig. 2.) As a result, and also supported by the ice-sheet model presented here, the total postglacial isostatic uplift in Scandinavia may reflect not only the ice-thickness distribution during the last glaciation, but also a large-scale, tectonic uplift of the Fennoscandian Shield. If this is correct, 60–70% of the post-glacial uplift may be due to glacio-isostasy and the remaining 30–40% due to a large-scale tectonic uplift of the Fennoscandian Shield.

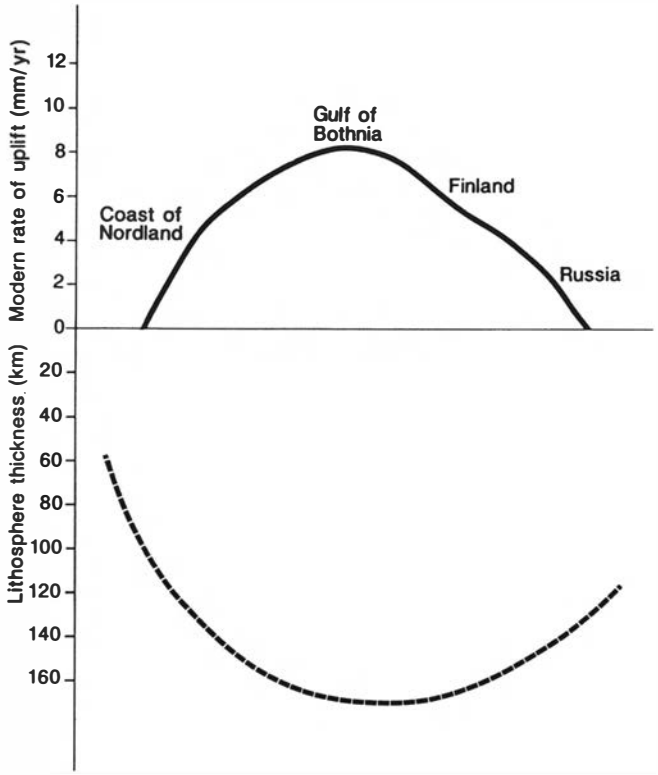

Fig. 2. East–west profile across Fennoscandia showing the present rate of crustal uplift (Ekman 1987) and the lithosphere thickness (Babuska et al. 1988).

Acknowledgements. – Vidar Valen did the computer processing and Jane Ellingsen prepared the Figures. Comments made by two referees are acknowledged.

Manuscript received October 1991

References

Andersen, B. G. 1981: Late Weichselian ice sheets in Eurasia, Greenland and Norway. *In* Denton, G. H. & Hughes, T. J. (eds.): *The Last Great Ice Sheets*, 20–27. John Wiley & Sons, New York.

Andrews J. T. 1982: On the reconstruction of Pleistocene ice sheets: a review. *Quaternary Science Reviews* 1, 1–30.

Andrews, J. T. 1987: The late Wisconsinan Glaciation and deglaciation of the Laurentide Ice Sheet. *In* Ruddiman, W. F. & Wright, H. E. Jr. (eds.): *North America and Adjacent Oceans During the Last Deglaciation*, 13–37. Boulder, Colorado, Geological Society of America.

Anundsen, K. 1985: Changes in shore-level and ice-front position in Late Weichsel and Holocene, southern Norway. *Norsk Geografisk Tidsskrift 39,* 205–225.

Anundsen, K. 1989: Late Weichselian relative sea levels in southwest Norway: observed strandline tilts and neotectonic activity. *Geologiska Föreningen i Stockholms Förhandlingar 111,* 288–292.

Anundsen, K. & Fjeldskaar, W. 1983: Observed and theoretical Late Weichselian shore-level changes related to glacier oscillations at Yrkje, south-west Norway. *In* Schroeder-Lanz, H. (ed.): *Late- and Postglacial Oscillations of Glaciers: Glacial and Periglacial Forms*, 133–170. A. A. Balkema, Rotterdam.

Babuska, V., Plomerova, J. & Pajdusak, P. 1988: Seismologically determined deep lithosphere structure in Fennoscandia. *Geologiska Föreningen i Stockholms Förhandlingar 110,* 380–382.

Ballantyne, C. K. 1990: The Late Quaternary glacial history of the Trotternish Escarpment, Isle of Skye, Scotland, and its implications for ice-sheet reconstruction. *Proceedings of the Geologists' Association 101,* 171–186.

Boulton, G. S., Smith, G. O., Jones, A. S. & Newson, J. 1985: Glacial geology and glaciology of the last mid-latitude Ice Sheets. *Journal of the Geological Society of London 142,* 447–474.

Brookes, I. A. 1985: Weathering. *In* Rutter, N. W. (ed.): *Dating Methods of Plesitocene Deposits and Their Problems*, 61–72. Geoscience Canada, Reprint series 2.

Bäckblom, G. & Stanfors, R. 1989: Interdisciplinary study of post-glacial faulting in the Lansjärv area, northern Sweden 1986–1988. *Svensk Kärnbränslehantering Technical Report* 89–13.

Denton, G. H. & Hughes, T. J. 1981: *The Great Ice Sheets.* John Wiley & Sons, New York.

Ehlers, J. 1990: Reconstructing the dynamics of the north-west European Pleistocene ice sheets. *Quaternary Science Reviews 9,* 71–83.

Ekman, M. 1987: Postglacial uplift of the crust in Fennoscandia and some related phenomena. *International Association of Geodesy Section V: Geodynamics XIX General Assembly Vancouver*, 23 pp.

Grosswald, M. G. 1980: Late Weichselian ice sheet of northern Eurasia. *Quaternary Research 13,* 1–32.

Hjort, Chr., Ingolfsson, O. & Norddal, H. 1985: Late Quaternary geology and glacial history of Hornstrandir, northwest Iceland: a reconnaissance Study. *Jökull 35,* 9–28.

Kujansuu, R. 1964: Nuorista sirroksista Lapissa. Summary: recent faults in Lapland. *Geology 6,* 30–36.

Lagerbäck, R. 1979: Neotectonic structures in northern Sweden. *Geologiska Föreningen i Stockholms Förhandlingar 100,* 271–279.

Lagerbäck, R. 1990: Late Quaternary faulting and paleoseismicity in northern Fennoscandia, with particular reference to the Lansjärv area, northern Sweden. *Geologiska Föreningen i Stockholm Förhandlingar 112,* 333–354.

Lagerlund, E. 1977: Förutsättningar för moränstratigrafiska undersökningar på Kullen i Nordvästskåne – teoriutveckling och neotektonikk. Department of Quaternary Geology, University of Lund, Thesis 5, 1–106.

Lundquist, J. & Lagerbäck, R. 1976: The Pärvie Fault; a late-glacial fault in the Precambrian of Swedish Lapland. *Geologiska Föreningen i Stockholm Förhandlingar 98,* 45–51.

Mörner, N.-A. 1980: The Fennoscandian uplift: geological data and their geodynamical implications. *In* Mörner, N. -A. (ed.): *Earth Rheology, Isostasy and Eustasy*, 251–284. John Wiley & Sons, New York.

Nesje, A., Anda, E., Rye, N., Lien, R., Hole, P. A. & Blikra, L. H. 1987: The vertical extent of the Late Weichselian ice sheet in the Nordfjord–Møre area, western Norway. *Norsk Geologisk Tidsskrift 67,* 125–141.

Nesje, A., Dahl, S. O., Anda, E. & Rye, N. 1988: Block fields in southern Norway: significance for the Late Weichselian ice sheet. *Norsk Geologisk Tidsskrift 68,* 149–169.

Olesen, O. 1988: *The Stuoragarra Fault. Evidence of neotectonics in the Precambrian of Finnmark, northern Norway. Norsk Geologisk Tidsskrift 68,* 107–118.

Olesen, O., Rønning, J. S., Dalsegg, E. & Lile, O. B. 1989: Geofysiske undersøkelser av Stuoragurra postglasial forkastning, Finnmark. *Geolognytt 22,* 48.

Peltier, W. R. 1987: Glacial isostasy, mantle viscosity, and Pleistocene climatic change. *In* Ruddiman, W. F. & Wright, H. E. Jr. (eds.): *North America and Adjacent Oceans During the Last Deglaciation*, 155–182. Boulder, Colorado, Geological Society of America.

Peltier, W. R. & Andrews, J. T. 1983: Glacial geology and glacial isostacy, Hudson Bay, Canada. *In* Smith, D. E. (ed.): *Shorelines and Isostasy*, 285–319. Academic Press, New York.

Prest, V. K. 1984: The Late Wisconsinan glacier complex. *In* Fulton, R. J. (ed.): *Quaternary Stratigraphy of Canada, a Canadian Contribution to IGCP Project 24,* 21–38. Geological Survey of Canada Paper 84–10.

Riis, F., Eidvin, T. & Fjeldskaar, W. 1990: Seintertiær kvartær erosjon og heving i Skandinavia og Barentshavet. *Geonytt 1/90,* 94.

Roberts, D. 1991: A contemporary small-scale thrust-fault near Lebesby, Finnmark. *Norsk Geologisk Tidsskrift 71,* 117–120.

Sollid, J. L. & Sørbel, L. 1979: Deglaciation of western Central Norway. *Boreas 8,* 223-239.

Svensson, N.-O. 1989: Late Weichselian and Early Holocene shore displacement in the central Baltic, based on stratigraphical and morphological records from eastern Småland and Gotland, Sweden. *Lundqua Thesis 25,* 195 pp.

Sørensen, R., Bakkelid, S. & Torp, B. 1987: *Nasjonalatlas for Norge. Hovedtema 2: Landformer, berggrunn og løsmasser. Kartblad* 2.3.3.

Vorren, T. O. 1977: Weichselian ice movements in South Norway and adjacent areas. *Boreas 6,* 247–257.

Late Tertiary uplift and erosion in the Skagerrak area: magnitude and consequences

LARS N. JENSEN & BIRTHE J. SCHMIDT

Jensen, L. N. & Schmidt, B. J.: Late Tertiary uplift and erosion in the Skagerrak area: magnitude and consequences. *Norsk Geologisk Tidsskrift*, Vol. 72, pp. 275–279. Oslo 1992. ISSN 0029-196X.

Neogene uplift and erosion in the order of 500–1500 m is documented in the Skagerrak area. The sediments generated during this erosion have been deposited in the Central Graben, where they caused accelerated Neogene subsidence of 1500–2000 m. On a regional scale these Late Tertiary movements were achieved by a gentle warping accompanied by only minor fault activity. These movements have important consequences for the hydrocarbon potential of the Farsund Basin. Due to deeper burial before this uplift, the possible Jurassic source rocks may be oil mature, and the Farsund Basin could become a future hydrocarbon province in the North Sea.

Lars N. Jensen, Statoil a/s, Postboks 300, N-4001 Stavanger, Norway; Birthe J. Schmidt, Geologisk Institut, Aarhus Universitet, DK-8000 Aarhus C, Denmark.

Major Neogene uplift and erosion has been recognized on Svalbard (Manum & Throndsen 1977), in the Barents Sea (Nyland et al. in press) and along the Norwegian coast to the North Sea. In this paper, we document a similar uplift and erosion in the Skagerrak area (Fig. 1), and discuss the magnitude, timing and consequences of this event.

Evidence of the Neogene erosion is clearly seen on seismic profiles (Fig. 2) where the Base Quaternary reflector is a major erosional unconformity, and Tertiary to Paleozoic sediments subcrop towards the Norwegian coast. In profile A–A′ weak erosion is seen in the Egersund Basin near the 9/2-2 well. The depth of erosion

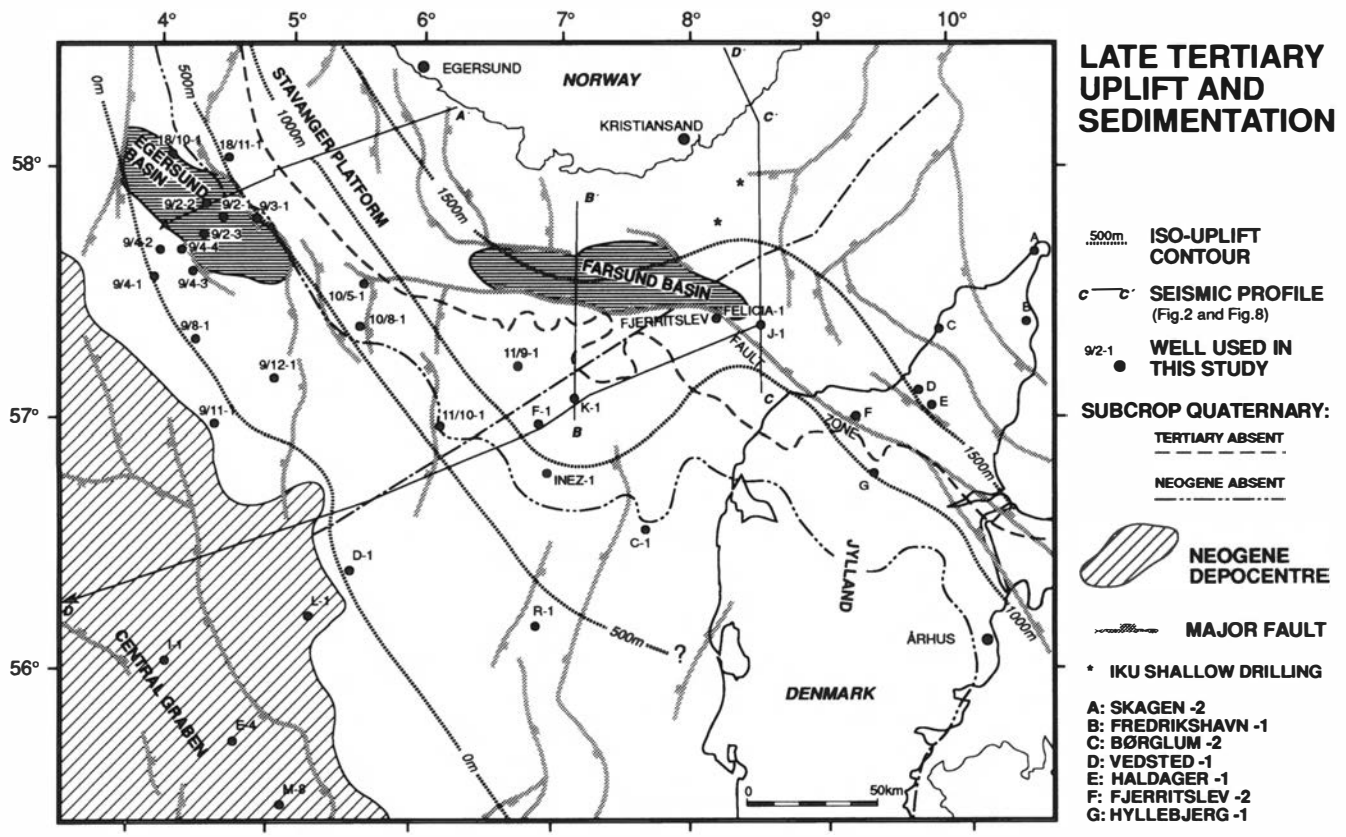

Fig. 1. Map of the Skagerrak area with wells used in this study. The Neogene depocentre in the Central Graben area is from Bjørslev-Nielsen et al. (1986). Lines indicating Tertiary and Neogene absent are the pre-Quaternary pinch-out lines of these sequences. Iso-uplift contours indicate the net-uplift of the area. The outline of the Farsund and Egersund Basin is shown with horizontal ruling.

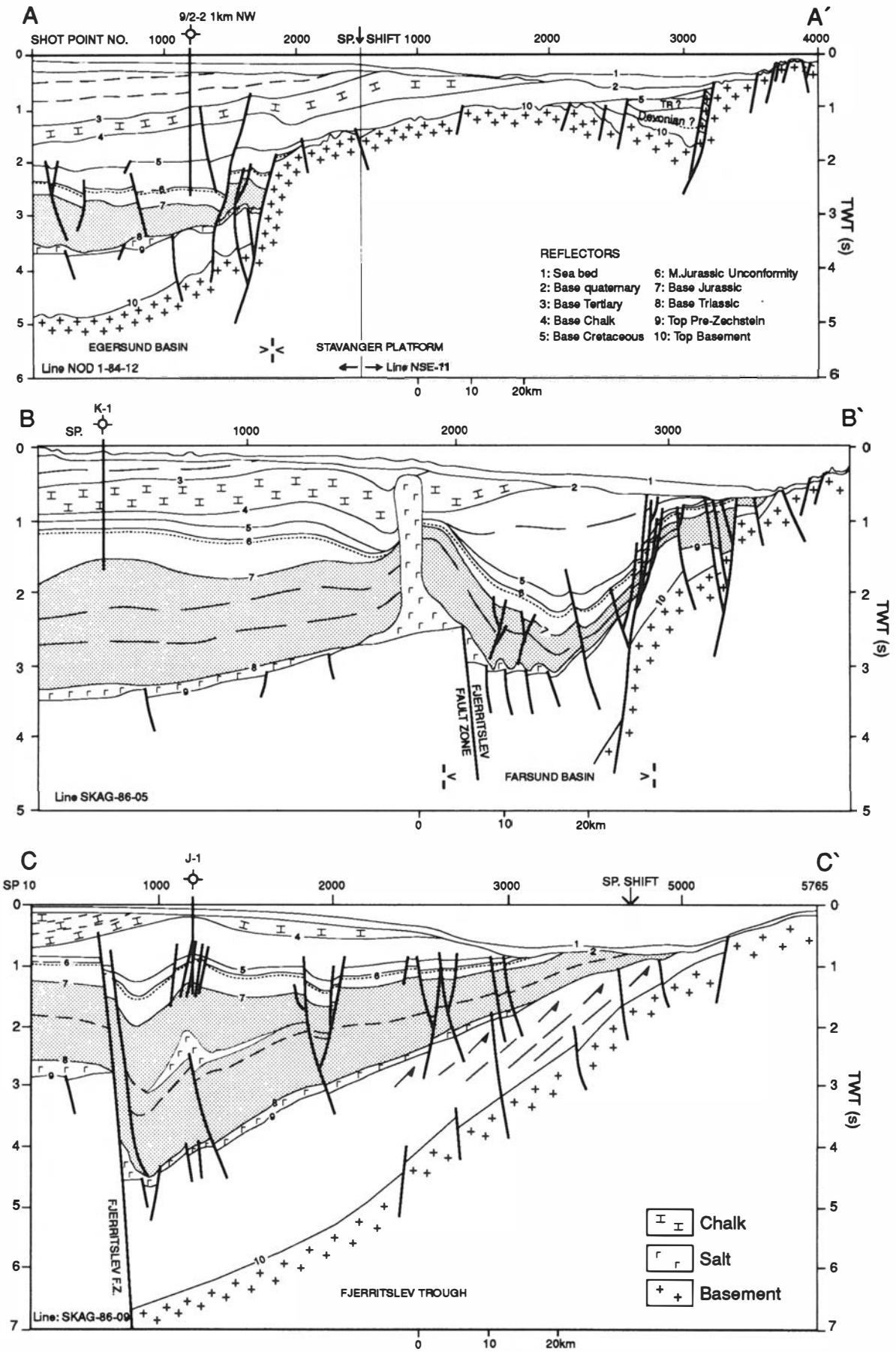

Fig. 2. Regional geoseismic profiles from the Skagerrak area. Their locations are indicated in Fig. 1. The Danian limestone is included in the chalk sequence.

increases across the Stavanger Platform where chalk and Lower Cretaceous strata subcrop the Quaternary towards the coast. A similar pattern is seen in profile B–B′ with clear erosion near the K-1 well and deeper erosion across the Farsund Basin. In profile C–C′ substantial erosion is seen near the J-1 well, and it increases towards the coast where Paleozoic sediments subcrop. Erosion is also evident on a Base–Quaternary subcrop map (e.g. Base Neogene and Base Tertiary subcrop lines, Fig. 1) where successively older strata are exposed in a coast-parallel pattern around southern Norway. This pattern is due to a general dip of the sediments away from the Fennoscandian Shield; the pattern continues into northern Jylland (Fig. 1) and along the west coast of Sweden.

Magnitude and timing of the uplift

Based on Statoil's experience from the Barents Sea (Nyland et al. in press; Skagen, this volume) shale compaction methods and vitrinite reflectance trends give the most consistent and reliable information in estimating magnitude of uplift. Both methods rely on irreversible depth and temperature-dependent processes. One or both of these methods have been applied to all the wells shown in Fig. 1. In the Felicia-1 well for example, shale compaction indicates 800–1000 m of uplift while chalk density indicates 1000–1200 m. Figure 3 shows vitrinite reflectance trends from all wells, grouped according to their geographic position and magnitude of uplift. In the Central Graben there is a clear vitrinite reflectance trend and no erosion. Here the trend line indicates a vitrinite reflectance of 0.2 at the surface. The next group of wells has been uplifted between 0 and 800 m, with a mean value of 400 m. Wells C-1, R-1 and S-1 have an uplift between 500 and 1100 m, but the trend is less clear. The uplift is about 1000 m in the wells to the south of the Farsund Basin (Fig. 3d) and more than 1200 m in northern Jylland and along the Norwegian coast. The substantial magnitude of uplift in northern Jylland (Fig. 3e) is due to the additional uplift caused by the Late Cretaceous–Early Tertiary inversion in the Sorgenfrei–Tornquist Zone (Jensen & Michelsen, in press). The iso-uplift contours (Fig. 1) are based on all available information, and show net-uplift. This is defined as the difference between maximum burial and the present depth of a given point in a well.

Most of the uplift is of Neogene age, contemporaneous with a similar uplift all along the Norwegian coast and Svalvard (Eidvin & Riis 1989, 1991; Manum & Throndsen 1977). Evidence of the timing in the study area is the accelerated Neogene sedimentation rate in the central North Sea (Bjørslev-Nilsen et al. 1986, Neo-

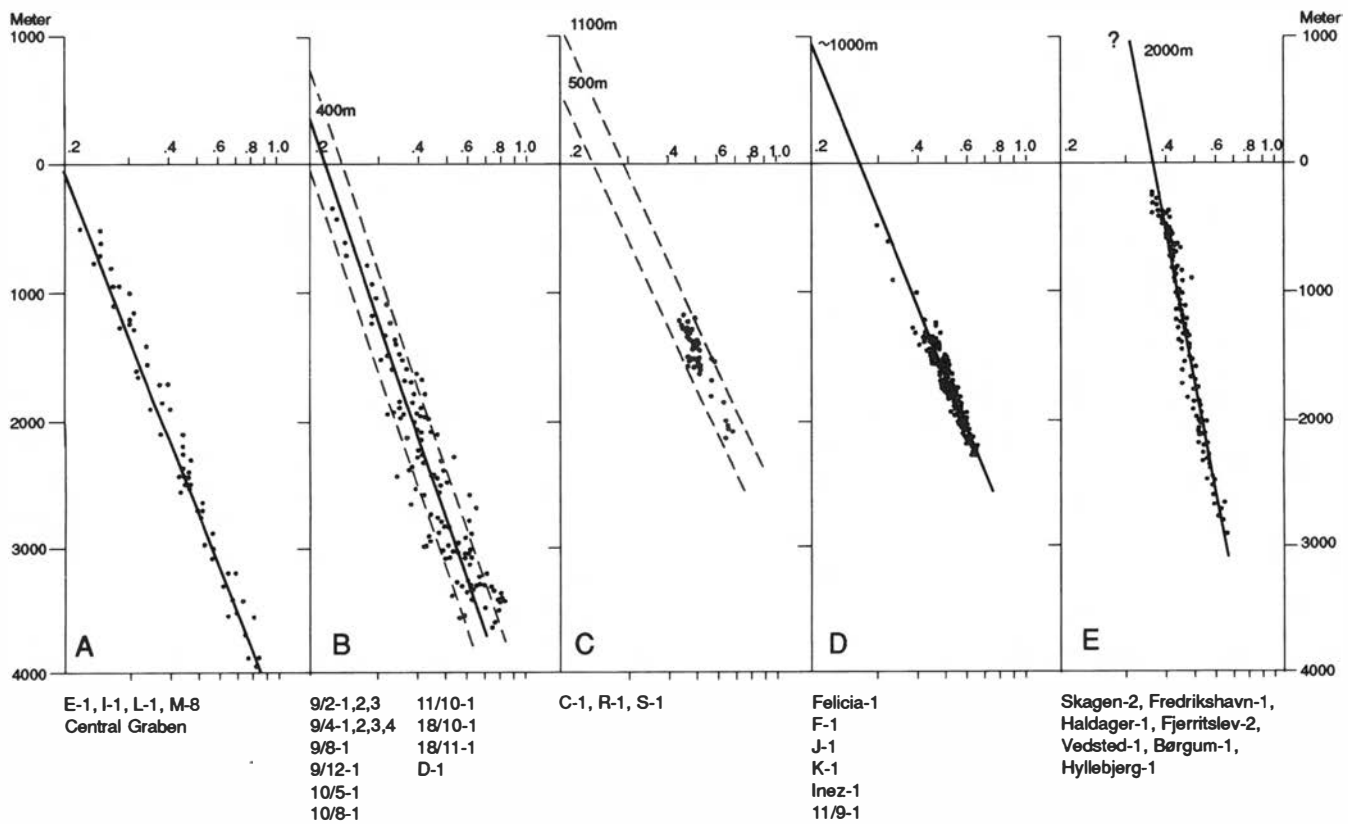

Fig. 3. Vitrinite reflectance trends from exploration wells grouped according to their geographic position and magnitude of uplift. Well locations are indicated in Fig. 1.

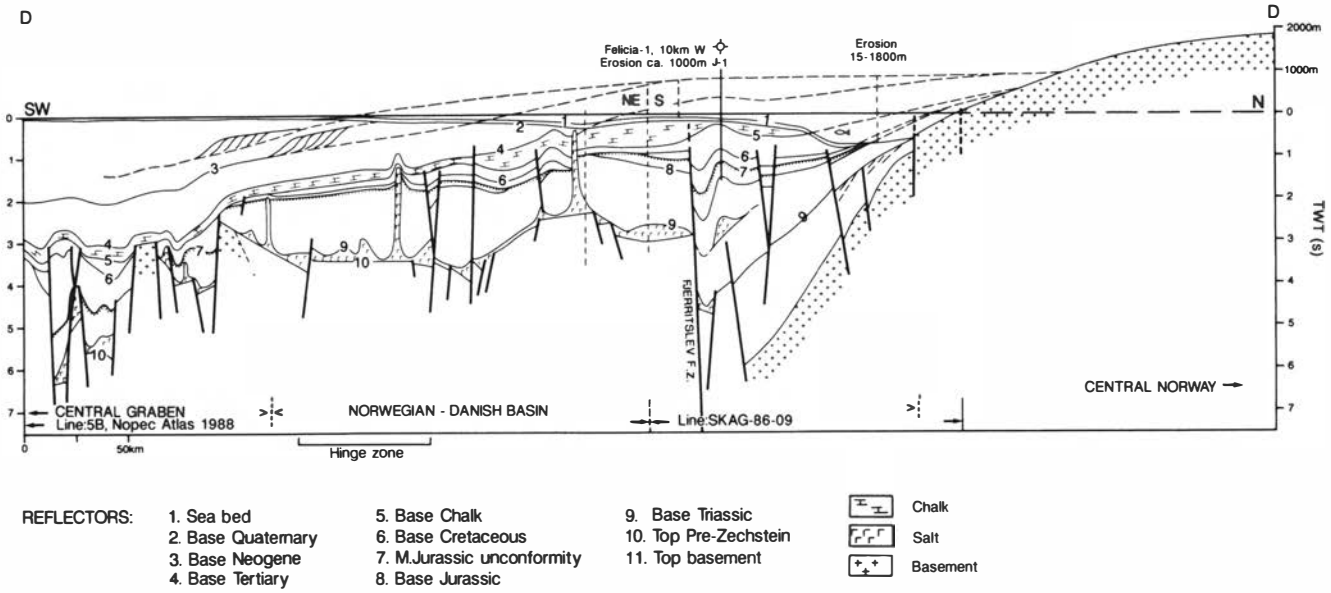

Fig. 4. A regional profile from central southern Norway across the Farsund Basin to the Central Graben (line D–D′, Fig. 1). Depth is in seconds (TWT) and height above sea level in meters. The profile is based on regional seismic lines, but the prograding Neogene sequences are shown schematically. The eroded pre-Neogene sequences are drawn tentatively, based on regional considerations and the documented magnitude of uplift.

gene depocentre Figs. 1 and 4). Based on stratigraphic evidence from the Central Graben area, most of the uplift and erosion is known to be of post-Mid Miocene age (CENOS 1991). More direct evidence of the timing is provided by apatite fission-track modelling (i.e. Green 1989). The 1500–2000 m Neogene uplift of the Norwegian mountains is believed to be part of the same event (Spjeldnæs 1975).

Discussion

These Neogene vertical movements have important consequences for hydrocarbon exploration in the affected areas. A source rock will be more mature than expected from its present depth in areas suffering uplift, while seal failure and gas expansion may affect existing hydrocarbon accumulations, as seen in the Barents Sea (Nyland et al. in press). The consequences for the Farsund Basin are as follows. If a Jurassic source rock in the basin had never been buried deeper than today, it would be immature, and the basin would be without interest for hydrocarbon exploration. But, as documented in this study (Figs. 1, 2 and 3d), possible Jurassic source rocks have been buried 1000–1500 m deeper than today, and basin modelling indicates that it will be oil mature in most of the Farsund Basin. A remaining problem is the existence and quality of Jurassic source rocks in the Farsund Basin, but regional studies (Hamar et al. 1983) indicate that the Lower Jurassic Fjerritslev Formation or the Upper Jurassic Børglum Formation may be present. In this case the Farsund Basin could become a new hydrocarbon province in the North Sea.

The Neogene uplift was due to broad-scale warping without major faulting, and the total amplitude of Neogene movements, from the base of the Neogene depocentre to the crestal peneplain of the Norwegian mountains, is about 4000 m (Fig. 4). Major Tertiary uplift is also evident in eastern Britain (Green 1989). In an intracratonic setting such as the central North Sea, the cause of the Neogene uplift and sedimentation is most likely a plate tectonic process (horizontal stress?) accentuated by the strong erosional effect of the glaciations (Jensen & Schmidt, in press).

Manuscript received October 1991

References

Bjørslev Nielsen, O., Sørensen, S., Thiede, J. & Skarbø, O. 1986: Cenozoic differential subsidence of North Sea. *American Association of Petroleum Geologists Bulletin, 70,* 276–298.

CENOS 1991: Cenozoic North Sea Study, Status Report No. 4, Geologisk Institut, Aarhus Universitet, January 1991, 22 pp.

Eidvin, T. & Riis, F. 1989: Nye dateringer av de tre vestligste borehullene i Barentshavet. Resultater og konsekvenser for den Tertiære hevingen. *NPD-Contribution 27,* 44 pp.

Eidvin, T. & Riis, F. 1991: En biostratigrafisk analyse av Tertiære sedimenter på kontinentalmarginen av Midt-Norge, med hovedvekt på øvre Pliocene vifteavsetninger. *NPD-Contribution 29,* 44 pp.

Green, P. F. 1989: Thermal and tectonic history of the East Midlands shelf (onshore UK) and surrounding regions assessed by apatite fission track analysis. *Journal of the Geological Society, London, 146,* 755–773.

Hamar, G. P., Fjæran, T. & Hesjedal, A. 1983: Jurassic stratigraphy and tectonics of the south-southeastern Norwegian offshore. *In* Kasschieter, J. P. H. & Reijers T. J. A. (eds.): Petroleum geology of the southeastern North Sea and the adjacent onshore areas. The Hague 1982. *Geologie en Mijnbouw 62,* 103–114.

Jensen, L. N. & Schmidt, B. J.: Neogene uplift and erosion in the northeastern North Sea; magnitude and consequences for hydrocarbon exploration in the Farsund Basin. *In* Spencer, A. M. (ed.): *Generation, Accumulation and*

Production of Europe's Hydrocarbons III. Special Publication of the European Association of Petroleum Geoscientists No. 3. Springer Verlag, Heidelberg (in press).

Jensen, L. N. & Micheisen, O.: Tertiær hævning og erosion i Skagerrak, Nordjylland og Kattegat. *Dansk Geol. Foren., Årsskrift* (in press).

Manum, S. B. & Throndsen, T. 1977: Rank of coal and dispersed organic matter and its geological bearing in the Spitsbergen Tertiary. *Norsk Polarinstitutt Årbok 1977,* 159–177.

Nyland, B., Jensen, L. N., Skagen, J., Skarpnes, O. & Vorren, T.: Tertiary uplift and erosion in the Barents Sea; magnitude, timing and consequences. *In* Larsen, R. M. & Larsen, B. T. (eds.): *Structural and Tectonic Modelling and Its Application to Petroleum Geology*. Norwegian Petroleum Society, Elsevier (in press).

Skagen, J. 1992: Methodology applied on uplift and erosion. *In* Jensen, L. N. & Riis, F. (eds.): Post-Cretaceous uplift and sedimentation along the western Fennoscandian shield. *Norsk Geologisk Tidsskrift*. This volume.

Spjeldnæs, N. 1975: Paleogeography and Facies Distribution in the Tertiary of Denmark and Surrounding Area. *Norges geologiske undersokelse 316,* 289–311.

The Karmsundet Basin, SW Norway: stratigraphy, structure and neotectonic activity

REIDULV BØE, STEINAR SØRENSEN & MARTIN HOVLAND

Bøe, R., Sørensen, S. & Hovland, M.: The Karmsundet Basin, SW Norway: stratigraphy, structure and neotectonic activity. *Norsk Geologisk Tidsskrift*, Vol. 72, pp. 281–283. Oslo 1992. ISSN 0029-196X.

The Karmsundet Basin, a newly discovered sedimentary basin located on the innermost continental shelf of SW Norway, has an areal extent of approximately 28 × 5 km and contains a tilted succession of sedimentary rocks with a maximum thickness of approximately 600 m. The sedimentary rocks are downthrown along the N–S trending Kvitsøy Fault, and are preserved in a half-graben. A succession of Quaternary deposits overlying these rocks shows features indicating sediment instability, including faults, slide scars and slump deposits. It is tentatively suggested that these features are related to fault reactivation and earthquake activity.

Reidulv Bøe, Geological Survey of Norway, PO Box 3006 Lade, N-7002 Trondheim, Norway; Steinar Sørensen, Elf Aquitaine Norge A/S, PO Box 168, N-4001 Stavanger, Norway; Martin Hovland, Statoil, PO Box 300, N-4001 Stavanger, Norway.

The Karmsundet Basin (new informal name) is a recently discovered sedimentary basin located on the innermost continental shelf of SW Norway (Bøe 1990; Bøe & Hovland 1990). The basin has an areal extent of approximately 28 × 5 km (Fig. 1) and contains a tilted sedimentary succession with a maximum thickness (measured normal to the bedding) of approximately 600 m (assuming a compressional wave velocity of 4.0 km/s). The sedimentary rocks are preserved in a half-graben with reflectors dipping towards the east–southeast. The eastern boundary fault of the half-graben is a major N–S trending structure (the Kvitsøy Fault) (new informal name) separating the sedimentary rocks in the half-graben from Precambrian and Cambro-Silurian metamorphic rocks to the east (Fig. 2). Towards the north the Kvitsøy Fault runs into a thrust of Caledonian age (Fig. 1). At the western margin of the half-graben, the sedimentary sequence rests unconformably upon rocks of the Caledonian West Karmøy Igneous Complex, rocks of the Karmøy Ophiolite Complex and meta-sedimentary rocks of the Ordovician and Silurian Skudenes Group (Thon 1980).

The Karmsundet Basin reaches its maximum width (ca. 5 km) just west of Kvitsøy (Fig. 1), and becomes narrower both northwards and southwards. In the southernmost part of the basin the sedimentary rocks are strongly faulted, and there is an unconformity present within the succession. In this southern area the rocks of the half-graben are buried beneath sedimentary rocks of probable Cretaceous age. The dip of bedding of the sedimentary rocks within the Karmsundet Basin varies from 5°ESE to 25°ESE.

The age of the sedimentary rocks in the Karmsundet Basin is unknown. A Jurassic age is possible, as Jurassic rocks crop out beneath the Quaternary close to the coast to the west of Karmøy (Rokoengen & Sørensen 1990). Other basins along the coast of southern Norway showing similar geometries are assumed to contain Triassic–Jurassic rocks and to have formed during extensional tectonism in mid–late Jurassic times (Holtedahl 1988; Rokoengen et al. 1988; Bøe & Bjerkli 1989; Bøe 1991). We propose that a late Palaeozoic age of the sediments in the Karmsundet Basin should also be considered. Thick successions of probable Carboniferous–Permian age are observed in deep half-grabens outside the coast of Jæren (Fig. 1) (S. Sørensen, pers. comm. 1991). The marginal faults of these half-grabens trend sub-parallel to the Kvitsøy Fault, and the basins exhibit very similar geometries. It is possible that the Karmsundet Basin is structurally connected with one of these basins (Fig. 1). It is also possible that the Karmsundet Basin contains both late Palaeozoic and Mesozoic rocks, separated by unconformities.

A succession of Quaternary deposits overlie the sedimentary rocks (Figs. 2 and 3). Based on seismic signature these are interpreted as late- (glaciomarine) and post-glacial clays. At their base there is locally a till layer. To the west of Kvitsøy the clays reach a thickness of almost 300 ms TWT. The uppermost part of the clay succession overlying the Karmsundet Basin has similarities to a contourite deposit (Pickering et al. 1989) (Fig. 3). This may be due to the presence of extraordinary ocean current systems, with strong NE–SW tidal currents to the north of Kvitsøy and a strong N–S coastal current in Karmsundet (Gade 1986).

There are several features indicating sediment instability in the Quaternary deposits in this area (Bøe 1990). Shallow seismic reflection records show faults, slide scars and slump deposits in the clays. One large slide has transported several million cubic metres of sediments in a southeasterly direction. These features occur in that part of Karmsundet with greatest water depth (approximately

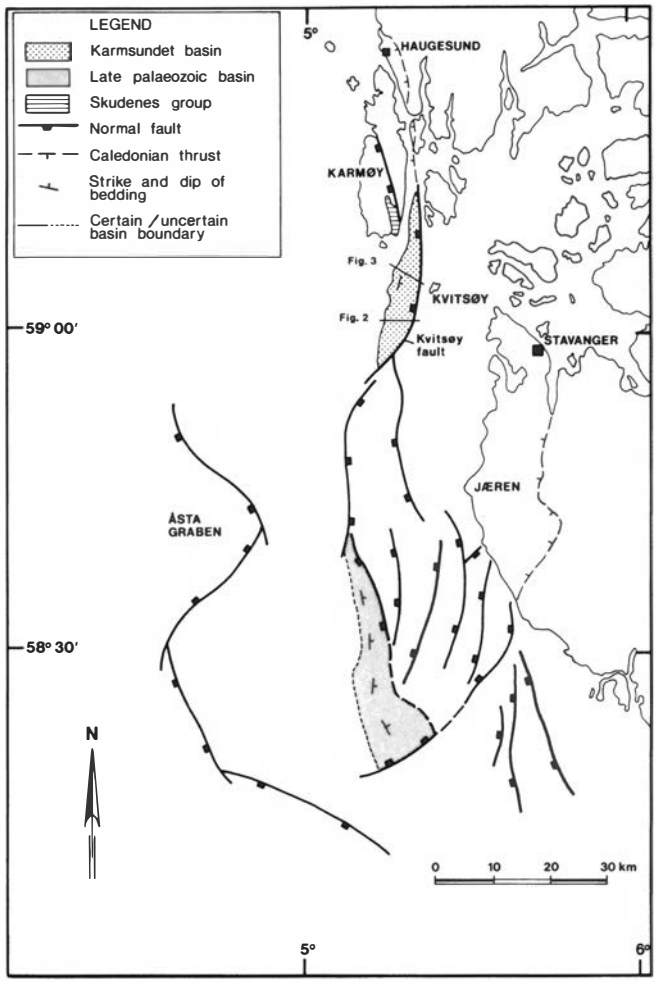

Fig. 1. Geological map showing the location of the Karmsundet Basin and tectonic elements in the SE North Sea and in SW Norway. The geology south of 58°45'S is based on unpublished data from Elf Aquitaine Norge A/S.

350 m), or in the slope to the west of this deep area, i.e. close to or directly above the Kvitsøy Fault.

The close spatial relationship between the sediment instability features in the Quaternary deposits and the Kvitsøy Fault may suggest that reactivation along the Kvitsøy Fault was the triggering mechanism for the slides. The lower terminations of some faults, in the Quaternary clay succession, appear to coincide with the position of faults in the underlying sedimentary rocks. It is evident from earthquake activity and observed faulting along some fjords that this part of Norway is still tectonically active (Feyling-Hansen 1966; Bakkelid 1986; Havskov & Bungum 1987; Sejrup 1987; Anundsen 1988; Bungum 1989; Gabrielsen 1989).

However, without knowing the age of the Quaternary clays, loading by glaciers must also be considered as a possible explanation for the faulting in the clays. An unconformity is present in the clays along the western slope of Karmsundet (Fig. 2). This may have been produced by glacial erosion below sea level. Furthermore, it is possible that the sediment mass movements mentioned above might be the result of sediment instability following deposition on unstable slopes. The special ocean current systems in this region lead in some areas to deposition, in other areas non-deposition. Slumps and slides redistribute the sediments.

A weak bottom simulating reflector (BSR), as defined by Paull & Dillon (1981), is evident in the deep-water parts of Karmsundet. Such a reflector is normally caused by gas hydrates. If hydrates occur in these sediments their destabilization during earthquakes could also trigger slides on the seabed.

These investigations, of which some preliminary results are presented above, will be followed up by a more

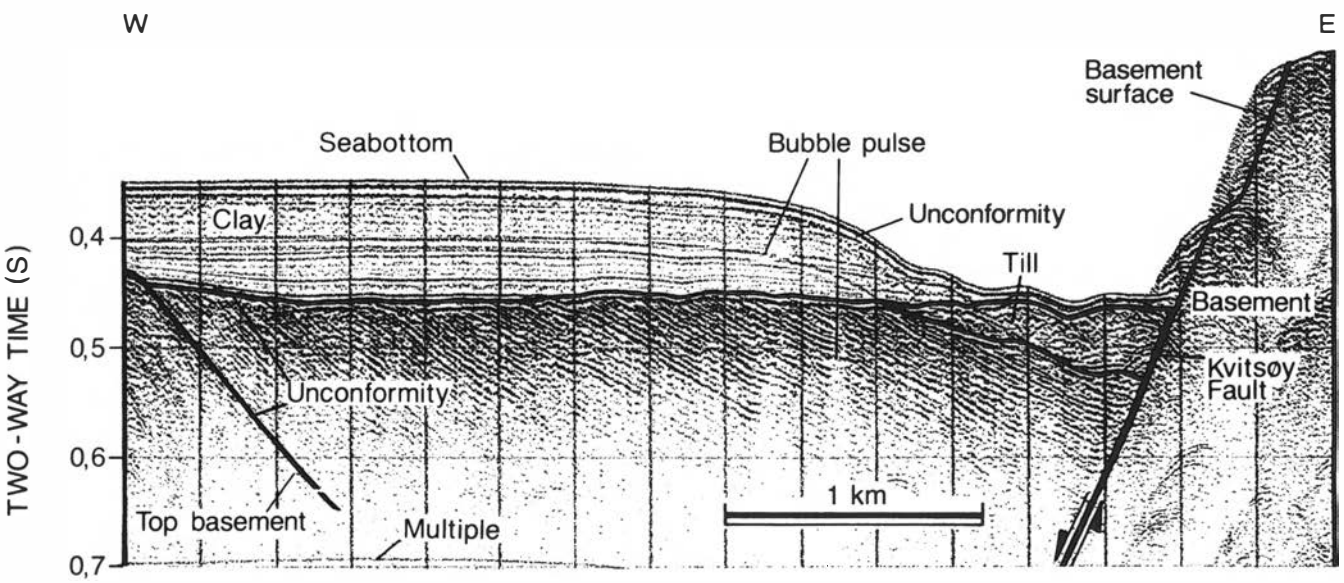

Fig. 2. Seismic reflection profile (single-channel, analogue mini-airgun) across the Karmsundet Basin illustrating downfaulting of a layered, sedimentary rock succession of late Palaeozoic–Mesozoic age along the Kvitsøy Fault. See Fig. 1 for location of profile. Vertical exaggeration is approximately ×2.

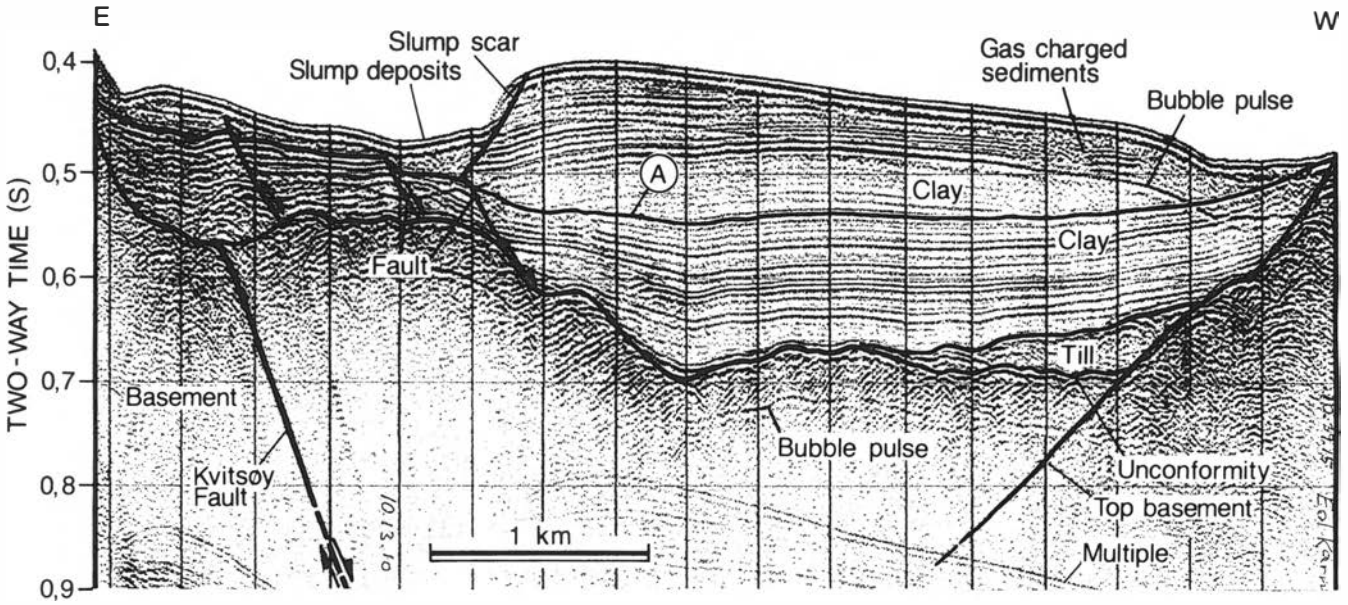

Fig. 3. Seismic reflection profile (single-channel, analogue mini-airgun) across the Karmsundet Basin illustrating downfaulting of a layered, sedimentary rock succession along the Kvitsøy Fault and tectonic disturbances in the Quaternary deposits. Note that faults cut the lowermost glaciomarine clay sequence beneath reflectory A, and that these faults, the slump scar and the slump deposits are all situated close to or immediately above the Kvitsøy Fault. Also note the contourite-like pattern of the clays above reflector A and the occurrence of gas-charged sediments. See Fig. 1 for location of profile. Vertical exaggeration is approximately ×2.

detailed shallow seismic profiling and sampling programme that will provide better correlation to dated seismic sections. This will perhaps enable us to be more precise about the age of the sedimentary rocks, the age of the Quaternary deposits and the sequence of tectonic events and mass movements that have occurred.

Acknowledgements. – The authors would like to thank Elf Aquitaine Norge A/S, Statoil and the Geological Survey of Norway for the opportunity to publish these data.

Manuscript received October 1991

References

Anundsen, K. 1988: Variations in Quaternary (Late Weichselian) relative sea-levels in southwest Norway; observations of isostatic/eustatic movements and active faulting (abstract). *In* Mørner, N. A. (ed.): *Proceedings of the Lejoland Symposium on Neotectonics*, Stockholm.

Bakkelid, S. 1986: The determination of rates of land uplift in Norway. *Tectonophysics 130,* 307–326.

Bungum, H. 1989: Earthquake occurrence and seismotectonics in Norway and surrounding areas. *In* Gregersen, S. & Basham, P. W. (eds.): *Earthquakes at North Atlantic Passive Margins: Neotectonics and Postglacial Rebound*, 501–520. Kluwer, Dordrecht.

Bøe, R. 1990: Regionalseismisk undersøkelse i ytre del av Boknafjorden. Unpublished report 90.093, Norges geologiske undersøkelse, 7 pp.

Bøe, R. 1991: Structure and seismic stratigraphy of the innermost mid-Norwegian continental shelf: an example from the Frohavet area. *Marine and Petroleum Geology 8,* 140–151.

Bøe, R. & Bjerkli, K. 1989: Mesozoic sedimentary rocks in Edøyfjorden and Beitstadfjorden, central Norway: implications for the structural history of the Møre–Trøndelag Fault Zone. *Marine Geology 87,* 287–299.

Bøe, R. & Hovland, M. 1990: Neotectonism and sediment instability along the Norwegian coast south of Karmøy (Abstract). *In* NGF's Tectonics and Structural Geology Studies Group TSGS 7th annual meeting: *Post-Cretaceous Uplift and Sedimentation Along the Western Fennoscandian Shield.*

Feyling-Hansen, R. W. 1966: Geologiske observasjoner i Sandnesområdet. *Norges geologiske undersøkelse 242,* 26–43.

Gabrielsen, R. H. 1989: Reactivation of faults on the Norwegian continental shelf and its implications for earthquake occurrence. *In* Gregersen, S. & Basham, P. W. (eds.): *Earthquakes at North Atlantic Passive Margins. Neotectonics and Postglacial Rebound*, 67–90. Kluwer, Dordrecht.

Gade, H. G. 1986: Brief overview of the physical oceanography. *In* Hurdle, B. G. (ed.): *The Nordic Seas*, 183–189. Springer Verlag, New York.

Havskov, J. & Bungum, H. 1987: Source parameters for earthquakes in the northern North Sea. *Norsk Geologisk Tidsskrift 67,* 51–58.

Holtedahl, H. 1988: Bedrock geology and Quaternary sediments in the Lista Basin, S. Norway. *Norsk Geologisk Tidsskrift 68,* 1–20.

Paull, C. K. & Dillon, W. P. 1981: Appearance and distribution of the gas hydrate reflection in the Blake Ridge region, offshore South Carolina. Map and Information Sheet. *United States Geological Survey.*

Pickering, K. T. Hiscott, R. N. & Hein, F. J. 1989: *Deep-Marine Environments. Clastic Sedimentation and Tectonics*, 219–245. Unwin Hyman, London.

Rokoengen, K. & Sørensen, S. 1990: Late Jurassic sedimentary bedrock north of Utsira, offshore western Norway. *Norsk Geologisk Tidsskrift 70,* 61–63.

Rokoengen, K., Riise, L., Bugge, T & Sættem, J. 1988: Bedrock geology on the Mid Norwegian Continental Shelf. Map in scale 1:1 000 000. *Institutt for kontinentalsokkelundersøkelser, Publication 118.*

Sejrup, H. P. 1987: Molluscan and foraminiferal biostratigraphy of an Eemian–Early Weichselian section on Karmøy, south-western Norway. *Boreas 16,* 27–42.

Thon, A. 1980: Steep shear zones in the basement and associated deformation of the cover sequence on Karmøy, SW Norwegian Caledonides. *Journal of Structural Geology 2,* 75–80.

Cenozoic uplift in the Stord Basin area and its consequences for exploration

SAMIR A. GHAZI

Ghazi, S. A.: Cenozoic uplift in the Stord Basin area and its consequences for exploration. *Norsk Geologisk Tidsskrift*, Vol. 72, pp. 285–290. Oslo 1992. ISSN 0029-196X.

A thorough evaluation of the tectonic development of the Stord Basin during the Cenozoic was undertaken in order to understand the state of maturity and the hydrocarbon potential of the primary Upper Jurassic source rock. Study of the Tertiary sequences within the basin reveals several episodes of uplift and subsequent erosion resulting in the deposition of westwardly prograding sedimentary wedges during the Late Paleocene, Late Oligocene and Mio-Pliocene. Maturation modelling of the present-day central parts of the Stord Basin shows that the source rocks have not reached the peak oil generation stage. It is estimated that approximately 400 to 600 m of Mio-Pliocene sediments have been removed from the central parts of the basin, as a result of the Tertiary uplift. It is anticipated that regional warping is the predominant mechanism by which Fennoscandia was uplifted during the Cenozoic. The initial phases of flank-uplift were most probably triggered by the opening of the Norwegian–Greenland Sea, with plate reorganizations in the North Atlantic and Tethyan closure providing the remaining impetus for the subsequent phases of uplift during the Tertiary.

S. A. Ghazi, Conoco Norway Inc., PO Box 488, N-4001 Stavanger, Norway.

The largely unexplored Stord Basin is a shallow depression confined between 59°N and 60°N; it is flanked to the east (Fig. 1) by the Fennoscandian landmass and to the west by the Utsira High. The basin was formed by extension during the Late Paleozoic to Late Jurassic period. During the Cretaceous thermal subsidence prevailed. However, inversion and reverse movement by rejuvenation along older major normal faults is apparent.

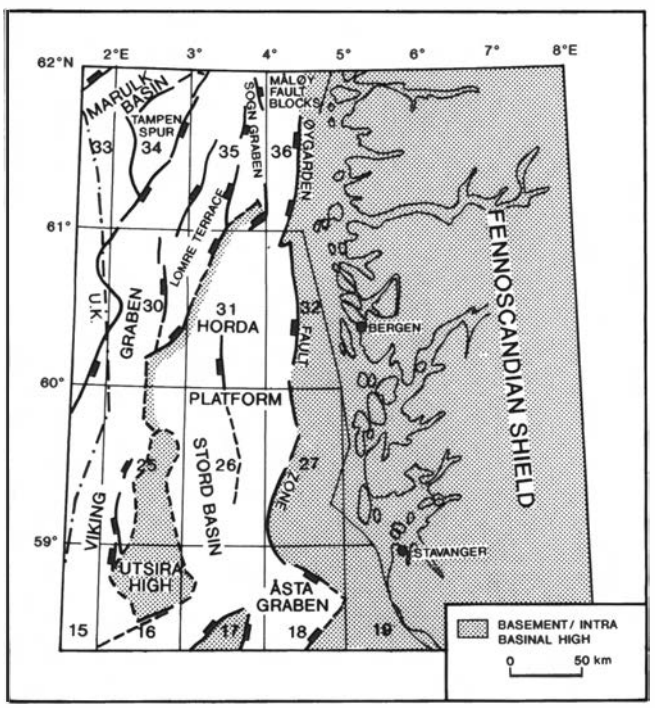

Fig. 1. Location map.

The period of inversion is thought to have occurred in the Late Cretaceous to Early Paleocene.

Cenozoic structural development

It is unfortunate that a major part of the Tertiary sedimentary record proximal to the Fennoscandian Shield has been removed by erosion. Nevertheless, the structural evolution can be reconstructed by interpreting what is seen at present from the observed configuration of stratigraphic units on seismic lines (Fig. 2). A schematic drawing summarizing the Cenozoic structural evolution of the study area is shown in Fig. 3. The Paleocene section in the Stord Basin is seismically transparent and generally uniform in thickness, except on the eastern flank where a distinct thicker wedge is present. The development of the wedge-shaped geometry, together with the presence of internal westwardly downlapping events (Fig. 2), signals an early phase of uplift and subsequent erosion of the adjacent Fennoscandian landmass. This movement took place during the Late Paleocene and is coeval with the first phase of sea-floor spreading in the Norwegian–Greenland Sea (Eldholm & Thiede 1980). The Eocene and most of the Oligocene appear to have been tectonically quiescent. Renewed tectonic activity took place at the close of the Oligocene. This, again, is apparent by the progradational nature of the sedimentary package in the uppermost part of the Oligocene sequence (Figs. 2, 3) on the eastern flank of the Stord Basin. The overlying Miocene section is characterized by large westward prograding clinoforms downlapping the Utsira Formation sands. The Pliocene

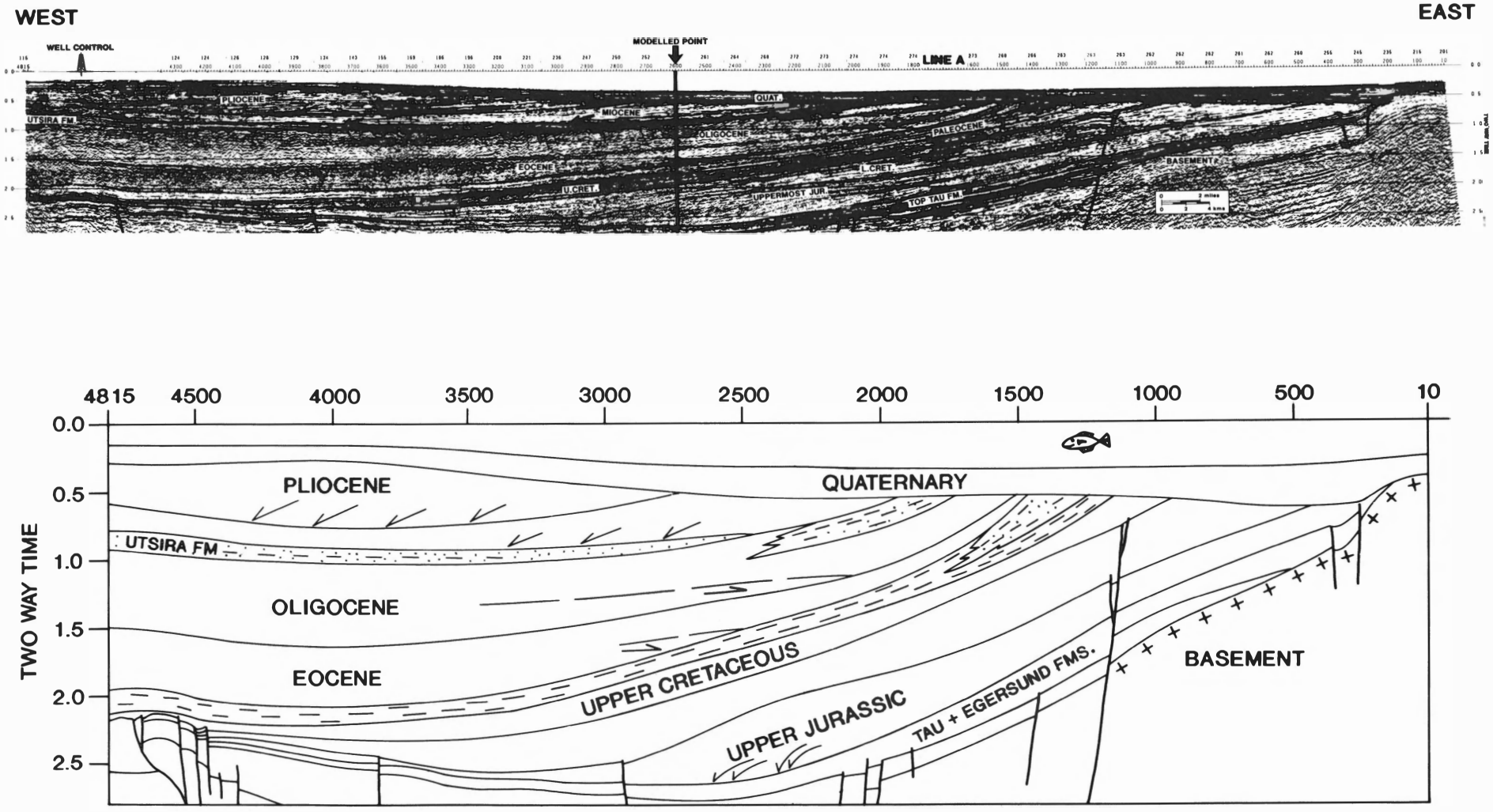

Fig. 2. (a) Seismic line A (see Fig. 4 for location) showing location of modelled point in center of Stord Basin. (b) Geologic interpretation of line A.

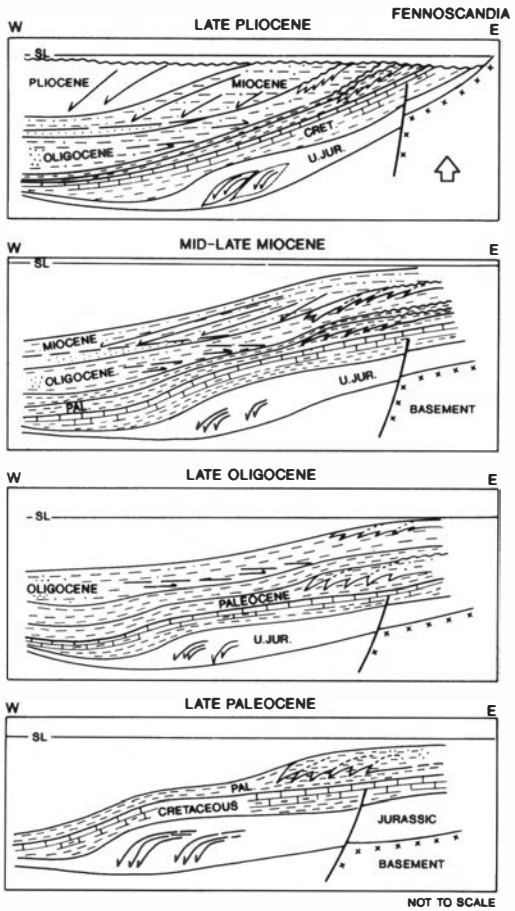

Fig. 3. Cenozoic structural evolution along an east–west transect in the Stord Basin.

epoch represents a continuation of the regime established during the Miocene. A thick sedimentary sequence displaying westwardly prograding clinoforms with downlap terminations typifies this package.

The Mio-Pliocene period represents the main phase of uplift of the eastern flank of the Stord Basin and the adjoining Fennoscandian Shield. Finally, by the Late Pliocene–Early Pleistocene the whole area was tilted, resulting in a massive angular unconformity. This episode coincides with the glaciation/deglaciation phenomena in the area and is estimated to have taken place at ca. 2.2 Ma (Rundberg 1989). Table 1 summarizes the various tectonic phases influencing the development of the Stord Basin area.

Source rock maturity

Regional seismic correlations indicate that the Tau Formation shales are present in the Stord Basin. The Tau Formation is Kimmeridgian to Early Volgian in age and is a rich (TOC = 2–8%) oil-prone source rock in the Åsta Graben (Fig. 1). Estimates based on known thicknesses from surrounding wells and the corresponding observed thicknesses on seismic lines indicate that for the

Table 1. Summary of Cenozoic structural activity in the Stord Basin.

Time	Tectonic activity	Sedimentary response
Early Pleistocene–Late Pliocene	Glaciation/deglaciation isostatic rebound	Glacial deposits
Pliocene	Fennoscandia: major uplift with concurrent basin subsidence	Thick progradational sedimentary packages
Miocene		
Late Oligocene	Renewed uplift	Westwardly prograding thin wedge
Early Oligocene	Quiescent	Fine-grained clastics eastward onlap/downlap
Eocene	Quiescent	Basinal shales
Late Paleocene	Uplift of Fennoscandia	Small prograding wedge

central portion of the Stord Basin between 400 and 600 m of Mio-Pliocene sediments have been removed as a result of the Tertiary uplift. The structural history as previously defined (Table 1), together with the calculated amounts of eroded section, were used to model a location (Fig. 4) in the present-day deepest part of the basin using the Yukler one-dimensional basin modelling software. Several scenarios involving various amounts of uplift (400–600 m) at slightly differing geologic ages were performed. Of these, only the two most appropriate models are shown in Fig. 5. Only two uplift periods were modelled, since the Late Paleocene phase was considered to have a negligible effect on the depth of burial of the source rock. The models show (Fig. 5a, b) that the Tau Formation has never reached the peak oil-generation stage. Very limited amounts of hydrocarbons have therefore been generated as indicated by the hydrocarbon transformation diagrams (Fig. 5c, d). Only when the total amount of uplift and erosion is increased to 1000 m does the source rock reach the peak oil-generation stage. This, however, is not considered a likely scenario at this particular location. Nevertheless, it is anticipated that at least 1500 m of section may have been removed from the more eastern portions adjoining the western margin of the Fennoscandian Shield.

Uplift mechanism

Examination of seismic data indicates that the Cenozoic section in the Stord Basin is undisturbed by major faults (Fig. 2). Major fault activity along the Øygarden Fault Zone ceased during the early part of the Late Cretaceous. Therefore the uplift of the landmass adjacent to the Stord Basin was not accomplished through fault rejuvenation. This, in addition to the marked northward increase in topographic relief of Fennoscandia, points to the rifting pulses in the Norwegian–Greenland Sea (Fig. 6) as the most logical and plausible triggering agent for the ensuing flank uplift of the adjacent continental margins (Torske 1972). It is suggested, however, that the

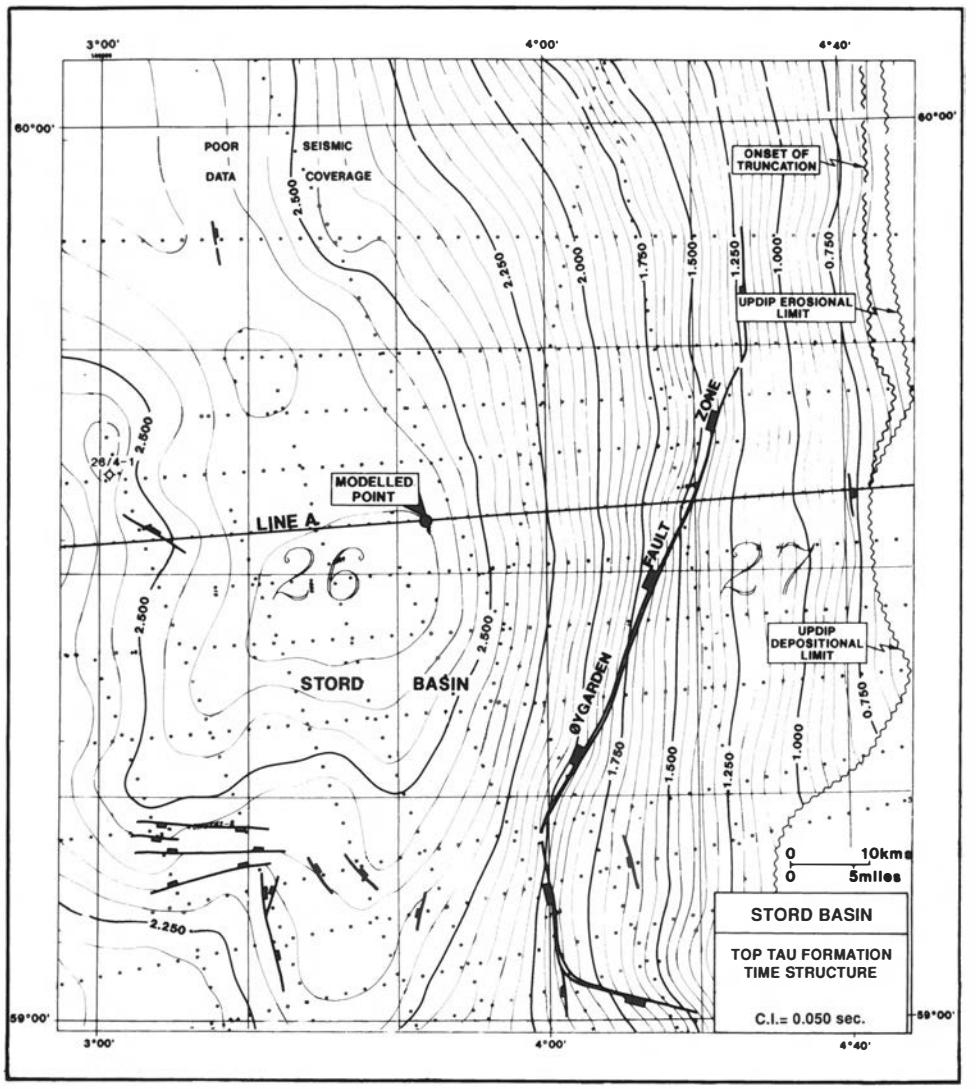

Fig. 4. Basin morphology at top Tau Formation, and location of line A with the position of the modelled shot point.

uplift is partially due to regional warping resulting in a broad fold as shown in Fig. 7. Once the initial flank uplift is initiated (time = t_0, Fig. 7) erosion of the 'bulge' takes place and the adjoining lithosphere (basinal area) is down-loaded by sediments. The immediate response is the isostatic adjustment of the adjacent highs, with corresponding down-bending of the lithosphere and the process is then re-established (time = t_1, then t_2. . .). Normally, this process should be of a self-perpetuating nature, until erosion to a certain base level is accomplished. Plate reorganization in the North Atlantic and Tethyan closure events (Doré, this volume) may, however, have triggered new uplift phases and sustained this process through the Cenozoic. Later glaciation and deglaciation amplified the extent of uplift through isostatic adjustments during the Plio-Pleistocene.

Conclusions

Several phases of *episodic* uplift during the Cenozoic affected the eastern flank of the Stord Basin and the adjacent Norwegian mainland. This resulted in the removal of between 400 and 600 m of sediments from the central part of the basin and more than 1500 m from the eastern margin adjoining the Fennoscandian Shield.

Thermal maturation modelling of the primary Upper Jurassic source – the Tau Formation – in the deeper parts of the Stord Basin indicates that it is still in the early oil-maturation stage and that the main phase of expulsion has not yet been reached.

Examination of seismic data from the Stord Basin indicates that regional warping was the predominant mechanism by which Fennoscandia was elevated. However,

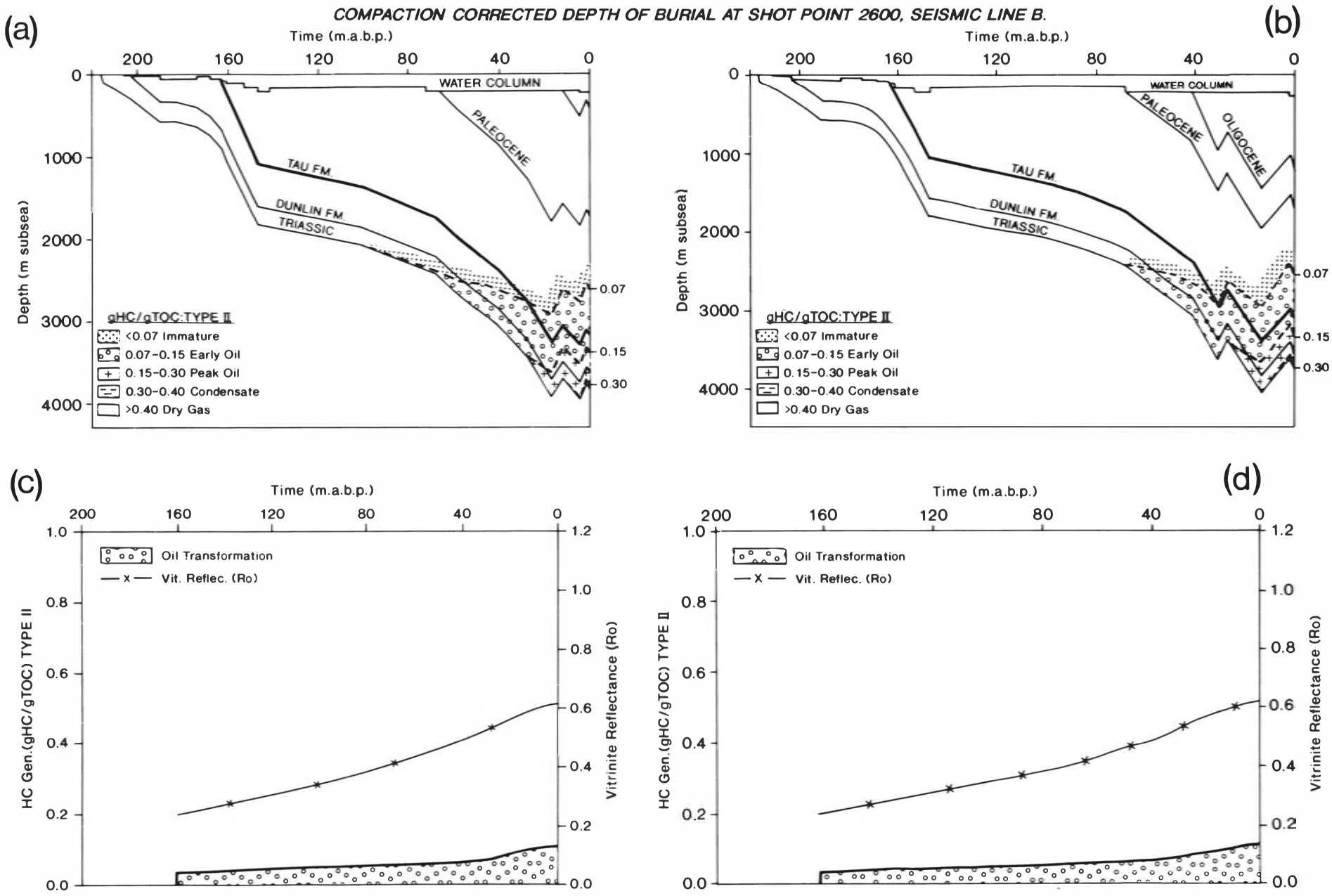

Fig. 5. (a) Uplift at Mid-Miocene and Late Pliocene with 200 m removed respectively. (b) Uplift at end of Oligocene and Mid-Miocene with 200 m and 400 m removed respectively. (c) Hydrocarbon generation and modelled vitrinite reflectance (Ro) versus time for top Tau Formation at shot point 2600, seismic line A; 200 m removed. (d) Hydrocarbon generation and modelled vitrinite reflectance (Ro) versus time for top Tau Formation at shot point 2600, seismic line A; 200 m and 400 m removed respectively.

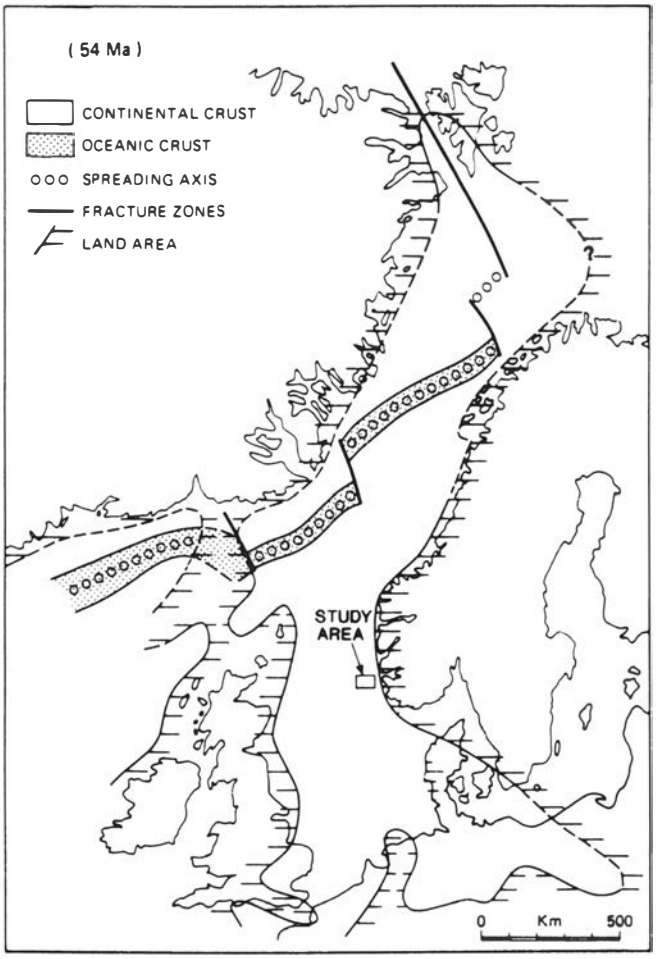

Fig. 6. Paleogeographic reconstruction of NW Europe in Late Paleocene time; anomaly 23 (Rundberg 1989).

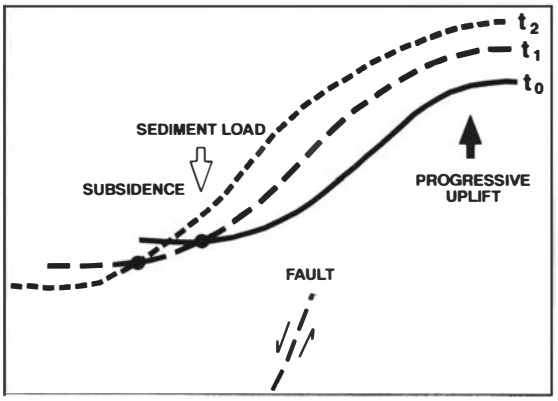

Fig. 7. Schematic representation of uplift by gentle warping of the lithosphere.

proximity to the spreading centres in the Norwegian–Greenland Sea may have caused the initial phases of flank uplift.

Acknowledgements. – I thank the management of Conoco Norway Inc. for permission to publish this paper. I also extend my thanks to Tony Doré and Bruce Reid, both of whom edited the manuscript and offered helpful suggestions.

Manuscript received October 1991

References

Doré, A. G. 1992: The Base Tertiary Surface of southern Norway and the Northern North Sea. *Norsk Geologisk Tidsskrift 72.* This volume, pp. 259–265.

Eldholm, O. & Thiede, J. 1980: Cenozoic Continental Separation between Europe and Greenland. *Paleogeogr., Paleoclimat., Paleoecol. 30,* 243–359.

Rundberg, Y. 1989: *Tertiary Sedimentary History and Basin Evolution of the Norwegian North Sea between* 60°*N and* 62°*N. An Integrated Approach.* Dr. Ing. thesis. Univ. of Trondheim, Norway.

Torske, T. 1972: Tertiary oblique uplift of Western Fennoscandia; crustal warping in connection with rifting and break-up of the Laurasian continent. *Norges geologisk undersøkelse 273,* 43–48.

Uplift study of the Jameson Land basin, East Greenland

FLEMMING G. CHRISTIANSEN, HANS CHRISTIAN LARSEN, CHRISTIAN MARCUSSEN, KIRSTEN HANSEN, HELLE KRABBE, LOTTE M. LARSEN, STEFAN PIASECKI, LARS STEMMERIK & W. STUART WATT

Christiansen, F. G., Larsen, H. C., Marcussen, C., Hansen, K., Krabbe, H., Larsen, L. M., Piasecki, S., Stemmerik, L. & Watt, W. S.: Uplift study of the Jameson Land basin, East Greenland. *Norsk Geologisk Tidsskrift*, Vol. 72, pp. 291–294. Oslo 1992. ISSN 0029-196X.

This extended abstract briefly outlines the results of a study of the uplift history of the Jameson Land basin, East Greenland. The interpretation of the timing and magnitude of the uplift is based on a combination of geometric (basin configuration from seismic and surface data) and analytical data (maturity parameters, apatite fission track analyses, porosity, seismic velocity and zeolite minerals). All data are in accordance with an uplift between 1.5 and 3 km during the Tertiary.

F. G. Christiansen, H. C. Larsen, C. Marcussen, L. M. Larsen, S. Piasecki, L. Stemmerik & W. S. Watt, Geological Survey of Greenland, Øster Voldgade 10, DK-1350, Copenhagen K, Denmark; K. Hansen & H. Krabbe, Geological Institute, University of Copenhagen, Øster Voldgade 10, DK-1350 Copenhagen K, Denmark.

The Jameson Land basin in East Greenland comprises a thick succession of Upper Palaeozoic–Mesozoic sediments which are well exposed due to considerable uplift during the Tertiary. Several decades of studies have provided a multidisciplinary background for the discussion of magnitude, timing and tectonic mechanisms of this uplift.

Mapping in the scale 1:100,000 was carried out from 1968 until 1972 and was followed by detailed stratigraphic studies of the Mesozoic succession (e.g. Surlyk et al. 1973; Birkelund & Perch-Nielsen 1976). Later studies by the Geological Survey of Greenland concentrated on more specific petroleum related subjects like reservoir and source rocks and thermal history (e.g. Surlyk et al. 1986).

Exploration for petroleum has been carried out with Atlantic Richfield Company (ARCO) as operator in 1985–1990. In this period, 1798 km of onshore seismic data (both dynamite and vibro-seismic) were acquired. Together with the 520 km of offshore seismic data from Scoresby Sund, which were obtained by the NAD-project (GGU) in 1980, these data provide a good background for geometric considerations (Fig. 1.)

ARCO has, however, decided to give up exploration by the end of 1990. Apparently this was done under the influence of the low oil price at the time of decision. Another factor was a high risk due to uncertainties of the Tertiary thermal and uplift history, which of course stresses the importance of the present contribution.

Techniques

Interpretation of uplift and erosion is based on a combination of geometric and analytical data. The thickness variation and geometry of Late Palaeozoic–Mesozoic sediments and Tertiary volcanics from seismic and surface interpretation provide some direct clues on differential vertical movements, as noted already by Larsen (1984, 1990).

These ideas can be tested against analytical data like thermal maturity parameters (TAI, R_0, T_{max}, isomerization of hopanes and steranes), parameters from apatite fission track analysis (FT-age, track length distribution), diagenetic parameters (porosity), seismic velocities (average or interval velocity from stacking velocities), and zeolite mineral zonation in the basalt succession.

The main problem in an accurate estimation of uplift is the lack of wells in Jameson Land. The extrapolation methods where the depth versus trend of maturity parameters or petrophysical properties are used to give a direct uplift value cannot be applied.

Basin geometry

The post mid-Permian succession of the Jameson Land basin is a structurally simple, sag-shaped fill with a NNE–SSW orientated depocenter. The oldest sediments are exposed along the eastern and western margin of the basin; strata exposed in central Jameson Land are younging towards south (Fig. 1). The strata dip between 1° and 2° to the south in longitudinal sections, parallel to the basin axis with a minor flexure approximately 40 km north of the southern tip of Jameson Land (Fig. 2). The cross-sections indicate a considerable variation in thicknesses and it is evident that differential vertical movement must have taken place during subsidence and possibly also during uplift. This is further substantiated by the subhori-

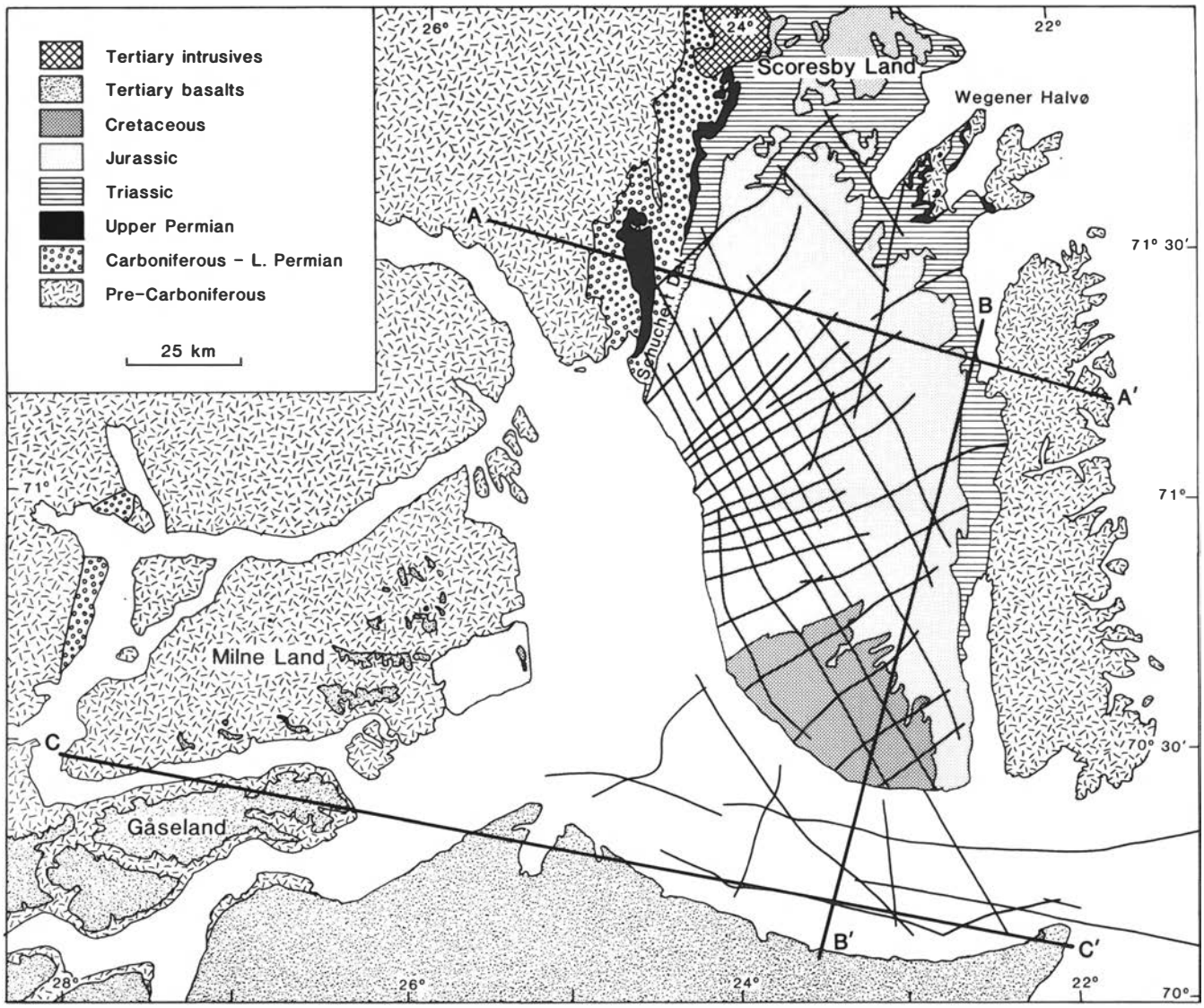

Fig. 1. Simplified geological map of the Jameson Land region with position of onshore ARCO seismic lines and offshore GGU seismic lines. The longitudinal and cross-sections are shown in Fig. 2.

zontally formed basalts south of Scoresby Sund, which now define a syncline with an axis close to the depocenter of the underlying sediments (Fig. 2). Further west, in Milne Land, the basalts which extruded on top of the basement display significantly higher present-day altitudes.

Analytical data

The measured maturity parameters are all from outcropping organic-rich units, especially the Upper Permian Ravnefjeld Formation, the Lower Jurassic Kap Stewart Formation, and the Upper Jurassic Hareelv Formation. The maturity pattern of the surface sediments is relatively simple (Fig. 3). By far the most of the area has immature surface sediments ($R_0 < 0.6$, $TAI < 2$, $T_{max} < 445$, steranes not in equilibrium). This is the case for all of central and southern Jameson Land except for a few abnormal zones in the vicinity of dolerite dykes and sills. This suggests that between 1.5 and 3 km of overburden has been removed. In the northernmost part of Jameson Land all surface sediments are postmature. In some areas this maturity is due to the effect of large mid-Tertiary intrusions, in others like the Wegener Halvø, the maturity of the Upper Permian is the result of deep subsidence combined with circulation of hot hydrothermal fluids (Christiansen et al. 1990).

The apatite fission track data recorded from sandstones of Carboniferous through Jurassic age are in accordance with the maturity data (Hansen 1988). In southern and central Jameson land, roughly corresponding to the immature zone, the apatite fission tracks are only slightly reset and the FT ages are very old, often older than the depositional ages, and therefore mainly provide information on the uplift of the source area. A few samples in this zone are reset with young ages (40–67 Ma). These samples are probably thermally affected by Late Paleocene–Eocene dolerite sills and

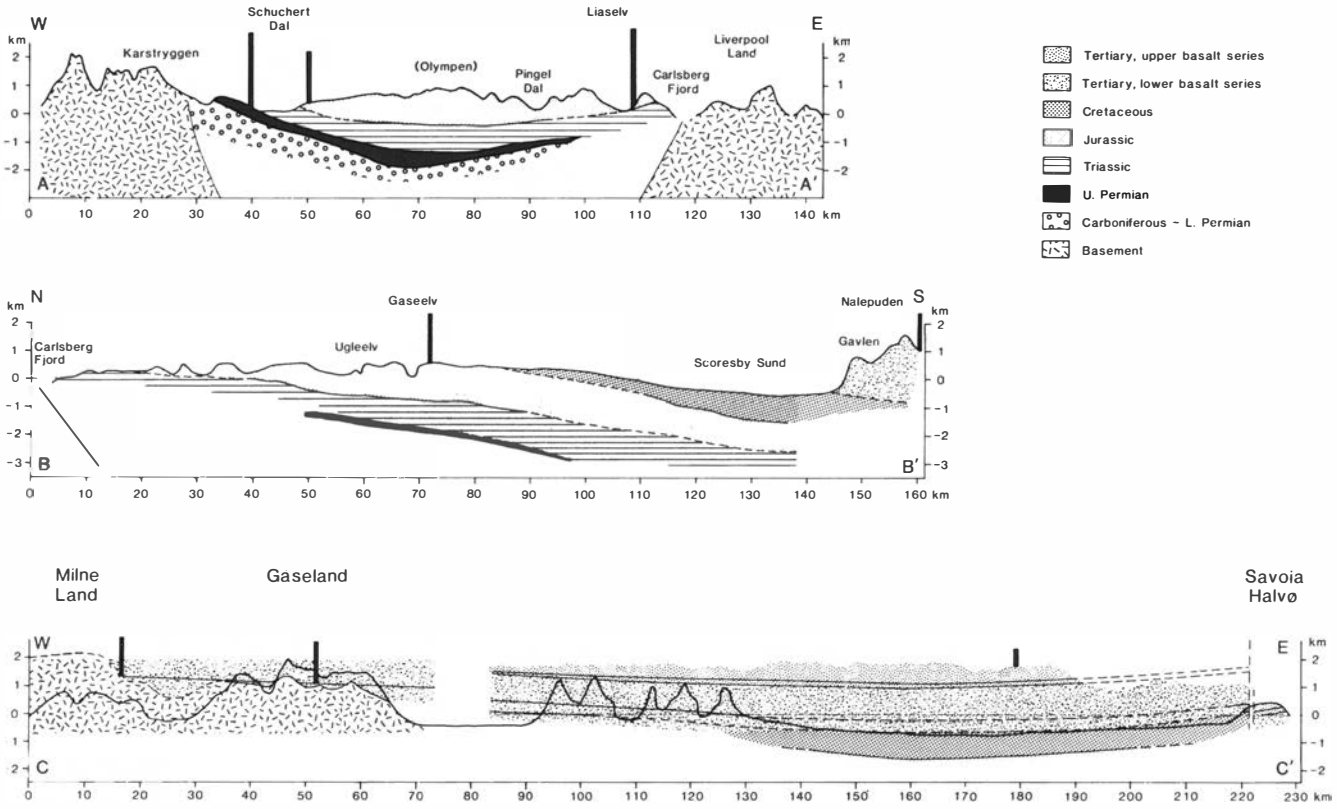

Fig. 2. Cross and longitudinal sections. See Fig. 1 for location. The vertical bars show the maximum overburden at various locations empirically deduced from maturity data (sterane isomerization, zeolite minerals).

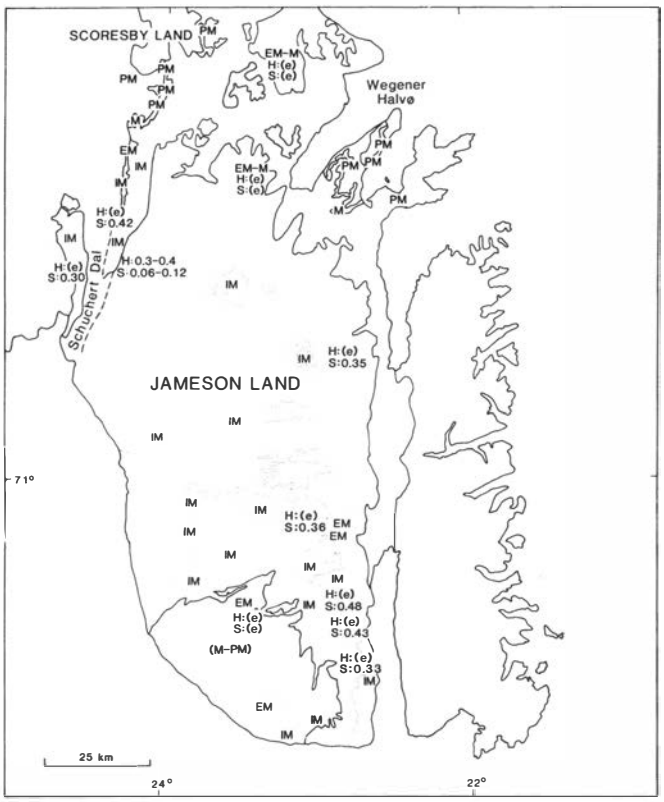

Fig. 3. Surface thermal maturity map. IM: early diagenetic – immature ($R_0 < 0.6$, TAI < 2 , $T_{max} < 435$, Steranes not in equilibrium); EM-M: early mature–mature; PM: postmature ($R_0 > 1.3$, TAI > 3⁻, $T_{max} > 460$). H and S: hopane and sterane isomerization values or equilibrium (e).

dykes, and therefore they record cooling ages subsequent to local contact metamorphism. In the northern area, roughly corresponding to the postmature zone, the fission tracks are completely reset and the FT ages are very young (15–25 Ma).

The few obtained sandstone porosity values of the Middle Jurassic in central Jameson Land (average: 21.6%) and the Upper Jurassic in southern Jameson Land (average: 23.8%) empirically suggest uplift values between 2 and 3 km.

The seismic velocity distribution also has a potential for determining the magnitude of uplift, although the lack of well control makes it difficult to make lithological corrections. As a test, the average seismic velocity versus depth curves has been calculated at a number of shot-points from the stacking velocities. A significant increase in velocity with depth and in near-surface velocity is observed from south towards north, and the high near-surface velocities (2.7–3.4 km/sec) suggest an uplift of several km.

The vertical zonation of zeolite minerals in the Tertiary basalts (mesolite–scolecite, analcime, chabazite–thomsonite and zeolite free zones) can be applied for estimates of erosion. South of Scoresby Sund (Geikie Plateau) less than 400 m of basalts have been removed. The bottom of the chabazite zone (ca. 70°C) is here situated 900 m above sea level. This is in contrast to the somewhat higher altitudes (1100–1300 m) in Gåseland

and Milne Land (Watt et al. 1989) and may support a model with greater uplift of the marginal areas.

Cretaceous and Tertiary history

The analytical data seem to provide a rather consistent pattern of uplift, which raises a number of questions on the thickness, facies and age of previously overlying Cretaceous and Tertiary strata. The thickness and facies distribution of the Upper Permian to Upper Jurassic is well known from fieldwork and seismic mapping and may be extrapolated to most of Jameson Land without serious problems. The depositional history of Jameson Land during the Cretaceous and Tertiary may be partially interpreted based on data from southern Jameson Land (Surlyk et al. 1973), Milne Land (Birkelund et al. 1974), offshore Scoresby Sund (GGU, unpublished), south of Scoresby Sund (Watt et al. 1989), northernmost Jameson Land and Traill Ø (Donovan 1953; Nielsen 1987).

This information, together with depositional and subsidence history models and the measured parameters, suggests that most of Jameson Land has been covered by more than 1 km of Cretaceous sediments comprising a rather thin (Volgian)–Barremian package of shallow marine-fluvial sandstones and a considerably thicker succession of Aptian–Albian marine shales. A thick cover of Tertiary basalts probably only covered the southernmost 30–40 km of Jameson Land, but this cover was thinner (max. 1–2 km) than south of Scoresby Sund (Fig. 2).

In central and southern Jameson Land this Upper Jurassic, Cretaceous and Tertiary package was removed during relatively stable uplift and erosion. In contrast northern Jameson Land (including Scoresby Land and Wegener Halvø) suffered a structurally and thermally complex Tertiary history, probably with considerably higher uplift.

Acknowledgements. – Finn Surlyk is thanked for discussions on especially the Cretaceous and Tertiary history of the area. The authors are grateful to J. Halskov, B. S. Hansen, N. Turner, V. Hermansen and J. Lautrup for technical assistance. The paper is published with the permission of the Geological Survey of Greenland.

Manuscript received October 1991

References

Birkelund, T. & Perch-Nielsen, K. 1976: Late Palaeozoic–Mesozoic evolution of central East Greenland. *In* Escher, A. & Watt, W. S. (eds.): *Geology of Greenland.* Grønlands Geologiske Undersøgelse, 305–339.

Christiansen, F. G., Piasecki, S. & Stemmerik, L. 1990: Thermal maturity history of the Upper Permian succession in the Wegener Halvø area, East Greenland. *Rapport Grønlands Geologiske Undersøgelse 148*, 109–114.

Donovan, D. T. 1953: The Jurassic and Cretaceous stratigraphy and palaeontology of Traill Ø, East Greenland. *Meddelelser om Grønland 111*, 150 pp.

Hansen, K. 1988: Preliminary report of fission track studies in the Jameson Land basin, East Greenland. *Rapport Grønlands Geologiske Undersøgelse 140*, 85–89.

Larsen, H. C. 1984: Geology of the Greenland shelf. *In* Spencer, A. M. et al. (eds.): *Petroleum Geology of the North European Margin*, 329–339. Graham & Trotman, London.

Larsen, H. C. 1990: The East Greenland Shelf. *In* Granz, A., Johnson, L. & Sweeney, J. F. (eds.): *The Arctic Ocean Region: The Geology of North America L*, 185–210, Boulder, Colorado, Geological Society of America.

Nielsen, T. F. D. 1987: Tertiary alkaline magmatism in East Greenland: a review. *In* Fitton, J. G. & Upton, B. G. J. (eds.): *Alkaline Igneous Rocks. Geological Society Special Publication 30*, 489–515.

Surlyk, F., Callomon, J. H., Bromley, R. G. & Birkelund, T. 1973: Stratigraphy of the Jurassic–Lower Cretaceous sediments of Jameson Land and Scoresby Land, East Greenland. *Bulletin Grønlands Geologiske Undersøgelse 105*, 76 pp.

Surlyk, F., Hurst, J. M., Piasecki, S., Rolle, F., Scholle, P. A., Stemmerik, L. & Thomsen, E. 1986: The Permian of the western margin of the Greenland Sea – a future exploration target. *In* Halbouty, M. T. (ed.): *Future Petroleum Provinces of the World. American Association of Petroleum Geologists Memoir 40*, 629–659.

Watt, W. S., Watt, M. & Larsen, L. M. 1989: Part 1: Geology. Geology and petrology of the Lower Tertiary plateau basalts of the Scoresby Sund region, East Greenland. *Bulletin Grønlands Geologiske Undersøgelse 157*, 5–48.

The Cenozoic sequence stratigraphy of the Halten Terrace and the Outer Vøring Plateau based on seismic and biostratigraphic data

ROBERT M. GOLL & JØRGEN W. HANSEN

Goll, R. M. & Hansen, J. W.: The Cenozoic sequence stratigraphy of the Halten Terrace and the Outer Vøring Plateau based on seismic and biostratigraphic data. *Norsk Geologisk Tidsskrift*, Vol. 72, pp. 295–299. Oslo 1992. ISSN 0029-196X.

The Cenozoic succession of the Halten Terrace consists of four major sedimentary sequences separated by hiatuses of long duration. Only two of these hiatuses, Base Tertiary and Inter-Oligocene, are clearly represented by regional seismic reflectors. Although the Cenozoic sequences of the Outer Vøring Plateau are more complex, the bounding hiatuses of these two adjoining regions are correlative.

R. M. Goll & J. W. Hansen, Institutt for Kontinentalsokkelundersøkelser og Petroleumsteknologi A/S, PO Box 7034, Trondheim, Norway.*
** New address: Statoil, PO Box 300, 4001 Stavanger, Norway.*

Investigations of a seismic grid compiled from various sources and biostratigraphic data from seven commercial wells from the Halten Terrace (Fig. 1) indicate that the Cenozoic succession of this region is composed of four major sedimentary sequences bounded by four regional unconformities with hiatuses of large magnitude (Fig. 2). A proprietary set of numerically determined biostratigraphic event markers with estimated precisions of ± 0.5 to ± 2.0 m.y. has been used to identify and date these sequences, determine the positions and durations of hiatuses, and re-establish chronostratigraphic unit boundaries (Goll et al. 1990). Our analyses indicate that the successions of these Halten Terrace wells include records of only 30–51% of Cenozoic time. The Halten Terrace sequences are compared to the sequences of the Outer Vøring Plateau that have been penetrated on DSDP Leg 38 and ODP Leg 104 (Goll 1989).

Sequence 1 has the most variable occurrence and most complex history of the Halten Terrace Cenozoic succession. This sequence is bounded below by the Cretaceous–Tertiary unconformity (reflector BT), and it includes 135–663 m of sediments assigned to the Rogaland Group and the lower Brygge Formation. Sediments at the base of this sequence have ages of 62–64 Ma at the various well sites, and the uppermost sediments have ages of 44–57 Ma. The sequence is locally interrupted by small hiatuses of 3–5 m.y. The complexity of this sequence is believed to have resulted from Eocene tectonism of the mid-Norwegian margin, which has been documented on the Vøring Plateau (Skogseid & Eldholm 1989). The unconformity bounding the top of sequence 1 has a hiatus of 10–19 m.y. This unconformity is not obvious from the seismic data. At well localities where sequence 1 ranges up to as young as 44 Ma, sequence 2 is absent.

Sequence 2 includes 55–178 m of upper Middle to Upper Eocene sediments of the upper Brygge Fm. Sediments at the base of this sequence have ages of 38–42 Ma at the various well sites, and the uppermost sediments have ages of 36–37 Ma. The boundary between sequences 2 and 3 is represented by the Inter-Oligocene (IO) reflector, and the hiatus associated with this unconformity has a duration of 7–14 m.y. The Brygge Fm/Kai Fm contact is coincident with this unconformity, as indicated by Dalland et al. (1988, Fig. 6), but the distinction of these two formations is not obvious on the basis of log data alone.

Sequence 3 has been observed in all the wells, and it includes 45–247 m of Upper Oligocene to Lower Miocene sediments of the Kai Fm. Sediments at the base of this sequence have ages of 24–30 Ma at the various well sites, and the uppermost sediments have ages of 20–21 Ma. The hiatus associated with the unconformity separating sequences 3 and 4 has a duration of 7–15 m.y. This unconformity is not recognized on the seismic data.

Sequence 4 includes 1400–1855 m of Middle Miocene to Holocene sediments of the Naust Fm and upper Kai Fm, which have basal ages of 5–14 Ma at the various well sites. The contact between these formations is marked by the Mid Pliocene (MP) reflector, which represents a surface of downlap for the overlying thick unit of clinoforms. On the Trøndelag Platform to the east, the MP reflector merges with the IO reflector, indicating increasingly more extensive eastward truncation of the Paleogene section. However, there is presently no biostratigraphic evidence of a hiatus associated with the MP reflector at the well sites we have studied on the Halten Terrace, and we conclude that any loss of sediments at this reflector must have been of undetectably

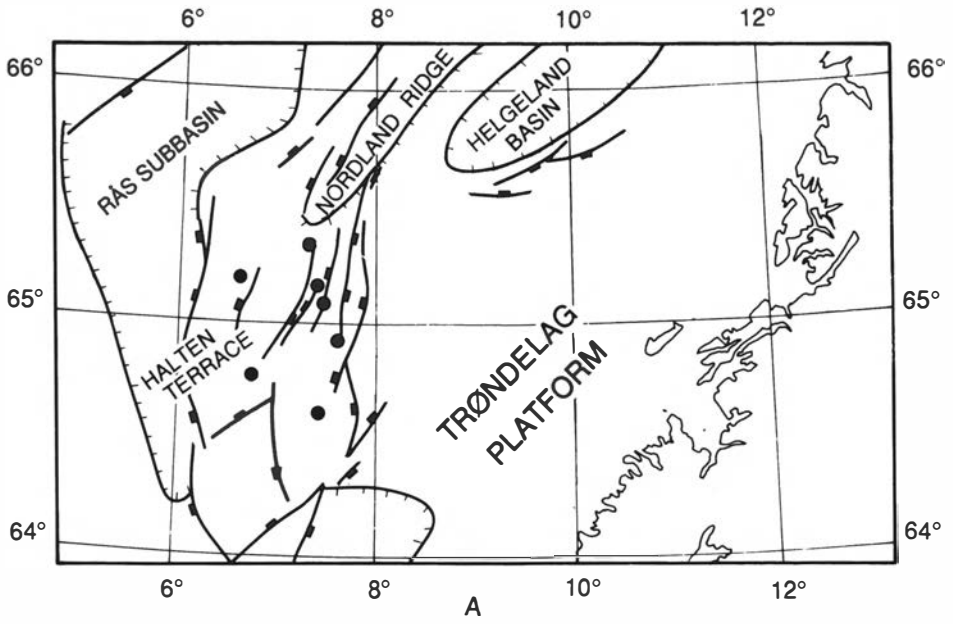

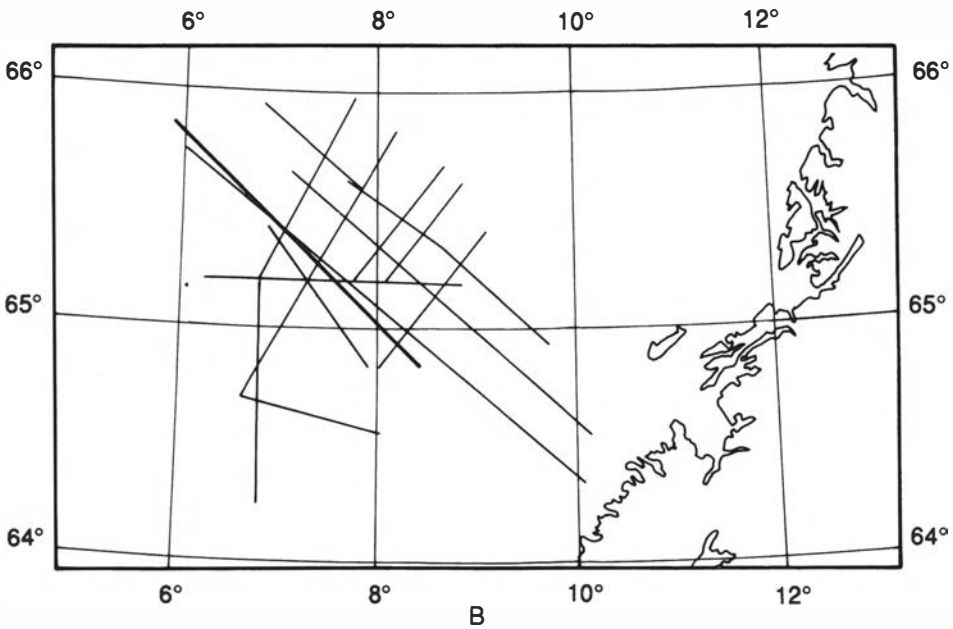

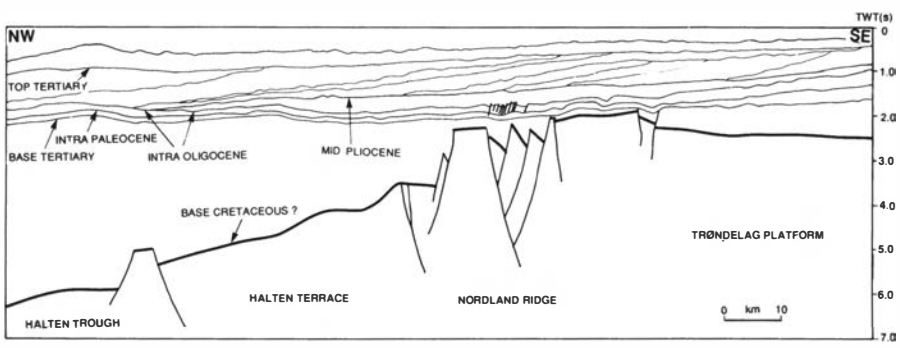

Fig. 1. (A) Structural provinces of the Haltenbanken region (from Blystad et al., in prep.). The seven well locations are indicated by black dots. (B) Distribution of the seismic grid used in this study. (C) Geoseismic cross-section of the bold line in Fig. 2B showing five of the six regional Cenozoic reflectors. The Intra Paleocene (IP) and Base Eocene (BE, not shown) reflectors are parallel and almost coincident on this seismic line.

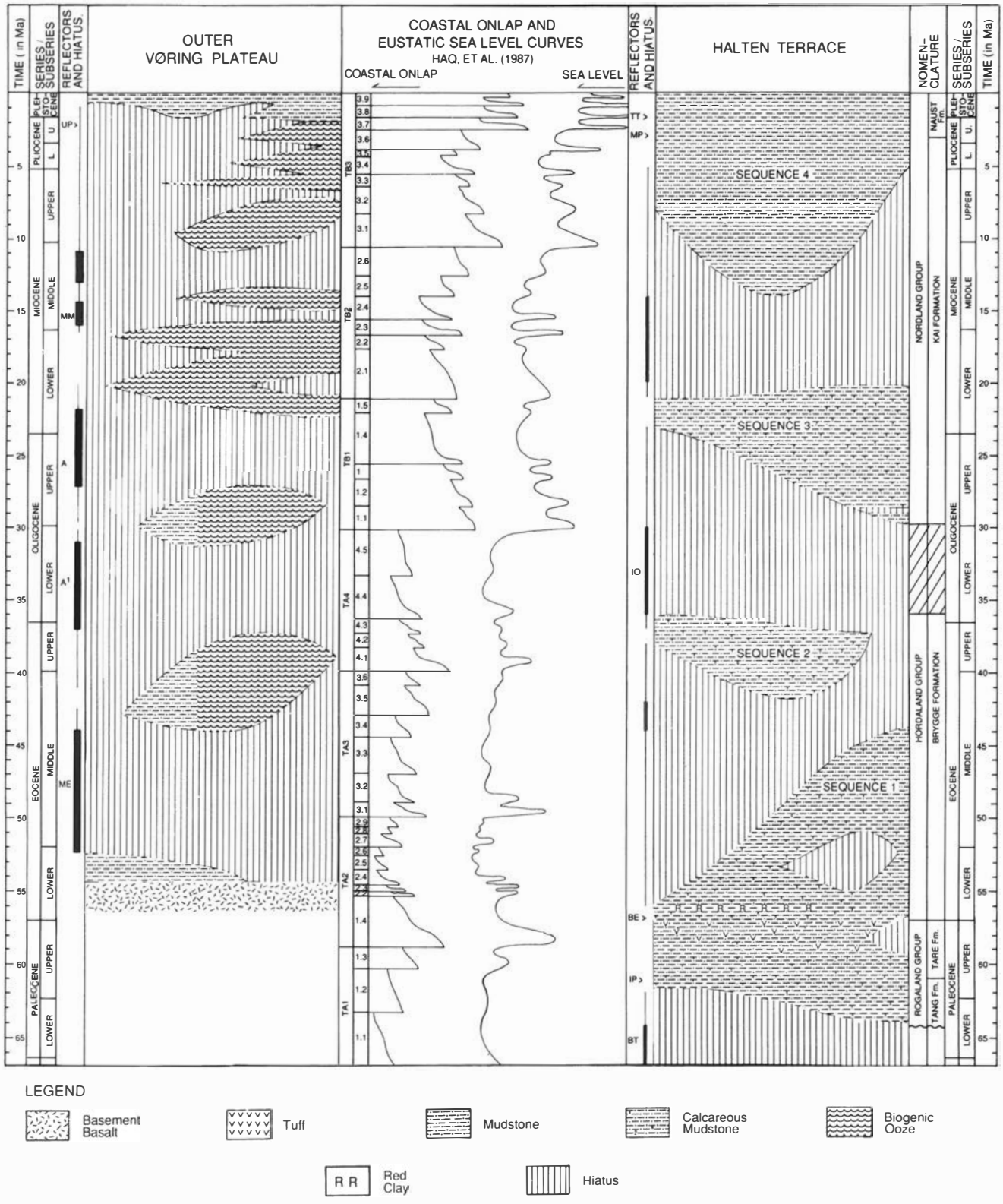

Fig. 2. A chronological comparison of Cenozoic sequences of the Halten Terrace and Outer Vøring Plateau with the eustatic sea level curve of Haq et al. (1987), which has been modified to conform with the Berggren et al. (1985) time scale.

short duration immediately preceding the advent of dominantly glaciomarine sedimentation at ca. 2.5–3.0 Ma.

In Halten Terrace well 6507/12-4 immediately to the southwest of our study area, Eidvin & Riis (1991) document evidence of an unconformity at the Naust Fm/Kai Fm contact (the MP reflector of our nomenclature). We conclude that this formational contact is essentially conformable at well 6507/12-4, contrary to the conclusion of these authors. We agree with Eidvin & Riis (1991) that sediments of the age range 2.5–4.5 Ma are missing at the

same contact in Træn Basin well (6607/5-1). Only the upper Kai Fm is present at both of these localities, and Sequence 4 directly overlies abbreviated Sequence 1 sections.

There are numerous similarities as well as anomalies between the Cenozoic sequences of the Halten Terrace and those of the Outer Vøring Plateau (Fig. 2). The significantly greater detail apparent particularly in the Neogene sequences of the later region are partially the result of the availability of continuously cored sections. Even if present, such fine-scale definition of the sediment record on the Halten Terrace would not be detectable in ditch cutting samples. A second factor is the very considerable deep ocean erosion that has truncated the sediment column of much of the Norwegian Sea, especially after sea-floor spreading commenced on the Knipovich Ridge after magnetic anomaly 5 time (9.5 Ma).

With one exception, all of the major Cenozoic hiatuses of the Outer Vøring Plateau are associated with major seismic reflectors, unlike the Halten Terrace. The Paleogene sequences of these two regions are approximately correlative, but Neogene correlations are far less obvious.

The hiatus separating sequences 1 and 2 of the Halten Terrace is approximately correlative with the hiatus on the Outer Vøring Plateau associated with the ME reflector of Skogseid & Eldholm (1989). Only a scant record exists of sediments on the Outer Vøring Plateau that are correlative with sequence 1 of the Halten Terrace, partly as a result of the onset of rifting under the plateau at ca. 54 Ma. The basal 117–175 m of mudstones and volcanics at Sites 338 and 343 (52–54 Ma) and the older thin shale intercalations in the dipping reflector basalts at Site 642 (Eldholm et al. 1987) are the only known Vøring Plateau equivalents to sequence 1.

The muds and biogenic oozes occurring between reflectors A′ and ME of the Outer Vøring Plateau are correlative with sequence 2 of the Halten Terrace. The hiatus associated with the IO reflector of the Halten Terrace correlates with the hiatus associated with the A′ reflector of the Outer Vøring Plateau.

The sequence between A and A′ of the Outer Vøring Plateau is correlative with lower sequence 3 of the Halten Terrace, but correlations are less clear in the overlying sections. The hiatus associated with reflector A occupies much of the upper age range of sequence 3.

There is a much more complete sedimentary record for the latest 22 m.y. of Cenozoic time at Sites 642 and 643 on the Outer Vøring Plateau than at any of the well sites on the Halten Terrace. Although occurrences are interrupted by local small-scale truncation, the two sequences separated by the hiatuses associated with the A and MM reflectors and immediately above the MM reflector are coeval with much of the hiatus between sequences 3 and 4 of the Halten Terrace. The hiatus associated with the MM reflector of the Outer Vøring Plateau appears to be the most plausible match to the Sequence 3/sequence 4 hiatus of the Halten Terrace, however. The strongly erratic, youngest two sequences of the Outer Vøring Plateau are approximately correlative with sequence 4.

In conclusion, the three younger hiatuses separating the four sequences of the Halten Terrace appear to have approximately coeval hiatuses on the Vøring Plateau, although it is not now possible to make confident direct seismic ties between these two regions. The unconformities bounding sequence 1/sequence 2, sequence 2/sequence 3, and sequence 3/sequence 4 of the Halten Terrace appear to be approximately correlative with the unconformities associated with the ME reflector, the A′ reflector, and the MM reflector, respectively, of the Vøring Plateau (Skogseid & Eldholm 1989). The recently revised ages of the hiatuses associated with these Vøring Plateau reflectors are shown in Fig. 2. However, the sequence stratigraphies of these two adjacent regions have become progressively more dissimilar during Cenozoic time. The two Paleogene sequences of the Halten Terrace are thicker and more complete than those of the Vøring Plateau, although the bounding hiatuses are approximately coeval. As a generalization, the Neogene sequences of the Outer Vøring Plateau are more numerous than those of the Halten Terrace, and the bounding hiatuses are of significantly shorter duration. Many portions of the Outer Vøring Plateau have been the subject of intensive erosion, but these Neogene sequences are preserved at localities such as Sites 642 and 643.

There appears to be a very poor correlation between the Cenozoic sequences of the Halten Terrace and the sea level curve of Haq et al. (1987), even at supercycle scale. If eustatic sea level fluctuations were responsible for the formation of these sequences, the hiatuses should coincide with the rapid large-scale sea level falls between the supercycles. This is not observed, however. Sequence 1 sediments were deposited and partially truncated during the interval immediately preceding and following rifting of the adjacent sea floor, and relatively continuous sedimentation during late TA1–early TA3 time can be explained by tectonic overprinting. Sequences 2 and 3 were deposited after tectonic quiescence, and the relative contemporaneity of their upper surfaces is consistent with sequence configurations proposed by Vail et al. (1977). However, sequence 2 occupies an interval of low relative sea level, whereas the high stands preceding and following this sequence are associated with hiatuses. Correlations are even weaker between the sequence stratigraphy of the Outer Vøring Plateau and the sea level curve. For example, the sequence between reflectors A and A′ is approximately coeval with the lowest relative sea level stands of mid-Cenozoic time, according to Haq et al. (1987). These results suggest that, at outer shelf and plateau localities such as these, unconformities bounding major sequences must be attributed to origins other than eustatic sea level fluctuation.

Manuscript received October 1991

References

Berggren, W. A., Kent, D. V., Flynn, J. J. & Van Couvering, J. A. 1985: Cenozoic geochronology. *Geological Society of America Bulletin 96*, 1407–1418.

Blystad, P., Færseth, R. B., Tørudbakken, B., Larsen, B. T. & Skogseid, J.: Structural elements on the Norwegian shelf between Møre and Troms. *Norwegian Petroleum Directorate* (in preparation).

Dalland, A., Worsley, D. & Ofstad, K. 1988: A lithostratigraphic scheme for the Mesozoic and Cenozoic succession offshore mid- and northern Norway. *Norwegian Petroleum Directorate Bulletin 4*, 65 pp.

Eidvin, T. & Riis, F. 1991: En biostratigrafisk analyse av tertiære sedimenter pa kontinentalmarginen av Midt-Norge, med hovedvekt pa øvre pliocene vifteavsetninger. *Norwegian Petroleum Directorate, Contribution 29*, 44 pp.

Eldholm, O. et al. 1987: *Proceedings of the Ocean Drilling Program, Initial Reports 104*, 783 pp.

Goll, R. M. 1989: A synthesis of Norwegian Sea biostratigraphies: ODP Leg 104 on the Vøring Plateau. *In*: *Proceedings of the Ocean Drilling Program, Scientific Results 104*, pp. 777–826.

Goll, R. M., Hansen, J. W. & Skarbø, O. 1990: The Cenozoic stratigraphy of Haltenbanken: an integrated seismic and biostratigraphic study. *IKU Report No. 23.1364.01/01/90*, 127 pp. (Restricted).

Haq, B., Hardenbol, J. & Vail, P. R. 1987: Chronology of fluctuating sea level since the Triassic. *Science 235*, 1156–1167.

Skogseid, J. & Eldholm, O. 1989: Vøring Plateau continental margin: seismic interpretation, stratigraphy, and vertical movements. *In*: *Proceedings of the Ocean Drilling Program, Scientific Results 104*, pp. 993–1030.

Vail, P. R., Mitchum, R. M. & Thompson, S. 1977: Seismic stratigraphy and global changes of sea level, part 3: relative changes of sea level from coastal onlap. *In* Payton, C. E. (ed.): Seismic stratigraphy – applications to hydrocarbon exploration. *American Association of Petroleum Geologists Memoir 26*, 63–81.

Neotectonics in the Precambrian of Finnmark, northern Norway

ODLEIV OLESEN, HERBERT HENKEL, OLE BERNT LILE, EIRIK MAURING, JAN STEINAR RØNNING & TROND HELGE TORSVIK

Olesen, O., Henkel., H., Lile, O. B., Mauring, E., Rønning, J. S. & Torsvik, T. H.: Neotectonics in the Precambrian of Finnmark, northern Norway. *Norsk Geologisk Tidsskrift*, Vol. 72, pp. 301–306. Oslo 1992. ISSN 0029-196X.

The postglacial Stuoragurra Fault (SF) lies within the Mierujav'ri-Sværholt Fault Zone (MSFZ), which is located in the extensive Proterozoic terrain of Finnmark, northern Norway. The SF is a southeasterly dipping reverse fault and an approximately 1 m thick fault-rock zone, detected in drillholes, is considered to represent the actual fault surface. Magnetic fabric data demonstrate that the SF parallels the schistosity of the surrounding bedrock. Resistivity measurements within the Fidnajåkka area reveal low-resistivity zones in both the hanging-wall and the foot-wall blocks of the SF. These low-resistivity zones lie within a several hundred metre wide belt and are interpreted to originate from strongly fractured and water-bearing quartzites along the regional MSFZ. The resistivity of the hanging-wall block of the SF is typically lower than that of the foot-wall, indicating more intense fracturing in the hanging-wall. Precision levelling data have shown that the foot-wall has subsided relative to the hanging-wall block by 2.3 mm between 1987 and 1991. We suggest that plate tectonic processes constitute the most important fault-generating mechansim in Finnmark.

Odleiv Olesen, Eirik Mauring, Jan Steinar Rønning & Trond Helge Torsvik, Geological Survey of Norway, PO Box 3006, N-7002 Trondheim, Norway; Herbert Henkel, Geological Survey of Sweden, Uppsala, Sweden. Present address: Royal Institute of Technology, S-100 44 Stockholm, Sweden; Ole Bernt Lile, University of Trondheim, Norwegian Institute of Technology, NTH, N-7034 Trondheim, Norway.

The traditional view on the stability of the Norwegian bedrock has changed significantly in recent years. Direct stress measurements and interpretation of seismic activity have shown that Fennoscandia is currently undergoing NW–SE to NNW–SSE compression (Zoback et al. 1989; Bungum et al. 1991). Accumulating evidence suggests that this compressional field, which is believed to be mostly related to the plate tectonic 'ridge push' force, causes faulting within Fennoscandia (Skordas et al. 1991). Opinions differ, however, both with regard to the role which other mechanisms play in the observed stress regime and also with regard to the mechanisms that have triggered postglacial faulting in northern Fennoscandia.

The Stuoragurra Fault (SF) was identified in 1983 during the course of a collaborative project between the Geological Surveys of Finland, Norway and Sweden, and details of the SF have been reported by Olesen (1988, 1991), Muir Wood (1989) and Olesen et al. (in press). The SF, located within the Mierujav'ri Sværholt Fault Zone (MSFZ), is an 80 km long fault zone (Figs. 1, 2) which contains numerous segments of eastward dipping (30–60°) faults (Fig. 3A) with up to 10 m of reverse displacement and a 7 m high escarpment. The SF cross-cuts glaciofluvial deposits northeast of Iešjav'ri (Olesen 1988) and an esker northeast of Masi (Fig. 3B). Similar fault scarps (cf. inset map in Fig. 1), interpreted to be post- or late-glacial, occur in adjacent parts of Finland (Kujansuu 1964), Sweden (Lundqvist & Lagerbäck 1976; Lagerbäck 1979, 1990), the USSR (Tanner 1930) and in Troms, northern Norway (Grønlie 1922; Tolgensbakk & Sollid 1988). At Skipskjølen on Varangerhalvøya similar escarpments can be observed on aerial photographs within the Trollfjord–Komagelv Fault Zone. It is not possible to date the youngest movements along this latter fault zone since the glacial overburden is absent. A 5.8 cm reverse-fault offset of a drillhole during a 3-year period has been reported (Roberts 1991) at a road-cut in Laksefjord, Finnmark.

Regional tectonic setting

Aeromagnetic and gravity data have been utilized to interpret the regional fault pattern within western Finnmark and northern Troms (Olesen et al. 1990). Details of the fault geometry have been obtained within the Masi area using processed images of aeromagnetic, gravimetric and topographical data and geological maps combined with the geophysical method, VLF, measured at ground level (Olesen et al. in press). The images were generated using an ERDAS PC system (cf. Image processing module, version 7.4, January 1990. ERDAS Inc., Atlanta). The 230 km long MSFZ (Olesen et al. 1990) is the main fault zone which separates the flat-lying, thin (up to 2 km), volcano-sedimentary sequences to the west of the Masi area from the Jer'gul Gneiss Complex to the southeast. The MSFZ (Fig. 1) extends from Mierujav'ri 30 km north of Kautokeino in a northeasterly direction through Masi, Iešjav'ri and Lakselv and can be traced below the Caledonian nappes on the Sværholt Peninsula

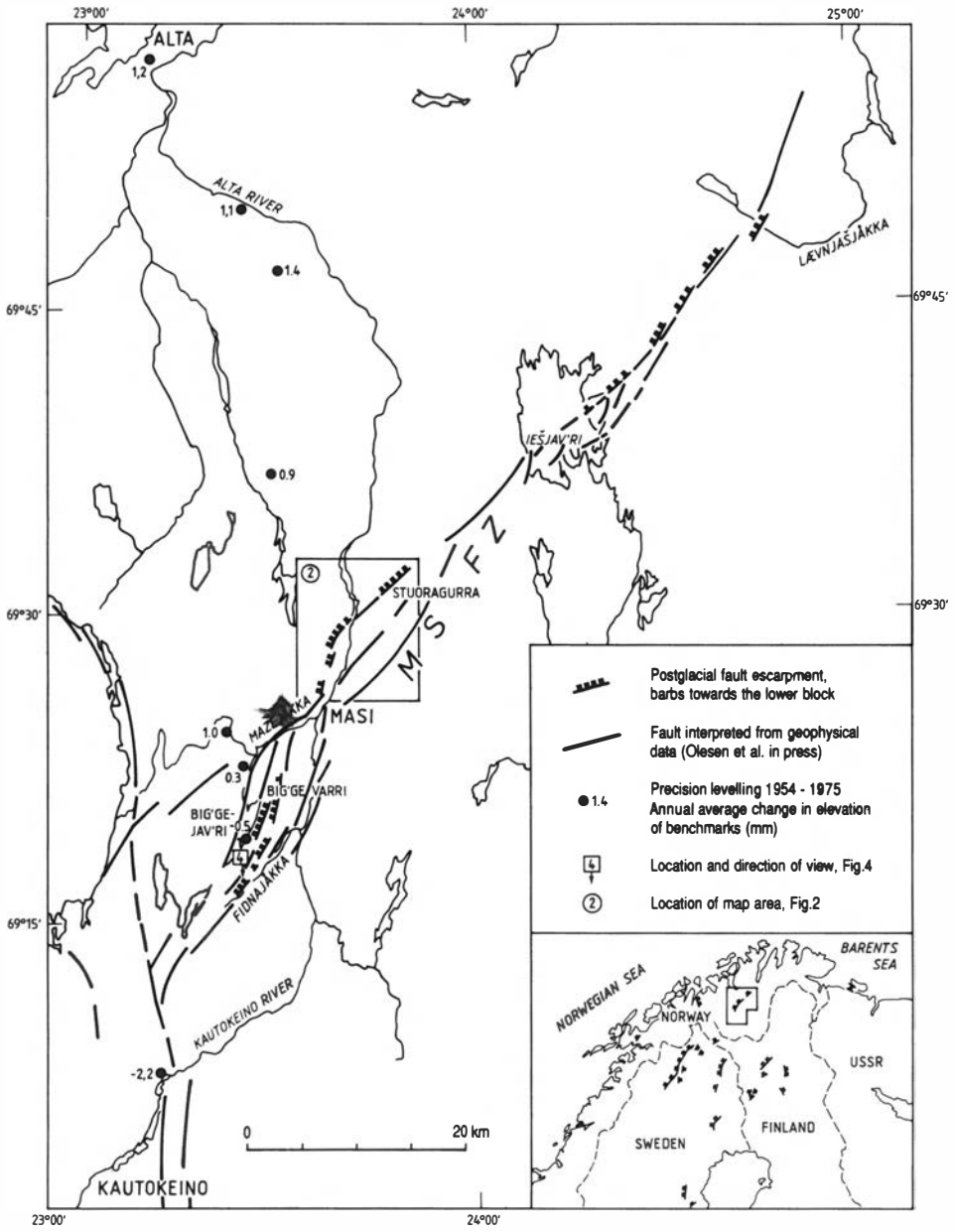

Fig. 1. Postglacial faults on Finnmarksvidda. Inset map shows Late Quaternary faults in northern Fennoscandia (from Olesen 1988). MSFZ–Mierujav'ri-Sværholt Fault Zone. The annual average change in elevation of benchmarks is based on precision levelling in 1954 and 1975 (Sørensen et al. 1987).

from the aeromagnetic and gravimetric data. To the south, the MSFZ terminates towards the eastern margin of the Alta–Kautokeino Rift. The 1815 ± 24 Ma albite diabases (Krill et al. 1985), responsible for the characteristic magnetic anomalies in the Masi area, have intruded along the MSFZ. A later episode of deformation of these diabases can be observed locally. A system of duplexes can be delineated along the MSFZ from the geophysical images (Fig. 1). The interpreted structures have been confirmed by electromagnetic (VLF) ground measurements in the till-covered area (Olesen 1991; Olesen et al. in press). In the Masi-Iešjav'ri area breccias occur along the MSFZ, and albite–carbonate alteration occurs along the borders of the Big'gevarri Duplex (Olesen 1991). Folding and imbrication in the Masi-Iešjav'ri area are thought to be associated with movement along the MSFZ.

The correlative Archaean–Early Proterozoic Gåldeenvarri and Vuomegielas Formations (Siedlecka et al. 1985; Siedlecka 1985; Solli 1988), which represent the lowermost stratigraphical unit within the Kautokeino Greenstone Belt, are dextrally displaced 20 km along the MSFZ (Olesen et al. 1990; Olesen 1991). Along the MSFZ to the northeast of Iešjav'ri a synsedimentary movement during the deposition of the Cambrian Dividal Group and a post/late Caledonian displacement which cuts through the Gaissa Thrust have been reported earlier (Townsend et al. 1989). Furthermore, an apparent offshore extension of the MSFZ coincides with one of the major basement faults on the continental shelf (Lippard & Roberts 1987); but this need not be exactly the same fault. As the earliest detectable displacement is of Proterozoic age and the latest movement occurred less than 9000 years ago, the MSFZ thus represents an

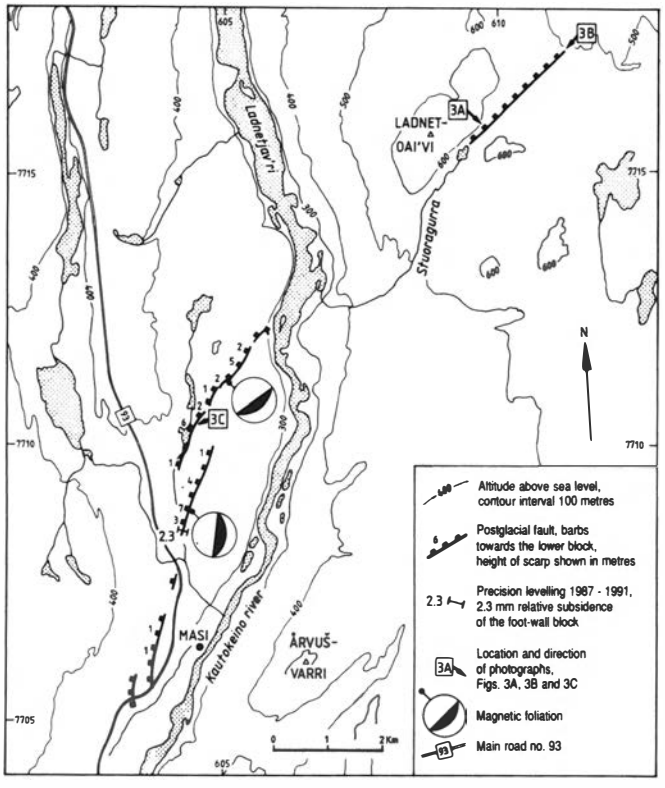

Fig. 2. Detailed topographical map from the Masi area. The relative depression of the footwall block of 2.3 mm from 1987 to 1991 has been recorded by precision levelling (Skjøthaug 1991). Magnetic foliation planes (downward-dipping planes in equal-angle stereoplots) demonstrate that the postglacial fault-break parallels the surrounding bedrock schistosity. The location of the map area is shown in Fig. 1.

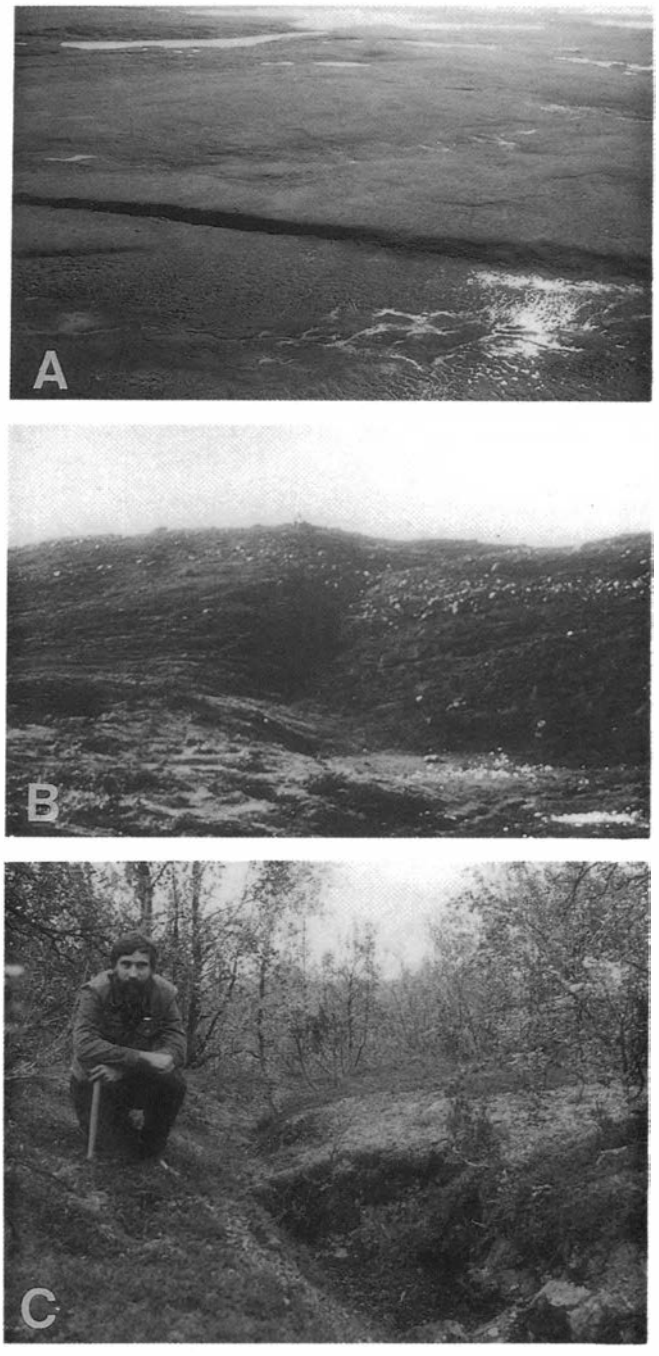

Fig. 3. (A) Oblique aerial photograph of the Stuoragurra Fault (UTM 610200-7716200) looking east, approximately 10 km to the NNE of Masi. (B) The SF (in the middle of the picture) cutting through a left to right trending esker 12 km NNE of Masi (UTM 611400-7717300); looking SW. The offset is approximately 2 m vertically and 0–5 m dextrally. (C) A 30 m long, 1 m wide and 1 m deep trench subparallel to the escarpment in the hanging-wall block of the SF (UTM 604600-7710400). The distance from the slightly curved trench to the escarpment is 40 m. The trench is interpreted as an accommodation fault formed during the postglacial faulting along the SF. The locations and directions of the photographs are shown in Fig. 2.

extremely long-lived fault zone. Furthermore, seismicity occurs along an elongate tract oriented NE–SW nearly parallel to the neotectonic structures, lying about 30 km to the southeast (Olesen 1988; Bungum et al. 1991). This indicates that the stress regime which produced the faulting may still be operative.

Figure 1 shows the annual average change in elevation of benchmarks in relation to mean sea level. These data are based on precision levelling in 1954 and later in 1975 along the old road from Alta to Kautokeino (Sørensen et al. 1987; P. Skjøthaug pers. comm. 1991) and show a significant deviation from the general postglacial upheaval of Fennoscandia (cf. Bjerhammar 1980). Instead of an increasing uplift from 2 mm/year in Alta to 5 mm/year in Kautokeino as assumed by Sørensen et al. (1987), a subsidence of the inland area is observed. From Fig. 1, one should also note that the Alta–Kautokeino levelling profile approaches the SF when moving to the south, and so indicates that the foot-wall block of the SF is being depressed rather than the hanging-wall block being uplifted. Repeated precision levelling across the SF in 1987 and 1991 has revealed a relative depression of the foot-wall block of 2.3 mm (Skjøthaug 1991). This gives an annual average of 0.6 mm, which is in the same order of magnitude as the annual depression of 0.5 mm observed along the Alta–Kautokeino levelling profile at the eastern shore of Biggejav'ri 2 km to the west of the SF (Fig. 1).

Detailed geophysical investigations

Detailed geophysical investigations have been carried out along the SF in the Fidnajåkka area 10 km to the south of Masi (Olesen 1991; Olesen et al. in press). The geology of the area is dominated by folded quartzites, with the

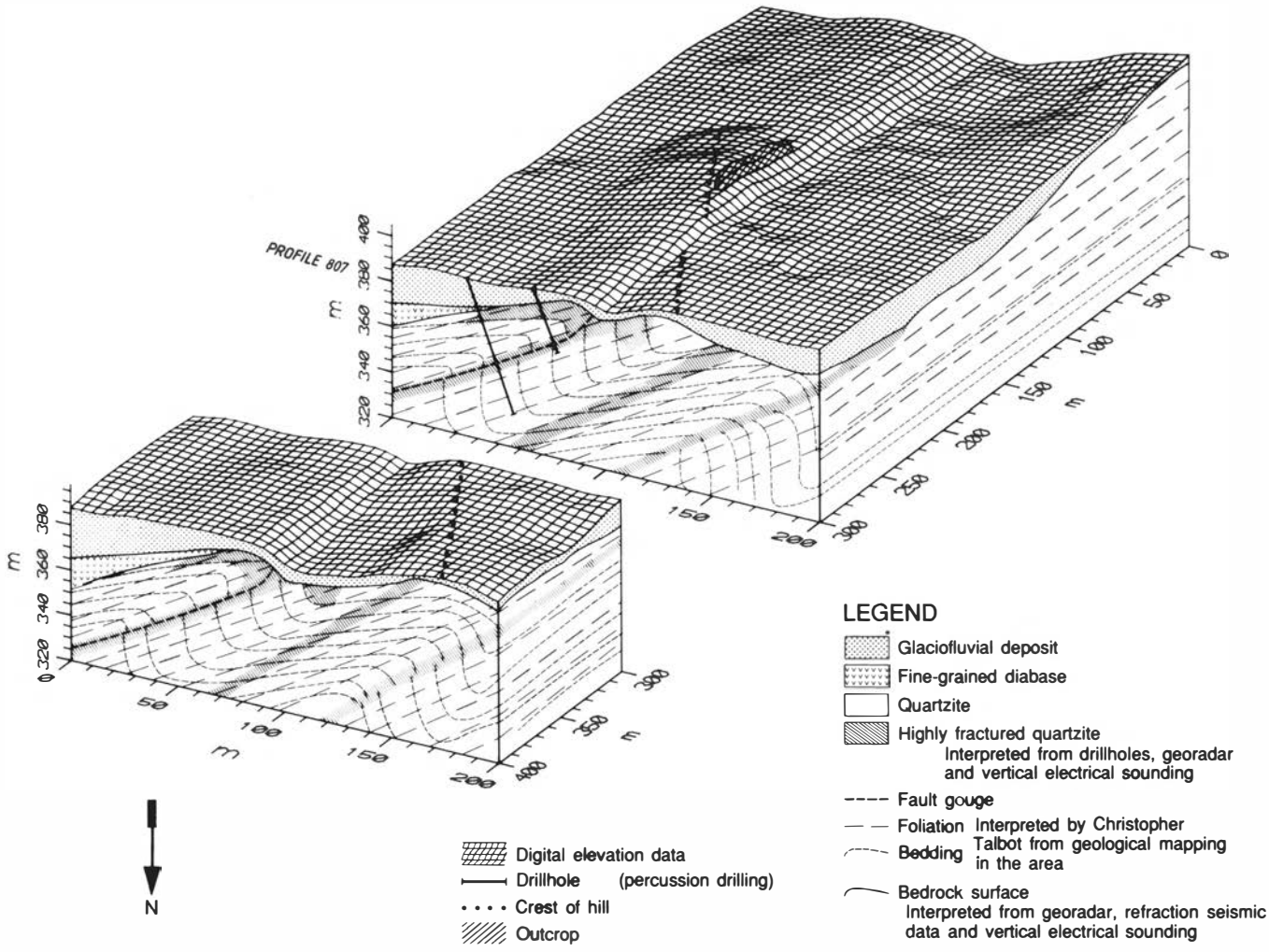

Fig. 4. Interpretation synthesis of model A (listric fault) as a block diagram. The view is towards the south along the SF (UTM 59700-7688000). The location is shown in Fig. 1. The N-S trending hill with a core of bedrock is cut by the SF.

fold axes lying parallel to the MSFZ. Alternating thin and thick limbs of the folds dip 20° to the southeast and almost vertically, respectively, and an axial plane foliation dips at approximately 30° to the southeast (Chr. Talbot pers. comm. 1988). The postglacial fault itself is thought to be represented by an approximately 1 m thick layer of fault gouge which has been detected in drillholes (Fig. 4).

Anisotropy of magnetic susceptibility (AMS) measurements (conducted on a modified Molspin delineator system) from two outcrops (14 samples) along the SF escarpment in the Masi area (Fig. 2) have been used to map the schistosity of the surrounding amphibolite. These magnetic fabric data reveal well-defined magnetic foliation (K_{max}–K_{min}) planes and oblate-shaped magnetic ellipsoids. The degree of anisotropy (percentage ratio of K_{max}/K_{min}) varies between 9 and 17%. The postglacial fault-break parallels the strike of the magnetic foliation which represents the schistosity. From the dips of the magnetic foliation at the northern and southern sites, 49° and 36° to the southeast and east respectively, we conclude that this is also the dip of the SF at those sites.

Electrical resistivity measurements in the Fidnajåkka area reveal low-resistivity zones in both the hanging- and foot-wall blocks of the SF, a feature which is inferred to be due to fracturing (Olesen 1991; Olesen et al. in press). An observed low seismic velocity in the quartzites is also interpreted to be caused by a generally high incidence of fracturing and faulting of the bedrock within the survey area. The SF is consequently interpreted to lie within a several hundred metre wide fault zone which is part of the regional MSFZ. Generally within the Fidnajåkka area, however, it can be stated that the electrical resistivity of the hanging-wall block of the SF is lower than in the foot wall, indicating a more intense fracturing in the hanging-wall. A generally intense brittle deformation of the hanging-wall block of the SF is also indicated by a 1 m wide accommodation fault which is situated 40 m from the SF scarp to the north of Masi (Fig. 3C). Vertical electrical soundings show a low-resistivity layer at depth in the eastern hanging-wall block, consistent with the observation of eastward-dipping faults.

Detailed topographical data proved to be useful for estimating the dip of the fault zones in the upper part of

the ground using the stratum contour method. Additional data from measurements with a ground penetrating radar (GPR) have been used to map the thickness of the overburden. When combined with the digital topography, these measurements could be used to map the topography of the bedrock surface. Highly reflective bedrock on the radar diagrams is interpreted to represent fractured and weathered quartzite and single reflectors can be interpreted as fault zones (Fig. 4).

Within the survey area, there exist two possibilities for the course of the reverse post-glacial fault at depth:

(a) The fault is listric with a dip of approximately 50° (from the digital topography) in the uppermost 10 m and a dip of 30° (from percussion drilling) at a depth between 25 and 40 m (Fig. 4).
(b) The fault continues at a depth from the surface with a dip of 50°–60°.

If model (a) is correct, the SF will be represented by a 1 m thick fault gouge which occurs in drillholes and the fault will be parallel to the foliation at depth. On the other hand, if model (b) proves to be correct, the drillholes in the hanging-wall block were abandoned prematurely and did not penetrate the fault. When combining the different geophysical results and geological features we find model (a) to be the more likely solution.

Discussion and conclusions

Resistivity, ground penetrating radar, percussion drilling, VLF and aeromagnetic data indicate that the SF is governed by older faulting, on a local as well as on a regional scale. Postglacial faulting most commonly occurs along margins of duplex structures or within them. Northeast of Iešjav'ri, however, the young faulting occurs within the main fault zone. The SF is a southeasterly dipping reverse fault and an approximately 1 m thick fault-rock zone, detected in drillholes, is considered to represent the actual fault surface. The existence of a minor dextral strike-slip component, however, cannot be ruled out (Olesen 1991). A relative depression of the foot-wall block of 2.3 mm from 1987 to 1991 has been recorded by precision levelling (Skjøthaug 1991).

Important contributors to the mechanism generating the postglacial faults are generally believed to be 'ridge push' forces associated with spreading on the Mohns, Knipovich and Nansen Ridges and viscous drag beneath the lithosphere. Deviation in the regional stress pattern may be induced by mass excess (Mareschal & Kuang 1986), as for instance within the Seiland Igneous Province (Olesen 1991). Henkel (1988) and Talbot & Slunga (1989) have argued that the compressional stress regime in Fennoscandia is caused by a wrenching which is related to strike-slip movements along the extrapolated extensions of the Jan Mayen and Iceland transforms.

The Stuoragurra Fault and the Pärvie Fault (Lagerbäck 1979) in Sweden coincide with a physiographic border. The mountainous area to the northwest has a higher average elevation than the area to the southeast. Using present analogies with Greenland and Antarctica, the inland ice was thickest in the southeastern area. Olesen (1988) and Muir Wood (1989) suggested that this would involve more depression during the glaciation and consequently a greater contribution to the subsequent postglacial stress regime during uplift. The differential loading of ice across a pre-stressed fault line might consequently be sufficient to cause fracturing and reactivation of faults. The observed subsidence of the foot-wall block rather than uplift of the hanging-wall block is, however, not in agreement with this model and we therefore suggest that plate tectonic processes constitute the most important fault-generating mechanism in Finnmark. The release of the stresses caused by plate tectonic forces could, however, still have been triggered during the deglaciation period.

Acknowledgements. – This work was partially financed by the Royal Norwegian Council for Scientific and Industrial Research (Grant 13220 to Odleiv Olesen), the Geological Survey of Norway and the Norwegian Institute of Technology, University of Trondheim. Roy Gabrielsen, David Roberts, Jan Sverre Sandstad, Per Skjøthaug, Arne Solli and Christopher Talbot have contributed with valuable advice and discussions. The manuscript has been critically reviewed by Arild Andresen, Karl Anundsen, David Roberts and Peter Walker and their comments have led to many improvements of the paper. The English text of the final manuscript was corrected by Rognvald Boyd. Gunnar Grønli and Bjørg Inger Svendgård prepared the figures. To all these persons and institutions we express our sincere thanks.

Manuscript received October 1991

References

Bjerhammar, A. 1980: Postglacial uplifts and geopotentials in Fennoscandia. *In* Mörner, N. A. (ed.): *Earth Rheology, Isostasy and Eustasy*, 323–326. John Wiley & Sons, New York.

Bugum, H., Alsaker, A., Kvamme, L. B. & Hansen, R. A. 1991: Seismicity and seismotectonics of Norway and nearby continental shelf areas. *Journal of Geophysical Research 96*, 2249–2265.

Grønlie, O. T. 1922: Strandlinjer, moræner og skjælforekomster i den sydlige del av Troms fylke. *Norges geologiske undersøkelse 94*, 39 pp.

Henkel, H. 1988: Tectonic studies in the Lansjärv region. Swedish Nuclear Fuel and Waste Management Co. Technical Report 88–07, 66 pp.

Krill, A. G., Berg, S., Lindahl, I., Mearns, E. W., Often, O., Olerud, S., Olesen, O., Sandstad, J. S., Siedlecka, A. & Solli, A. 1985: Rb–Sr, U–Pb, and Sm–Nd isotopic dates from the Precambrian rocks of Finnmark, *Norges geologiske undersøkelse Bulletin 403*, 37–54.

Kujansuu, R. 1964: Nuorista sirroksista Lapissa. Summary: Recent faults in Lapland. *Geologi 16*, 30–36.

Lagerbäck, R. 1979: Neotectonic structures in northern Sweden. *Geologiska Föreningens i Stockholm Förhandlingar 100(1978)*, 271–278.

Lagerbäck, R. 1990: Late Quaternary faulting and paleoseismicity in northern Fennoscandia, with particular reference to the Lansjärv area, northern Sweden. *Geologiska Föreningens i Stockholm Förhandlingar 112*, 333–354.

Lippard, S. J. & Roberts, D. 1987: Fault systems in Caledonian Finnmark and the southern Barents Sea. *Norges geologiske undersøkelse Bulletin 410*, 55–64.

Lundqvist, J. & Lagerbäck, R. 1976: The Pärvie fault: a late-glacial fault in the Precambrian of Swedish Lapland. *Geologiska Föreningens i Stockholm Förhandlingar 98*, 45–51.

Mareschal, J.-C & Kuang, J. 1986: Intraplate stresses and seismicity: the role of topography and density heterogeneities. *Tectonophysics 132*, 153–162.

Muir Wood, R. 1989: Extraordinary deglaciation reverse faulting in northern Fennoscandia. *In* Gregersen, S. & Basham, P. W. (eds.): *Earthquakes at North-Atlantic Passive Margins: Neotectonics and Postglacial Rebound.* NATO ASI series. Series C, Mathematical and Physical Sciences, vol. 266, 141–173. Kluwer, Dordrecht, The Netherlands.

Olesen, O. 1988: The Stuoragurra Fault, evidence of neotectonics in the Precambrian of Finnmark, northern Norway. *Norsk Geologisk Tidsskrift 68*, 107–118.

Olesen, O. 1991: A geophysical investigation of the relationship between old fault structures and postglacial faults in Finnmark, northern Norway. Unpubl. Doktor ingeniør thesis. University of Trondheim, Norwegian Institute of Technology. 126 pp.

Olesen, O., Roberts, D., Henkel, H., Lile, O. B. & Torsvik, T. H. 1990: Aeromagnetic and gravimetric interpretation of regional structural features in the Caledonides of West Finnmark and North Troms, northern Norway. *Norges geologiske undersøkelse Bulletin 419*, 1–24.

Olesen, O., Henkel, H., Lile, O. B., Mauring, E. & Rønning J. S.: Geophysical investigations of the Stuoragurra postglacial fault, Finnmark, northern Norway. *Journal of Applied Geophysics* (in press).

Roberts, D. 1991. A contemporary small-scale thrust-fault near Lebesby, Finnmark. *Norsk Geologisk Tidsskrift 71*, 117–120.

Siedlecka, A. 1985: Geology of the Iešjav'ri–Skoganvarre area, northern Finnmarksvidda, North Norway. *Norges geologiske undersøkelse Bulletin 403*, 103–112.

Siedlecka, A., Iversen, E., Krill, A. G., Lieungh, B., Often M., Sandstad, J. S. & Solli, A. 1985: Lithostratigraphy and correlation of the Archean and Early Proterozoic rocks of Finnmarksvidda and the Sørvaranger district. *Norges geologiske undersøkelse Bulletin 403*, 7–36.

Skjøthaug, P. 1991: Rapport fra nivellement over Stuoragurraforkastningen 1991. Norwegian Mapping Authority (Statens kartverk) Report, 2 pp.

Skordas, E., Meyer, K., Olsson, R. & Kulhánek, O. 1991: Causality between interplate (North Atlantic) and intraplate (Fennoscandian) seismicities. *Tectonophysics 185*, 295–307.

Solli, A. 1988: *Masi, 1933 IV, berggrunnsgeologisk kart M 1:50 000.* Norges geologiske undersøkelse, Trondheim.

Sørensen, R., Bakkelid, S. & Torp, B. 1987: *Land uplift*. Scale 1:5 mill. Statens kartverk, Hønefoss.

Talbot, C. J. & Slunga, R. 1989: Patterns of active shear in Fennoscandia. *In* Gregersen, S. & Basham, P. W. (eds.): *Earthquakes at North-Atlantic Passive Margins: Neotectonics and Postglacial Rebound.* NATO ASI series. Series C, Mathematical and Physical Sciences, Vol. 266, 441–466. Kluwer, Dordrecht, The Netherlands.

Tanner, V. 1930: Studier över kvartäsystemet i Fennoskandias nordliga delar IV. *Bulletin de la Commission Géologique de Finlande 88*, 594 pp.

Tolgensbakk, J. & Sollid, J. L. 1988: *Kåfjord, kvartærgeologi og geomorfologi 1:50 000, 1634 II.* Geografisk institutt, Universitetet i Oslo.

Townsend, C., Rice, A. H. N. & Mackay, A. 1989: The structure and stratigraphy of the southwestern portion of the Gaissa Thrust Belt and the adjacent Kalak Nappe Complex, Finnmark, N Norway. *In* Gayer, R. A. (ed.): *The Caledonide Geology of Scandinavia*, 111–126. Graham & Trotman, London.

Zoback, M. L., Zoback, M. D., Adams, J., Assumpção, M., Bell, S., Bergman, E. A., Blümling, P., Brereton, N. R., Denham, D., Ding, J., Fuchs, K., Gay, N., Gregersen, S., Gupta, H. K., Gvishiani, A., Jacob, K., Klein, R., Knoll, P., Magee, M., Mercier, J. L., Müller, B. C., Paquin, C., Rajendran, K., Stephansson, O., Suarez, G., Suter, M., Udias, A., Xu, Z. H. & Zhizhin, M. 1989: Global patterns of tectonic stress. *Nature 341*, 291–298.

Methodology applied to uplift and erosion

JAN I. SKAGEN

Skagen, J. I.: Methodology applied to uplift and erosion. *Norsk Geologisk Tidsskrift*, Vol. 72, pp. 307–311. Oslo 1992.
ISSN 0029-196X.

Several methods have been developed and applied to estimating the Post-Cretaceous uplift and erosion in the Barents Sea. Earlier estimates show a spread in results which may indicate the inaccuracy of the methods. To attain the accuracy required, several methods covering a wide field of subjects, such as geochemistry, drilling, petrophysics, sedimentology and mineralogy, have to be applied. New methods along with new techniques applied to well-known methods have improved the accuracy of the results.

Jan I. Skagen, Statoil A/S, PO Box 40, N-9401 Harstad, Norway.

Methodological aspects

The methods applied to estimating Post-Cretaceous uplift and erosion in industry today can be divided on the basis of how precisely the magnitude of the uplift can be evaluated. Methods such as opal-CT transition, crystallinity index of illite and apatite fission track analysis are imprecise. These methods typically give 'yes' or 'no' answers to whether or not an uplift has occurred. Such methods are also expensive to carry out in the laboratories.

Based on experience from the Barents Sea, the following methods have a potential for an accuracy of ± 200 m in uplift evaluation: vitrinite reflectance profiles, shale compaction and a new method developed to apply drilling parameters. These methods are based on data that are commonly available from exploration wells and do not necessarily require extra laboratory costs.

Opal-CT transition

The method is based on observation of the diagenetic reaction Opal-A – Opal-CT – quartz, related to burial depth. This is based on assumptions of an increase of Opal-CT at 40–50°C and a transition to quartz at 80°C. The geothermal gradient must therefore be known. A limitation to the method is the fact that the transition to quartz is normally gradual, reducing the accuracy of depth determination. Quantification of transitions is uncertain, and a reference well is necessary. In our experience this method is semiquantitative and the accuracy of the calculated net uplift is ± 500 m.

Crystallinity index of illite

This method is based on the evaluation of the degree of diagenesis of authigene illite, which is related to the maximum burial depth. Temperature and depth are the main factors influencing the crystallinity index of illite. To be used in uplift evaluation the geothermal gradient must be known and a reference well with no uplift is necessary. In addition, pore water composition, reaction kinetics and time will influence the growth of illite, and the distinction between detrital and authigene illite is difficult. The accuracy of this method is thought to be within ± 500 m of the net uplift.

Apatite fission track analysis

This method is based on the measurement of fission track density and length in apatite. At increased temperatures (70–125°C) these tracks are shortened and healed. To calculate the magnitude of uplift the thermal history has to be known, and the method is very sensitive to abnormal changes in the geothermal gradient. A great advantage is that this is the only method that gives an indication of the timing of the events.

The biggest disadvantage is the laboratory costs. Based on a study initiated by Statoil and NPD the method is not more accurate than ± 500–1000 m.

Vitrinite reflectance profiles

The method is based on plotting profiles of vitrinite reflectance measurements versus depth using a semi-logarithmic scale. An extrapolation of the trendline of this data to a known surface value (VR = 0.20%) directly gives the magnitude of net uplift (Nyland et al., in press). The measurement of vitrinite reflectance is known to be subjective, and the pick of 'representative' vitrinite values and the drawing of the trend are normally done manually. With reliable vitrinite data the method is thought to have an accuracy of ± 200 m.

Shale compaction

The method is based on the comparison of porosity log responses in shale to a 'normal' reference curve of shale porosity versus depth. It gives direct estimates of the net uplift. The reference curve has to be valid for the area and there must be similarity in the lithology and mineralogy to the area where the reference curve was established. Abnormal pore pressures will influence the porosities and thereby the accuracy of this method. The method is lithology-dependent, but the large volume of data in each well increases its reliability. The method is regarded by Statoil to be more accurate than $\pm$ 200 m.

Drilling parameters

A new method for estimating net uplift has been developed based on comparison of drilling parameters to a valid reference curve of the compaction of normally pressured shale versus depth. This method gives direct estimates of the net uplift. The principles of the method are as follows: The rate of penetration (ROP) is a function of compaction versus depth. So are the porosities of shales, the densities of shales and thereby also the overburden pressure gradient which is calculated by integrating the densities.

The drilling exponent (dc-exponent) is a logarithmic function of the ROP. Several mechanical drilling parameters like weight on bit, revolutions per minute, bit diameter and mud weight are needed to calculate the dc-exponent. These parameters should be kept constant while drilling. The dc-exponent is used to calculate the pore pressure for a well and the pore pressure is a function of the overburden gradient. The dc-exponent can be expressed as a function of the pore pressure, the overburden pressure and depth. The method developed by Eaton (1976) and the equivalent depth method, also called the matrix stress method (Hottman & Johnson 1965), are commonly used for the calculation of the pore pressure from analysis of the dc-exponent. Both methods are based on the same analytical technique. By combining the two methods a simple expression of the dc-exponent can be achieved as a function of the pore pressure, the overburden pressure and depth. This expression describes the increase of the dc-exponent with increase in depth if the pore pressure is normal, the mechanical drilling parameters are kept constant and a reference overburden gradient exists. By picking an initial dc-exponent from the actual drilling in normally pressured shales, any new dc-exponent is calculated. Plotting the calculated dc-exponents on a linear scale shows that the dc-exponents follow a straight line. By extrapolating this line to the depth axis the net uplift is achieved directly from the plot. This is similar to the technique applied on vitrinite reflectance values. The method is in our experience thought to be more accurate than $\pm$ 200 m.

Discussion of the quantitative methods

Vitrinite reflectance

The maturity parameter T_{max} should be plotted to control the vitrinite reflectance measurements of difficult samples. The subjective evaluation part should be limited to each individual sample and trendlines should be solved mathematically. The trendline should be a logarithmic regression of the chosen values. In addition, a new weighted regression technique of the profile should also be used (Fig. 1). This has the advantage of weighting each value by the number within the population, causing a much larger number of calculations. If the weighted trendline coincides with the normal regression line a more reliable result is obtained. Only the largest

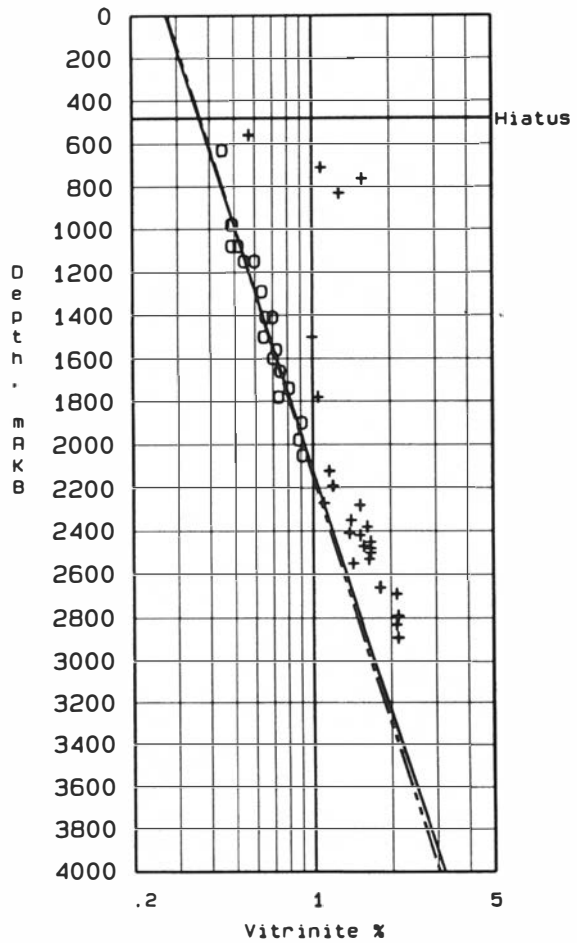

———Normal
R2: .942
No. of calculations: 19.
Uplift (0.16%): – 933 m.
Uplift (0.20%): – 560 m.
Erosion (0.16%): – 1413 m.
Erosion (0.20%): – 1040 m.
———Weighted.
R2: .931.
No. of calculations: 316.
Uplift (0.16%): – 888 m.
Uplift (0.20%): – 524 m.
Erosion (0.16%): – 1368 m.
Erosion (0.20%): – 1004 m.

\+ not used.
O used.

Fig. 1. Vitrinite reflectance profile showing Tertiary erosion from a Barents Sea well by use of logarithmic regression and weighted logarithmic regression. This example shows the results of both methods for two surface values (0.16 and 0.20%). Both the net uplift and the erosion are indicated.

indigenous populations and VR values of less than 1% should be used. In addition, since the surface value is a matter of discussion, consistent use is essential.

Shale compaction

Both the sonic log and the density log readings follow a compaction trend. Most published reference curves are based on the porosity of shale or shaly sands versus depth. Magara (1976) suggests a relation between porosity and the sonic transit time for the Western Canada Basin. This proved to be quite good also for the Barents Sea area compared with the results from other methods. Sonic log readings do not give the correct porosities of shales. Therefore, the equation presented by Wyllie et al. (1956) for porosities from the sonic log is limited to sandstones with porosities within a range of 25 to 30% (Raymer et al. 1980). Porosities outside this range have to be corrected by a compaction factor C. This factor is known for shale and is variable with depth. A method has been published for calculating porosities in shale from the sonic log, but this method uses the density of the shales from the density log in the calculations (Raymer et al. 1980). Critical for both the sonic and the density log readings is the reference curve of shale porosities versus depth. The best reference curve so far has been presented by Sclater & Christie (1980), based on Cretaceous shales in the North Sea. Checking these parameters in a Barents Sea well where only a small amount of uplift has taken place, indicates good agreement with their proposal. A valid reference curve should be developed for each area if possible. Figure 2 shows the use of this reference curve applied on a Barents Sea well.

Drilling parameters

This method requires a 'paleo' overburden pressure gradient. By integrating shale densities calculated from the shale porosities suggested by Sclater & Christie (1980), an overburden pressure gradient is achieved which can be applied to this method. Figure 3 shows the shale densities from this method together with the resulting overburden pressure gradient. The dc-exponent is normally plotted on a semilogarithmic scale versus depth. Plotting the calculated 'paleo' dc-exponents and the actual dc-exponents observed in a well gives two curved lines (left graph, Fig. 4). Plotting the same dc-exponents on a linear grid gives two almost straight lines (right graph, Fig. 4). In a zone of interest, the uplift can either be calculated from a linear regression of the dc-exponents within the interval or by a matrix operation. The matrix operation will give rise to numerous sets of calculations within an interval of normally pressured shales and with constant mechanical drilling parameters. All pairs of dc-exponents within that interval might be solved as a straight line, except for the cases where the slope is negative, i.e. where the initial dc-exponent is greater than the other dc-

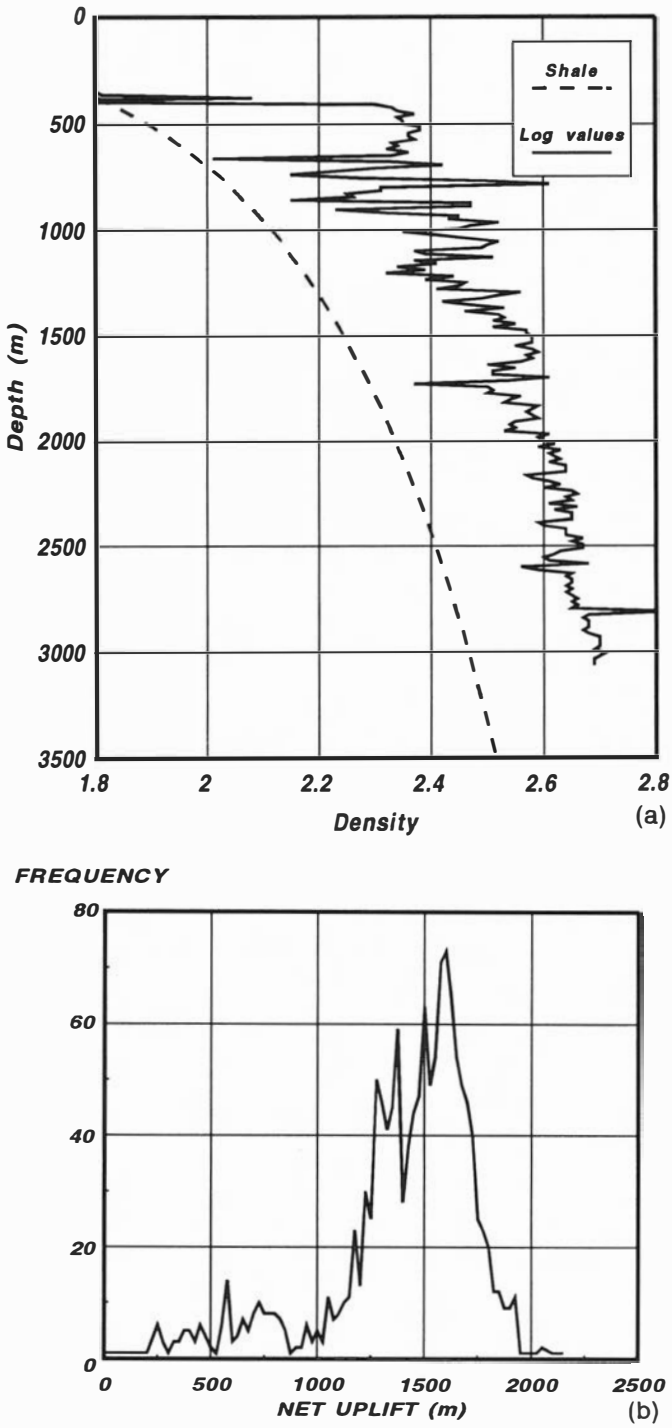

Fig. 2. Uplift estimation from shale compaction from a Barents Sea well by use of the density log. The dashed line in the bottom graph is the shale density curve as suggested by Sclater & Christie (1980). The solid curve is the actual density log. The histogram at the top shows the distribution of all the calculations. Mean values of these are most commonly used.

exponents. By doing that, thousands of calculations are performed, which will help to achieve a statistically more reliable result for the net uplift. It is recommended that 1 m data are obtained from the mud logging company.

Only calculations of the net uplift greater or equal to zero are valid. The method is dependent on the lithology, and calculations of the net uplift should only be carried out in homogeneous shales. The mechanical parameters

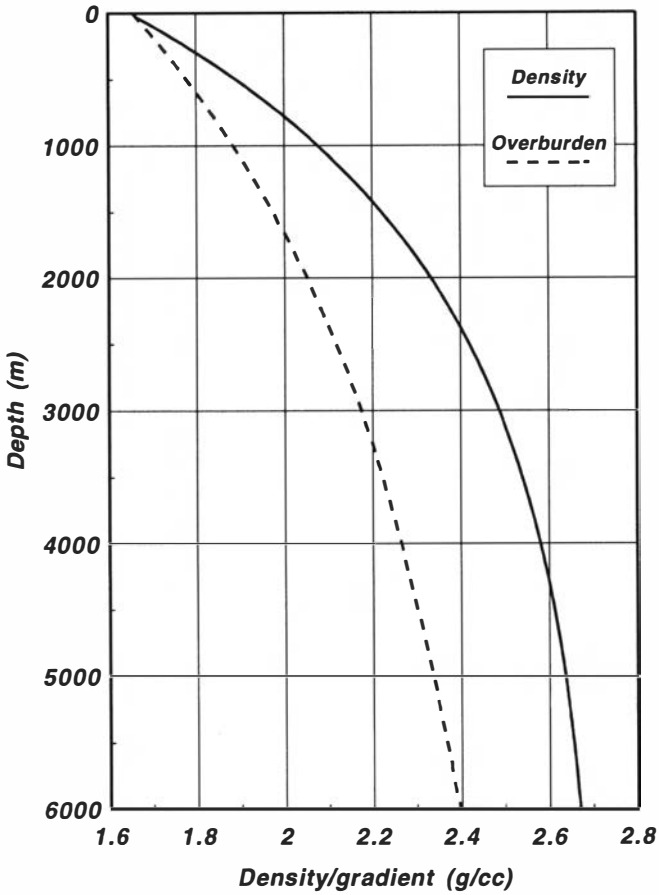

have to be constant within the calculation zone, and the normal pore pressure analysis technique has to be followed. This kind of analysis requires a software package to ease the amount of data computation. Figure 5 is an example from a well in which this method has been applied. Calculations were done in the boxed interval, where 4899 calculations were valid. The histogram at the right of Fig. 5 shows the intensity of the calculations where the most frequent range always indicates 100% intensity.

Conclusions

Accurate estimates of the uplift and erosion are essential for hydrocarbon exploration in the affected areas. As an

Fig. 3 (Left). Compaction curves based on the suggestion by Sclater & Christie (1980) of shale porosities versus depth. Shale density and overburden pressure gradient versus depth of shale.

Fig. 4. (A) Principles for uplift calculations from dc-exponent on logarithmic scale. The dashed line is the dc-exponents versus depth for normally pressured shales (dcn) where no uplift and erosion have occurred. The solid line is the dc-exponents for normally pressured shales where an uplift and erosion have occurred. (B) Similar to (A) but plotted on a linear scale, resulting in parallel lines. The dashed line intersects the depth axis at zero, while the solid line intersects the depth axis above the zero level. In this example it indicates a net uplift of 1000 m.

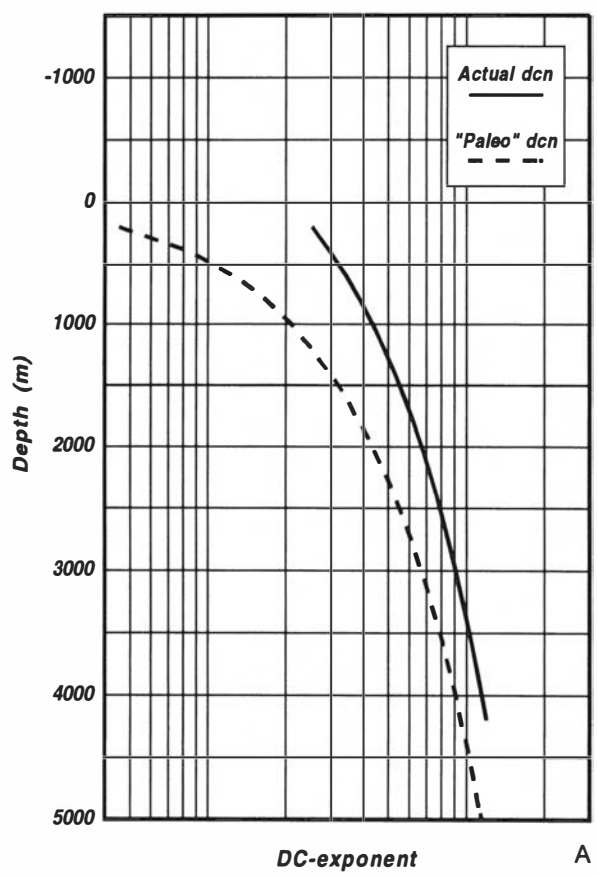

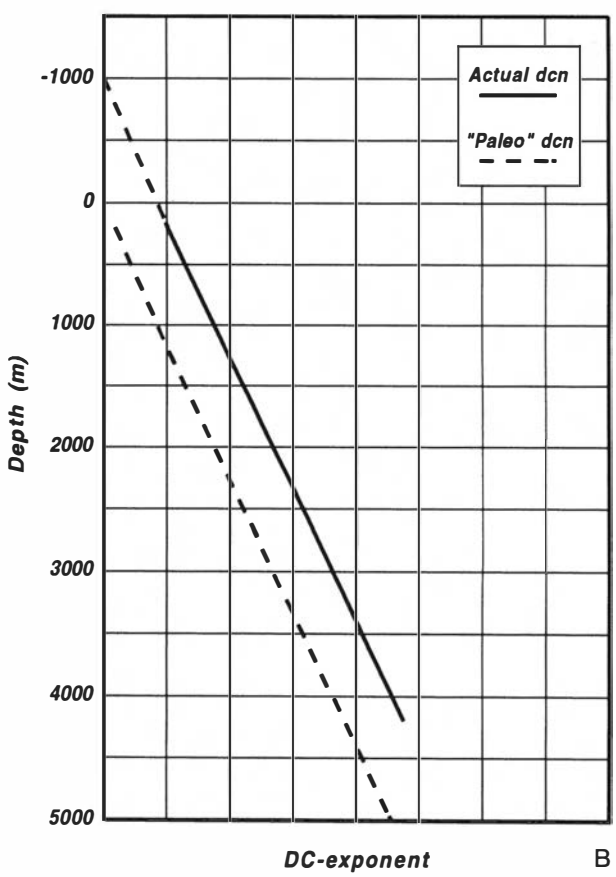

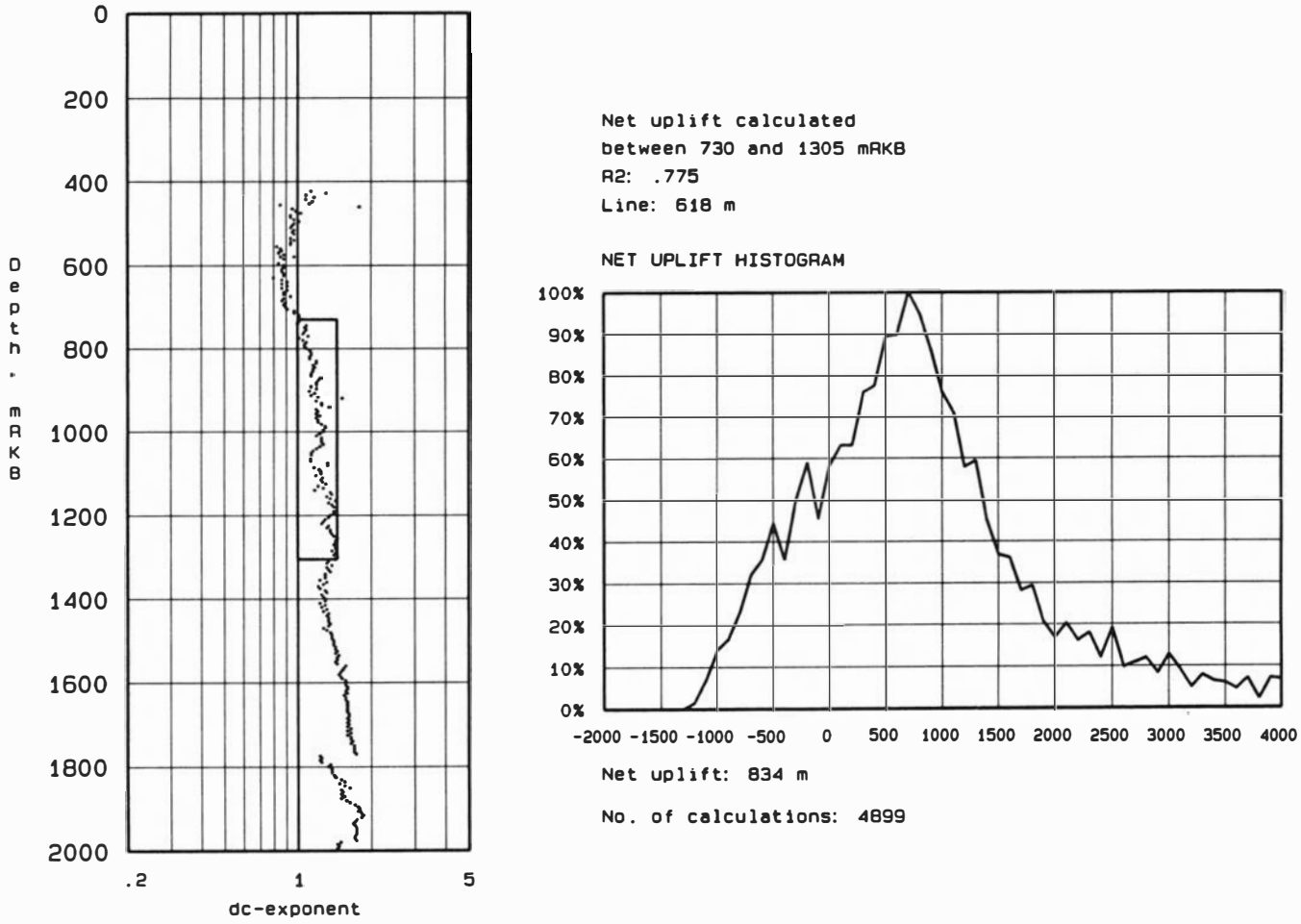

Fig. 5. Example of calculation of the net uplift in the Tertiary by use of dc-exponent from a Barents Sea well. Linear regression of values within the boxed interval in this example gives a correlation coefficient of 0.775 and a net uplift of 618 m. A matrix operation gives 4899 calculations with a mean value of the net uplift of 834 m. The histogram shows the distribution of all calculated results.

example, an additional uplift of 150 m in the Snøhvit area would have completely emptied the reservoir of oil due to gas expansion and gas liberation, which again would have caused the oil to spill at spillpoint (Skagen, in press). The method applying drilling parameters is the cheapest and one of the most accurate methods applicable on uplift and erosion. All quantitative methods are cheap, simple to use and accurate, but these methods are based on large amounts of data and statistical treatment is necessary for accurate analyses. Careful use of all methods, keeping the limitations in mind, will help in an accurate mapping of the Post-Cretaceous uplift and erosion along the Western Fennoscannian shield.

Acknowledgements. – Thanks to my colleagues Per Emil Eliassen and Rolf Magne Pettersen, Statoil, Harstad who helped on the different methodical aspects. Thanks also to Robert Evans who helped me with the language. Statoil is acknowledged for allowing me to publish this article.

Manuscript received October 1991

References

Baldwin, B. & Butler, C. O. 1985: Compaction Curves. *American Association of Petroleum Geology Bulletin 69,* 622–626.

Dzevanshir, R. D., Buryakovskiy, L. A. & Chilingarian, G. V. 1986: Simple quantitative evaluation of porosity of argillaceous sediments at various depth of burial. *Sedimentary Geology 46,* 169–175.

Eaton, B. A. 1975: *The Equations for Geopressure Prediction from Well logs.* Society of Petroleum Engineers 5544.

Hottman, C. E. & Johnson, R. K. 1965: Estimation of formation pressures from log-derived shale properties. *Journal of Petroleum Technology*, June 1965.

Magara, K. 1976: Thickness of removed sedimentary rocks, paleopore pressure, and paleotemperature, southwestern part of Western Canada Basin. *American Association of Petroleum Geology Bulletin 60,* 554–565.

Nyland, B., Jensen, L. N., Skagen, J. I., Skarpnes, O. & Vorren, T. 1992: Tertiary uplift and erosion in the Barents Sea; magnitude, timing and consequences. *In* Larsen, R. M. et al. (eds.): *Structural and Tectonic Modelling and Its Application to Petroleum Geology*, Norwegian Petroleum Society, Elsevier.

Raymer, L. L., Hunt, E. R. & Gardner, J. S. 1980: *An Improved Sonic Transit Time-to-Porosity Transform.* Society of Professional Well Log Analysts, twenty-first annual logging symposium, July 8–11, 1980.

Sclater, J. G. & Christie, P. A. F. 1980: Continental stretching: An explanation of the Post-Mid-Cretaceous subsidence of the Central North Sea Basin. *Journal of Geophysical Research 85,* 3711–3739.

Skagen, J. I.: Effects on hydrocarbon potential caused by Tertiary uplift and erosion in the Barents Sea. *In* Vorren, T. et al. (eds.): *Arctic Geology and Petroleum Potential*, Norwegian Petroleum Society (in press).

Quantitative geodynamic modelling of Barents Sea Cenozoic uplift and erosion

GUOJIANG LIU, STEPHEN LIPPARD, STEIN FANAVOLL, ØYVIND SYLTA, STIG VASSMYR & ANTHONY DORÉ

Liu, G., Lippard, S., Fanavoll, S., Sylta, Ø., Vassmyr, S. & Doré, A.: Quantitative geodynamic modelling of Barents Sea Cenozoic uplift and erosion. *Norsk Geologisk Tidsskrift*, Vol. 72, pp. 313–316. Oslo 1992. ISSN 0029-196X.

Geodynamic modelling has been carried out to explain the Cenozoic uplift and erosion in the Barents Sea. Three erosion models are considered: instantaneous, constant rate and elevation-dependent erosion. The first gives the maximum erosion, whereas the last is preferred as it gives more realistic results. Three theoretical models are proposed to account for the Barents Sea uplift: subcrustal mantle lithospheric extension, crustal thickening and magmatic intrusion into the crust, and are modelled against the erosion distribution and present-day crustal thicknesses. Modelling of subcrustal extension gives a maximum β factor for lithospheric mantle extension of 1.7. The crustal thickening model predicts a maximum shortening of 14%. The magma intrusion model predicts an intrusion thickness of 2.7 km. The consequences of these models for the Cenozoic heat flow history are briefly considered.

G. Liu, S. Fanavoll & Ø. Sylta, IKU Petroleum Research A/S, N-7034 Trondheim, Norway; S. Lippard. Department of Geology and Mineral Resources Engineering, Norwegian Institute of Technology (NTH), N-7034 Trondheim, Norway; S. Vassmyr & A. Doré, Conoco Norway Inc., PO Box 488, N-4001 Stavanger, Norway.

The underlying causes of the widespread Cenozoic uplift and erosion in the Barents Sea have been the subject of much recent discussion. For example, Kjemperud & Fjeldskaar (1989) proposed that they are largely an isostatic response to glacial erosion and overdeepening in the Plio-Pleistocene. Sættem (1990) has demonstrated some of the dramatic effects of ice erosion in the area. The problem here is whether glacial erosion alone can have caused the 1–2 km of uplift over such a large region. Riis & Fjeldskaar (1989) proposed that relief of pressure following erosion can have caused phase changes in the upper mantle and provided an extra uplift. On the other hand, Sales (1989) related the uplift to largely tectonic causes, in particular, Tertiary rift flank uplift. Wood et al. (1989) proposed a non-uniform two-layer stretching model related to mid-Tertiary rifting of the margin in which extra heat is input into the lower part of the lithosphere.

The intention of this paper is to investigate some of the possible geodynamic mechanisms involved in the uplift and erosion. The aim is to quantify the uplift and erosion for different models as well as modelling the theoretical heat flow. We have tested three erosion models which are quantitatively formulated with three potential uplift mechanisms: (1) non-uniform lithospheric extension, (2) crustal thickening, and (3) magmatic intrusion in the crust. For each of these a 2-D physical model is demonstrated according to the distribution of erosion and crustal thicknesses along a representative profile across the southwest Barents Sea.

Quantitative erosion modelling

In erosion modelling, the elevation is important. The elevation variation can be influenced by many geological factors; for instance, thermal conditions in the lithosphere, erosion rate, tectonic activity, eustatic sea-level changes, etc. In our modelling, however, only two factors related to the elevation variation – erosion rate and thermal subsidence – are considered. The relationship between these variables can be formulated mathematically by the following equation:

$$\frac{dE(t)}{dt} + \frac{\rho_m - \rho_s}{\rho_m} P(t, E(t), C) + \frac{dS(t)}{dt} = 0 \qquad (1)$$

$E(t)$ = elevation evolution with time; ρ_m, ρ_s = densities of the subcrustal lithosphere and sediments; $P(t, E(t), C)$ = erosion rate function; $S(t)$ = thermal subsidence.

According to the erosion rate variation, three erosion processes can be defined with the assumption of local isostatic compensation. Instantaneous erosion implies a very large erosion rate such that the influence of thermal subsidence is negligible. Constant rate erosion is unchanged with time even if the magnitude can change with tectonic and geological situations. Elevation-dependent erosion implies that the erosion has a linear relationship with elevation. In the case of instantaneous erosion the amount of erosion (ER) can be expressed as:

$$ER = E_0 \frac{\rho_m}{\rho_m - \rho_s} \qquad (2)$$

E_0 = Initial elevation.

In the case of constant rate erosion, the erosion equation takes the form:

$$ER = P \cdot t \tag{3}$$

P = Erosion rate function.

On the assumption that erosion rate has a linear relationship with the elevation, equation (1) can be solved analytically and written as:

$$E(t) = \exp(-C_k \cdot t)\left\{\int^t S(s)\exp(C_k \cdot s)ds + C\right\} \tag{4}$$

where:

$$C_k = \frac{\rho_m}{\rho_m - \rho_s} \cdot K \tag{5}$$

K is the erosion time constant. C_k is a constant determined by the initial conditions. The cumulative erosion is an integral of instantaneous erosion with the form of:

$$ER(t) = \int^t K \cdot E(v)dv + C \tag{6}$$

By substituting (4) in (6) we get:

$$ER(t) = -K\int^t \exp(-C_k \cdot v) \times \left\{\int^v S(s) \cdot \exp(C_k \cdot s)ds + C_1\right\}dv + C_2 \tag{7}$$

C_1 and C_2 are constants which can be evaluated by two initial conditions:

$$E(t = t_1) = 0 \tag{8}$$

$$S(t = t_2) = S_1 \tag{9}$$

The elevation-dependent erosion model has been generally used (Ahnert 1970; Murrell 1986). Ahnert proposed that the erosion time constant (K) should be around 0.151 (m.y.)$^{-1}$ (m.y. = million years). In our computations, we use a range from 0.01 to 3.0 (m.y.)$^{-1}$. When the erosion time constant approaches 3.0, the erosion process will be almost the same as that for instantaneous erosion. The theoretical results of erosion modelling are demonstrated in Fig. 1, where a constant erosion rate of 50 m/m.y. and an erosion time constant of 3.0 (m.y.)$^{-1}$ have been used.

It should be noted that in erosion modelling the total erosion period must be pre-computed by the condition $e(t) = 0$ from equations (3) or (7) for the constant rate and elevation dependent erosions respectively.

Investigation of the Barents Sea uplift and erosion

The erosion distribution in the southwestern part of the Barents Sea based largely on a study of shale velocities in wells is shown in Fig. 2. The erosion generally increases towards the northeast from 0 to 1500 m. The present-day crust thickness distribution (Fig. 3.) increases in the same direction from 15 to 35 km. These two pieces of information have been used to investigate the following three uplift mechanisms: subcrustal lithospheric extension, crustal thickening and magmatic intrusion in the crust along a NE–SW profile (CC′).

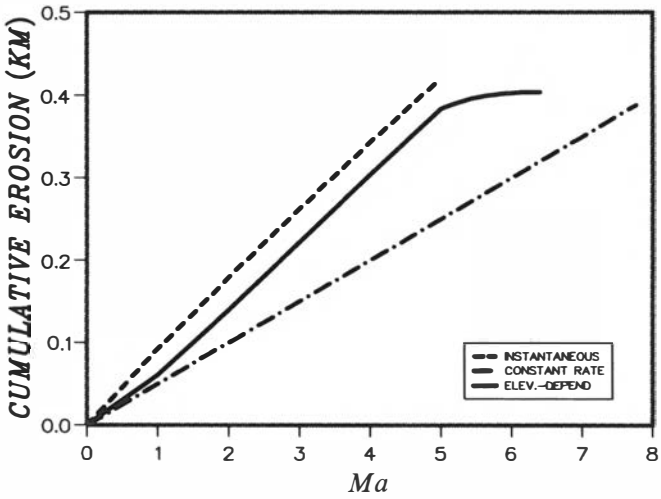

Fig. 1. A comparison of cumulative erosion for instantaneous (dashed line), constant rate (dash-dot line) and elevation dependent (solid line) erosion models (Ma = million years). See test for details.

Pure shear subcrustal lithospheric extension has been modelled giving a maximum mantle stretching factor (β) of 1.7 at the end of the profile (Fig. 4). The input parameters were: active stretching began 15 Ma ago and lasted 2 m.y., with an initial lithosphere thickness of 125 km. The predicted present-day heat flow is increased to 0.2 hfu above background. This model simulates a mantle plume. In addition, simple-shear lithospheric detachment (Wernicke 1985) could be incorporated in the subcrustal lithospheric extension model. However, this is highly speculative because there is as yet no evidence of such a detachment underlying the area.

The crustal thickening model (Murrell 1986) is apparently supported by the increase in crustal thickness towards the northeast in the same direction as increased erosion. A maximum shortening of 14% ($\beta = 0.86$) is predicted according to the distribution of erosion and crustal thickness along the profile (Fig. 5). In this case the crustal thickness variation would be interpreted as the result of Cenozoic crustal thickening. However, it is more likely that the present thickness variations are the result of older Paleozoic and Mesozoic stretching events (Roufosse 1987) and there is no evidence for Cenozoic compressional tectonics in the area to support the model. The crustal thickening model predicts lower than normal heat flow.

Eocene and later magmatic activity has been recognized along the western Barents Sea margin (Faleide et al. 1988) and Cenozoic to Recent volcanism is known on Svalbard, but at present there is no evidence for Cenzoic magmatic activity further east. Modelling the intrusion of a mantle-derived, sheet-like basic intrusion (density 2.95 gm/cc, temperature 1300°C) in the crust shows that: (1) intrusion thickness has a more or less linear relationship with the cumulative erosion (Fig. 6) and, (2) the

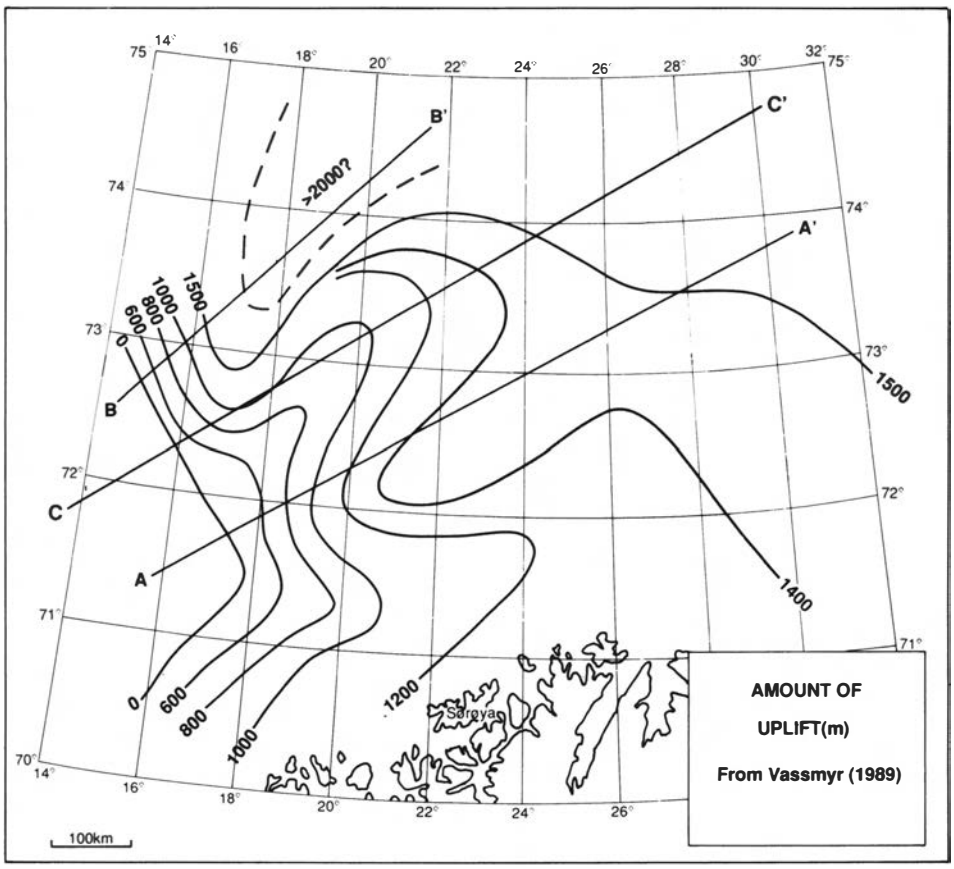

Fig. 2. Thickness of erosion (m) in the southwest Barents Sea. Based on shale interval velocity data from selected wells and other data sources.

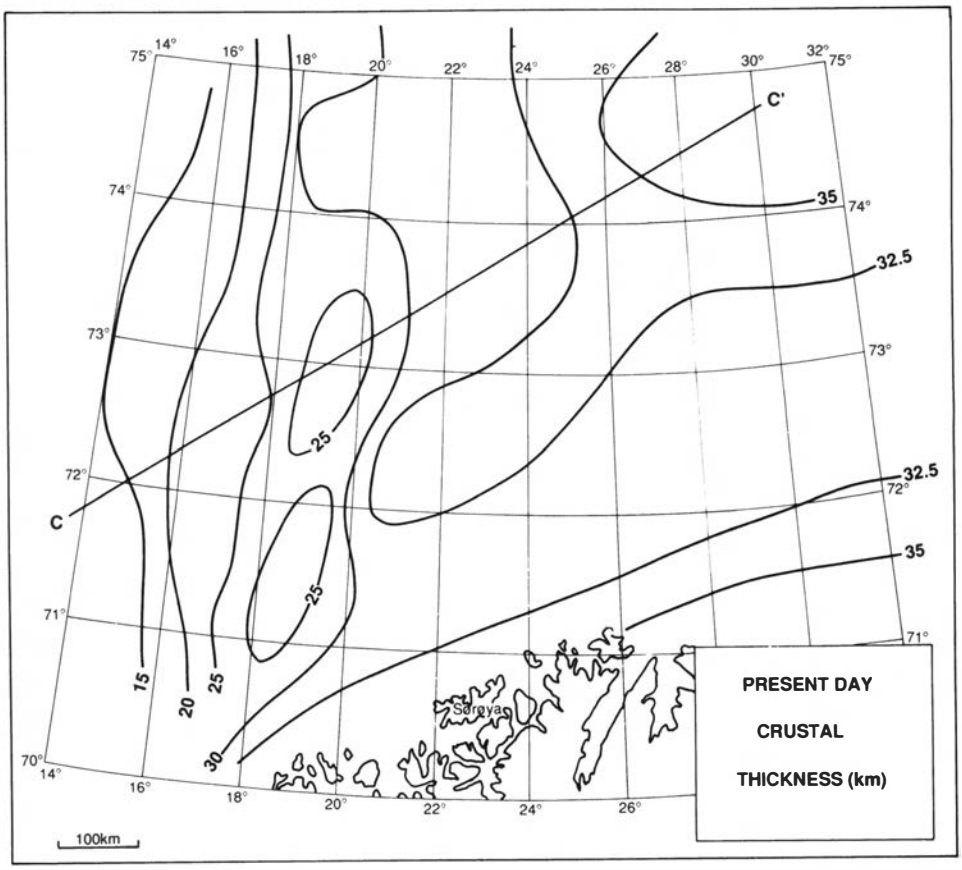

Fig. 3. Present-day crustal thickness (km) in the southwest Barents Sea. Based on an analysis of IKU deep seismic data and other data sources (in cooperation with J. I. Faleide and others at the University of Oslo).

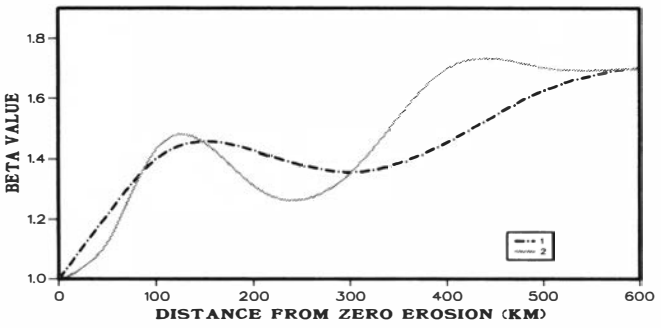

Fig. 4. Distribution of the subcrustal lithospheric extension factor ($\beta = 1.0-1.8$) along line CC′ (see Fig. 2). Solid line based on present-day crustal thickness; dash-dot line is based on a constant crustal thickness of 27 km.

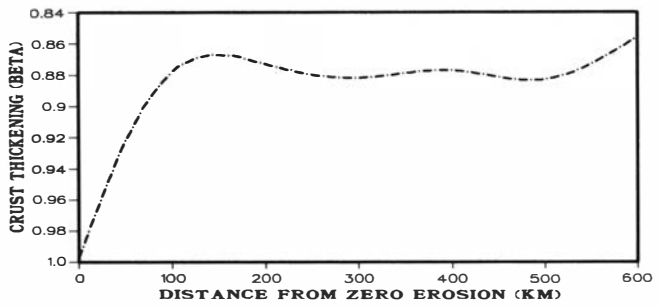

Fig. 5. Crustal thickening factor ($\beta = 1.0-0.86$) distribution along line CC′.

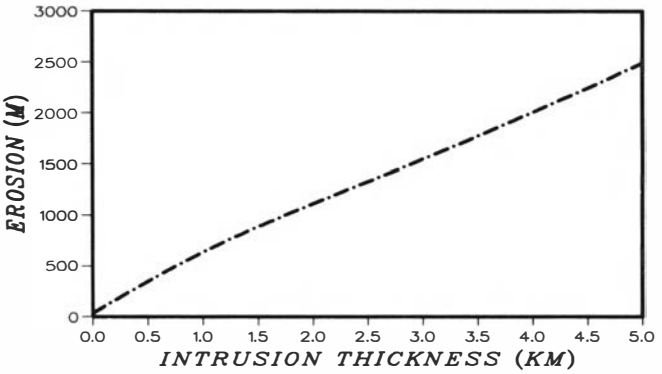

Fig. 6. The influence of intrusion thickness on the maximum erosion.

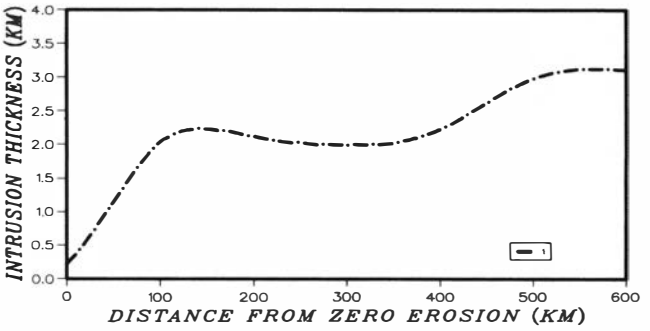

Fig. 7. Modelled intrusion thickness distribution along line CC′.

intrusion depth has little effect on the uplift but is inversely proportional to the surface heat flow. Based on the amount of erosion, the intrusion thickness has been modelled to a maximum of 2.7 km along profile CC′ (Fig. 7). The intrusion depth can be tentatively modelled using the limited amount of data available on the present-day surface heat flow as about 15 km, by assuming that the intrusion was emplaced at 15 Ma. A deeper intrusion, for example at the base of the crust, would have to have been emplaced more recently.

Conclusions

Three erosion models; instantaneous erosion, constant rate erosion and elevation dependent erosion, have been tested to simulate erosion processes. The elevation-dependent erosion model is the most realistic process with the erosion time constant ranging from 0.01 to 3.0 $(\text{m.y.})^{-1}$.

Three uplift mechanisms, subcrustal lithospheric extension, crustal thickening and magmatic intrusion have been modelled to explain the Tertiary uplift and erosion along a chosen profile in the Barents Sea. The subcrustal lithospheric extension model predicts a maximum mantle stretching factor of 1.7 while the crustal thickening model gives a maximum crustal shortening factor of 0.86. The magmatic intrusion model predicts a thickness of 2.7 km at a depth of 15 km for a basic intrusion emplaced 15 m.y. ago. None of these mechanisms is yet supported by any deep seismic or other geophysical data, so at present, we do not have sufficient data to give priority to any of the proposed models.

Manuscript received October 1991

References

Ahnert, F. 1970: Functional relationships between denudation, relief and uplift in large mid-latitude drainage basins. *American Journal of Science 268,* 243–263.

Faleide, J. I., Myhre, A. M. & Eldholm, O. 1988: Early Tertiary volcanism at the western Barents margin. *In* Morton, A. C. & Parson, L. M. (eds.): *Early Tertiary Volcanism and the Opening of the NE Atlantic. Geological Society Special Publication 39,* 135–146.

Kjemperud, A. & Fjeldskaar, W. 1989: Glacial isostasy – a tectonic effect neglected by petroleum geologists. *Structural and Tectonic Modelling and its Application to Petroleum Geology*, NPF Meeting Stavanger October 1989, Abstract Volume, p. 20.

Murrell, S. A. F. 1986: Mechanics of tectogenesis in plate collision zones. *In* Coward, M. P. & Ries, A. C. (eds.): *Collision Tectonics, Geological Society Special Publication 19,* 95–111.

Riis, F. & Fjeldskaar, W. 1989: The importance of erosion and mantle phase changes for the late Tertiary uplift of Scandinavia and the Barents Sea. *Structural and Tectonic Modelling and its Application to Petroleum Geology*. NPF Meeting Stavanger October 1989, Abstract Volume, p. 22.

Roufosse, M. 1987: The formation and evolution of sedimentary basins in the Western Barents Sea. *In* Brooks, K. & Glennie, K. W. (eds.): *Petroleum Geology of Northwest Europe*, 1149–1162. Graham & Trotman, London.

Sales J. 1989: Late Tertiary uplift – west Barents Shelf, character, mechanisms and timing. *Structural and Tectonic Modelling and its Application to Petroleum Geology*, NPF Meeting Stavanger October 1989, Abstract Volume, p. 21.

Sættem, J. 1990: Glaciotectonic forms and structures on the Norwegian continental shelf, observations, process and implications. *Norsk Geologisk Tidsskrift 70,* 81–94.

Wood, R. J. Edrich, S. P. & Hutchison, I. 1989. Influence of North Atlantic tectonic on the large-scale uplift of Stappen High and Loppa High, Western Barents Sea. *In* Tankard, A. J. & Balkwill, H. R. (eds.): *Extensional Tectonics and Stratigraphy of the North Atlantic Margins, AAPG Memoir 46,* 559–566.

Wernicke, B. 1985. Uniform normal simple shear of the continental lithosphere. *Canadian Journal of Earth Sciences 22,* 108–125.

Shallow faulting around the Nordkapp Basin and its possible relation to regional uplift

STEPHEN LIPPARD & STEIN FANAVOLL

Lippard, S. J. & Fanavoll, S.: Shallow faulting around the Nordkapp Basin and its possible relation to regional uplift. *Norsk Geologisk Tidsskrift*, Vol. 72, pp. 317–320. Oslo 1992. ISSN 0029-196X.

Numerous small high-level normal extensional faults occur in Cretaceous sediments on the platform areas surrounding the Nordkapp Basin in the eastern part of the Norwegian sector of the Barents Sea. The amount of extension represented by the faulting, which is more or less detached from underlying unfaulted sequences, is at least 8%. Several mechanisms are considered: gravity sliding, salt tectonics and plate boundary-related extension during the early Tertiary, but the faults can be interpreted as the result of differential stresses that were generated during one or more phases of regional uplift in the late Cretaceous or, more likely, Cenozoic time.

Stephen Lippard, Department of Geology and Mineral Resources Engineering, Norwegian Institute of Technology (NTH), N-7034 Trondheim, Norway; Stein Fanavoll, IKU Petroleum Research A/S, N-7034 Trondheim, Norway.

A NNE–SSW to N–S trending composite 2.5 s twt seismic line (IKU-01-88/IKU-3015-88) (Fig. 1) reveals in fine detail numerous small (up to 70 ms, majority 10–20 ms, throw) normal faults in Cretaceous sediments in the eastern part of the Norwegian sector of the Barents Sea. The area of high-level faulting is known from regional seismic data to cover a wide area east of 29°E between 71°30 and 74°N on the flanks of the Nordkapp Basin and on adjacent parts of the Finnmark and Bjarmeland Platforms (structural elements from Gabrielsen et al. 1990).

Description of the faulting

The faulting occurs in well-bedded Cretaceous sediments, believed to be mainly shales, that occur between the near sea floor base Quaternary unconformity and the base Cretaceous unconformity. The great majority of the faults appear to die out near the base of the Cretaceous section although south of the Nordkapp Basin a few can be directly connected to deeper faults with larger throws that extend into the underlying Jurassic and Triassic sequences (Fig. 2). These deep-seated faults were active during a period of late Jurassic regional extension in the area. North of the basin no such connection between the pre- and post-Cretaceous faulting has been recognized and a northward thickening sequence of unfaulted Lower Cretaceous sediments lies between the faulted section and the base Cretaceous unconformity (Fig. 3). The top of the unfaulted unit appears to have acted as a zone of decollement below the high-level faults. There are no indications that the faulting was active during the deposition of the sediments.

Some of the larger faults south of the Nordkapp Basin can be tied on the regional seismic grid (NPD data) and

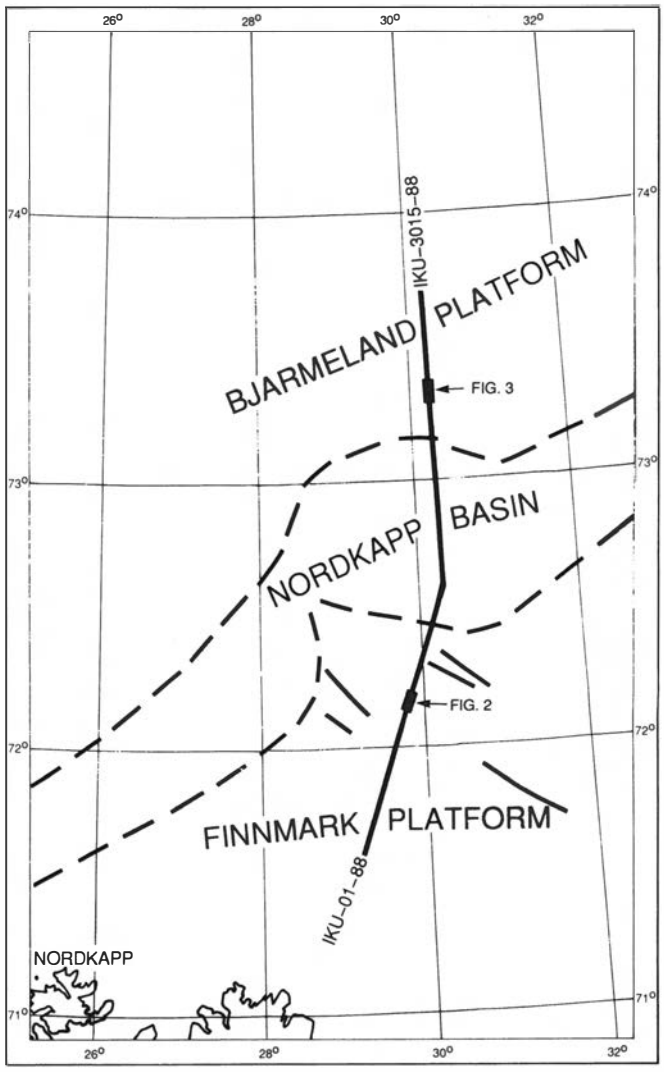

Fig. 1. Location map showing positions of lines IKU-01-88 and IKU-3015-88. Structural features based on Gabrielsen et al. (1990).

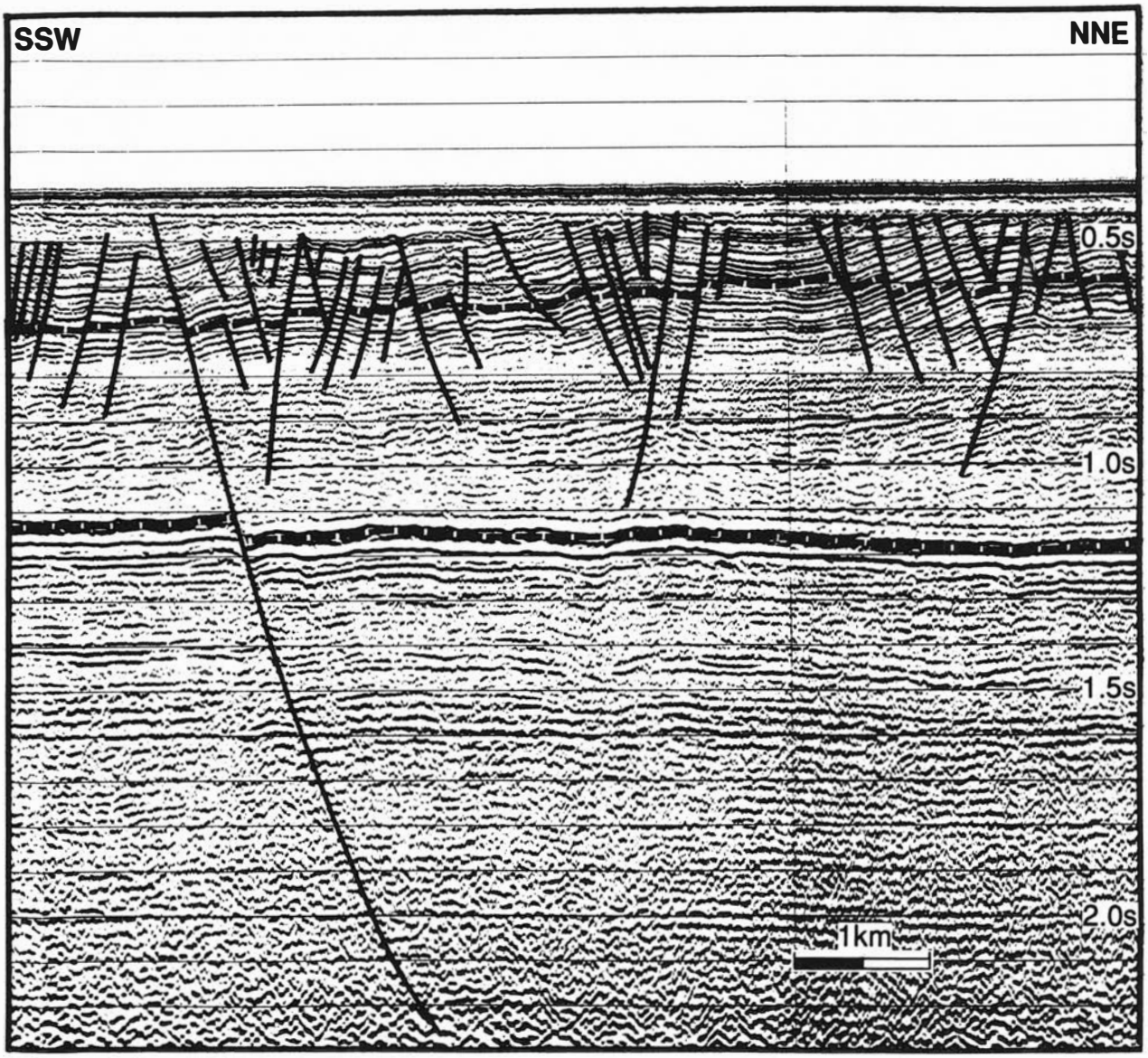

Fig. 2. Part of line IKU-01-88 south of the Nordkapp Basin (location shown in Fig. 1). The upper marker shows the shallow faulting; the lower marker is the Base Cretaceous Unconformity. Note that the majority of the faults die out above the base of the Cretaceous except for one which reactivates a deep-seated fault.

show predominantly NW–SE trends. We consider that this is also the most likely trend for the shallow detached faults as they appear to parallel the major faults and are best seen on the seismic lines that trend between E and N; i.e. more than 45° to the assumed trend.

The faults have an average spacing of 400–500 m and are seen to dip between 64° and 82° (mean 72°) on the seismic data which represents 40° to 70° (mean 50°) when depth converted and corrected for vertical exaggeration. They are mostly planar to slightly listric in form. The beds are tilted between the faults with high (>60°) cut-off angles. Parallel sets of up to 15 adjacent faults can show the same dip (facing) direction and conjugate pairs of faults showing opposite facing directions are relatively rare. On the southern part of line IKU-01-88 (faults 1–100 on Table 1a) there is a 2:1 predominance of south-facing faults but further north roughly equal numbers of north- and south-facing faults are present just to the south of the Nordkapp Basin (Table 1a). All of the larger faults which cut through the base Cretaceous unconformity face to the north. On line IKU-3015-88 to the north of the basin, there is an almost 2:1 predominance (63% of the total) of north-facing faults (Table 1b). This is thus in contrast to the area south of the basin where south-facing faults predominate (57%).

The net extension, i.e. present length/original length of a chosen marker horizon, calculated by summing the heaves of up to 50 faults over several measured sections, is about 8%. The extension due to faulting on the underlying base Cretaceous reflector appears to be much less (<2%).

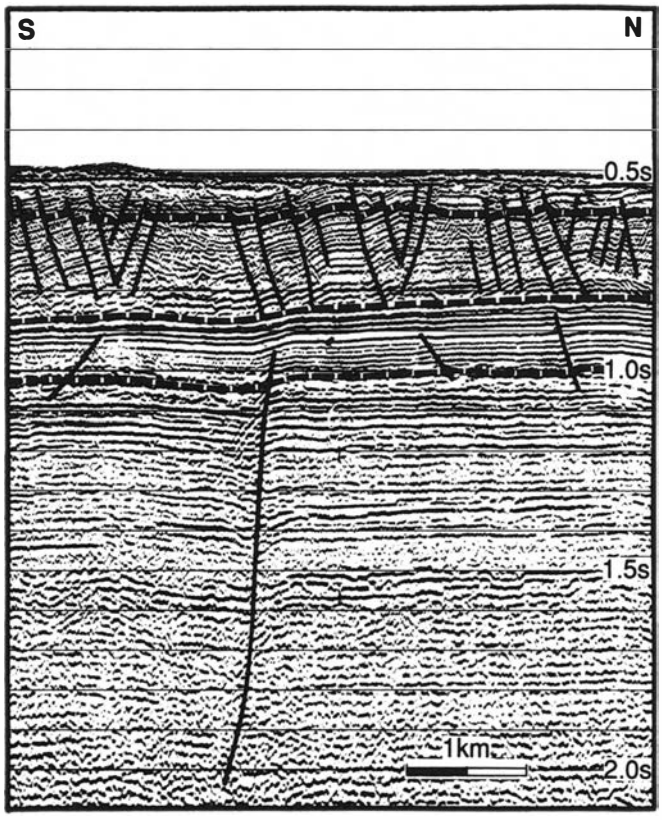

Fig. 3. Part of line IKU-3015-88 north of the Nordkapp Basin (location shown in Fig. 1). The upper marker shows the shallow faulting, the middle marker the 'decollement' horizon and the lower marker the Base Cretaceous Unconformity. Note that the high level faults are confined to the upper part of the Cretaceous section above the decollement. The one deep-seated fault is not connected with the high level faults.

Table 1. Analysis of fault facing directions.

(a) Line IKU-01-88 sp 4650-12725. South of the Nordkapp Basin.
Length 101 km. Trend N24°E.
Number of faults: 265. Average spacing: 380 m.

		S-facing	N-facing
Faults	1–50*	32	18
	51–100	36	14
	101–150	25	25
	151–200	22	28
	201–250	28	22
	251–265	9	6
	Total	152 (57%)	113 (43%)

(b) Line IKU-3015-88 sp 5400–9600. North of the Nordkapp Basin.
Length 52.5 km. Trend N.
Number of faults: 97. Average spacing: 540 m.

		S-facing	N-facing
Faults	1–50*	21	29
	51–97	14	33
	Total	35 (36%)	62 (64%)

* Faults numbered from southern ends of lines.

Possible origins of the faulting

Gravity sliding

As described above, many of the faults, especially north of the basin, appear to die out above a decollement horizon above the base Cretaceous unconformity. A possible mechanism for the formation of the faults is therefore as a result of gravity sliding on the decollement. In this case the faults would be expected to show preferred facing directions down slope, i.e. towards the Nordkapp Basin. In fact the opposite seems to be the case with a predominance of south-facing faults on the southern flank and north-facing faults on the northern flank of the basin (Table 1). A gravity sliding mechanism is therefore considered unlikely.

Salt tectonics

The high-level faulting could be related to Cenozoic salt movements that occurred in the Nordkapp Basin, there being no evidence for contemporaneous salt movements during the deposition of the Cretaceous sequence. However, although the faults occur on the platform areas surrounding the basin, they are largely absent within the basin and in the rim synclines between the salt domes. In addition, they are clearly different in style from the listric, collapse faults that occur over and on the flanks of the domes. Finally, the high-level faulting shows no clear relationship to the deep-lying salt pillows on the basin margins and extends well beyond the limits of salt movement. As a result, salt tectonics is excluded as a cause of the faulting.

Regional extension

Another possible cause of the faulting is late Cretaceous to Cenozoic regional extension. A likely period for this to occur was during the early to mid-Cenozoic time when a new plate boundary was developing along the western margin of the Barents Sea. However, the faulting associated with Tertiary rifting appears to be confined to the western part of the Barents Sea (Riis et al. 1986). In addition, the faulting in question is largely confined to Cretaceous sediments and is partly detached from underlying unfaulted or less severely faulted sequences where the amount of post-Jurassic extension appears to be negligible. This would appear to rule out regional extension as a cause unless extension in the underlying beds was accommodated in some other way.

Uplift

The final explanation considered here is that the faulting is related in some way to regional uplift. Cenozoic uplift of up to 2 km is thought to have occurred over wide areas of the Barents Sea (Nyland et al. 1989; Løseth et al. in press), including the area in question. In addition, late Cretaceous uplift may have occurred. Antonsen et al. (1991) have described high-level normal faults in Jurassic and Cretaceous sediments on the Storbanken High in the northern Barents Sea which they relate to late Cretaceous uplift of the region.

The association between extension and regional uplift is generally considered to be the result of expansion of the surface area. Hafner (1951) showed that variable vertical stresses will cause conjugate high-angle normal faults to develop on the upper part of the uplift and that increasing strains will cause the zone of faulting to expand downwards. Sanford (1959) showed from analytical and experimental studies of stress trajectories that extensional shear fractures form in the cover over a basement undergoing sinusoidal uplift. The normal faults on the flanks of the uplift face in the direction of increasing uplift as suggested by the preferred facing directions of the faults on the flanks of the Nordkapp Basin. A more specific mechanism for extensional fault formation during uplift is described by Price (1966) in which the lateral stresses decrease more rapidly than the vertical gravitational stress which then becomes the greatest principal stress (σ_1) giving rise to vertical shear fractures. A problem is that the differential stresses developed during uplift are normally small and probably generally insufficient to cause faulting. It may, however, be significant that the faults in question are largely restricted to a dominantly shaley sequence which could have suffered overpressuring during burial. Overpressures will generally lower the effective stress and may promote fracturing.

Conclusions

Numerous small, conjugate normal faults affecting uplifted, dominantly shaley Cretaceous sediments around the Nordkapp Basin do not appear to be related to local gravity or salt tectonics, nor can they be easily related to regional tectonics, for example, the early Tertiary rifting along the western margin of the Barents Sea. An alternative explanation is differential stresses generated by the up to 2 km of regional uplift that occurred during the late Cretaceous or, more likely, Cenozoic time. There may be a causal relationship between the highly faulted formations and overpressures generated during maximum burial.

Acknowledgements. – We thank IKU and Conoco Norway Inc., owners of the seismic data, for permission to publish. We thank Bjørn T. Larsen and an anonymous reviewer for comments.

Manuscript received October 1991

References

Antonsen, P., Elverhøi, A., Dypvik, H. & Solheim, A. 1991: Shallow bedrock geology of the Olga Basin area, northwestern Barents Sea. *American Association of Petroleum Geologists Bulletin 75*, 1178–1194.

Gabrielsen, R. H., Færseth, R. B., Jensen, L. N., Kalheim, J. E. & Riis, F. 1990: Structural elements of the Norwegian continental shelf. Part 1: The Barents Sea Region. *NPD-Bulletin No 6*, 33 pp.

Hafner, W. 1951: Stress distribution and faulting. *Geological Society of America Bulletin 62*, 373–398.

Løseth, H., Lippard, S. J., Sættem, J., Fanavoll, S., Fjerdingstad, V., Leith, L. T., Ritter, U., Smelror, M. & Sylta, Ø.: Cenozoic uplift and erosion of the Barents Sea – evidence from the Svalis Dome area. *Proceedings NPF Conference on Arctic Geology and Petroleum Potential, Tromsø*. In press.

Nyland, B., Jensen, L. N., Skagen, J. I., Skarpnes, O. & Vorren, T. 1989: Tertiary uplift and erosion in the Barents Sea, timing and consequences. Paper presented at NPF Conference on Structural and Tectonic Modelling and its Application to Petroleum Geology, Stavanger, October 1989.

Price, N. J. 1966: *Fault and Joint Development in Brittle and Semibrittle Rock*, 176 pp. Pergamon Press.

Riis, F., Vollset, J. & Sand M. 1986: Tectonic development of the western margin of the Barents Sea and adjacent areas. *In* Halbouty, M. J. (ed.): Future Petroleum Provinces of the World. *American Association of Petroleum Geologists Memoir 40*, 661–667.

Sanford, A. R. 1959: Analytical and experimental study of simple geological structures. *Bulletin of the Geological Society of America 76*, 19–52.

Magnitude of uplift of the Stø and Nordmela Formations in the Hammerfest Basin – a diagenetic approach

OLAV WALDERHAUG

Walderhaug, O.: Magnitude of uplift of the Stø and Nordmela Formations in the Hammerfest Basin – a diagenetic approach. *Norsk Geologisk Tidsskrift*, Vol. 72, pp. 321–323. Oslo 1992. ISSN 0029-196X.

The quartzitic sandstones of the Jurassic Stø and Nordmela Formations are located only 1.5 km below the sea floor in well 7120/9-1 in the Hammerfest Basin. Despite the moderate burial depth, the sandstones are extensively quartz-cemented, contain well-developed stylolites and have a mean helium porosity of only 16.7%. This advanced degree of quartz cementation and stylolitization, and the low porosities, would not be expected at depths of less than 3–3.5 km in similar sandstones in the North Sea or Haltenbanken area. Calcite cement in the Stø Formation contains hydrocarbon inclusions trapped or re-equilibrated at temperatures of around 125 C. Assuming geothermal gradients of 30–40 C and a sea floor temperature of 5 C, temperatures of 125 C correspond to burial depths of 3–4 km. It is consequently suggested that the Stø and Nordmela Formations in this part of the Hammerfest Basin have been uplifted 1.5–2 km.

O. Walderhaug, Rogaland Research, PO Box 2503, N-4004 Stavanger, Norway.

Several lines of evidence indicate that major uplift has taken place in the Hammerfest Basin area and in other parts of the Barents Sea shelf at some time during the Tertiary (Olaussen et al. 1984; Walderhaug 1985; Berglund et al. 1986; Bjørlykke et al. 1989; Riis and Fjeldskaar, in press Nyland et al. in press). One way of estimating the magnitude of this uplift is by studying the diagenetic evolution of reservoir sandstones in the area. In this study magnitude of uplift is estimated by detailed study of the diagenetic history of the quartzitic sandstones of the Jurassic Stø and Nordmela Formations in well 7120/9-1 in the Hammerfest Basin.

Quartz cementation

The top of the Stø Formation is presently situated exactly 1500 m from the sea floor in well 7120/9-1. Similar sandstones from other parts of the Norwegian shelf with only 1.5 km overburden are typically loose and uncemented, except for carbonate-cemented intervals, and do not contain quartz overgrowths. Stø and Nordmela Formation sandstones in the studied well are, on the other hand, hard and quartz-cemented with typical quartz cement contents of 5–10%. Furthermore, stylolites are well developed. This degree of quartz cementation and stylolitization would not be expected at depths of less than approximately 3 km in the North Sea area or offshore mid-Norway (Olaussen et al. 1984; Berglund et al. 1986; Bjørlykke et al. 1986).

Porosity

Mean helium-porosity for sandstone samples in the studied cores is 16.7%, maximum helium-porosity is 23%. These porosities are exceptionally low for clay-poor quartzitic sandstones at 1.5 km burial depth elsewhere on the Norwegian shelf (Olaussen et al. 1984; Bjørlykke et al. 1986; Bjørlykke et al. 1989). Normally such porosity values in this type of sandstone would only be expected after burial to depths of 3–3.5 km (Fig. 1).

Oxygen isotopes

$\delta^{18}O_{PDB}$-values for calcite cement in the Stø Formation in well 7120/9-1 are as negative as -14.3%(Fig. 2). This corresponds to temperatures of precipitation of 73°C, 100°C and 130°C assuming $\delta^{18}O_{SMOW}$-values of -4, 0 and 4 respectively for the pore water at the time of calcite precipitation. However, no reliable way of determining the correct $\delta^{18}O_{SMOW}$-value at the time of calcite precipitation is available in this case. Nevertheless, all the calculated temperatures of precipitation are above the present formation temperature of approximately 60–65°C. It is also interesting that the third and youngest calcite cement generation in the Stø Formation (CALC3) has less negative $\delta^{18}O$-values than the second generation (CALC2) of calcite cement (Fig. 2). This may possibly be a consequence of uplift and cooling between the precipitation of CALC2 and CALC3.

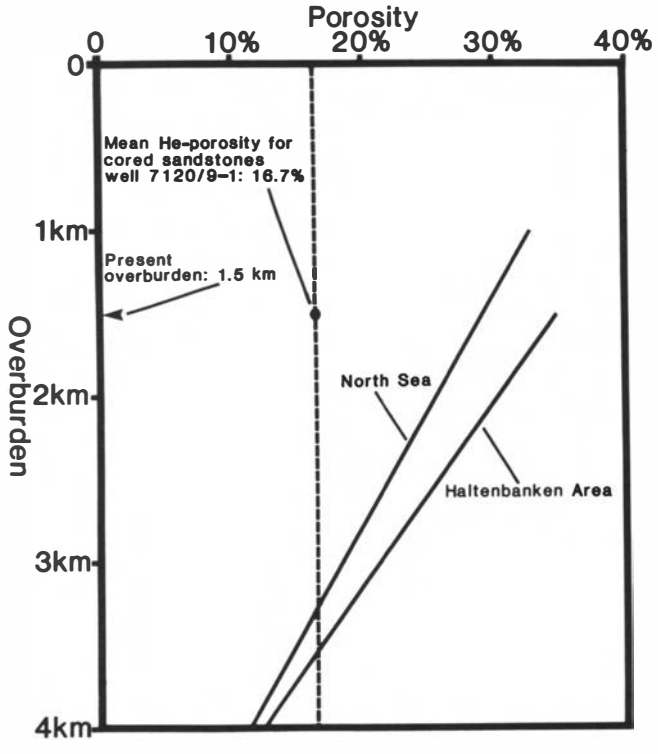

Fig. 1. Porosity versus depth trends for Jurassic sandstones from the North Sea (Selley 1978) and from the Haltenbanken area (Bjørlykke et al. 1986)

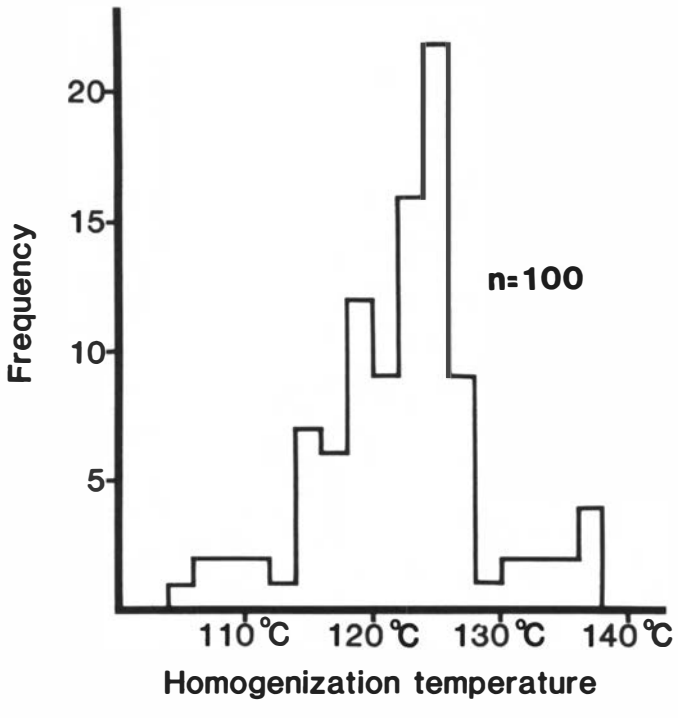

Fig. 3. Homogenization temperatures of hydrocarbon inclusions in calcite cement (CALC2) in the Stø Formation.

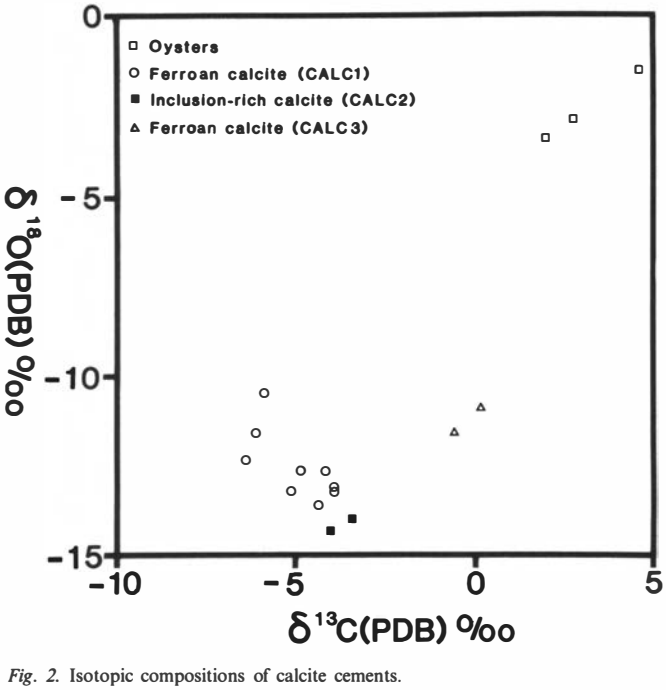

Fig. 2. Isotopic compositions of calcite cements.

Fluid inclusions

The second generation of calcite cement (CALC2) in the Stø Formation contains abundant hydrocarbon fluid inclusions which at room temperature consist of a colourless liquid and a gas bubble. Measurement of one hundred homogenization temperatures for the hydrocarbon inclusions gave results within the temperature range 104–138°C (Fig. 3). Mean and modal homogenization temperatures are 123°C and 125°C respectively; i.e. twice as high as present formation temperatures of 60–65°C. The homogenization temperatures are not thought to be subject to significant pressure corrections due to probable gass-saturation in the pore fluids at the time of entrapment. Whether the homogenization temperatures record original trapping temperatures or re-equilibration temperatures is not certain. However, since the objective of this study is to determine the magnitude of uplift, re-equilibration of the inclusions at progressively higher temperatures would in fact be an advantage as the homogenization temperatures might then record the maximum temperature that the inclusions have been subjected to. In any case, the homogenization temperatures recorded are very good evidence for temperatures of at least 125°C in the Stø and Nordmela Formations at this well location at some point in time. Assuming geothermal gradients in the range 30–40°C/km and sea floor temperatures between 5°C and 15°C, a temperature of 125°C corresponds to burial depths of 2.8–4 km.

Fractures

The Stø and Nordmela Formation cores from well 7120/9-1 contain common vertical to subvertical fractures with lengths of up to 5 cm and widths of up to 50 μm. The

fractures very often extend upwards or downwards from vertical stylolite segments but do not cut across stylolites, observations that suggest formation of the fractures after the stylolites. No movement has taken place along the fracture planes, and the fractures are therefore thought to be a result of horizontal tension. Such a stress regime could be a result of slight doming during uplift and/or contraction due to uplift-induced cooling of the sandstones. The same type of fractures are common in many other Stø and Nordmela Formation cores in other wells.

Conclusions

The degree of quartz cementation and stylolitization, the low porosities plus the homogenization temperatures of fluid inclusions in calcite cement all indicate that the Stø and Nordmela Formations in well 7120/9-1 have been buried to a depth of at least 3 km. $\delta^{18}O$-values for calcite cement are in accordance with this view, and vertical fracturing of the sandstones may also indicate that uplift has taken place. The present burial depth of the top of the Stø Formation in well 7120/9-1 is 1.5 km, and it is consequently suggested that the Stø and Nordmela Formations have been uplifted 1.5–2 km at this well location. The diagenetic study performed does not date the time of uplift directly, but as the largest stratigraphic break in the well studied is between Paleocene siliceous shales and Pleistocene sediments, the uplift has probably taken place after the Paleocene.

Manuscript received October 1991

References

Berglund, L. T., Augustson, J., Færseth, R., Gjelberg, J. & Ramberg-Moe, H. 1986: The evolution of the Hammerfest Basin. *In* Spenser, A. M. et al. (eds.): *Habitat of Hydrocarbons on the Norwegian Continental Shelf*, 319-338. Graham & Trotman, London.

Bjørlykke, K., Aagaard, P., Dypvik, H., Hastings, D. S. & Harper, A. S. 1986: Diagenesis and reservoir properties of Jurassic sandstones from the Haltenbanken area, offshore Mid Norway. *In* Spencer, A. M. et al. (eds.):*Habitat of Hydrocarbons on the Norwegian Continental Shelf*, 275–286. Graham & Trotman, London.

Bjørlykke, K., Ramm, M. & Saigal, G. C. 1989: Sandstone diagenesis and porosity modification during basin evolution. *Geologische Rundschau 78,* 243–268.

Nyland, B., Jensen, L. N., Skagen, J., Skarpnes, O. & Vorren, T. 1992: Tertiary uplift and erosion in the Barents Sea: magnitude, timing and consequences. *In* Larsen, R. M. & Larsen, B. T. (eds.): *Structural and Tectonic Modelling and its Applications to Petroleum Geology*. Elsevier, Amsterdam.

Olaussen, S., Dalland, A., Gloppen, T. G. & Johannessen, E. 1984: Depositional environment and diagensis of Jurassic reservoir sandstones in the eastern part of Troms I area. *In* Spencer, A. M. et al (eds.): *Petroleum Geology of the North European Margin*, 61–79. Graham & Trotman, London.

Riis, F. & Fjeldskaar, W.: On the magnitude of the Late Tertiary and Quaternary erosion and its significance for the uplift of Scandinavia and the Barents Sea. *In* Larsen, R. M. et al. (eds.): *Structural and Tectonic Modelling and Its Application to Petroleum Geology*. Norwegian Petroleum Society, Graham & Trotman, London (in press).

Selley, R. C. 1978: Porosity gradients in North Sea oil-bearing sandstones. *Journal of the Geological Society of London 135,* 119–132.

Walderhaug, O. 1985: Et studium av tidlig jurassiske sandsteiner fra brønn 7120/9-1, Hammerfestbassenget, med hovedvekt på diagenese. Cand. scient. thesis, University of Bergen, 204 pp.

Dating and measuring of erosion, uplift and subsidence in Norway and the Norwegian shelf in glacial periods

FRIDTJOF RIIS

Riis, F. Dating and measuring of erosion, uplift and subsidence in Norway and the Norwegian shelf in glacial periods. *Norsk Geologisk Tidsskrift*, Vol. 72, pp. 325–331. Oslo 1992. ISSN 0029-196X.

The large Plio-Pleistocene deposits off the coast of Norway and in the Barents Sea indicate a significant increase in erosion rates and in vertical movements in Norway and the Barents Sea in the last 2–3 Ma. This activity had impact on several hydrocarbon accumulations on the shelf. Results from ongoing research projects suggest that parts of the Norwegian mainland were also uplifted in the Paleogene. In South Norway, important vertical movements are indicated later than 1 Ma ago, causing tilting of Lower and Middle Pleistocene sediments along the eastern boundary of the Norwegian Channel.

F. Riis, Norwegian Petroleum Directorate, PO Box 600, N-4001 Stavanger, Norway.

Results from petroleum exploration in the Norwegian part of the Barents Sea indicate that in most of the explored area, several hundreds of metres of Tertiary and older sediments have been removed by erosion (e.g. Nyland et al., in press). In the northern and western parts, the erosion cuts into older rocks, and data from Bjørnøya and Svalbard suggest removal of as much as 3000 m or more of overburden in the Tertiary (Manum & Throndsen 1978; Wood et al. 1990). Figure 1 is based mainly on well data. In the north, contours are extrapolated by using bathymetry and outcrop patterns.

Studies of the properties of reservoir liquids and gases show that this amount of erosion will have a great impact on the petroleum accumulated in traps (Skagen 1990). The effects related to uplift and erosion in the Barents Sea are therefore now the subject of study in many oil companies and in the Norwegian Petroleum Directorate. Some of these effects are summarized in Fig. 2.

Large amounts of Tertiary erosion also occurred in the western part of Fennoscandia, and the deposition of the erosional products took place along most of the Norwegian shelf (Riis & Fjeldskaar, in press).

Biostratigraphic studies of the uppermost clastic wedges off the coast of central Norway and in the western Barents Sea (Eidvin & Riis 1989, 1991; Eidvin et al. 1991) indicate that an important part of the erosion in the whole region took place in the Late Pliocene and Pleistocene, and was related to glaciation. Similar conclusions were reached by Nøttvedt et al. (1988) and Vorren et al. (1990), although the dating of some of the stratigraphic units has been disputed.

In addition to the clastic wedges which can be correlated to the period of glaciation, Paleocene to Eocene depocentres can be identified in the northern North Sea, off Møre, in the Lofoten area and in the area west of the Stappen High in the Barents Sea. These depocentres could be related to the Early Tertiary opening of the North Atlantic, high heat flows and tectonic movement (Sales, in press). The central parts of the North Sea have a differing geological history with a more continuous subsidence through the Tertiary and in particular a thick Miocene section was deposited.

Therefore, a model for the Tertiary uplift and erosion north of 62° should be divided into a Paleogene part, which can be modelled by plate tectonics, and a recent part which is related to glaciations in the last 2–3 Ma (Eidvin & Riis 1989; Jansen et al. 1988). South of 62°, the geological development may have been more complicated.

Riis & Fjeldskaar (in press), calculated the isostatic responses of erosion from the Barents Sea and Fennoscandia and the corresponding deposition on the shelves. Using maximum models for the amount of glacial erosion (Figs. 1 and 3), they concluded that there is a component of tectonic uplift in Fennoscandia which cannot be explained by the calculation. This is consistent with modelling work by other authors (Doré, in press). Similarly, the subsidence of the shelves seems to be larger than what the models predict. The part of the uplift which cannot be modelled seems to be greater in the onshore mountain areas and smaller in the Barents Sea.

Uplift and erosion in the period of glaciations

The results of the regional study by Riis and Fjeldskaar (in press) caused the Norwegian Petroleum Directorate

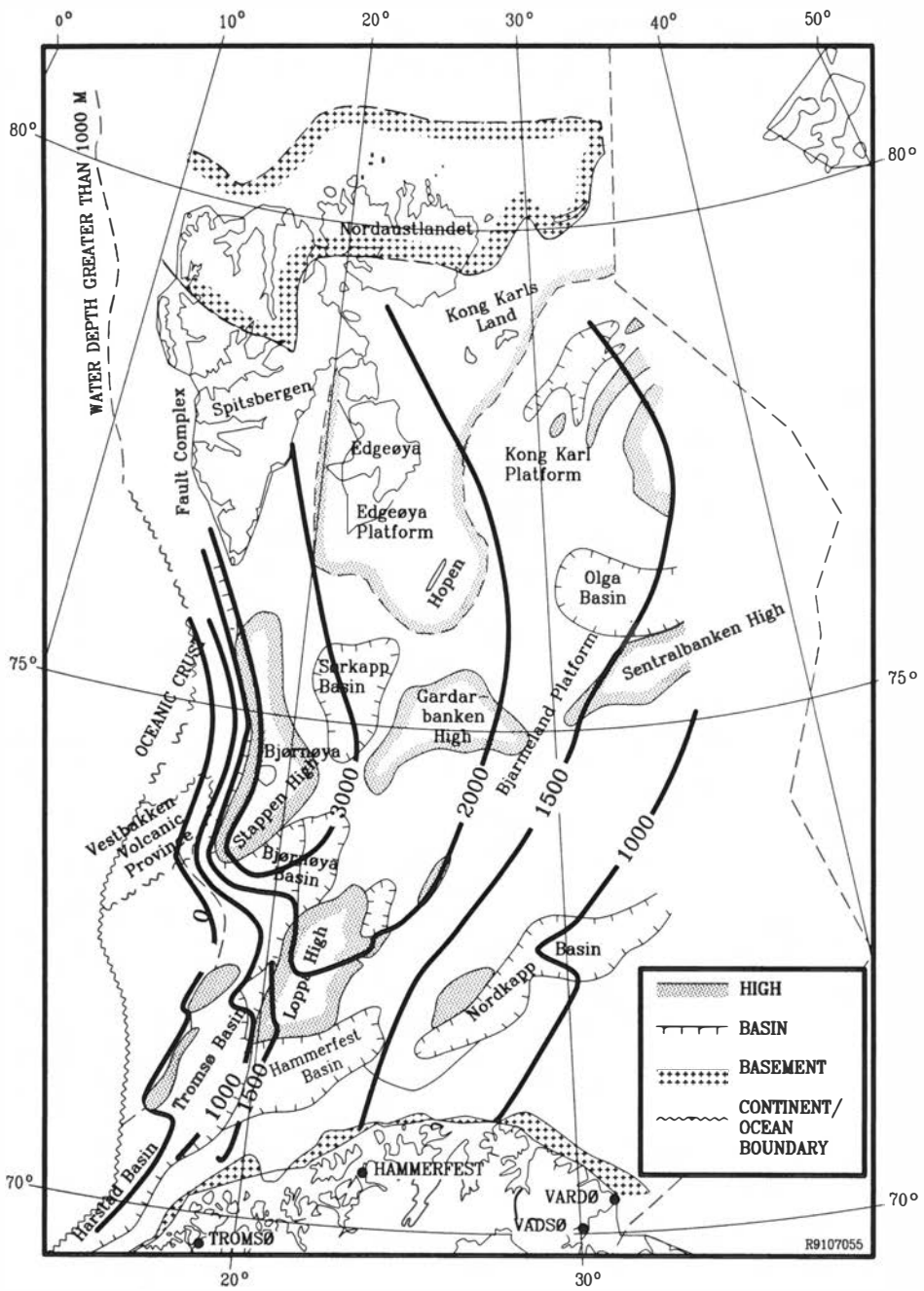

Fig. 1. Sketch map of the western part of the Barents Sea showing an interpretation of the amount of overburden which has been removed by erosion in the Tertiary and Quaternary. Contour interval 1000 m (500 m). The map is based mainly on geochemistry data from wells (vitrinite reflectance and pyrolysis T_{max} data) and on seismic interpretation of the reflector interpreted to represent the opal A to CT transformation. In the north there are few data points.

to concentrate its studies to the Norwegian Channel and southern-central Norway. The objective is to obtain more precise data on the timing and amounts of erosion, deposition and tectonic movements through the Late Pliocene and Pleistocene.

Different lines of approach have been used to obtain better data, and research carried out by several academic groups in Norway is essential for the project.

Precise dating within the Plio-Pleistocene section is important for correlation of major events between different parts of the shelf. Also, if the Neogene wedges can be divided into sedimentary packages of known age, a more detailed mass balance study can be made. The biostratigraphy (foraminifera) in the clastic wedges in the Northern North Sea, mid-Norway and Barents Sea was examined by Eidvin & Riis (1989, 1991) and Eidvin et al. (1991). In the Troll Field, core material allows dating of the complete Quaternary section in the Norwegian Channel (Sejrup et al. 1989; unpublished data).

The results indicate that the volume of late Pliocene sediments in the wedges exceeds the volume of Pleistocene sediments. In the Norwegian Channel, the basal glacial deposits are overlain by Lower to Middle Pleistocene marine clays and silts (Sejrup pers. comm.).

The calculations by Riis & Fjeldskaar (in press) were based on the assumption that it is possible to define

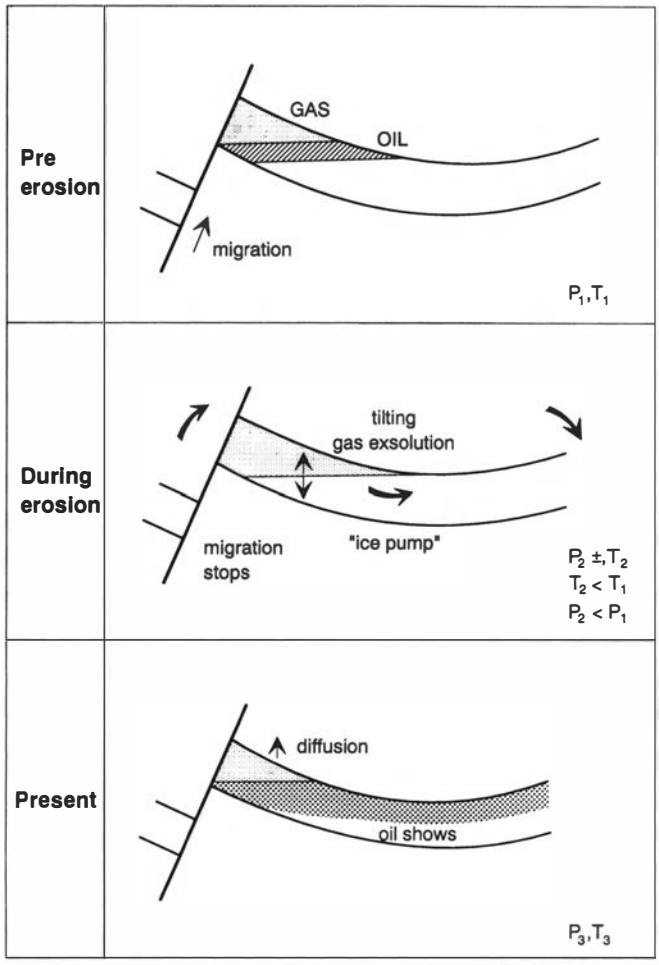

Fig. 2. Effects of erosion and uplift on hydrocarbon accumulations. If the cooling caused by erosion blocks the generation of hydrocarbons, oil will tend to be redistributed in the reservoir rock by the processes of gas expansion and gas exsolution caused by pressure and temperature drop. Tilting of the reservoir is an additional effect. It is also suggested that replacement of the water with a thick ice cap will result in hydrostatic pressures in excess below the ice. This would cause a free gas cap to contract, while it would expand when the ice melts. This is referred to as the 'ice pump' effect in the sketch.

certain morphological levels onshore which can be regarded as low relief plains formed relatively close to sea level. The erosion below these levels, and the deformation of the levels (Doré, this volume), will then give important information about the recent erosion and uplift. If the block fields as defined by Nesje et al. (1988) represent pre-glacial weathering surfaces, the block field level could represent such a marker surface. This level can be defined in the mountains of South Norway and North Norway (Thoresen 1990).

Also, the topography of the paleic surface (Gjessing 1967) as mapped by Nesje (reported by Riis & Fjeldskaar, in press) contains important information. Nesje et al. (in press) calculated that the volume eroded below the paleic surface in the Sognefjord basin exceeds 7000 km^3, corresponding to an average erosion of more than 600 m in the drainage area of the Sognefjord. Using an average Quaternary thickness of 250 m in the Norwegian Channel, the eroded volume exceeds the sediment volume deposited in the Quaternary in the northern part of the Norwegian Channel between 61° and 62°30′.

This study therefore gives an impression that the paleic surface in the Sognefjord area could have existed prior to the major glaciations in the Quaternary. However, more exact volume comparison must await better data of the outer parts of the Plio-Pleistocene wedge off the Norwegian Channel where a large volume of Pleistocene sediments was deposited. As is indicated in Fig. 3, there is a great Pliocene–Pleistocene sediment volume in the wedge, so the mass balance method does not necessarily indicate a pre-glacial minimum age for the paleic surface in West Norway.

Another approach to the detailed study of the onshore uplift and erosion is to examine the cave deposits in the major caves in Nordland, Central Norway. Some of the larger caves show erosion levels which can be dated by speleothems, and ages back to at least 300,000 years have been reported (Lauritzen et al. 1990). These deposits are the oldest post-Cretaceous deposits recorded so far onshore in Norway. Since there are mountains rising more than 1000 m above the dated levels in the caves, these data suggest that a considerable relief existed far back in the Quaternary in Central Norway, and that the onshore uplift was not pronounced in the last few hundred thousand years in this area.

The study of neotectonics may also give relevant data on the uplift problem. Neotectonics in Norway is mainly related to the glacio-isostatic rebound. The present uplift rates seem to be fairly regular on a regional scale (Sørensen et al. 1987). However, detailed studies across fault zones indicate that differential movements may take place locally (Anundsen 1990; Olesen et al., in press).

The neotectonics is also strongly related to earthquake activity. The seismic activity of Norway is concentrated along some of the well known major fault zones and rifts (Bungum et al. 1990). Also, on the maps produced by Bungum et al. (1990), it can be noted that there is a concentration of epicenters along the west coast of Norway, in the area where the Tertiary and Quaternary erosion was at a maxium, and where Quaternary vertical movement took place along the Norwegian Channel as discussed below. Bungum et al. (1990) suggest that 'ridge push', sedimentary loading effects and postglacial uplift are important sources of stress.

Similarly, it is suggested here that the vertical movements observed today could have one short-term component related to glacio-isostasy and one component which is a response to forces and loads acting over longer periods of time.

Quaternary vertical movement along the coast of South Norway

In the platform areas along the coast, Mesozoic and Cenozoic strata have a regional dip away from the coast.

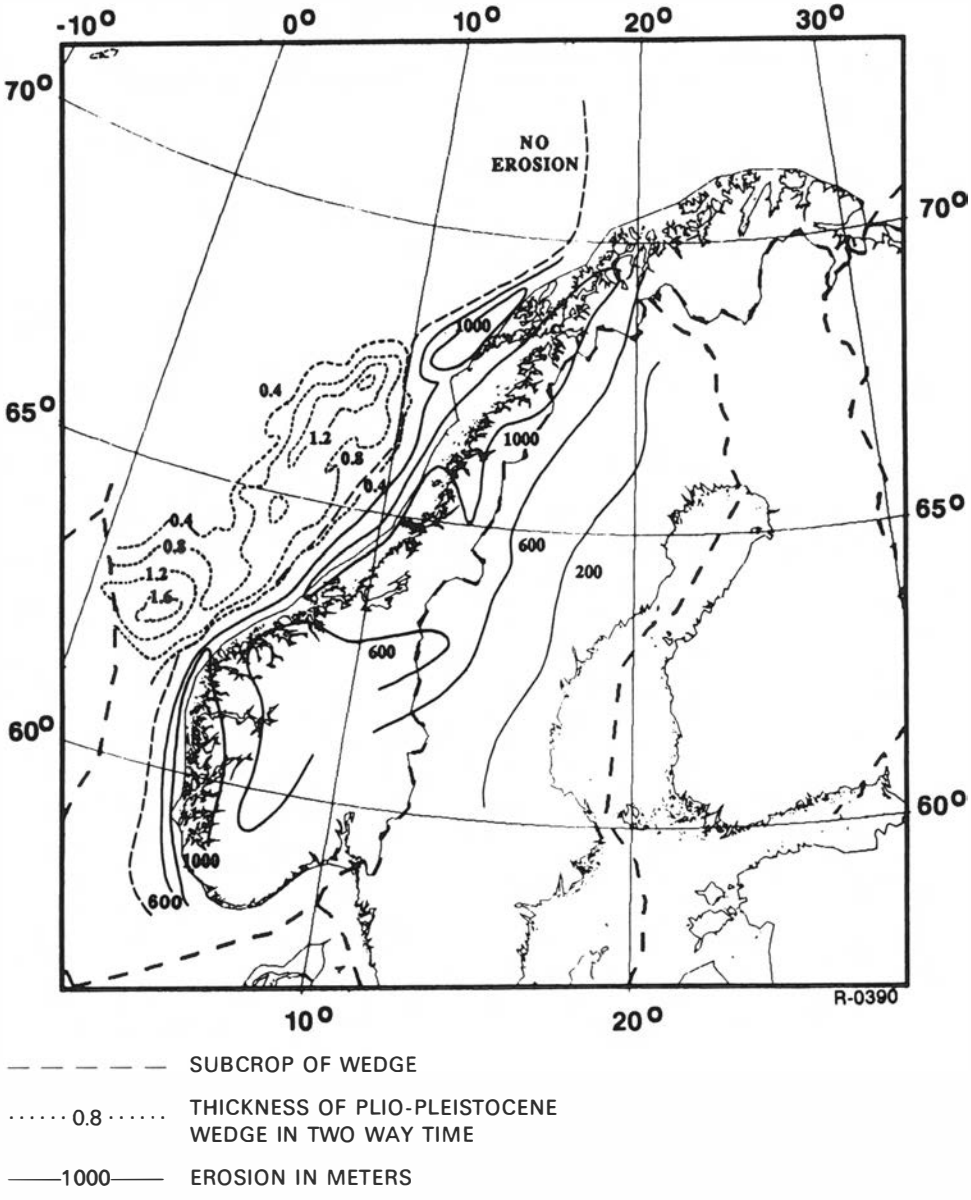

Fig. 3. Composite map showing the averaged amount of overburden removed between the present surface and the summit level in Mid-Norway, as well as an isopach map in two-way time of the thickness of the Plio-Pleistocene wedge deposited off Mid-Norway.

In an outcrop map this results in a geometry where the different horizons parallel the coast (Rokoengen et al. 1988; Sigmond, in press). The tilted layers are truncated by the base of Quaternary unconformity (Fig. 4), suggesting a late Pliocene or early Quaternary phase of tilting.

However, seismic lines shot close to the coast of SW Norway may be interpreted to show tilting of even the Quaternary beds. The tilted area is located at the eastern flank of the Norwegian Channel, and only the deeper parts of the Quaternary section have been locally preserved from later erosion. Fig. 4 shows an interpretation of parts of two shallow seismic sections close to the island of Utsira (profiles AA′ and BB′). The seismics was acquired for IKU by Geoteam.

In these seismic sections, the older part of the Quaternary section dips to the west, and there are at least two erosional events (tentatively correlated with major phases of glaciation) in the upper part of the section.

Obviously, care must be taken to distinguish dips due to progradation and dips due to draping over pre-existing topography from tectonic tilting of the layers. The suggested tectonic tilt is based on the following description of the sections.

The base of the Quaternary section (BQ, Fig. 4) is an angular discordance which truncates dipping Mesozoic and Tertiary sediments. This unconformity is close to horizontal in the Norwegian Channel, but along a coast parallel line, this horizontal attitude changes to a pronounced dip towards the channel. The dip is apparently not related to lithological changes in the underlying sediments (Fig. 4, profile AA′).

The section overlying the unconformity is interpreted as a Lower Pleistocene basal till succeeded by marine sediments which in the lower part are older than 0.7 Ma (Sejrup pers. comm.). These marine sediments are well developed with a consistent reflection pattern in the northern part of the Norwegian channel. In general they

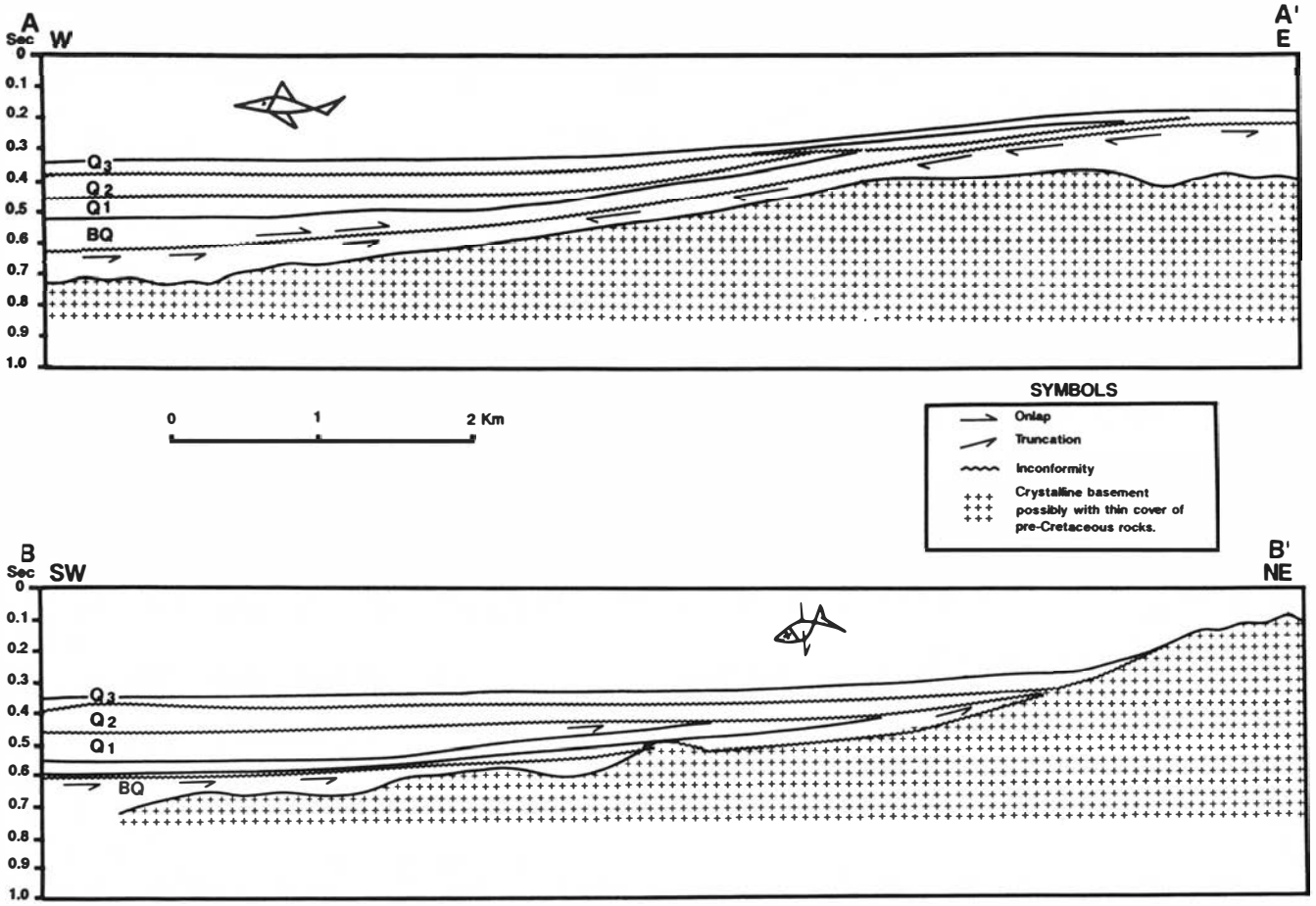

Fig. 4. Two geoseismic sections in the Utsira area, southwest Norway. The interpretation is based on seismics collected by IKU in 1988. Onlaps and truncations are indicated by arrows.

are parallel to the basal unconformity, but in the western flank of the channel, they onlap the base of the channel. However, on the eastern flank, which at present has a much more pronounced topography, these reflectors continue to be parallel with the basal unconformity even in the dipping part of the section. Onlaps can be defined only in a small area in the deepest part of the channel. Farther updip, there is little change in thickness in the dipping lower Quaternary section (Fig. 4).

The unconformities Q1 and Q2 (Fig. 4) which are interpreted as erosive events in the channel, do not tend to erode into the dipping part of the section, rather these unconformities also show dips indicating a progressive tilting taking place.

The difference in elevation of the base of Quaternary across the structure in Fig. 4 is in the order of 350 m, and it is thought that an important part of this differential uplift must be explained by tectonic movements.

Similar observations can be made in selected localities also along the coast of Jæren (Fugelli & Riis, in press) and north to Møre. In Fig. 5, the coastal hinge zone has not been drawn continuously to the north because of erosion of the key area close to the coast. Onshore, the Quaternary geology of Jæren suggests important vertical movements as recent as approximately 100,000 years (Fugelli & Riis, in press).

In conclusions, it is suggested that relative vertical motion in the order of several hundred metres could have taken place in the Quaternary along a gentle monoclinal structure (hinge zone) parallelling the west coast of southern Norway. The hinge zone cannot be mapped in detail, because the older Quaternary sections are too deeply eroded in many localities. However, the hinge zone seems to parallel more or less the bathymetrical eastern slope of the Norwegian Channel. It parallels the boundary of outcropping basement, and it has a trend similar to the major faults separating the Triassic-Jurassic fault blocks of the Horda Platform from the uplifted basement block of the continent. However, these faults are situated to the west of the hinge zone (Fig. 5).

If this interpretation is correct, it will be important for the modelling of the tectonic events since the motion was more rapid than previously anticipated. Also, our understanding of the tilting and migration of hydrocarbons into the Troll Field reservoir will be affected, since the Troll Field is within the zone of tilted Tertiary strata and fairly close to the Quaternary hinge zone (Fig. 5).

Acknowledgements. – The support from the Norwegian Petroleum Directorate has been very important for the present research on the Tertiary/Quaternary uplift problems. IKU kindly allowed publication of the geoseismic sections.

Manuscript received October 1991

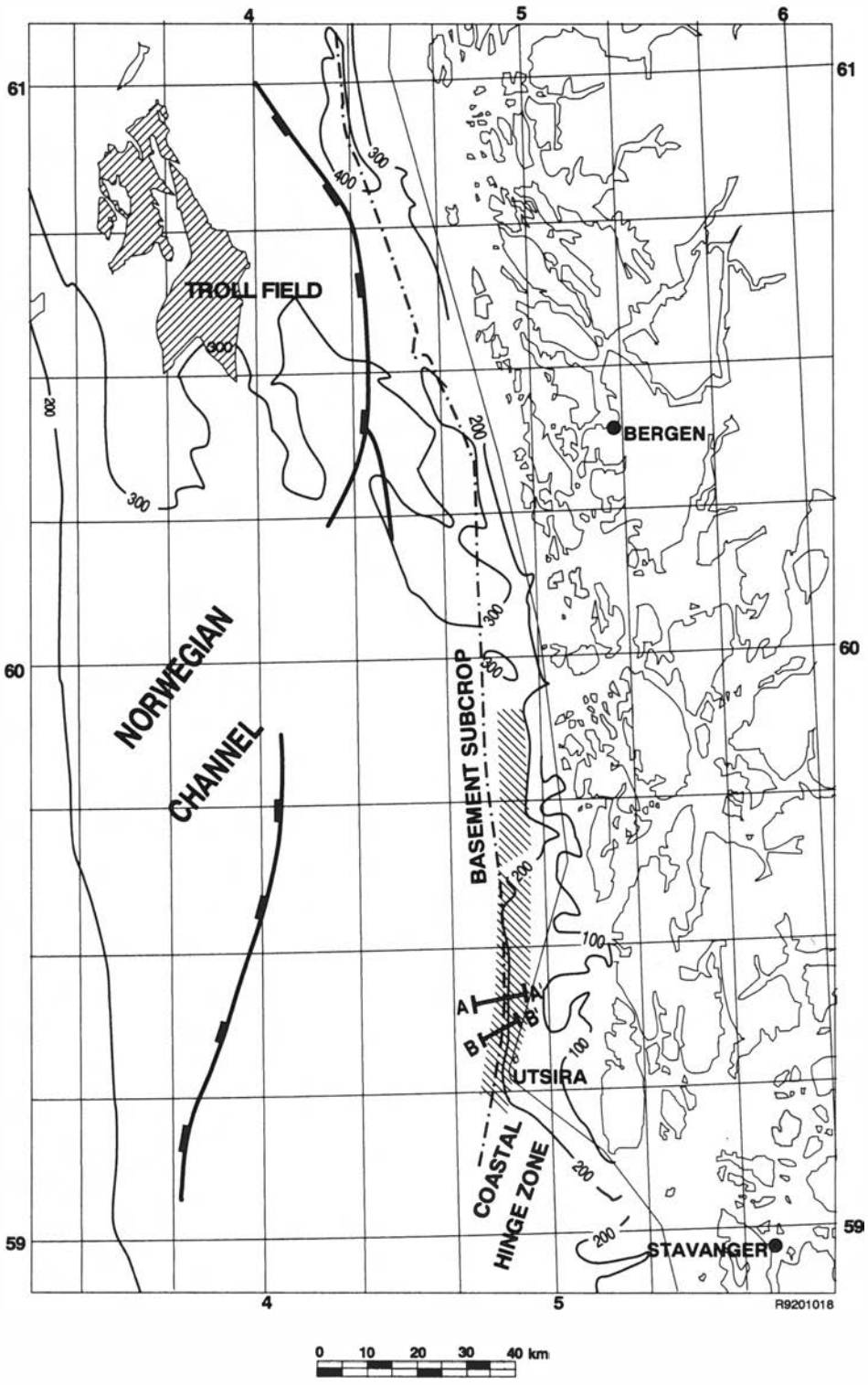

Fig. 5. Tectonic map of a part of the Norwegian Channel, showing bathymetry (contour interval 100 m), locations of the profiles AA′ and BB′, as well as the main faults and the basement subcrop below the Quaternary, modified from Brekke et al. 1992. The faults are mapped at the Base Cretaceous level, and they separate the faulted Triassic basins to the west from the upthrown crystalline basement to the east. The coastal hinge zone indicates the area where Quaternary layers are dipping. This zone probably continues to the north, but is difficult to map due to lack of data and deep erosion into the older parts of the Quaternary section.

References

Anundsen, K. 1990: Precise measurements of active faulting in southwest Norway. Abstract, 19. Nordiske Geologiske Vintermøte, Stavanger. *Geonytt 17*, 24.

Brekke, H., Kalheim, J.-E., Riis, F., Egeland, B., Johnsen, S. & Ragnhildstveit, J. 1992: Norges kontinentalsokkel. Formkart over inkonformitetsflaten under henholdsvis overjuralagrekken (nord for 69°) og krittlagrekken (sør for 69°), med geologiske hovedtrekk fra fastlandet. Målestokk 1:2000000. Oljedirektoratets sokkelkart nr 1. Oljedirektoratet/Norges geologiske undersøkelse.

Bungum, H., Alsaker, A., Kvamme, L. B. & Hansen, R. A. 1990. Seismicity and seismotectonics of Norway and nearby continental shelf areas. *NORSAR Contribution 399*, 24 pp.

Doré, A. G. 1992: The Base Tertiary surface of southern Norway and the northern North Sea. *In* Jensen, L. N. & Riis, F. (eds.): Post-Cretaceous uplift and sedimentation along the western Fennoscandian shield. *Norsk Geologisk Tidsskrift*. This volume, pp. 259–265.

Eidvin, T. & Riis, F. 1989: Nye dateringer av de tre vestligste borehullene i Barentshavet. Resultater og konsekvenser for den tertiære hevingen. *NPD Contribution 27* 43 pp.

Eidvin, T., Fugelli, E. M. G. & Riis, F. 1991: En biostratigrafisk analyse av sedimenter over og under basal pleistocen, regionale vinkeldiskordans i nordøstlige deler av Nordsjøen. *NPD Contribution 28*, 22 pp.

Eidvin, T. & Riis, F. 1991: Enobiostratigrafisk analyse av tertiære sedimenter på kontinentalmarginen av Midt-Norge, med hovedvekt på øvre pliocene vifteavsetninger. *NPD Contribution 29*, 44 pp.

Fugelli, E. M. G. & Riis, F. 1992: Neotectonism in the Jæren area, southwest Norway. *In* Jensen, L. N. & Riis, F. (eds.): Post-Cretaceous uplift and sedimentation along the western Fennoscandian shield. *Norsk Geologisk Tidsskrift*. This volume, pp. 267–270.

Gjessing, J. 1967: Norway's paleic surface. *Norsk Geografisk Tidsskrift 21* 69–132.

Jansen, E., Bleil, U., Henrich, R., Kringstad, L. & Slettemark, B. 1988: Paleoenvironmental changes in the Norwegian Sea and the Northeast Atlantic during the last 2.8 Ma.: DSDP/ODP Sites 610, 642, 643 and 644. *Paleoceanography 3*, 563–581.

Lauritzen, S.-E., Løvlie, R., Moe, D. & Østbye, E. 1990: Paleoclimate deduced from a multidisciplinary study of half million year old stalagmite from Rana, Northern Norway. *Quaternary Research 34*, 306–316.

Manum, S. & Thorndsen, T. 1978: Rank of Coal and dispersed organic matter and its geological bearing in the Spitsbergen Tertiary. *Norsk Polarinst. Årbok 1977*, 159–177.

Nesje, A., Dahl, S. O., Anda, E. & Rye, N. 1988: Block fields in southern Norway. significance for the Late Weichselian Ice Sheet. *Norsk Geologisk Tidsskrift 68*, 149–169.

Nesje, A. & Dahl, S. O., Valen, V. & Øvstedal, J. in press: Quaternary erosion in the Sognfjord drainage Basin, Western Norway. *Geomorphology*.

Nyland, B., Jensen, L. N., Skagen, J. I., Skarpnes, O. & Vorren, T. O.: Tertiary uplift and erosion in the Barents Sea; magnitude, timing and consequences. *In* Larsen, R. M. et al. (eds.): *Structural and Tectonic Modelling and Its Application to Petroleum Geology*. Norwegian Petroleum Society. Elsevier, Amsterdam (in press).

Nøttvedt, A., Berglund, T., Rasmussen, E. & Steel, R. 1988: Some aspects of Tertiary tectonics and sediments along the western Barents Shelf. *In* Morton A. C., & Parson, L. M. (eds.): Early Tertiary volcanism and the opening of the NE Atlantic. *Geol. Soc. Spec. Publ. 39*, 421–425.

Olesen, O., Henkel, H., Lile, O. B., Mauring, E. & Rønning, J. S. 1992: Neotectonics in the Precambrian of Finnmark, Northern Norway. *In* Jensen, L. N. & Riis, F. (eds.): Post-Cretaceous uplift and sedimentation along the western Fennoscandian shield. *Norsk Geologisk Tidsskrift*. This volume, pp. 301–306.

Riis, F. & Fjeldskaar, W.: On the magnitude of the Late Tertiary and Quaternary erosion and its significance for the uplift of Scandinavia and the Barents Sea. *In* Larsen, R. M. et al. (eds.): *Structural and Tectonic Modelling and Its Application to Petroleum Geology*. Norwegian Petroleum Society, Elsevier, Amsterdam (in press).

Rokoengen, K., Rise, L., Bugge, T. & Sættem, J. 1988: Bedrock geology on the Mid Norwegian Continental shelf. Map in scale 1:1,000,000. *IKU publication 118*. Continental Shelf and Petroleum Technology Research Institute *A/S*.

Sales, J.: Late Tertiary uplift – West Barents shelf. Character, mechanisms and timing. *In* Larsen, R. M. et al. (*eds.*): *Structural and Tectonic Modelling and Its Application to Petroleum Geology*. Norwegian Petroleum Society, Graham & Trotman, London (in press).

Sejrup, H. P., Nagy, J. & Brigham-Grette, J. 1989: Foraminiferal stratigraphy and amino acid geochronology of Quaternary sediments in the Norwegian Channel, northern North Sea. *Norsk Geologisk Tidsskrift 69*, 111–124.

Sigmond, E. M.: Berggrunnskart over Norge og kontinentalsokkelen. 1:3000000. Norges geologiske undersøkelse (in press).

Skagen, J. 1990: Effects on hydrocarbon potential caused by uplift and erosion in the Barents Sea. Abstract, International conference on arctic geology and petroleum potential, 15–17 august 1990. Norwegian Petroleum Society. p. 31.

Sørensen, R., Bakkelid, S. & Torp, B. 1987: Landhevning. *In Nasjonalatlas for Norge. Map sheet* 2.3.3. Statens Kartverk.

Thoresen, M. K. 1990: *Kvartærgeologisk kart over Norge. Tema: Jordarter. M: 1:1 mill.* Norges Geologiske Undersøkelse.

Vorren, T. O., Richardsen, G., Knutsen, S.-M. & Henriksen, E. 1990: The western Barents Sea during the Cenozoic. *In* Bleil, U. & Thiede, J. (eds.): *Geologic History of the Polar Oceans: Arctic versus Antarctic*, 95–118 NATO ASI Series, Kluwer, Dordrecht.

Wood, R. J., Edrich, S. P. & Hutchinson, I. 1990: Influence of North Atlantic tectonics on the large-scale uplift of the Stappen High and Loppa High, Western Barents Shelf. *In* Tankard, A. J. & Balkwill, H. R. (eds): Extensional tectonics and stratigraphy of the North Atlantic Margins. *American Association of Petroleum Geologists Memoir 43*, 559–566.

Glacial erosion and tectonic uplift in the Barents Sea

ERLING VÅGNES, JAN INGE FALEIDE & STEINAR THOR GUDLAUGSSON

Vågnes, E., Faleide, J. I. & Gudlaugsson, S. T.: Glacial erosion and tectonic uplift in the Barents Sea. *Norsk Geologisk Tidsskrift*, Vol. 72, pp. 333–338. Oslo 1992. ISSN 0029-196X.

A large part of the Cenozoic erosion in the Barents Sea was apparently accommodated by lowering of the erosional basis several hundred meters below early Oligocene sea level. This was a combined effect of glacio-eustatic lowering of global sea level and erosion by marine ice sheets covering the Barents Sea during the late Cenozoic ice ages. The amount of erosion accommodated by this lowering of the erosional basis may be estimated from the present bathymetry of the Barents Sea. Comparison with independent erosion estimates suggests that at least the Svalbard–Bjørnøya area has been affected by Late Cenozoic tectonic uplift in the order of 1000 m.

E. Vågnes[1], J. I. Faleide & S. T. Gudlaugsson, Department of Geology, University of Oslo, PO Box 1047, Blindern, N-0316 Oslo, Norway; [1] Present address: Norsk Hydro as, PO Box 200, N-1321 Stabekk, Norway.

During the Late Cenozoic large-scale erosion occurred in the Barents Sea and caused significant reduction of the petroleum potential of the area (Nyland et al., in press; Riis & Fjeldskaar, in press). An average of 600 m of Late Cenozoic erosion has been inferred in the Western Barents Sea from volume estimates of glacial sediments in the Lofoten Basin (Eidvin & Riis 1989; Vorren et al. 1991). However, local erosion estimates tend to exceed this average: On Spitsbergen and on Bjørnøya a total of $\approx$3000 m of erosion has been inferred from vitrinite reflectance data (Manum & Throndsen 1978; Wood et al. 1989). Much or all of this erosion occurred in the Cenozoic. Estimates of Cenozoic erosion from wells in the Hammerfest Basin range from 1000 to 1500 m (Ramm 1990).

It is also generally agreed that the erosion was associated with uplift. As pointed out by for example Riis & Fjeldskaar (in press), uplift of the crust below the eroded strata is a necessary consequence of isostatic adjustment due to erosion. On the other hand, uplift may also be the driving force for erosion by elevating the terrain above the erosional basis, e.g. sea level. Such uplift may be caused by thermal, tectonic, magmatic, or metamorphic processes. Here such uplift is referred to as *tectonic uplift*.

When discussing Cenozoic erosion events, it is important to bear in mind that glaciations may initiate erosion by the opposite process, i.e. by *lowering the erosional basis*. In this respect glaciations operate on two levels: Globally by glacio-eustatic lowering of sea level and regionally by glaciers and ice sheets eroding below sea level (Fig. 1). Erosion accommodated by glacio-eustatic fall in sea level probably occurred in the Barents Sea already during the initial glaciations of Antarctica during Oligocene times (Barker et al. 1988). The final result of erosion by marine glaciers or ice sheets will be increased depth, but a substantial amount of related isostatic uplift will occur during the process (Fig. 1).

Here we summarize evidence suggesting the large-scale erosion by marine ice sheets did take place in the Barents Sea in the Late Cenozoic, then we show how a rough estimate of the amount of erosion accommodated by glacial driving forces alone can be obtained from the present bathymetry of the Barents Sea, and finally we show that although glacial driving forces were important this cannot explain all of the observed Late Cenozoic erosion in the Barents Sea, indicating that at least some areas must have been affected by tectonic uplift.

Importance of submarine glacial erosion

Strong evidence suggests that marine ice sheets caused extensive erosion on the Barents Shelf, although convincing mechanisms through which a marine ice sheet may effect large-scale erosion on a continental shelf have yet to be proposed (A. Elverhøi, pers. comm.).

Redating of strata in the westernmost wells in the Barents Sea indicates that most of the sediments forming the Bjørnøyrenna Delta (Fig. 2) cannot be much older than 2.3 Ma, and that they postdate the first evidence of ice-dropped material (Eidvin & Riis 1989). The amount of glacial sediments in the Bjørnøyrenna Delta corresponds to $\approx$600 m of erosion in the southern Barents Sea (Vorren et al. 1991).

The above observations clearly demonstrate the importance of glacial erosion, but they do not indicate whether the glaciers eroded uplifted terrain or whether the erosional basis was below sea level. That the latter was the case is supported by the morphological differences of the continental shelves around the Arctic (Perry

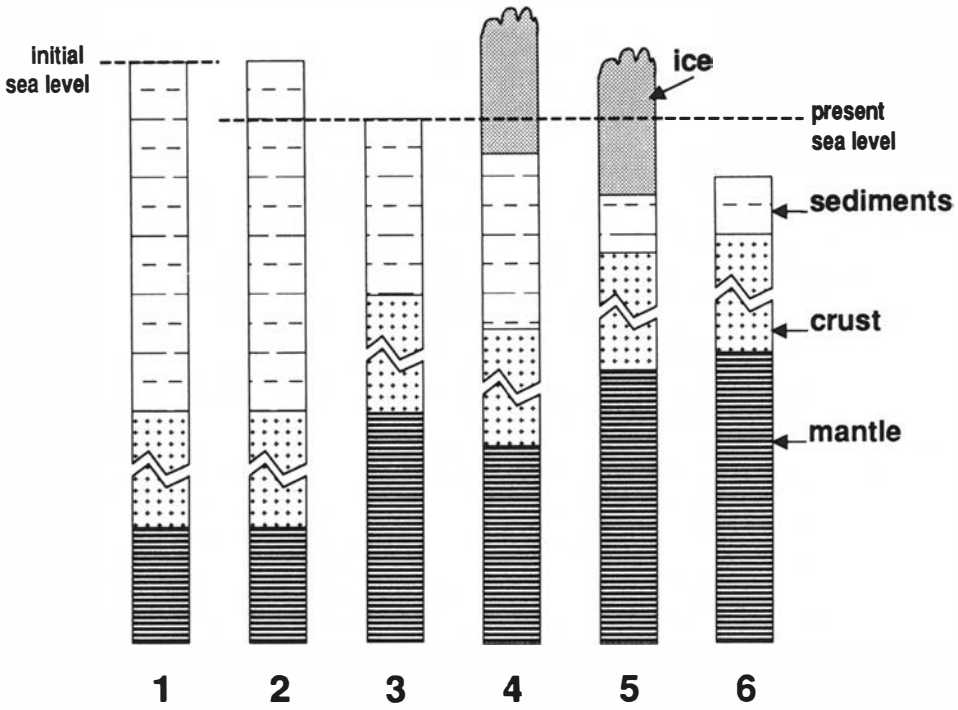

Fig. 1. Schematic illustration of erosion due to glacial driving forces on the Barents Shelf. A column of mantle, crust, sediments with present water depth of 200 m is chosen as an example, and its evolution since Oligocene times has been divided into six stages. (1) Initial situation, the column is at sea level, (2) a 200 m fall in sea level has 'elevated' the shelf above the erosional basis, (3) erosion has leveled the terrain to the new sea level, (4) initial glaciation, (5) ice sheets erode below sea level, (6) the ice sheet has melted and the present water depth of 200 m is established.

& Flemming 1986). The Barents Shelf was a center for accumulation of an ice sheet, and the Canadian Arctic Islands were probably covered by part of the Laurentide ice sheet during the last glaciation (Denton & Hughes 1981). Both areas are incised by prominent submarine valleys where water depths exceed those of mature shelves by several hundred meters.

The shelves of the Alaskan North Slope and the Laptev Sea, on the other hand, exhibit very low relief and depths typical of mature shelves. These latter shelves were situated adjacent to areas not much affected by the last glaciation (e.g. Denton & Hughes 1981). It seems reasonable to infer that a similar distribution of ice sheets existed during the previous Late Cenozoic glaciations, and that ice sheets in the Canadian Arctic Islands and the Barents Sea repeatedly lowered the erosional basis below sea level, causing the peculiar morphology of these areas.

Erosion due to glacial driving forces

Utilizing some simplifying assumptions, the erosion due to glacial driving forces may be estimated from the present bathmetry of the Barents Sea (cf. Appendix). The following assumptions are made:

1. The Barents Sea is in local isostatic equilibrium, i.e. the effects of flexural compensation of the bathymetry are negligible. This is probably a good approximation for features like Bjørnøyrenna (width = 150 km), but not for the Svalbard region which is incised by narrow fjords (width ≈ 10 km).

2. The Barents Shelf was at sea level, and in local isostatic equilibrium, prior to the onset of Cenozoic glaciations in Antarctica.

3. Present sea level is ≈200 m below that of the early Oligocene (Haq et al. 1987).

4. The average density of the eroded sediments in the Barents Sea area was 2.2 g/cm^3, and the density of the mantle 3.3 g/cm^3.

Formulas relating the amount of erosion to present water depth are obtained from isostatic balance equations in the Appendix. A map of the amount of erosion accommodated by glacial driving forces in the Barents Sea based on the above assumptions is shown in Fig. 2.

The uncertainty in eustatic sea-level fluctuations is the single largest source of uncertainty in the construction of Fig. 2. An alternative to the ≈200 m of sea-level fall since the Early Oligocene (Haq et al. 1987) would be to assume that the fall in the sea level since the early Oligocene is 75 m, i.e. equal to the expected sea-level rise if all present glaciers and ice sheets melted (e.g. Alley 1991). In this case ≈400 m of erosion should be subtracted from the estimates in Fig. 2. On the basis of available evidence it is incorrect to attribute more than 75 m of sea-level fall to glacio-eustasy, the remaining 125 m of eustatic sea-level fall since the Oligocene (Haq et al. 1987) must be attributed to other causes. Thus, strictly speaking, one should consider erosion accommodated by a glacio-eustatic sea-level fall (75 m) and erosion accommodated by a eustatic sea-level fall from other causes (125 m) separately. However, both must be corrected for in order to isolate tectonic uplift, and here

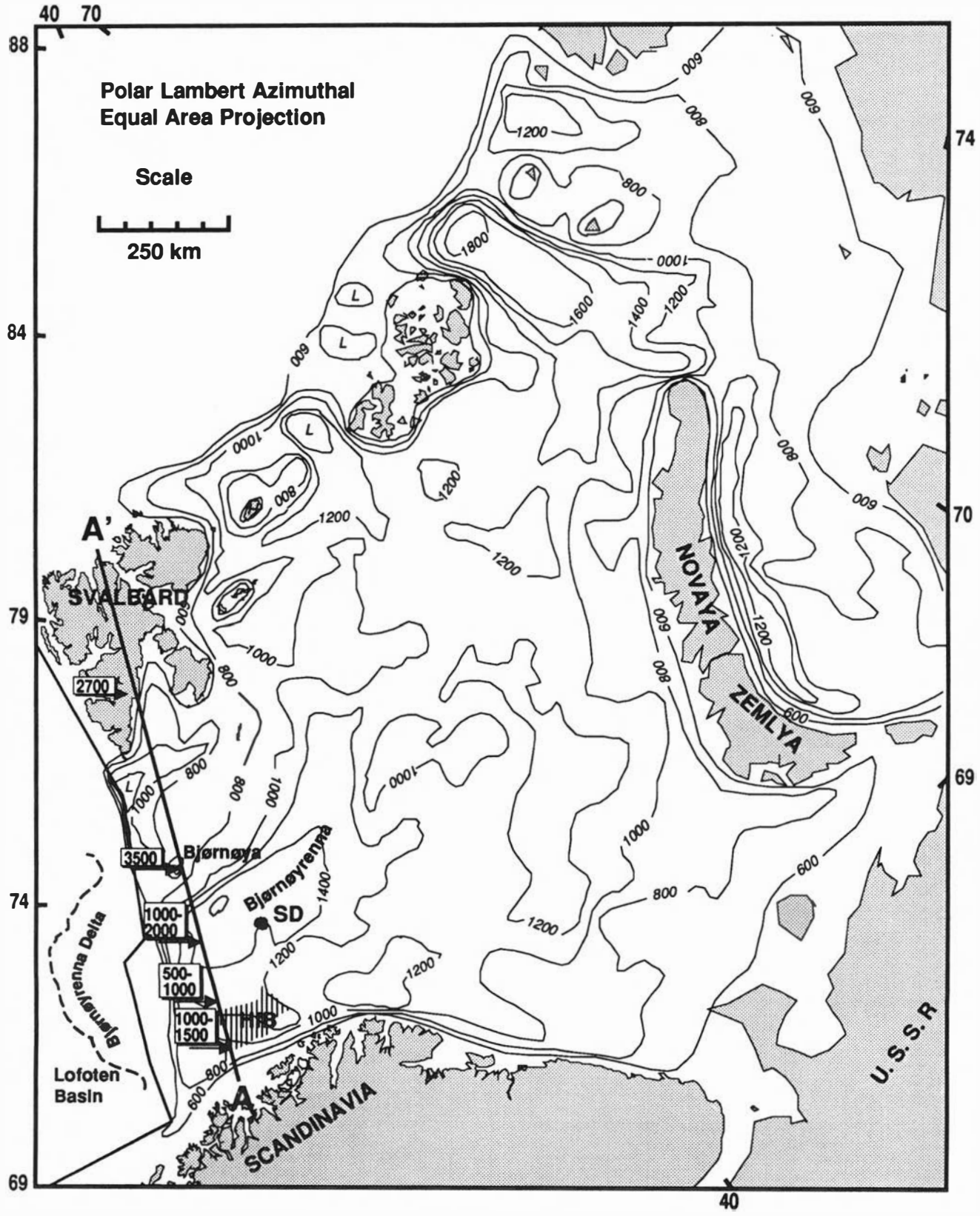

Fig. 2. Maximum estimate of erosion from glacial driving forces alone. The map is constructed from present water depth, assuming an average density of 2.2 g/cm^3 for the eroded material. The post-Oligocene fall in sea level has been incorporated by adding 600 m of erosion to that estimated from bathymetry. Profile A-A′ refers to Figs. 3 and 4; arrows indicate position of erosion estimates from geochemical and straigraphic data. HfB = Hammerfest Basin, SD = Svalis Dome.

the entire 200 m sea-level fall since the Oligocene is included in the discussion of glacial driving forces.

Another source of uncertainty is the density of the eroded material; a sea-level fall of 100 m may accommodate 550 m of erosion in basement rocks (density = 2.7 g/cm^3) vs. 200 m in sediments (density = 2.2 g/cm^3). This has probably helped create the characteristic subcrop pattern towards the coast of Norway. With regard to Fig. 2, it is worth noting that the average density of eroded sediments will increase with increasing depth of erosion due to compaction. Therefore the estimate used here (2.2 g/cm^3) may be on the low side for Bjørnøya and Svalbard.

Furthermore, the assumption of zero water depth is important for the estimates; if the Oligocene water depth was 100 m rather than zero, 200 m should be subtracted from the erosion estimates in Fig. 2. On the other hand, if the area was at an elevation of 50 m in the Oligocene, 150 m should be added to the estimates in Fig. 2.

Finally, where flexural isostatic compensation of the bathymetry is important the amount of erosion in the troughs in Fig. 2 is exaggerated, and the erosion on their flanks is underestimated. On a regional scale these effects will cancel out.

Tectonic uplift

We consider the erosion estimates in Fig. 2 to be maximum estimates of the amount of erosion that can be accommodated by glacial driving forces, because the maximum difference in sea level since the Early Oligocene is incorporated. Therefore areas in the Barents Sea where erosion exceeds that inferred from Fig. 2 must have been affected by tectonic uplift in order to explain the erosion.

Conversion of erosion estimates into estimates of tectonic uplift can be accomplished by first correcting for erosion accommodated by glacial driving forces, and then correcting the remaining erosion for isostatic rebound (cf. Appendix).

Erosion estimates (Wood et al. 1989; Ramm 1990; Manum & Throndsen 1978) along a profile from the coast of north Norway to the northern tip of Svalbard are annotated on Fig. 2. Figure 3 shows the differences between the erosion estimates from bathymetry and the other erosion estimates. Figure 4 shows the difference between the two sets of erosion estimates converted into tectonic uplift estimates.

The tectonic uplift in the SW Barents Sea from Fig. 4 seems to be small, arguably below the resolution of present erosion estimate methods. On the other hand the ≈1750–2050 m of erosion reported near the Svalis Dome (Løseth et al. in press), indicates ≈100–200 m of tectonic uplift in this area.

Both on Svalbard and on Bjørnøya ≈1000 m of tectonic uplift is indicated by vitrinite reflectance data and present elevation. On Svalbard the vitrinite reflectance

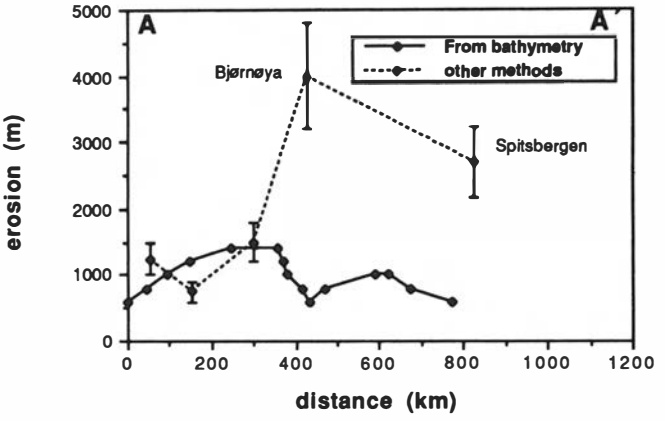

Fig. 3. Comparison of maximum glacial erosion estimated from bathymetry and erosion estimates from geochemical and stratigraphic data along profile A-A′. We have corrected the erosion estimate on Bjørnøya for the present elevation of the sampled Triassic shales (≈500 m), increasing the estimate to ≈4000 m from the 3500 m reported by Wood et al. (1989). Error bounds of 20% indicate the variations in reported erosion estimates.

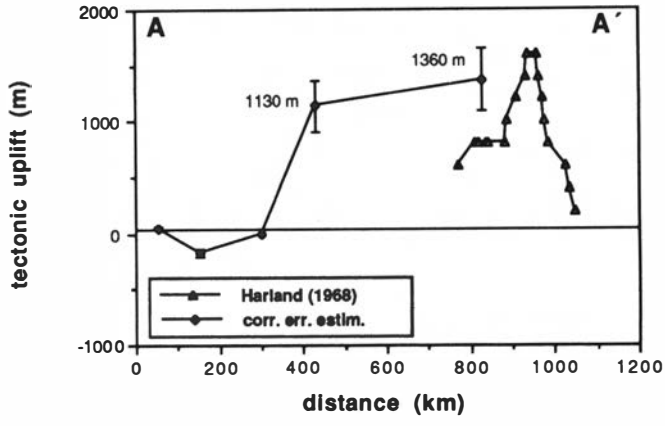

Fig. 4. The difference in erosion estimates from Fig. 2 reduced to tectonic uplift by subtracting glacial erosion and correcting for isostatic rebound. Note that Bjørnøya has less tectonic uplift than Spitsbergen, although erosion estimates are greater on Bjørnøya. This is because the erosion estimates on Spitsbergen come from the inner part of Van Keulen Fjorden and local isostatic compensation for the fjord relief is likely to be small. We have therefore assumed infinite flexural rigidity in this area, instead of local isostatic equilibrium. The present uplift on Spitsbergen from the summit-height surface of Harland (1968) is also shown. Note that because the correction for erosion accommodated by glacial driving forces is a maximum, the estimates of tectonic uplift in this figure are minimum estimates.

data were measured in Paleocene sediments, thus the entire tectonic uplift must have occurred in the Cenozoic. It is generally agreed that Spitsbergen underwent compressional deformation and crustal thickening during the Eocene (Harland 1969; Steel et al. 1985) and some of the erosion may reflect relief formed in the Spitsbergen thrust and fold belt. However, this does not explain the present uplift of Svalbard, which affects a post-orogenic peneplain (Harland 1968). Instead, the present high heatflow on Spitsbergen, the geochemical signature of the sequence of Late Cenozoic volcanism and the high oceanic heatflow adjacent to Spitsbergen suggest that the present uplift of Svalbard is due to an anomalously thin mantle lithosphere (Vågnes & Amundsen in prep.).

The vitrinite reflectance data from Bjørnøya were measured in Triassic rocks (Bjorøy et al. 1981), providing little constraint on the amount of Cenozoic uplift. However, the presence of high velocity Early Cretaceous sediments nearby on the Svalbard Platform (Edwards 1975; Houtz 1980) suggests that maximum burial in the area did not occur any earlier than the Mid-Cretaceous. This suggests important Cenozoic tectonic uplift. The large amounts of Eocene and younger pre-glacial sediments in the Vestbakken Volcanic Province (Faleide et al. 1988; Gabrielsen et al. 1990) indicate that the Stappen High/Bjørnøya underwent breakup-related uplift and erosion in the Eocene–Oligocene, probably due to influx of heat across the continental margin to the west. However, this heat influx cannot be responsible for the present uplift of the area, because erosion and subsidence due to cooling of the lithosphere would have caused the area to submerge tens of millions of years ago. In light of the regional uplift pattern we suggest that Bjørnøya is affected by the same broad uplift as Svalbard, and that the Late Cenozoic tectonic uplift may well be in the order of 1000 m on Bjørnøya also.

Conclusions

Three major Cenozoic phases of erosion may be expected in the Barents Sea, the first during the Eocene due to break up-related tectonic uplift along the plate boundary, the second in the Oligocene due to glacio-eustatic lowering of the sea level, and the third during the Late-Pliocene and Pleistocene due to erosion by marine ice sheets. Analysis of erosion, bathymetry and elevation indicates that glacial erosion may explain much but not all of the observed erosion in the Western Barents Sea. When glacial effects are removed, tectonic uplift in the NW Barents Sea appears to be in the order of 1000 m; an order of magnitude greater than in the SW Barents Sea.

Acknowledgements. – This study was funded by BP-Norway. A. Elverhøi made constructive comments on an early version of the manuscript, as did I. J. Stewart on a later version. F. Riis made a manuscript available prior to publication. Two anonymous reviewers provided valuable suggestions and criticisms.

Manuscript received October 1991

References

Alley, R. B. 1991: West Antarctic collapse – How likely? *Episodes 13*, 231–238.

Barker, P. F., Kennett, J. P. et al. 1988: Proc. *ODP, Init. Repts. 113*, 5–11. College Station TX.

Bjorøy, M., Mørk, A. & Vigran, J. O. 1981: Organic geochemic studies of the Devonian to Triassic succession on Bjørnøya and the implications for the Barents Shelf. *In* Bjorøy, M. et al. (eds.): *Advances in Organic Geochemistry – 1981*, 49–59. Wiley, Chichester.

Denton, G. H. & Hughes, T. J. 1981: *The Last Great Ice Sheets*, 484 pp. John Wiley & Sons, New York.

Edwards 1975: Gravel fraction on the Spitsbergen Bank, NW Barents Shelf. *Norges geologiske undersøkelse 316*, 205–217.

Eidvin, T. & Riis, F. 1989: Nye dateringer av de tre vestligste borehullene i Barentshavet. Resultater og konsekvenser for den Tertiære landhevningen. *NPD Contribution no. 27*, 44 pp.

Faleide, J. I., Myhre, A. M. & Eldholm, O. 1988: Early Tertiary volcanism at the western Barents Sea margin. *In* Morton, A. G. & Parson, L. M. (ed.): *Early Tertiary Opening and the Opening of the NE Atlantic. Geological Society Special Publication 39*, 135–146. Blackwell, Oxford.

Gabrielsen, R. H., Færseth, R. B., Jensen, L. N., Kalheim, J. E. & Riis, F. 1990: Structural elements of the Norwegian continental shelf. Part I: The Barents Sea Region. *NPD-Bulletin 6*, 33 pp.

Haq, B. U., Hardenbol, J. & Vail, P. 1987: Chronology of fluctuating sea levels since the Triassic. *Science 235*, 1156–1167.

Harland, W. B. 1968: Mantle changes beneath the Barents Shelf. *Transactions New York Academy of Sciences 31*, 25–41.

Harland, W. B. 1969: Contribution of Spitsbergen to understanding of tectonic evolution of the North Atlantic region. *In* Kay, M. (ed.): *North Atlantic Geology and Continental Drift. American Association of Petroleum Geologists Memoir 12*, 817–851.

Houtz, R. E. 1980: Seafloor and near surface velocities from Barents Sea sonobuoy data. *Journal of Geophysical Research 85*, 4838–4844.

Løseth, H., Fanavoll, S., Fjæringstad, V., Leith, L. T., Lippard, J. S., Ritter, U., Smelror, M., Sylta, Ø. & Sættem, J.: Cenozoic uplift and erosion of the Barents Sea; evidence from the Svalis Dome area. *In* Vorren, T. O. et al. (eds.): *Arctic Geology and Petroleum Potential*, Norwegian Petroleum Society (in press).

Manum, S. B. & Throndsen, T. 1978: Rank of Coal and dispersed organic matter and its geological bearing in the Spitsbergen Tertiary. *Norsk Polarinstitutt Årbok 1977*, 159–177.

Nyland, B., Jensen, L. N., Skagen, J. L., Skarpnes, O. & Vorren, T. in press: Tertiary uplift and erosion in the Barents Sea; magnitude, timing and consequences (abstract). *In* Larsen, R. M. & Larsen, B. T. (eds.): *Structural and Tectonic Modelling and Its Application to Petroleum Geology*. Norwegian Petroleum Society Special Publication, 1. Elsevier, Amsterdam.

Perry, R. K. & Flemming, H. S. 1986: *Bathymetry of the Arctic Ocean*. Naval Research Laboratory, Washington DC.

Ramm, M. 1990: Diagenesis and porosity evolution of reservoir sandstones in Troms well 7119/12-1 (*abstract*). *Geonytt 17*, 92.

Riss, F. & Fjeldskaar, W.: On the magnitude of the Late Tertiary and Quaternary erosion and its significance for the uplift of Scandinavia and the Barents Sea. *In* Larsen, R. M. & Larsen, B. T. (eds.): *Structural and Tectonic Modelling and Its Application to Petroleum Geology*. Norwegian Petroleum Society. Graham & Trotman, London (in press).

Steel, R. J., Gjelberg, J., Nøttvedt, A., Helland-Hansen, W., Kleinspehn, K. & Rye-Larsen, M. 1985: The Tertiary strike-slip basins and orogenic belt of Spitsbergen. *Society of Economic Paleontologists and Mineralogists Special Publication 37*, 339–359.

Vorren, T., Richardsen, G., Knutsen, S. M. & Henriksen, E. 1991: Genozoic erosion and sedimentation in the western Barents Sea. *Marine and Petroleum Geology 8*, 317–340.

Vågnes, E. & Amundsen, H. E. F. 1991: Late Cenozoic uplift and volcanism on Spitsbergen: Caused by mantle convection? *In* Amundsen, H. E. F.: *Igneous Processes and Lithosphere Evolution: Evidence from Upper Mantle and Lower Crustal Xenoliths from Northwestern Spitsbergen and the Canary Islands*. Dr. Philos. Thesis, University of Oslo. 142 pp.

Wood, R. J., Edrich, S. P. & Hutchison, I. 1989: Influence of North Atlantic Tectonics on the large-scale uplift of the Stappen High and Loppa High, Western Barents Shelf. *In* Tankard, A. J. & Balkwill, H. R. (eds.): *Extensional Tectonics and Stratigraphy of the North Atlantic Margins. American Association of Petroleum Geologists Memoir 46*, 559–566.

Appendix: Relationships between tectonic uplift, waterdepth and erosion from isostatic balancing

Assuming local isostatic equilibrium the relationship between tectonic uplift (U) above sea level in an area and the amount of erosion (E) needed to erode the area to sea level may be obtained from the condition for isostatic balance; i.e. that the pressure at the depth of compensation (H) is the same before and after erosion. Assuming that the erosion occurs in sedimentary rocks:

$$h_s\rho_s + h_c\rho_c + (H - (h_s - U) - h_c)\rho_m$$
$$= (h_s - E)\rho_s + h_c\rho_c + (H - h_c - (h_s - E))\rho_m$$

Where the left-hand side corresponds to the situation before erosion, and h_s is the height of the sedimentary column (including the uplift, U), H is the depth of compensation measured from sea level; h_c is the thickness of the crystalline crust; ρ_c, ρ_m, ρ_s are the density of the crust, mantle and the average density of the eroded sediments, respectively. This gives:

$$E = U(\rho_m)/(\rho_m - \rho_s)$$

or conversely if the amount of erosion is known the tectonic uplift is given by

$$U = E(\rho_m - \rho_s)/(\rho_m)$$

For submarine erosion the isostatic balance condition is:

$$h_s\rho_s + h_c\rho_c + (H - h_s - h_c)\rho_m = h_w\rho_w + (h_s - E)\rho_s + h_c\rho_c + (H - h_c - (h_s - E) - h_w)\rho_m$$

Where the left-hand side corresponds to the situation before erosion, ρ_w is the water density and h_w is the present water depth. This gives:

$$E = h_w(\rho_m - \rho_w)/(\rho_m - \rho_s)$$